PHARMACOLOGICAL DETERMINANTS OF ANTI-TUBERCULOSIS DRUG ACTIVITY

Thesis submitted in accordance with the requirements of the University of Liverpool for the degree of Doctor of Philosophy

By
Ruben Christiaan Hartkoorn
April 2006

CONTENTS

	Abstract	i
	Preface	ii
	Acknowledgements	iii
	List of Publications	iv
	Abbreviations	vi
Chapter 1-	General introduction	1
Chapter 2-	Effect of P-glycoprotein and MRP1 on the cellular accumulation of anti-tuberculosis drugs	59
Chapter 3-	Characterisation of the time and concentration dependent bacteriostatic activity of anti-tuberculosis drugs on extracellular H37Rv	109
Chapter 4-	Intracellular anti-tuberculosis activity and the influence of P-glycoprotein	143
Chapter 5-	Characterisation of OATP expression and function in cell lines and alveolar macrophages	163
Chapter 6-	Method Development for the Quantitative Analysis of Plasma Rifampicin, Isoniazid and Pyrazinamide by HPLC, HPLC-MS and HPLC-MS/MS	186
Chapter 7-	The impact of drug transporters on rifampicin cellular accumulation *in vivo*	222
Chapter 8-	General discussion	250
	References	259

ABSTRACT

Pathogenic *Mycobacteria* tuberculosis (MTB) exist as a 'mixed population', containing bacilli in different metabolic states as well as within or outside alveolar macrophages and granuloma. Despite the availability of numerous anti-tuberculosis drugs, the duration of tuberculosis therapy is still at least 6 months. Current drugs are highly effective at killing actively growing bacilli in the extracellular space; however they are less effective at killing semi-dormant and intracellular bacilli (persisting bacilli). Active drug influx and efflux transporters may play a role in the accumulation of anti-tuberculosis drugs into macrophages, and thereby contribute to the decreased bactericidal activity against intracellular bacilli.

Active efflux transporters P-glycoprotein (P-gp) and multidrug resistance polypeptide 1 (MRP1) were found to be expressed on monocyte derived macrophages and alveolar macrophages. Using cell line models, rifampicin and ethambutol were found to be substrates for P-gp but not MRP1. Pyrazinamide and isoniazid were not substrates for either transporter. Rifampicin accumulation remained unaltered by inhibition of basal P-gp on PBMCs and no relationship was found between rifampicin accumulation and P-gp or MRP1 expression on PBMCs.

Alveolar macrophages were also found to express two of the examined solute carrier mRNA (SLCO1B3 and 3A1). As rifampicin is a substrate for OATP1B3 (product of SLCO1B3), active influx transporters may contribute to the intracellular potency of anti-tuberculosis drugs.

When using a modified microplate alamar blue assay (MABA) to determine drug mediated early bactericidal activity (EBA), it was found that H37Rv developed time dependent phenotypic tolerance against rifampicin and suspected genotypic resistance against isoniazid. Ethambutol susceptibility remained unchanged over time. Using a newly developed assay to determine intracellular antibacterial drug activity it was found that rifampicin, isoniazid and ethambutol showed concentration dependent activity. Inhibition of P-gp significantly improved the intracellular anti-tuberculosis activity of rifampicin and ethambutol.

The development and validation of analytical methods for the quantification of plasma rifampicin, pyrazinamide and isoniazid allowed for the determination of pharmacokinetics in patients. Rifampicin receiving patients were found to show no relationship between *in vivo* rifampicin accumulation and P-gp expression. However, patients receiving rifampicin did show marked P-gp induction compared to healthy volunteers. The quantitative analysis of plasma concentrations of rifampicin, isoniazid and pyrazinamide is underpinning pharmacokinetic trials in different groups.

Drug accumulation into alveolar macrophages is a combination between active influx, efflux and diffusion. Rifampicin and ethambutol are substrates for P-gp, although basal expression had limited influence on drug accumulation. Further work needs to be done to establish the role of OATPs for drug accumulation in alveolar macrophages. Further, this thesis describes novel assays that will be helpful in determining extracellular and intracellular activity of novel anti-tuberculosis drugs.

PREFACE

Chapter 1: Introduces the pathogenesis of tuberculosis, the pharmacology of current first line anti-tuberculosis drugs and active drug transporters.

Chapter 2: Demonstrates the expression of P-glycoprotein and MRP1 on alveolar macrophages and monocyte derived macrophages. Further it investigates whether first line anti-tuberculosis drugs are substrates for P-glycoprotein and MRP1 using in vitro cell line models (T-lymphoblastoid cell, MDCKII epithelial cells) and *ex vivo* PBMCs.

Chapter 3: Details a study investigating the time and concentration dependent killing of anti-tuberculosis drugs on log-phase extracellular H37Rv.

Chapter 4: Introduces a novel assay for the analysis of anti-mycobacterial activity of drugs against H37Rv residing within macrophages. It also investigates the impact of P-glycoprotein inhibition on the efficiency of drug activity.

Chapter 5: Determines the expression of active drug influx transporters (OATPs) on alveolar macrophages, and their potential influence on rifampicin accumulation.

Chapter 6: Presents a description and validation of novel assays for the quantification of rifampicin, pyrazinamide and isoniazid.

Chapter 7: Details on *In vivo* determination of the impact of P-glycoprotein on the accumulation of rifampicin in patients with tuberculosis and staphylococcal infection.

Chapter 8: Discusses the principle findings and suggests further work.

ACKNOWLEDGEMENTS

The studies presented in this thesis were carried out at the University of Liverpool (Department of Pharmacology and Therapeutics) and the Liverpool School of Tropical Medicine between 2002 and 2006.

I would like to thank both Professor David Back and Dr Saye Khoo for giving me this wonderful opportunity to research in a very interesting and important field of tropical medicine and pharmacology. They have both been very supportive supervisors, giving me great guidance and support. I am also very grateful to Dr Becky Jubb, Dr. Andrew Owen, Dr Omar Janneh and Dr Gerry Davies who have been a huge source of information, ideas and were invaluable both in the laboratory and outside. Thanks go to everyone else in the HIV pharmacology group that have made working at the University pleasant and fun, JT, Sara, Maria, Stevy, Neill, Phil, Clare, Wai San and the Laura's; you have all been wonderful

I am very thankful to both Professor Steve Ward and Dr Andrew Ramsay at the Liverpool School of Tropical Medicine who have been incredibly supportive and have helped me develop new ideas, skills and assays in the lab. I would also like to thank Dr Mas Chaponda, Dr Catriona Waitt and the nurses that helped in the clinical study at the Royal Liverpool and Broadgreen University Hospitals for their help and clinical expertise.

Finally, I am greatly indebted to my family who have always supported me throughout IB, University and my PhD. I would never have had this opportunity unless they backed and encouraged me, 'Allemaal hartstikke bedankt!' Further, I would like to thank Chloe Palmer for keeping me sane (and largely in Paris) during the writing of my thesis.

LIST OF PUBLICATIONS

Published

Hider SL, Owen A, **Hartkoorn R**, Khoo S, Back DJ, Silman A, Bruce IN. (2006) Down-Regulation Of MRP1 Expression In Early RA Patients Exposed To Methotrexate As A First DMARD. *Ann Rheum Dis*, (Feb 27, Epub ahead of print).

Graham, S. M., Bell, D. J., Nyirongo, S., **Hartkoorn, R.**, Ward, S. A. & Molyneux, E. M. (2006) Low levels of pyrazinamide and ethambutol in children with tuberculosis and impact of age, nutritional status, and human immunodeficiency virus infection. *Antimicrob Agents Chemother*, 50, 407-13.

Owen, A., Janneh, O., **Hartkoorn, R. C.**, Chandler, B., Bray, P. G., Martin, P., Ward, S. A., Hart, C. A., Khoo, S. H. & Back, D. J. (2005) In vitro synergy and enhanced murine brain penetration of saquinavir coadministered with mefloquine. *J Pharmacol Exp Ther*, 314, 1202-9.

Janneh, O., Owen, A., Chandler, B., **Hartkoorn, R. C.**, Hart, C. A., Bray, P. G., Ward, S. A., Back, D. J. & Khoo, S. H. (2005) Modulation of the intracellular accumulation of saquinavir in peripheral blood mononuclear cells by inhibitors of MRP1, MRP2, P-gp and BCRP. *Aids*, 19, 2097-102.

Owen, A., **Hartkoorn, R. C.**, Khoo, S. & Back, D. (2003) Expression of P-glycoprotein, multidrug-resistance proteins 1 and 2 in CEM, CEM(VBL), CEM(E1000), MDCKII(MRP1) and MDCKII(MRP2) cell lines. *Aids*, 17, 2276-8.

Conference Abstracts and Posters

Alfirevic A, Carr D, Mills T, **Hartkoorn R,** Owen A, Tugwood J, Smith JC, Park BK and Pirmohamed M. Multidrug resistance 3 (MDR3) protein and tacrine-induced hepatotoxicity, 9th European ISSX Meeting, Manchester June 2006.

Hartkoorn R., Waitt C., Chaponda M., Davies G., Chandler B., Owen A., Ward S., Back D. and Khoo S. P-glycoprotein and MRP-1 interactions with rifampicin. 12th Conference on Retroviruses and Opportunistic Infections. Boston, USA. 2005.

Owen A., Almond L., **Hartkoorn R.**, Walsh T., Youle M., Bonington A., Turner F., Smith C., Garretti A.M., Phillips A., Janneh O., Back D. and Khoo S., Relevance of Drug Transporters and Drug Metabolism Enzymes to Nevirapine: Superimposition of Host Genotype, 12th Conference on Retroviruses and Opportunistic Infections. Boston, USA. 2005.

Hartkoorn R.C., Janneh O., Owen A., Davies G.R., Chandler B., Back D.J. and Khoo S.H., Active drug transporters and rifampicin accumulation, DMDG, Cambridge, UK, 2004.

Janneh O., Owen A., **Hartkoorn R.C.,** Chandler B., Back D.J. and Khoo S.H., Drug efflux transporters: role in the intracellular accumulation and activity of antiretroviral agents, British Society for antimicrobial chemotherapy (BSAC) meeting, Birmingham, 2004

Hartkoorn R., Chandler B., Khoo S., Back D., The interaction between anti-tuberculosis drugs and P-glycoprotein. BPS focussed meeting on transporters. Cambridge, UK, 2004.

Hartkoorn R.C., Janneh O., Owen A., Davies G.R., Chandler B., Back D.J. and Khoo S.H., The interaction between active drug transporters and rifampicin accumulation, The British Pharmacological Society, 2nd Focused Meeting March 2004, University of Cambridge (pA_2 online, Vol2, Issue1, Abst 003P)

Owen A., Janneh O., Bray P.G., **Hartkoorn R.C.**, Baba M., Ward S.A.,Back D.J. and Khoo S.H, Pharmacoenhancement of saquinavir by mefloquine via inhibition of multi-drug transporters, The British Pharmacological Society, 2nd Focused Meeting March 2004, University of Cambridge (pA_2 online, Vol2, Issue1, Abst 005P)

Hartkoorn R.C., Chandler B., Khoo S., Back D., Interactions between anti-tuberculosis drugs and P-glycoprotein. The British Pharmacological Society, Winter Meeting December 2004, University of London, (pA_2 online, Vol1, Issue4, Abst 205P)

Owen A., Janneh O., **Hartkoorn R.**, Chandler B., Back D. J., Khoo S. H., Modulation of intracellular saquinavir accumulation - Potential for augmenting anti-HIV effect. Federation of Infection Societies Tenth Anniversary Conference. Cardiff, UK. 2003.

Ellis S.W., Anderson M.C., **Hartkoorn R.C.**, Harlow J.R., Chowdry J.E., Mather B., Blaney F.E., Tucker G.T., Evidence for the role of Asp301, and not Glu216, as a ligandbinding residue in the active site of CYP2D6, Structural Biology in Drug Metabolism and Drug Discovery Meeting, AstraZeneca R & D Charnwood, Loughborough, Leicestershire, February 2003

ABBREVIATIONS

7H9GT	Glycerol and tween supplemented Middlebrook 7H9
7H11GT	Glycerol and tween supplemented Middlebrook 7H11
°C	Degrees Celsius
µL	Microlitre
µm	Micrometer
µM	Micromolar
%	Percentage
x g	Gravity
ABC	ATP- binding cassette
ACN	Acetonitrile
AcpM	Acyl carrier protein
Ag85C	Microbial antigen 85C
A-THP1	Activated THP1 cells
AUC	Area under the curve
BAL	Bronchoalveolar lavage
BSP	Sulfobromophthalein
c[Ca^{2+}]	Cytosolic calcium
Ca^{2+}-CaM	Calcium-calmodulin complex
CaM	Calmodulin
CaMKII	Calcium-calmodulin complex dependent protein kinase II
CAR	Cellular accumulation ratio
CD	Cluster of differentiation
CEM	Human T-lymphoblastoid cell line
CHO	Chinese hamster ovary cells
Cmax	Maximum concentration
CR	Complement Receptor
CYP	Cytochrome P450
DAB	Di-amino benzene
DMEM	Dulbecco's modified eagle's medium
DNA	Deoxyribonucleic acid
dpm	Disintegrations per minute
E-3-S	Estrone 3 sulphate
EBA	Early bactericidal activity
EC50	Concentration of drug inhibiting 50 percent of growth
EC90	Concentration of drug inhibiting 90 percent of growth
EDBA	2,2'(ethylenediamino)-dibutyric acid
EEA1	early endosomal autoantigen 1
ER	Endoplasmic reticulum
FA	Fast acetylator
FASI	Fatty acid synthase I
FcγRIIIB	IgG Fcγ receptor IIIB
FCS	Foetal calf serum
g	Gram
GABA	γ-amino butyric acid
GDI	Rab GDP dissociation inhibitor
hr	Hour
H37Rv	Laboratory virulent strain of MTB

HIV	Human Immunodeficiency Virus
HPLC	High performance liquid chromatography
HPLC-MS	HPLC tandem mass spectrometry
icl	Isocitrate lyase
IgG	Immunoglobulin G
IFN	Interferon
IL	Interleukin
IL-1R	Interleukin 1 receptor
InhA	Enoyl-acyl carrier protein reductase
iNOS	Inducible nitric oxide synthase
IRAK	Interleukin 1 receptor associated kinase
IS	Internal standard
J744	Mouse macrophage cell line
KasA	β-Ketoacyl-acyl carrier protein synthase
KatG	Mycobacterial enzyme – a catylase peroxidase
L	Litre
LAMP2	Lysosomal-associated membrane protein 2
LM	Lipomannan
n	Number of observation
NA	Nicotinic acid
NAD	β-nicotinamide adenine dinucleotide
ng	Nanogram
NMR	Nuclear magnetic resonance
MABA	Microplate based alamar blue assay
ManLAM	Mannose capped lipoarabinomannans
MCP-1	Monocyte chemoattractant protein
MDCKII	Madin-Darby Canine Kidney cell lines
MDM	Monocyte derived macrophage
MDR1	Gene that encodes fro P-gp (a.k.a ABCB1)
MHC	Major histocompatibility complex
MIC	Minimum inhibitory concentration
min	Minute
mL	Millilitre
MMA	Microplate based MTT assay
MOI	Multiplicity of infection
mRNA	Messenger RNA
MRP	Multidrug resistance associated polypeptide
MTB	*Mycobacterium* tuberculosis
MTT	Tetrazolium bromide
MyD88	Myeloid differentiation protein 88
MK571	Drug, MRP1 inhibitor
m/z	Mass to charge ratio
NBD	Nucleotide binding domain
NF-κB	Nuclear factor kappa B
NO	Nitric oxide
NOS	Nitric oxide synthase
NSF	N-ethylmaleimide-sensitive factor
OADC	Oleic acid, albumin, dextrose mix
OATP	Organic anion transport protein
p38-MAPK	p38 mitogen-activated protein kinase

PBMC	Peripheral blood mononuclear cells
PBS	Phosphate buffered saline
PCR	Polymerase chain reaction
P-gp	P-glycoprotein
PGL	A polyketide synthase-derived phenolic glycolipid
PIM	Phosphatidylinositol mannoside
PI3K	phosphatidylinositol 3-kinase
PI3P	phosphatidylinositol 3-phosphate
PKCα	A mammalian protein kinase C
PKnG	A bacterial protein kinase
PMA	Phorbol 12-myristate 13-acetate
PRR	pattern recognition receptors
PTK	Protein tyrosine kinases
PZase	Pyrazinamidase
QC	Quality control sample
Rab	A endosome GTP-binding protein
RANTES	T-lymphocytes and monocytes chemoattractant cytokine
RNA	Ribonucleic acid
rPE	r-phycoerythrin
RT-PCR	Reverse transcriptase polymerase chain reaction
RPMI	RPMI medium 1640
S1P	Sphingosine-1-phosphate
SA	Slow acetylator
SDS	Lauryl sulphate
SHP-1	A host tyrosine phosphatase
SIM	Single ion monitoring
SK	Sphingosine kinase
SLCO	Solute carrier, Gene that encode for OATP
SNARE	Soluble N-ethylmaleimide attachment protein receptor
STF	Soluble tuberculosis factor
$T_{1/2}$	Half-life
TB	Tuberculosis
TGN	*Trans*-Golgi Network
Th	T-helper
TIC	Total ion currunt
TLR	Toll Like Receptor
Tmac	Time at which maximum concentration occurs
TNF	Tumour necrosis factor
TRAF6	TNF receptor associated factor
v/v	Volume for volume
w/v	Weight for volume
WHO	World Health Organisation

CHAPTER 1

General Introduction

1.1 Mycobacterium Tuberculosis 3

1.1.1 Tuberculosis pathogenesis 7

1.1.2 Phagocytosis and MTB recognition 9

1.1.3 Phagosome maturation 9

1.1.4 Innate immune response to MTB 19

1.1.5 Adaptive immune response to MTB 24

1.1.6 MTB gene expression in phagosomes and in dormancy 27

1.2 Anti-tuberculosis therapy 31

1.2.1 Isoniazid 32

1.2.2 Pyrazinamide 38

1.2.3 Rifampicin 42

1.2.4 Ethambutol 45

1.2.5 Anti-microbial activity of the anti-tuberculosis drugs *in vivo* 47

1.3 Active drug transporters 50

1.3.1 P-glycoprotein (P-gp) 51

1.3.2 Multidrug resistance associated protein (MRP) 53

1.3.3 Organic anion transport protein (OATP) 54

1.4 Aims of thesis 58

1.1 Mycobacterium Tuberculosis

Tuberculosis is a major world disease that is responsible for the killing of 2 to 3 million people per year (http://www.who.int). The incidence rate of tuberculosis infection is greatest in sub-Saharan Africa and Southeast Asia (which has the greatest number of cases) (Fig. 1.1). The natural history of tuberculosis shows that most people are able to mount a sufficiently effective immune response against the bacterium making them resistant. However, of those exposed to *Mycobacterium tuberculosis* (MTB), around 10% are unable to mount an initial immune defence and become infected. 90% or more of people that become infected by MTB do not develop active tuberculosis and their adaptive immune response is able drive MTB into a non-proliferating latent phase. The remaining 10% of people are unable to control MTB and develop active tuberculosis (North and Jung, 2004). Failure of the immune system, (commonly due to HIV infection) can lead to reactivation of latent MTB many years after initial contact with the bacilli (Fig. 1.2). Because of this, the incidence of tuberculosis in HIV patients is far greater, at around 10% per year compared to 10 % lifetime risk in non-immune compromised patients (Markowitz *et al.*, 1997). The synergy between HIV and TB infection can also be seen when considering at the rise in number of TB cases occurring in sub-Saharan Africa following the start of the HIV epidemic (Fig. 1.3)

MTB was identified as the bacterium that causes most cases of tuberculosis by Robert Koch in 1882. MTB is a slow-growing (generation time approximately 18 hr), aerobic, facultative intracellular pathogen that can infect and survive inside mononuclear phagocytes such as macrophages. MTB bacilli are known as "acid-fast bacilli" because of their lipid-rich cell walls which are relatively impermeable to

various basic dyes (such as gram's stains with crystal violet) unless the dyes are combined with phenol. Once stained (using carbol fuchsin stain), the cells resist decolourisation with acidified organic solvents and are therefore called "acid-fast".

MTB are gram positive bacteria with a highly hydrophobic cell wall which tends to make them clump together. On top of the peptidoglycan layer, MTB cell walls contain arabinogalactan (D-arabinose and D-galactose) that are linked to high-molecular weight mycolic acids. This arabinogalactan/ mycolic acid layer is further covered with a layer of polypeptides and mycolic acids consisting of free lipids, glycolipids, and peptidoglycolipids. The dominant presence of mycolic acids in the cell wall is unique to mycobacterium, and make up more than 50% of their dry weight. Further, MTB cell wall consists of other important glycolipids including mannose capped lipoarabinomannans (ManLAM), lipomannan (LM), phosphatidylinositol mannoside (PIM) (Fig 1.4).

The full genome of the laboratory MTB strain H37Rv has been sequenced and published (Cole *et al.*, 1998). The genome was shown to contain around 4000 genes, of which many are involved in lipogeneses and lipolysis.

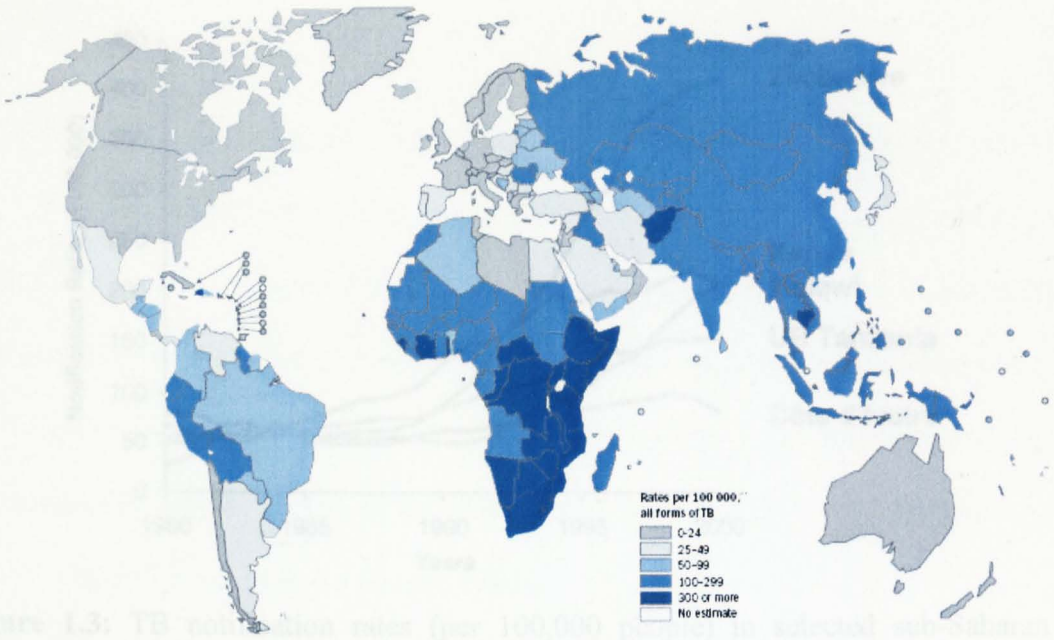

Figure 1.1: Estimated TB incidence rates, 2003 (taken from the WHO http://www.who.int)

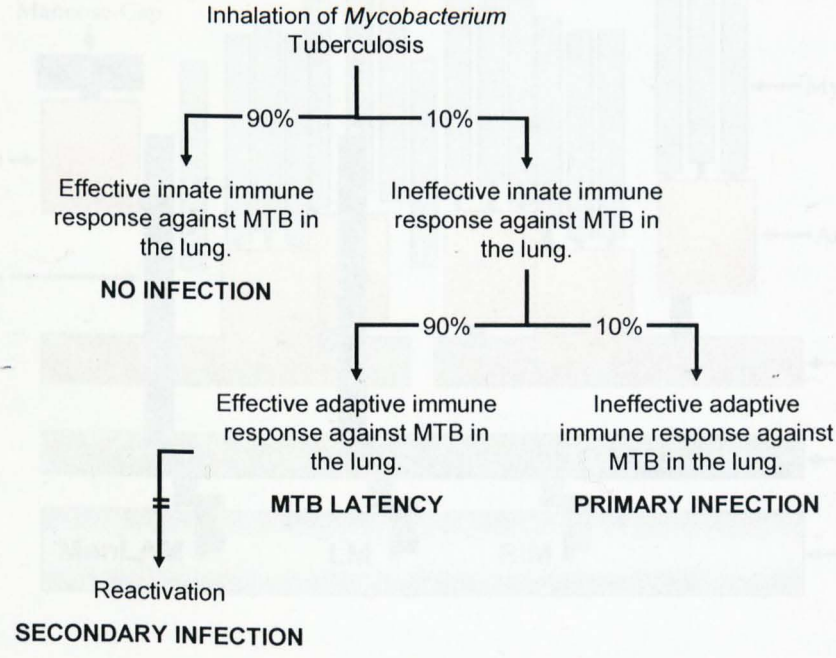

Figure 1.2: Chronological events following the inhalation of MTB. The majority of bacilli are killed by alveolar macrophages in the lung. Of those that survive only 10% are able to cause active tuberculosis while in the other 90% of cases the adaptive immune response drives the MTB into latency and prevents active tuberculosis. Months or years after the inhalation of tuberculosis, latent MTB can reactivate following the failing of the immune system.

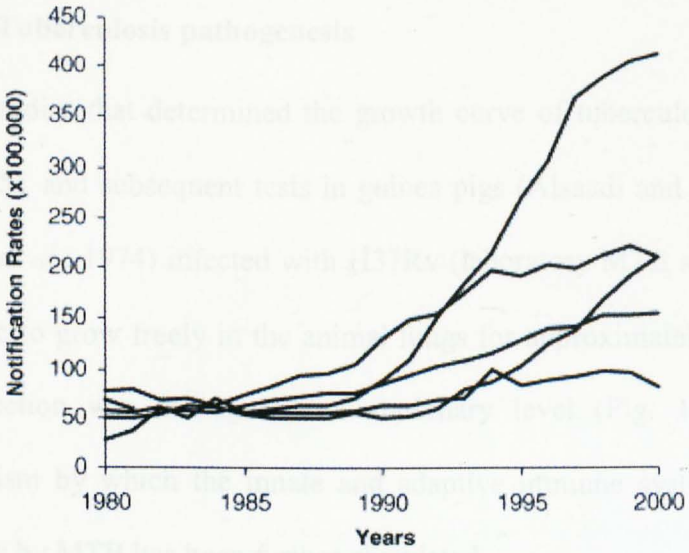

Figure 1.3: TB notification rates (per 100,000 people) in selected sub-Saharan African countries from 1980 to 2000. Largely due to the HIV epidemic, notifications have doubled or tripled in this period. Figure taken from Raviglione (2003).

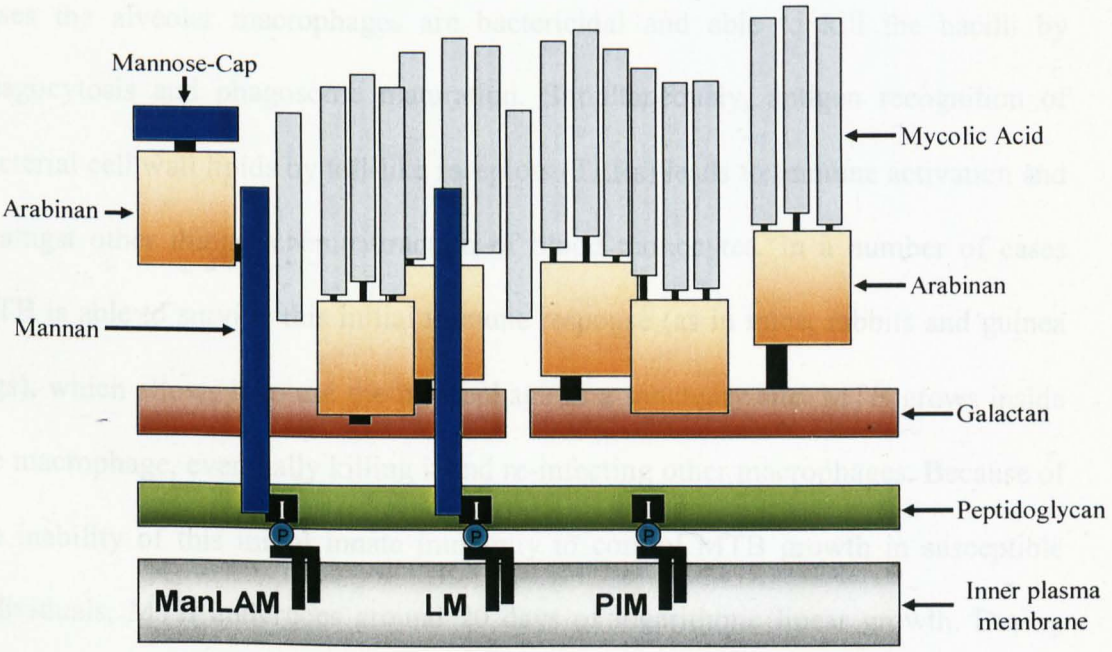

Figure 1.4: Model of mycobacterium cell wall components, containing mannose capped lipoarabinomannans (ManLAM), lipomannan (LM), phosphatidylinositol mannoside (PIM) and mycolic acids. Modified from (Chatterjee and Khoo, 1998).

1.1.1 Tuberculosis pathogenesis

Initial studies that determined the growth curve of tuberculosis in rabbits (Lurie *et al.*, 1955), and subsequent tests in guinea pigs (Alsaadi and Smith, 1973) and mice (Schell *et al.*, 1974) infected with H37Rv (laboratory MTB strain), found that MTB was able to grow freely in the animal lungs for approximately 3 weeks, after which the infection was managed at a stationary level (Fig. 1.5). Subsequently, the mechanism by which the innate and adaptive immune system responds following infection by MTB has been further elucidated.

The process of infection by MTB can be described in a number of steps. Firstly MTB inhaled into the lungs encounter alveolar macrophages (first line of defence). In most cases the alveolar macrophages are bactericidal and able to kill the bacilli by phagocytosis and phagosome maturation. Simultaneously, antigen recognition of bacterial cell wall lipids by toll-like receptors (TLRs) leads to immune activation and amongst other things, chemoattraction of blood monocytes. In a number of cases MTB is able to survive this initial immune response (as in mice, rabbits and guinea pigs), which allows it to use the macrophage as a sanctuary site. MTB grows inside the macrophage, eventually killing it and re-infecting other macrophages. Because of the inability of this initial innate immunity to control MTB growth in susceptible individuals, MTB undergoes around 20 days of logarithmic linear growth. During this 2-3 week period of MTB growth, adaptive T-cell immunity develops, which leads to activation of macrophages which in most cases stifles MTB growth. As a consequence MTB becomes stationary or dormant, allowing it to survive in the host. Under later failing of the host immune system (up to many years after the primary

infection), dormant bacilli are able to reactivate and cause a secondary tuberculosis infection.

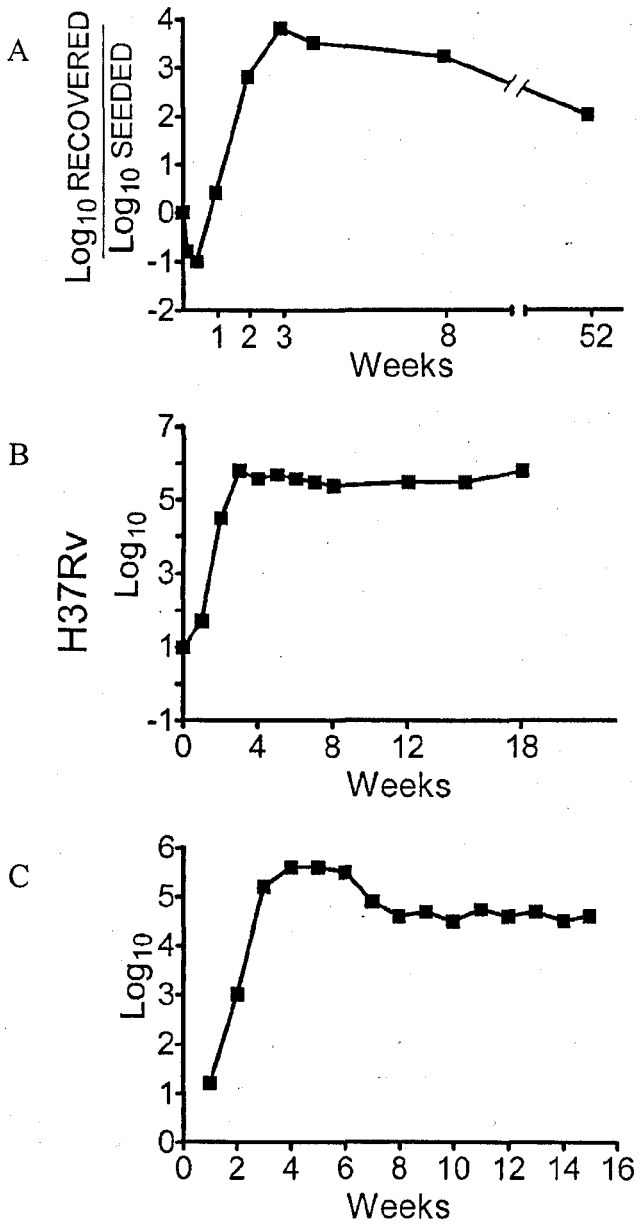

Figure 1.5: The pattern of MTB growth in the lungs of H37Rv infected (A) rabbits (Lurie *et al.*, 1955) (B) guinea pig (Alsaadi and Smith, 1973) and (C) mice (Schell *et al.*, 1974). In all case, inhibition of MTB growth occurs around 3 weeks post-infection, after which MTB growth is stationary but is not resolved. Diagram taken from North and Jung (2004).

1.1.2 Phagocytosis and MTB recognition

The first line of defence in multi-cellular organisms to microbial pathogens is the innate immune system. Macrophages play a key role as 'professional phagocytes' in this innate immune defence by engulfing the microbes into sub-cellular vacuoles named phagosomes by phagocytosis. Phagocytosis of microbes is a receptor mediated process that requires macrophage recognition of non-opsonic ligands on the microbial surface or of complement-opsonised microbes (Vieira *et al.*, 2002). In non-opsonic mediated phagocytosis of MTB, individual and/or multiple macrophage surface receptors (CR3, CD14, TLR and mannose receptor) are able to recognise bacterial lipopolysaccharides such as LAM and PIM as well as microbial antigen 85C (Ag85C) (Vieira *et al.*, 2002; Velasco-Velazquez *et al.*, 2003). MTB complement-opsonised mediated phagocytosis involves opsonisation of the bacilli with C3b and iC3b (Velasco-Velazquez *et al.*, 2003), which in turn interacts with complement receptors CR1, CR3 and CR4 on the host macrophage. Work by (Schlesinger *et al.*, 1990) showed that in this process CR3 is the main complement receptor involved, mediating approximately 80% of phagocytosis. Further, MTB opsonised with IgG antibodies can also be recognised and phagocytosis by macrophages through the Fcγ receptor IIIB (FcγRIIIB), however, by this mechanism, the resultant phagosomes undergo phagosome maturation which leads to the killing of MTB (Malik *et al.*, 2000; Vieira *et al.*, 2002).

1.1.3 Phagosome maturation

Following phagocytosis of microbes other than MTB, the phagosomes fuse with endocytic organelles (early endosomes, late endosomes and lysosomes) and organelles from the *trans*-Golgi network (TGN) to form phagolysosomes in a process

called phagosome maturation (Chua *et al.*, 2004). The formation of phagolysosomes leads to increased acidification and accumulation of degrading enzymes that consequently result in the killing of the microbe.

Pathogenic mycobacteria are however able to prevent the fusion of late endosomes and lysosomes to the phagosome (Armstrong and Hart, 1971; Armstrong and Hart, 1975; Russell, 2001; Mwandumba *et al.*, 2004). This ability to arrest phagosome maturation allows MTB to tolerate and survive within macrophages and use the nutrients provided by the host macrophage to grow and multiply. Numerous studies have been performed in recent years to elucidate the potential mechanisms that MTB utilises in order to arrest phagosome maturation.

During normal phagosome progression phagosomes accumulate markers from the different endosomal organelles, however phagosome progression of MTB is arrested between the phagosome recruitment of early endosomal markers (GTP-binding protein Rab5 and Transferrin receptors) and late endosomal markers (CD63, LAMP1, LAMP2 and GTP-binding protein Rab7)(Gomes *et al.*, 1999). The specific processes occurring between the recruitment of Rab5 and Rab7 that are different between phagocytosis of MTB and other microbes has been extensively studied so as to be able to pinpoint the mechanism by which MTB arrests phagosome progression.

Following the binding of opsonised microbes (other than mycobacteria) to the β subunit of CR3 (CD18), a number of signalling pathways are activated that cause the activation of tyrosine kinases (Hellberg *et al.*, 1996; Pettit and Hallett, 1996). Protein tyrosine kinases (PTK) in turn mediate the activation of sphingosine kinase (SK)

which then translocates from the cytosol onto the phagosome. SK then converts spingosine to sphingosine-1-phosphate (S1P) a bioactive lipid which in turn causes the release of intracellular stores of Ca2+ from the endoplasmic reticulum (ER)(Spiegel and Milstien, 2002; Malik *et al.*, 2003; Kusner, 2005)(Fig. 1.6). This increase in cytosolic calcium (c[Ca^{2+}]) is thought to trigger the generation of reactive oxygen species and play a vital role in phagosome maturation (Malik *et al.*, 2000; Malik *et al.*, 2001; Malik *et al.*, 2003; Kusner, 2005).

The proposed pathway through which an increase in c[Ca^{2+}] regulates the fusion of phagosomes with endocytic organelles (Fig. 1.7) is by binding to calmodulin (CaM). The calcium-calmodulin complex (Ca^{2+}-CaM) then activates calcium-calmodulin (Ca^{2+}-CaM) dependent protein kinase II (CaMKII) on the phagosome membrane. The activation of CaMKII leads to the recruitment of the Rab5 effector protein: type 3 phosphatidylinositol 3-kinase (PI3K: hVPS34 and a p150 subunit) to the phagosome membrane causing an increased production of phosphatidylinositol 3-phosphate (PI3P) from phosphatidylinositol (Christoforidis *et al.*, 1999; Vieira *et al.*, 2001; Vergne *et al.*, 2003). PI3P is a membrane trafficking regulatory lipid that is essential in the phagosome maturation (Fratti *et al.*, 2001).

PI3P functions as a ligand for proteins that contain FYVE domains (Itoh and Takenawa, 2002; Chua and Deretic, 2004). One of the proteins that contain this FYVE domain and which is recruited and strengthened by PI3P binding is another Rab5 effector protein: EEA1 (early endosomal autoantigen 1) (Simonsen *et al.*, 1998). EEA1 is a membrane tethering molecule that, in combination with Rab5 directly and specifically interacts with syntaxin-6 (Simonsen *et al.*, 1998; Simonsen

et al., 1999). Syntaxin-6 is a SNARE (Soluble N-ethylmaleimide attachment protein receptor) that is expressed on the endosomes derived from the TGN that traffic to the phagosomes. These TGN derived endosomes are responsible for the delivery of lysosomal components (lysosomal enzymes such as cathepsin D and the V_0H^+ATPase proton pump subunit) to the phagosome needed for phagosome acidification and microbe degradation (Malik *et al.*, 2000; Malik *et al.*, 2001; Fratti *et al.*, 2003b).

Complement opsonised MTB bacilli that are taken up through complement receptors importantly undergo arrested phagosome maturation between the acquisition of Rab5 and Rab7 leading to incomplete acidification and lack of mature lysosomal hydrolase (Ullrich *et al.*, 1999; Malik *et al.*, 2000; Malik *et al.*, 2001). Pivotal studies by (Malik *et al.*, 2000) demonstrated that phagocytosis of complement opsonised zymosan (fungal cell wall polysaccharide) induces a 4.6 fold increase in $c[Ca^{2+}]$ while there was no change in $c[Ca^{2+}]$ with complement opsonised MTB(Malik *et al.*, 2000). Further it was demonstrated that MTB only prevents a change in $c[Ca^{2+}]$ when it is phagocytosed through CR and is alive as ingestion of killed MTB and antibody opsonised MTB leads to a similar increase in $c[Ca^{2+}]$ as seen with complement opsonise zymosan. Antibody opsonised MTB (increase in $c[Ca^{2+}]$) show a 78% decreased chance of survival compared to complement opsonised MTB (no change in $c[Ca^{2+}]$) (Malik *et al.*, 2000). Phagosomal progression of antibody opsonised MTB could also be arrested artificially by decreasing $c[Ca^{2+}]$ with a Ca^{2+} chelator (Malik *et al.*, 2000; Malik *et al.*, 2001). These data suggests that the ability of MTB to prevent a change in $c[Ca^{2+}]$ is key in its ability to arrest phagosome maturation.

By preventing the increase in $c[Ca^{2+}]$, MTB is able to terminate the pathway described in Fig 1.7. The lack of $c[Ca^{2+}]$ leads to decreased formation of Ca^{2+}-CaM complexes and therefore CaMKII on the phagosomal membrane stays inactive. This leads to decreased recruitment of PI3K, a decrease in PI3P and a decreased recruitment and activation of EEA1. Overall this prevents the fusion of organelles formed in the TGN and therefore stops the delivery of lysosomal enzymes and proton pumps (cathepsin D and the V_0H^+ATPase proton pump subunit) needed for acidification and microbe degradation (Malik *et al.*, 2000; Fratti *et al.*, 2001; Malik *et al.*, 2001; Fratti *et al.*, 2003b; Vieira *et al.*, 2003; Kelley and Schorey, 2004).

ManLAM is a glycosylated MTB phosphatidylinositol found in the cell wall of MTB. Recent work has demonstrated that ManLAM is able to arrest phagosome maturation through the inhibition of PI3P dependent recruitment of EEA1 (Fig. 1.8) (Fratti *et al.*, 2003b; Vergne *et al.*, 2003). More specifically it was found that ManLAM coated beads were able to arrest phagosome maturation (Fratti *et al.*, 2003b) and that ManLAM from virulent MTB, but not avirulent MTB was able to block the increase in $c[Ca^{2+}]$ (Rojas *et al.*, 2000; Vergne *et al.*, 2003).

As mentioned above the increased in $c[Ca^{2+}]$ following phagocytosis of microbes is thought to be mediated through the activation of sphingosine kinase (SK) by protein tyrosine kinases (PTK) (Fig. 1.6). Following the phagocytosis of MTB, it has been demonstrated that sphinosine kinase is inhibited and thereby prevents the release of intracellular Ca^{2+} stores (Malik *et al.*, 2003). ManLAM has been shown to activate a host tyrosine phosphatase; SHP-1 following phagocytosis (Knutson *et al.*, 1998). It has been hypothesised by (Kusner, 2005) that SHP-1 may be responsible for the

depposphorylation and therefore inactivation of sphingokinase which in turn prevents the release of intracellular Ca^{2+} stores.

ManLAM has also been shown to have a secondary pathway by which it is able to prevent phagosome progression. As mentioned above, ManLAM causes increased activity of tyrosine phosphatase 1 (SHP-1), which in turn is able to activate p38 mitogen-activated protein kinase (p38-MAPK) (Knutson *et al.*, 1998). Activation of p38-MAPK leads to the phosphorylation and activation of Rab GDP dissociation inhibitor (GDI), a protein that either removes active Rab5 from the phagosome membrane (Cavalli *et al.*, 2001) or converts it to its inactive GDP form (Fratti *et al.*, 2003a). As a consequence, Rab5 is unable to bind EEA1 and recruit TGN derived organelles for acidification and lysosomal enzymes (Fratti *et al.*, 2003a; Chua *et al.*, 2004; Vergne *et al.*, 2004).

As we know, MTB is able to prevent the fusion of phagosomes with late endosomes and lysosomes, however this is not the case with early endosomes. Mycobacteria in phagosomes actually require the fusion of early endosomes in order to supply them with the essential nutrients; iron, transferrin and glycolipids (Clemens and Horwitz, 1996; Russell *et al.*, 1996; Schaible *et al.*, 2002; Kelley and Schorey, 2003; Vergne *et al.*, 2004). However, as described above, ManLAM inhibits fusion of early endosomes, a mechanism whereby MTB limits its own supply of iron. Recently however, it has been found that another phosphatidylinositol found in the cell wall of MTB; PIM specifically stimulates the fusion of early endosomes to phagosomes, thereby restoring the supply of iron to the mycobacterium (Vergne *et al.*, 2004). PIM stimulated early endosome fusion is ATP-, cytosol- and NSF (N-ethylmaleimide-

sensitive factor)-dependent (Vergne *et al.*, 2004) and requires Rabs in a neo-pathway independent of PI3P (Vergne *et al.*, 2003). PIM therefore provides MTB with a method of compensation for the LAM mediated inhibition of early endosome fusion.

PKnG is a MTB soluble protein kinase that closely resembles mammalian protein kinase C (PKCα). Interestingly PKnG is secreted by MTB into both the phagosome lumen as well as the macrophage cytosol. The importance of PKnG in phagosome maturation was identified when mycobacteria lacking the protein were unable to arrest phagosome maturation (Walburger *et al.*, 2004). However, the extent to which PKnG regulates and arrests phagosome maturation still needs to be elucidated.

Mycobacteria are very susceptible to nitric oxide (NO), which in macrophages is produced by inducible nitric oxide synthase (iNOS). Mice that lack functional iNOS die rapidly from mycobacterial infection (MacMicking *et al.*, 1997). However, MTB decreases NO production by preventing the proper localisation of iNOS to the phagosome, possibly by modifying the actin filament network (Guerin and de Chastellier, 2000; Miller *et al.*, 2004).

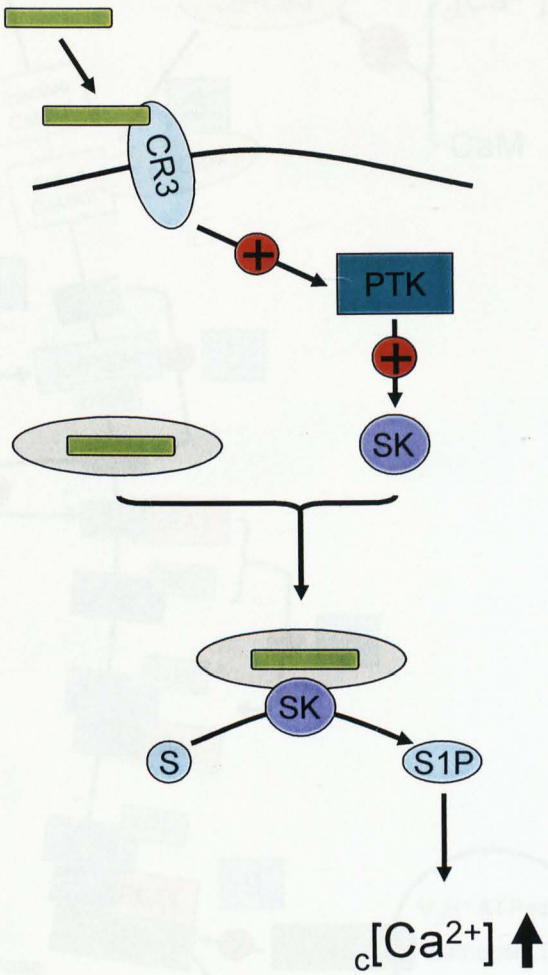

Figure 1.6: Diagrammatic representation of the pathway leading to increased cytosolic Ca^{2+} following phagocytosis of microbes other than pathogenic MTB. The binding of the microbe to complement receptor 3 (CR3) stimulates the activation of protein tyrosine kinases (PTK), which in turn activates sphingosine kinase (SK). SK then binds to the phagosome membrane and phosporylates sphingosine (S) to sphingosine-1-phosphate (S1P), which in turn causes the release of intracellular Ca^{2+} stores from the endoplasmic reticulum.

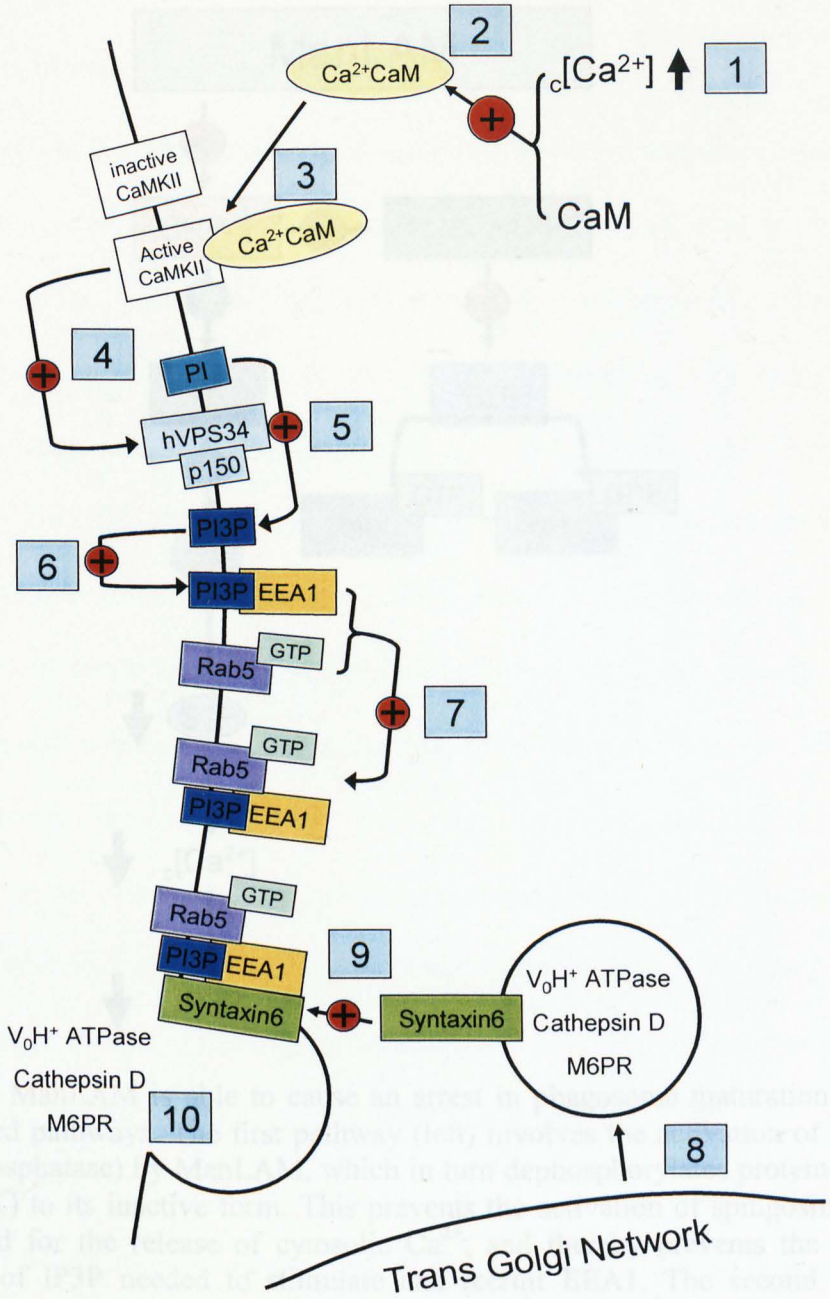

Figure 1.7: Diagrammatic representation of the proposed mechanism by which an increase in cytosolic [Ca^{2+}] modulates phagosome acidification and accumulation of lysosomal enzymes. An increase in c[Ca^{2+}] as a consequence of microbe phagocytosis (1) leads to an increase in Ca^{2+}CaM complex (2), which in turn results in the activation of CaMKII on the phagosome membrane (3). Ca^{2+}CaM recruits phosphatidylinositol 3-kinase (4) causing an increased production of phosphatidylinositol 3-phosphate (PI3P) from phosphatidylinositol (PI) (5). PI3P binds to EEA1 (6) which in turn binds to the active GTP form of Rab5 (7). The PI3P, EEA1 and Rab5 complex attracts TGN derived organelles (8) containing a specific SNARE (syntaxin6) to the phagosomal membrane (9). The fusion of the TGN organelle with the phagosome allows for release of V_oH^+ATPase, cathepsin D and Manose 6 protein receptor (M6PR) for the eventual acidification and lysosomal enzyme accumulation in the phagosome (10).

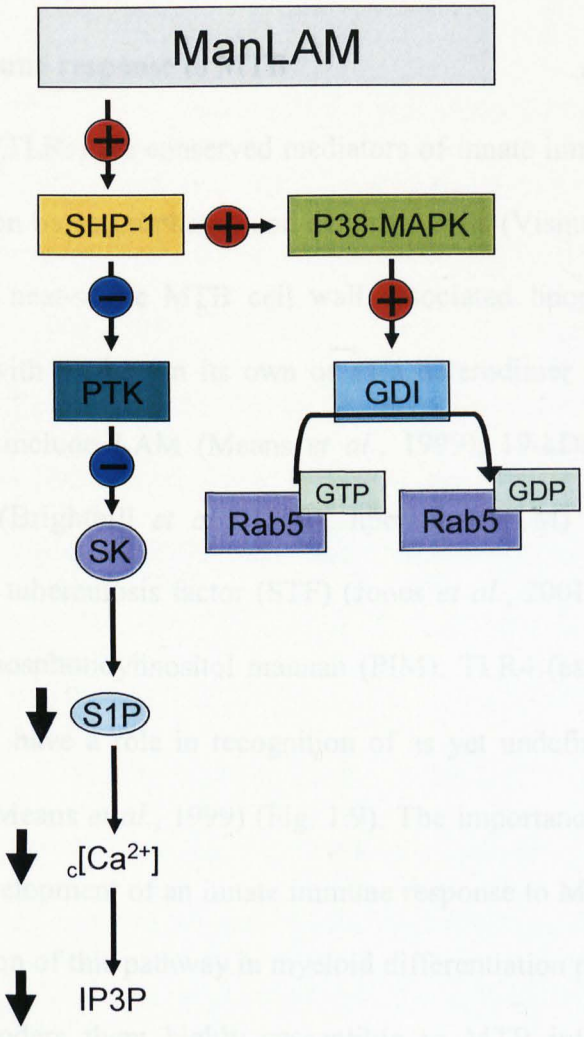

Figure 1.8: ManLAM is able to cause an arrest in phagosome maturation through two proposed pathways. The first pathway (left) involves the activation of SHP1 (a tyrosine phosphatase) by ManLAM, which in turn dephosphorylates protein tyrosine kinase (PTK) to its inactive form. This prevents the activation of spingosine kinase (SK) needed for the release of cytosolic Ca^{2+}, and thereby prevents the eventual production of IP3P needed to stimulate and recruit EEA1. The second pathway (right) involves SHP1 dephosphorylation and activation of P38-MAPK which phhosphorylates and activates Rab GTP dissociation inhibitor (GDI). Activation of GDI leads to the inactivation of Rab5-GTP to it inactive Rab5-GDP form. Both arms lead to decreased formation of the EEa1-Rab5 complex needed to recruit TGN derived organelles.

1.1.4 Innate immune response to MTB

Toll like receptors (TLRs) are conserved mediators of innate immunity essential for microbial recognition by macrophages and dendritic cells (Visintin *et al.*, 2001). A number of soluble heat-stable MTB cell wall associated lipoproteins have been shown to interact with TLR2 (on its own or as a heterodimer with TLR1/TLR6). These lipoproteins include LAM (Means *et al.*, 1999), 19-kDa MTB lipoprotein (secreted antigen) (Brightbill *et al.*, 1999), lipomanan (LM) (Quesniaux *et al.*, 2004b) and soluble tuberculosis factor (STF) (Jones *et al.*, 2001a), which has been found to contain phosphotidylinositol mannan (PIM). TLR4 (as a homodimer) has also been shown to have a role in recognition of as yet undefined heat labile cell associated factors (Means *et al.*, 1999) (Fig. 1.9). The importance of TLR mediated pathways in the development of an innate immune response to MTB is supported by the fact that inhibition of this pathway in myeloid differentiation protein 88 (MyD88) knock out mice renders them highly susceptible to MTB infection, despite the development of an adaptive immune response (Fremond *et al.*, 2004).

Activation of the innate immune system is initially mediated through recognition of the whole MTB bacilli rather than isolated and purified lipoproteins. Following infection of Chinese hamster ovary cells (CHO) transfected with the TLR2 or TLR4 (Means *et al.*, 1999), it was found that both virulent and attenuated bacilli use both TLRs. Work also showed that, even though some of the TLR interactions were mediated through MTB cell associated lipoproteins, with regard to whole MTB, they were independent of LAM.

Engagement of TLR2 or TLR4 by MTB, leads to activation of the cytoplasmic domain of TLRs that is homologous with the signalling domain of interleukin-1 receptors (IL-1R). IL-1R activation in turn leads to sequential activation of adaptor proteins: myeloid differentiation protein 88 (MyD88) and IL-1R associated kinase (IRAK) (Oddo *et al.*, 1998). IRAK is a serine kinase that activates TRAF6 (tumour necrosis factor [TNF] receptor associated factor) which in turn activates transcription factors such as NFκB (Oddo *et al.*, 1998; Heldwein and Fenton, 2002; van Crevel *et al.*, 2002; Krutzik and Modlin, 2004; North and Jung, 2004; Quesniaux *et al.*, 2004a) (Fig. 1.9).

The overall result of TLR2 engagement is to induce a predominantly pro-inflammatory response through the production of TNF and IL-12. Work using macrophages derived from TLR2 and TLR4 deficient mice showed that both receptors are responsible for the production of TNF and IL12 following contact with mycobacteria (Fremond *et al.*, 2003). Further, inhibition of the MyD88 which connects all TLR with IRAK (Fig 1.9) was able to inhibit TNF production (Quesniaux *et al.*, 2004a).

TNF has been shown to have a key role in macrophage activation and the formation of granulomas. TNF-α has been shown to be present at the site of infection in patients suffering from tuberculosis (Barnes *et al.*, 1993). Further, knock out mice lacking the ability to produce TNFα, showed increased susceptibility to MTB (Bean *et al.*, 1999). Overproduction of TNF-α during tuberculosis infection can however also be detrimental as it has been shown to be associated with fever and wasting (Cooper *et al.*, 1997). Further, IL-12 (pro-inflammatory cytokine) is critical in innate

immune protection as IL-12 knock out mice are highly susceptible to MTB infection (Cooper *et al.*, 1997).

Recently it has been shown that TLR2 engagement can also lead to the production of anti-inflammatory cytokines (Drennan *et al.*, 2004; Jang *et al.*, 2004). The main anti-inflammatory cytokine involved is IL-10 which is capable of antagonising the production of TNF-α, interferon-γ (INFγ) and IL-12 (Gong *et al.*, 1996; Fulton *et al.*, 1998; Hirsch *et al.*, 1999). The production of IL-10 has been shown to interfere with the protective immune response caused by pro-inflammatory cytokines. Indeed, IL-10 overexpressing transgenic mice show an increased bacterial burden, whilst IL-10 deficient mice have a decreased burden. It therefore seems that IL-10 production is detrimental to the innate immune system; however it may act to limit collateral damage caused by pro-inflammatory cytokines (Salgame, 2005).

TLRs have also been linked with induction of apoptosis through TLR2. Macrophages infected with MTB have been shown to have an increased rate of apoptosis, largely mediated by membrane bound or secreted 19 kDa lipoprotein through TLR2s (Lopez *et al.*, 2003). Apoptosis of macrophages has been shown to reduce mycobacterial viability and may be an important step in controlling MTB infection (Lopez *et al.*, 2003).

As well as TLR there are a host of other pattern recognition receptors (PRR) that play a role in the activation of immune cells through the recognition of mycobacterial components (Quesniaux *et al.*, 2004a). It is most likely that a combination of the

numerous TLRs and PRRs are responsible for signal transduction following MTB binding.

In the case of pathogenic MTB, activation of the innate immune response is insufficient to kill the intracellular pathogen. (Reed *et al.*, 2004) demonstrated that the degree of MTB virulence is also related to the cellular wall composition of specific MTB strains. Hypervirulent strains of MTB: HN878, and W-Beijing strains 210 and W4 were found to express a highly biologically active lipid species, a polyketide synthase- derived phenolic glycolipid (PGL). The presence of PGL led to a decrease in both the innate immune response (decrease in pro-inflammatory cytokines) and the adaptive immune response (decreased Th-1 T-cell response; see section 1.1.5). Loss or lack of PGL increased production of pro-inflammatory cytokine production and decreased the virulence of the MTB strain (Reed *et al.*, 2004). Expression of PGL may therefore contribute to the ability of MTB to evade the immune response.

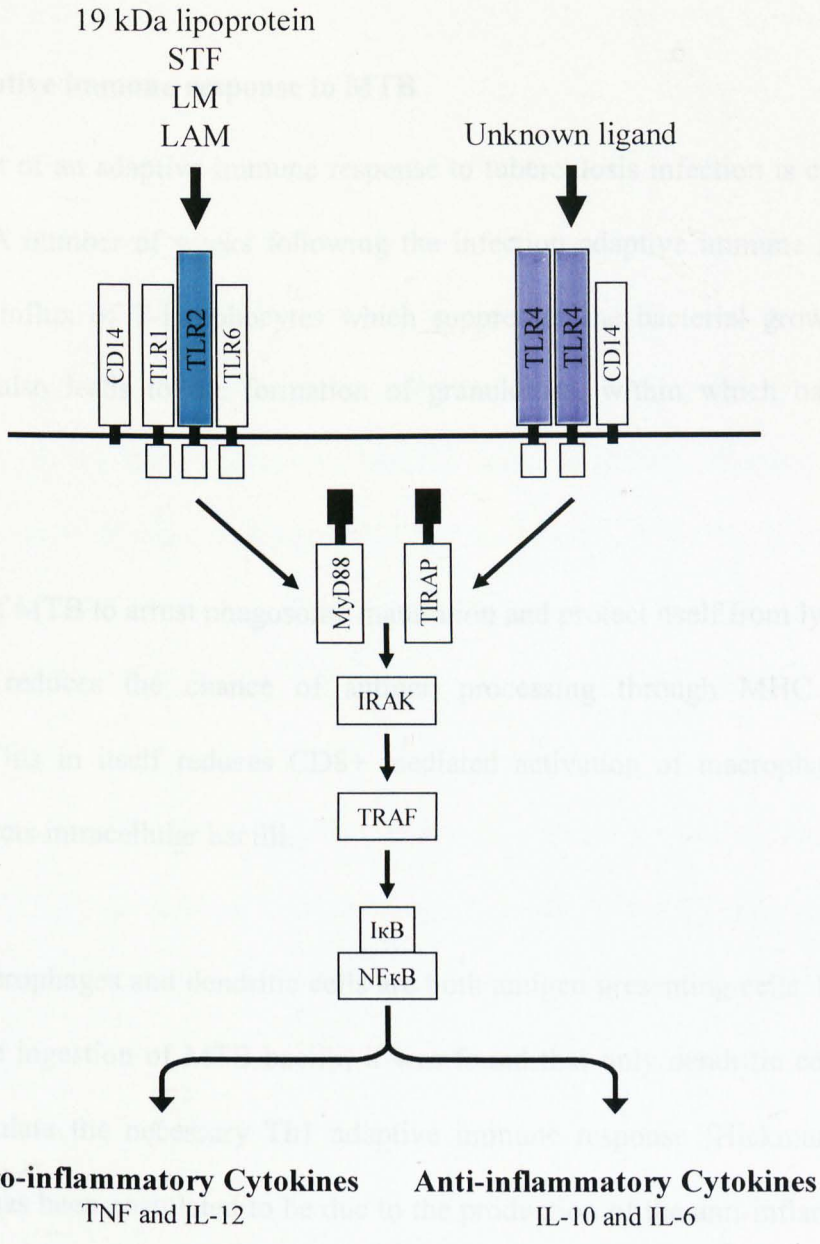

Figure 1.9: Taken and modified from (Quesniaux *et al.*, 2004a). Binding of MTB ligands to TLR2 (alone or in combination with TLR1/6) can lead to the induction of both pro- and anti-inflammatory cytokines that mediate the activation of macrophages during the innate immune response. TLR signalling is mediated through adaptators such as MyD88, IRAK, TRAF and transcription factor NFκB. It is thought that in the case of MTB, ligand binding to TLR4 leads to signal mediation through TIRAP (Tir domain containing adaptor protein) instead of MyD88. The balance between the induction of pro- and anti-inflammatory cytokines may influence the pathogenesis of MTB.

1.1.5 Adaptive immune response to MTB

Development of an adaptive immune response to tuberculosis infection is critical in its control. A number of weeks following the infection adaptive immune response leads to an influx of T-lymphocytes which suppresses the bacterial growth. Cell recruitment also leads to the formation of granulomas, within which bacilli are contained.

The ability of MTB to arrest phagosome maturation and protect itself from lysosomal degradation reduces the chance of antigen processing through MHC class I molecules. This in itself reduces CD8+ mediated activation of macrophages and thereby protects intracellular bacilli.

Alveolar macrophages and dendritic cells are both antigen presenting cells, however following the ingestion of MTB bacilli, it was found that only dendritic cells were able to stimulate the necessary Th1 adaptive immune response (Hickman *et al.*, 2002). This has been postulated to be due to the production of the anti-inflammatory cytokine; IL10, by infected macrophages but not dendritic cells (Hickman *et al.*, 2002). IL10, which is also secreted into the pleural fluid and alveolar lavage fluid (Barnes *et al.*, 1993; Gerosa *et al.*, 1999), results in dampening of the adaptive immune response in the lung, and thereby prevents antigen presenting cells from maturing. The ability of dendritic cells to leave the site of infection and travel to lymphoid tissue allows them to mature and release cytokines that strongly polarise T-cells towards a Th1 phenotype (Hickman *et al.*, 2002).

In mice, 1 week post MTB infection the number of CD4+ and CD8+ T-cells dramatically increases in the lymph nodes (Feng *et al.*, 1999). 2 to 4 weeks following the initial infection the CD4+ and CD8+ T-cells migrate into the lungs and interact with antigen presenting cells. This results in the production of pro-inflammatory cytokines (IFNγ and TNFα) that activate the macrophages. This leads to the induction of NOS2 (nitric oxide synthase) and the production of reactive nitrogen intermediates (Denis, 1991; Chan *et al.*, 1992; Roach *et al.*, 1993). Reactive nitrogen intermediates such as nitric oxide are able to kill intracellular MTB or control its growth both *in vivo* (Chan *et al.*, 1995; MacMicking *et al.*, 1997) and *in vitro* (Chan *et al.*, 1992; Roach *et al.*, 1993).

IFNγ release by T cells and natural killer cells during infection was found to be very important in MTB control in mice and humans. Mice without the IFNγ receptor were found to be very susceptible to mycobacterium infections (Huang *et al.*, 1993). This was also seen in children with a complete deficiency of IFNγ receptor (Jouanguy *et al.*, 1997).

CD4+ T-cells are critical in controlling MTB infection, as has been shown in mice with depleted or disrupted CD4+ T-cells (Muller *et al.*, 1987; Caruso *et al.*, 1999). The role of CD4+ T-cells is further demonstrated in patients with HIV infection, where the depletion of CD4+ T-cells is linked with increased susceptibility to acute and reactivated tuberculosis infection (Selwyn *et al.*, 1989). The function of CD4+ T-cells in controlling MTB infection is further demonstrated by CD4 knockout mice and MHC class II knockout mice that have greatly decreased IFNγ production following infection (Caruso *et al.*, 1999). Further, CD4 knockout mice show a

marked delay in the production of NOS2, needed for the production of bactericidal nitric oxide (Caruso *et al.*, 1999).

TLR have been found to play a part in the adaptive as well as the innate immune response to MTB infection. The role of TLR occupation in the adaptive immune response was proposed as MyD88 knock out mice (MyD88 is central to TLR mediated NF-κB activation, Fig. 1.9) are unable to stimulate a Th1 response against MTB infection (Schnare *et al.*, 2001). Further work shows that stimulation of TLR2 by 19 kDa lipoprotein reduces synthesis of MHC class II molecules and thereby limits antigen presentation by infected macrophages (Noss *et al.*, 2000; Noss *et al.*, 2001; Gehring *et al.*, 2003).

As well as activating infected macrophages to kill or control intracellular MTB bacilli, the adaptive immune response is responsible for preventing the spread of MTB and localising the inflammation and damage to the lungs by the formation of granulomas. Human tuberculosis granulomas are formed by the chemoattraction of epitheloid macrophages, dendritic cells, T-cells, B-cells and fibroblasts (Co *et al.*, 2004) around infected macrophages. By surrounding the MTB infection with leukocytes, the granuloma prevents the spread of MTB to other macrophages. The chemokines thought to be involved include IL-8, MCP-1 (monocyte chemoattractant protein) and RANTES (Lu *et al.*, 1998; van Crevel *et al.*, 2002; Raja, 2004).

Despite the elaborate adaptive immune response to MTB, activation of infected macrophages and formation of granulomas are unable to fully eradicate infection.

Instead a number of bacilli are able to adapt by switching to an asymptomatic latent state, which can reactivate if and when the host becomes immuno-compromised.

People who fail to control MTB and go on to have active tuberculosis have been linked with T-cell under-responsiveness (Hirsch *et al.*, 1999). Further, granuloma wall components in patients with active tuberculosis present a diffuse pattern of proliferating cells suggesting inadequate cell communication (Ulrichs *et al.*, 2005). An insufficient number of CD4+ T-cells in HIV infected patients prevents the adaptive immune system from effectively controlling MTB bacilli within granulomas, and thereby allows the reactivation of TB.

1.1.6 MTB gene expression in phagosomes and in dormancy

As an innate mechanism of survival, MTB is able to adapt its gene expression profile in reaction to changes in its environment. The ability of MTB to react to and compensate for host mediated challenges has been a hot topic in recent years. Numerous studies have tried to determine the changes in gene expression that allow MTB to survive both the innate and adaptive immune response.

In response to phagocytosis of MTB by naïve and INFγ activated macrophages, the expression of approximately 15 % of the MTB open reading frames were found to be altered (454 genes induced, 147 genes repressed). 68 of these genes were identified to be differentially expressed in the IFNγ activated compared to the naïve macrophages (suggesting that ~11 of the genes were controlled through IFNγ) (Schnappinger *et al.*, 2003). These changes were found to compensate for the hostile environment of the phagosome.

Due to the decrease in oxygen tension and availability of carbohydrates inside phagosomes, MTB undergoes metabolic adaptations from aerobic to anaerobic respiration. Changes in MTB respiration were first noted when it was observed that an enzyme needed for the metabolism of citrate (isocitrate lyase) was induced in persistently MTB infected mice (McKinney *et al.*, 2000). This induction was also found to be necessary for MTB survival in IFNγ activated macrophages, but not necessarily in naïve macrophages (McKinney *et al.*, 2000). Later it was found that the expression of all genes necessary for β-oxidation of fatty acids by MTB were also induced by MTB inside activated macrophages (Schnappinger *et al.*, 2003) (Fig.1.10). By being able to utilise fatty acids (also abundant in the necrotic centre of granulomas) as a source of energy, MTB is able to survive the phagosomal environment (Honer Zu Bentrup *et al.*, 1999; McKinney *et al.*, 2000; Schnappinger *et al.*, 2003).

The reduced concentrations of iron (essential MTB nutrient) in phagosomes lead to increased production and secretion of iron scavenging sideophores by MTB. This increase is seen in MTB inside naïve macrophages, and even more prominently in activated macrophages where IFNγ causes strong induction of low iron response genes (Schnappinger *et al.*, 2003).

The main bactericidal molecules produced by macrophages are reactive oxygen and nitrogen intermediates such as nitric oxide. Macrophage production of nitric oxide is greatly increased following the macrophage activation by IFNγ (adaptive immune response). As a reaction, MTB induces the expression of the alkyl hydroperoxide

reductase antioxidant genes; *ahpC* and *ahpD* (Schnappinger *et al.*, 2003) and *noxR1* (Ehrt *et al.*, 1997) to protect itself from reactive oxygen and nitrogen intermediates. High nitric oxide concentrations also induce expression of genes for the stabilisation and repair of the MTB cell wall and chromosomes (Schnappinger *et al.*, 2003).

MTB inside naïve macrophages are still proliferating but have increased fatty acid and decreased carbohydrate metabolism compared to extracellular bacilli. Further, genes for iron scavenging, antioxidant proteins and those for the reparation of the cell wall and DNA are induced. Following the activation of macrophages through IFNγ and nitric oxide, MTB often becomes non-replicating (dormant) and increases its iron scavenging and dependency on fatty acid metabolism (McKinney and Gomez, 2003; Schnappinger *et al.*, 2003) (Fig. 1.11).

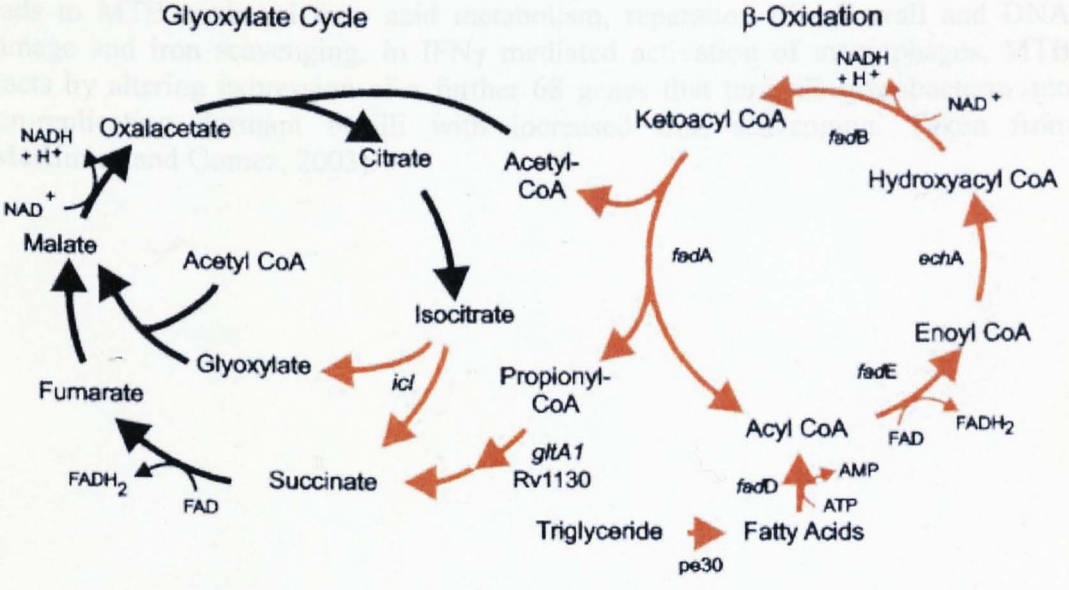

Figure 1.10: Phagocytosis of MTB by activated macrophages leads to the induction of all the MTB genes needed for the β-oxidation of fatty acids (induction indicated by red arrows). Further, phagocytosis also leads to the induction of isocitrate lyase (icl) which allows MTB to metabolise isocitrate in the glycolate cycle. These changes allow MTB to survive within the low carbohydrate, low oxygen environment of phagosomes and granumulomas. Taken from (Schnappinger *et al.*, 2003).

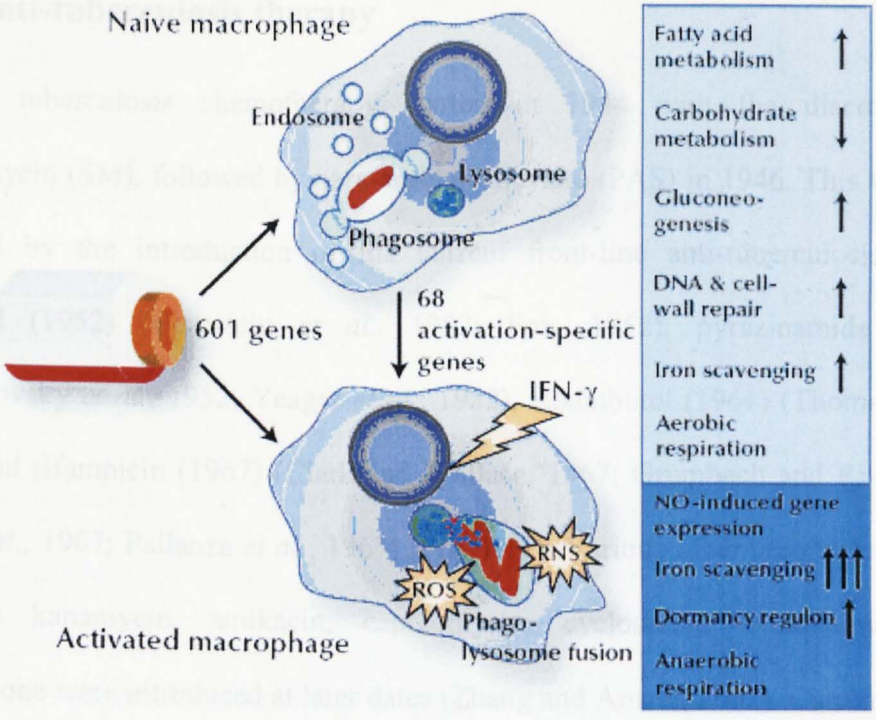

Figure 1.11: Phagocytosis of MTB by naïve and activated macrophages leads to changes in the expression of approximately 601 genes. In naïve macrophages this leads to MTB mediated fatty acid metabolism, reparation of cell wall and DNA damage and iron scavenging. In IFNγ mediated activation of macrophages, MTB reacts by altering expression of a further 68 genes that turn the mycobacteria into non-replicating dormant bacilli with increased iron scavenging. Taken from (McKinney and Gomez, 2003).

1.2 Anti-tuberculosis therapy

Modern tuberculosis chemotherapy started in 1944 with the discovery of streptomycin (SM), followed by para-amino-salicylate (PAS) in 1946. This was then followed by the introduction of the current front-line anti-tuberculosis drugs; isoniazid (1952) (Bernstein *et al.*, 1952; Fox, 1952), pyrazinamide (1952) (Solotorovsky *et al.*, 1952; Yeager *et al.*, 1952), ethambutol (1961) (Thomas *et al.*, 1961) and rifampicin (1967) (Clark and Wallace, 1967; Grumbach and Rist, 1967; Nitti *et al.*, 1967; Pallanza *et al.*, 1967) (Fig. 1.12). Various other second line drugs such as kanamycin, amikacin, capreomycin, cycloserine, ethionamide and thiacetazone were introduced at later dates (Zhang and Amzel, 2002). Current 'short-course' tuberculosis therapy consists of 2 months of isoniazid, rifampicin, pyrazinamide and often ethambutol, followed by 4 months of isoniazid and rifampicin.

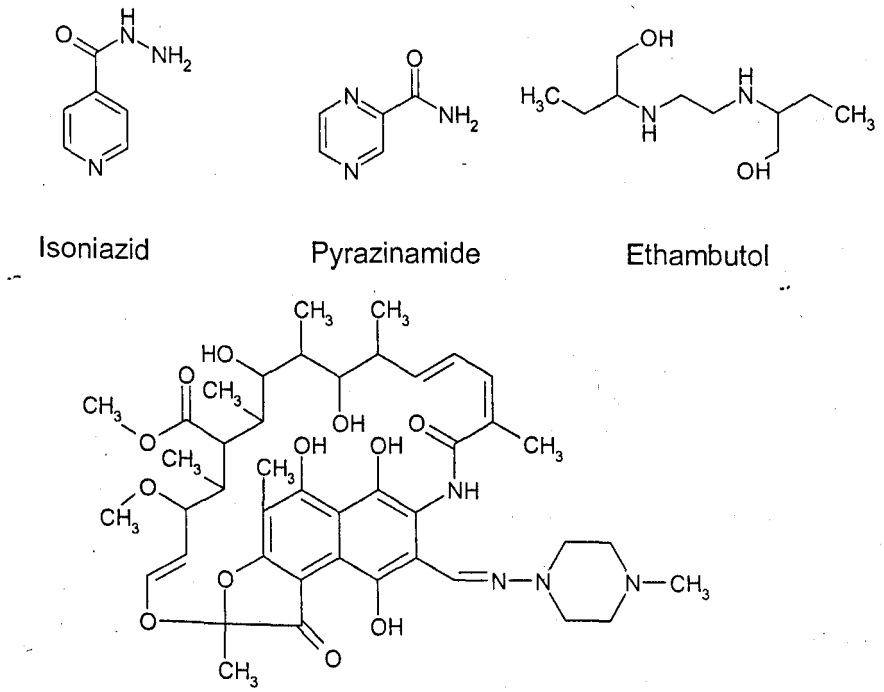

Figure 1.12: Structures of the first line anti-tuberculosis drugs.

1.2.1 Isoniazid

Isoniazid is highly bactericidal drug against actively growing bacilli and bacteriostatic for non-dividing MTB. Isoniazid (a structural analogue of nicotinamide) is a small hydrophilic compound that is thought to enter MTB through porins in the mycobacterial cell wall (Lambert, 2002). Recent work has also implied the role of an active efflux protein in the accumulation of isoniazid (Choudhuri *et al.*, 1999; Viveiros *et al.*, 2002; De Rossi *et al.*, 2006). Progress has been made in elucidating the mechanism by which isoniazid is bactericidal; however the exact mechanism is as yet unknown.

Isoniazid is a pro-drug, activated to its active metabolite through the mycobacterial enzyme KatG, a hemoprotein possessing catalase-peroxidase, Mn^{2+} dependent peroxidise, cytochrome P450-like oxygenase and peroxygenitritase activity (Zhang *et al.*, 1992; Wengenack *et al.*, 2000). Mutations in KatG have been shown to be responsible for the bulk (approximately 50%) of isoniazid resistant MTB strains (Zhang *et al.*, 1992; Ramaswamy and Musser, 1998). By purifiying KatG from MTB, a number of stable KatG mediated isoniazid metabolites have been identified which include isonicotinic acid, isonicotinamide and pyridine-4-carboxyaldehyde (Johnsson and Schultz, 1994). However, none of these stable metabolites themselves are bactericidal, and it is likely that reactive intermediate species such as isonicotinic acyl radicals and anions generate the bacteriocidal activity (Shoeb *et al.*, 1985; Rozwarski *et al.*, 1998) (Fig. 1.13).

In vitro, isoniazid is particularly effective at inhibiting the synthesis of mycolic acid needed for the MTB cell wall (Takayama *et al.*, 1972) (Fig. 1.4). Mycolic acid

synthesis in MTB is mediated through a number of proteins including an enoyl-acyl carrier protein reductase (InhA), an acyl carrier protein (AcpM) and a β-ketoacyl-ACP synthase (KasA) (Slayden and Barry, 2000; Slayden *et al.*, 2000; Somoskovi *et al.*, 2001). Mutations in these proteins (InhA, AcpM and KasA) have been shown to mediate low level isoniazid resistance and are therefore hypothesised as target proteins for the isoniazid active metabolites (Zhang and Amzel, 2002).

One of the proposed mechanisms by which isoniazid is able to inhibit InhA and therefore mycolic acid synthesis is by covalently binding to the nicotinamide ring of NAD(H) (beta-nicotinamide adenine dinucleotide) (Rozwarski *et al.*, 1998; Nguyen *et al.*, 2001). Here it is proposed that isonicotinic acyl radicals (reactive intermediate of isoniazid metabolism by KatG) covalently bind to NAD• radicals to form isonicotinic acyl NADH (Fig 1.13). InhA is a vital protein that catalyses the reduction of 2-*trans*-enoyl-acyl carrier protein which is vital in fatty acid biosynthesis and is NADH dependent. Isonicotinic acyl NADH is thought to inhibit InhA activity and thereby inhibit mycolic acid synthesis.

An alternative theory on isoniazid activity is the isonicotinic acid hypothesis (Thiemer-Kruger, 1958). In this theory, isoniazid is metabolised to it stable metabolite; isonicotinic acid, which at physiological pH remains in its ionic form. This leads to ion trapping and accumulation of isonicotinic acid in MTB. When the concentrations are high enough, isonicotinic acid competes with, and displaces nicotinic acid (NA) during the bacterial synthesis of NADH. This leads to the formation of the *meta*-isomer of NADH which inhibits InhA mediated fatty acid synthesis (Scior *et al.*, 2002)

Isoniazid taken on an empty stomach is well absorbed with peak plasma concentrations achieved 1-2 hours post dose. Protein binding is negligible and the volume of distribution is approximately equal to body weight. The rate of elimination of isoniazid is largely dependent on acetylator status (slow acelylator half life: 2-6.5 hr and fast acelylator half life: 0.5-2 hr). 95% of ingested isoniazid is excreted in the urine within 24hr mainly in the form of actylisoniazid and isonicotinic acid (Dollery, 1998). A summary of the pharmacokinetic parameters of isoniazid are given in Table 1.1 (Peloquin *et al.*, 1997).

Isoniazid metabolism is largely dependent on the interplay between N-acetyltransferase and aminohydrolase/amidase although CYP1A2 and CYP2E1 may also be involved (Sarich *et al.*, 1999). N-acetyltransferase converts isoniazid to acetylisoniazid, which in turn undergoes hydrolysis to isonicotinic acid and acetylhydrazine. Alternatively isoniazid can be directly hydrolysed to isonicotinic acid and hydrazine by amidohydrolase (Fig. 1.14). Further processing of hydrazine to acetylhydrazine by N-acetyltransferase (and *visa versa* by amidohydrolase), followed by the formation of diacetylhyrazine by N-acetyltransferase are also dependent on acetylator status (Fig. 1.14) (Sarich *et al.*, 1999).

The two main types of isoniazid related severe toxicity are peripheral neuropathy (which is the most common) and hepatotoxicity (which is the most dangerous). Peripheral neuropathy occurs most frequently in slow acetylators and is dependent on isoniazid exposure. It was found that isoniazid was able to react with and deplete pyridoxine (vitamin B_6), by forming a pyridoxyl-isoniazid schiff base. Pyridoxine

(vitamin B_6) is essential for the synthesis of the amino acid neurotransmitter γ-amino butyric acid (GABA) from glutamate, and depletion therefore results in peripheral neuropathy. To prevent this toxicity, isoniazid administration now requires co-administration with vitamin B_6 (Dollery, 1998).

The mechanism by which isoniazid mediated hepatotoxicity occurs is as yet unknown. 10 to 20 % of isoniazid receiving patients show a mild increase in liver enzymes (Mitchell *et al.*, 1975; Yu *et al.*, 2005), of which 1 to 2 % show severe liver toxicity. One of the possible mechanisms of toxicity is through the formation of hydrazine, a known hepatotoxin (Sarich *et al.*, 1996) (see Fig. 1.14) while others believe acetylhydrazine is responsible (Mitchell *et al.*, 1976).

Table 1.1: Previously published pharmacokinetic parameters of isoniazid in both fast (FA) and slow aceytlators (SA). Data from (Peloquin *et al.*, 1997) given as mean (range).

Cmax (μg/mL)	FA:	2.44 (1.04-2.96)
	SA:	3.64 (2.17-5.11)
Tmax (hr)	FA:	1.0 (0.5-1.0)
	SA:	1.0 (0.5-3.0)
$AUC_{0-\infty}$ (μg.hr/mL)	FA:	5.8 (3.0-7.0)
	SA:	17.3 (13.1-26.4)
Half life ($t_{1/2}$) (hr)	FA:	1.30 (1.10-1.78)
	SA:	2.81 (2.81-4.43)
Volume of distribution (L/kg)	FA:	1.10 (0.98-1.77)
	SA:	0.90 (0.78-1.25)
Clearance (L/hr)	FA:	42.7 (36.0-84.5)
	SA:	14.4 (9.5-19.1)

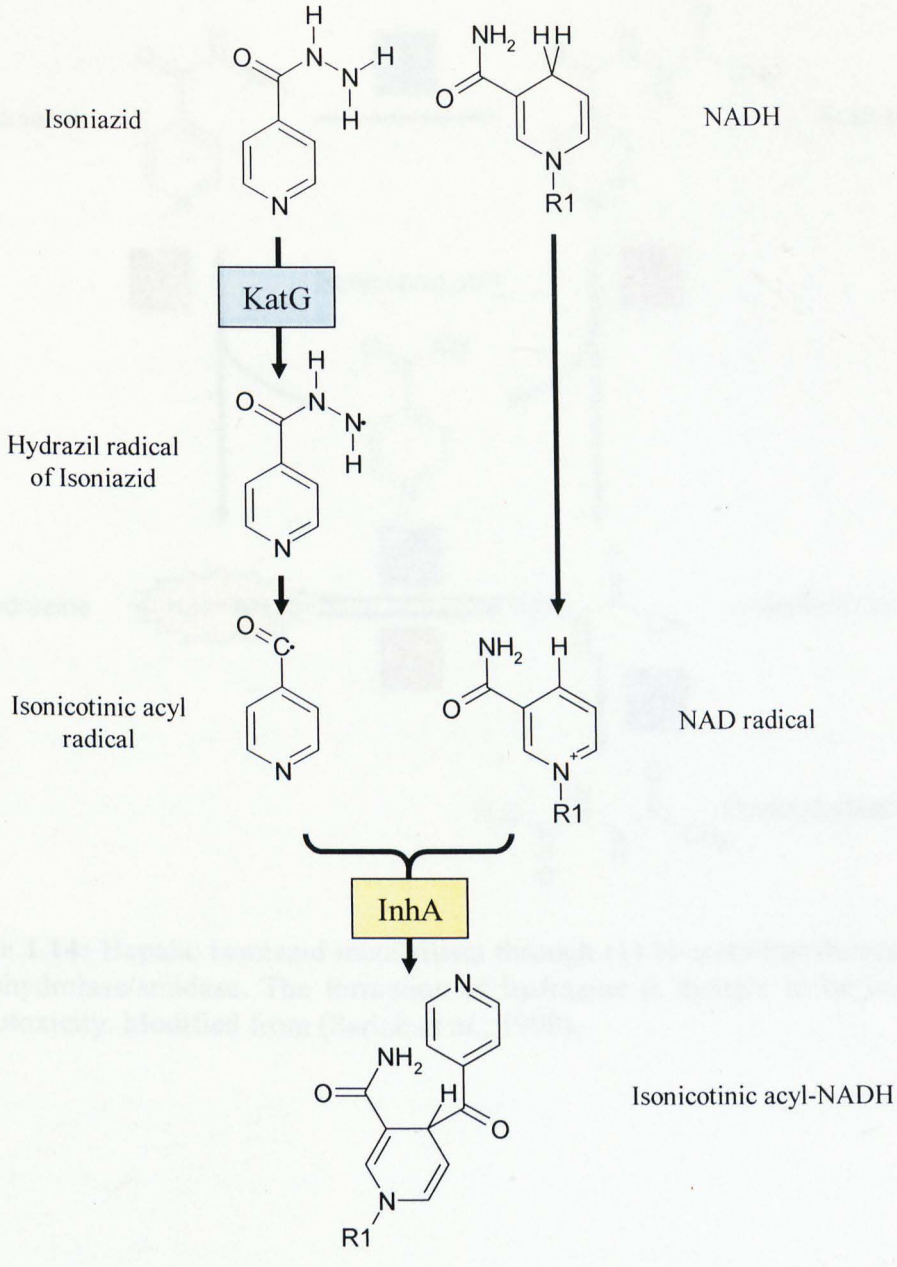

Figure 1.13: Proposed mechanism for the formation of isonicotinic acyl radicals and isonicotinic acyl-NADH as modified from (Scior *et al.*, 2002) and (Rozwarski *et al.*, 1998). MTB KatG catalyses the conversion of isoniazid into a hydrazil radical of isoniazid which in turn converts this to isonicotinic acyl radicals that are able to covalently bind to NAD radicals to form isonicotinic acyl-NADH, an inhibitor of InhA needed for fatty acid synthesis. .

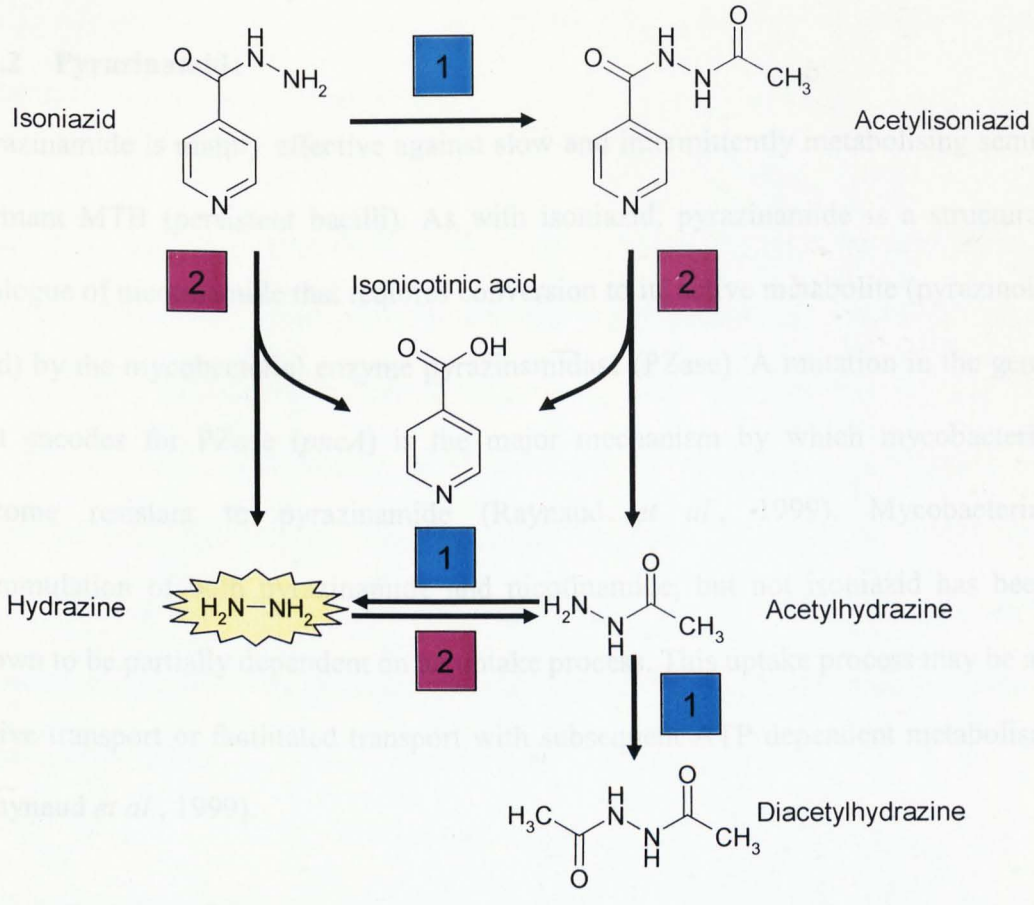

Figure 1.14: Hepatic isoniazid metabolism through (1) N-acetyltransferase and (2) amidohydrolase/amidase. The formation of hydrazine is thought to be linked with hepatotoxicity. Modified from (Sarich *et al.*, 1999).

1.2.2 Pyrazinamide

Pyrazinamide is mainly effective against slow and intermittently metabolising semi-dormant MTB (persistent bacilli). As with isoniazid, pyrazinamide is a structural analogue of nicotinamide that requires conversion to its active metabolite (pyrazinoic acid) by the mycobacterial enzyme pyrazinamidase (PZase). A mutation in the gene that encodes for PZase (*pncA*) is the major mechanism by which mycobacteria become resistant to pyrazinamide (Raynaud *et al.*, 1999). Mycobacterial accumulation of both pyrazinamide and nicotinamide, but not isoniazid has been shown to be partially dependent on an uptake process. This uptake process may be an active transport or facilitated transport with subsequent ATP dependent metabolism (Raynaud *et al.*, 1999).

Pyrazinamide is a paradoxical drug that shows good *in vivo* activity against tuberculosis (its introduction allowed TB therapy to shorten from 1 year to 6 months), however it shows no activity against MTB grown in standard culture conditions *in vitro* (Tarshis and Weed, 1953), unless acidic conditions are introduced (McDermott and Tompsett, 1954). The role of the acidic pH is most probably to facilitate the accumulation of pyrazinoic acid inside the bacilli (Zhang *et al.*, 1999; Zhang and Mitchison, 2003). It has been put forward by Zhang and colleagues (Zhang *et al.*, 1999; Zhang and Mitchison, 2003) that, pyrazinamide enters MTB through porins and is converted to pyrazinoic acid. Pyrazinoic acid in turn leaves the bacteria by passive diffusion or via a weak efflux pump. When the bacteria are in an acidic environment the pyrazinoic acid is uncharged and protonated which allows it to enter the bacteria. As the rate of influx of pyrazinoic acid in acidic conditions is greater than the rate of efflux, pyrazinoic acid accumulates within the bacilli (Fig.

1.15). Accumulation of pyrazinoic acid is thought to be vital in mediating the antimicrobial activity of pyrazinamide.

There are a number of postulated mechanisms of action of pyrazinoic acid. Firstly, the accumulation of protonated pyrazinoic acid brings protons into the bacilli which can eventually cause acidification of the cytosol. It has been hypothesised that this acidification leads to disruption of MTB membrane energetics by collapsing the membrane potential and affecting membrane transport (Zhang *et al.*, 2003). The ability to maintain a membrane potential is reduced when MTB become semi-dormant explaining why pyrazinamide is more effective against this population (Zhang *et al.*, 2003).

A second proposed hypothesis is that pyrazinoic acid inhibits fatty acid synthase I (FASI) of MTB (Zimhony *et al.*, 2000). FASI generates C_{16} from acetyl-CoA primers and can also elongate them to C_{24}/C_{26} fatty acids. It has been demonstrated that both pyrazinamide and pyrazinoic acid inhibit fatty acid synthesis of MTB in acidic conditions (pH 6) but not at pH 6.8, and that this occurs through the inhibition of FASI (Zimhony *et al.*, 2000).

In vivo the decrease in pH needed for pyrazinamide activity is thought to be created by either of two methods. Firstly, even though MTB inhibits phagosome maturation, a small decrease in phagosome pH still occurs due to binding of the early endosomes, which may be sufficient for pyrazinamide to function. Secondly, the acidic environment generated by early inflammation following MTB infection may allow pyrazinamide to function (Heifets *et al.*, 2000).

Following an oral dose of pyrazinamide, the drug is completely absorbed reaching peak concentrations 1 to 2 hours post dose. Pyrazinamide undergoes around 50 % protein binding and has a long plasma half-life (10-24 hr) (Dollery, 1998). 3 to 4 % of pyrazinamide is excreted unchanged in the urine, whilst 30 to 40 is metabolised to pyrazinoic acid by liver deaminase. Pyrazinoic acid is further metabolised to 5-hydroxypyrazinoic acid by xanthine oxidase (Yamamoto *et al.*, 1987) (Fig. 1.16). A summary of the pharmacokinetic parameters of pyrazinamide are given in Table 1.2 (Peloquin *et al.*, 1997).

Pyrazinamide is relatively non-toxic in terms of tuberculosis treatment. Pyrazinamide toxicity is dose dependent, and high doses (3 g daily) lead to hepatic disease in up to 15 % of patients, of whom 2 to 3 % develop jaundice and die because of hepatic necrosis.

Table 1.2: Previously published pharmacokinetic parameters of pyrazinamide. Data from (Peloquin *et al.*, 1997) given as mean (range).

Cmax (μg/mL)	28.8 (21.7-42.6)
Tmax (hr)	1.0 (0.5-2.0)
$AUC_{0-\infty}$ (μg.hr/mL)	396 (304-541)
Half life ($t_{1/2}$) (hr)	10.1 (8.1-12.9)
Volume of distribution (L/kg)	0.67 (0.60-0.93)
Clearance (L/hr)	3.78 (2.77-4.94)

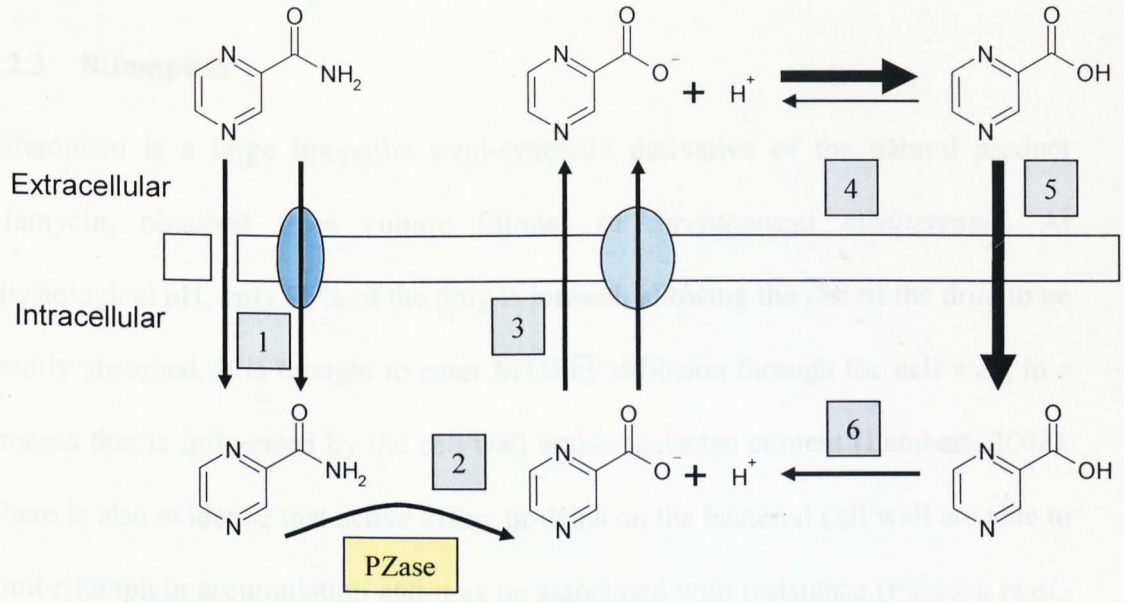

Figure 1.15: Pyrazinamide enters MTB bacilli through porins or possible active influx proteins (1). Deaminisation of pyrazinamide by pyrazinamindase (PZase) generates pyrazinoic acid, which with a pKa of 2.9 is mainly in its ionised form (2). Pyrazinoic acid leaves the bacteria by diffusion and a weak efflux pump to the extracellular environment. If the extracellular environment is acidic, pyrazinoic acid becomes protonated and therefore deionised (4) allowing it to enter back into the bacteria by diffusion (5). Once inside the bacteria, pyrazinoic acid ionises again, releasing protons into the MTB cytosol that are postulated to disrupt the membrane potential and trafficking. Further, because the rate of accumulation of pyrazinoic acid is greater than its efflux, its concentration builds up inside the bacteria which is postulated to inhibit FASI. Modified from (Zhang and Mitchison, 2003).

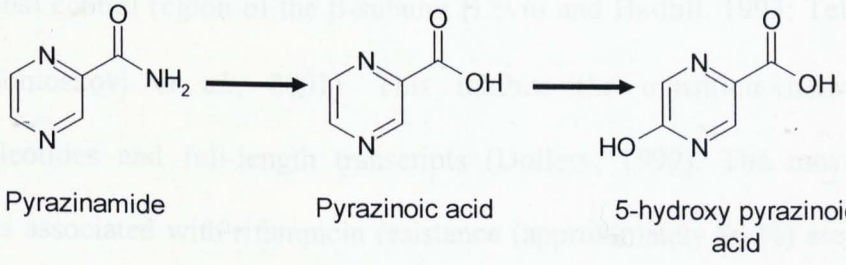

Figure 1.16: Hepatic pyrazinamide metabolism to pyrazinoic acid by deaminase, followed by oxidation by xanthine oxidase (Dollery, 1998).

1.2.3 Rifampicin

Rifampicin is a large lipophilic semi-synthetic derivative of the natural product rifamycin, obtained from culture filtrates of *Streptomyces mediterranei.* At physiological pH, only 25% of the drug is ionised, allowing the rest of the drug to be readily absorbed. It is thought to enter MTB by diffusion through the cell wall, in a process that is influenced by the cell wall arabinogalactan content (Lambert, 2002). There is also evidence that active efflux proteins on the bacterial cell wall are able to limit rifampicin accumulation and may be associated with resistance (Piddock *et al.*, 2000; Siddiqi *et al.*, 2004; De Rossi *et al.*, 2006).

Rifampicin is one of the essential drugs in modern chemotherapy, with resistance to it being a main reason for treatment failure and fatality (Mitchison and Nunn, 1986). Rifampicin is active against both actively growing and semi-dormant susceptible MTB bacilli. At low concentrations rifampicin acts as an inhibitor of bacterial DNA dependent RNA polymerase (encoded by the *rpoB* gene) by targeting an 81 base pair (27 codons) central region of the β-subunit (Levin and Hatfull, 1993; Telenti *et al.*, 1993; Somoskovi *et al.*, 2001). This inhibits the transition between short oligonucleotides and full-length transcripts (Dollery, 1999). The most common mutations associated with rifampicin resistance (approximately 96 %) are those that occur in this 81 bp region of rpoB.

Following an oral dose of rifampicin on an empty stomach, peak drug concentrations are achieved 2 to 4 hours post dose. Rifampicin protein binding is approximately 80 % and the volume of distribution is 1.1 L/kg. Around 85% of rifampicin is metabolised by the liver microsomal enzymes to its main and active metabolite,

desacetylrifampicin (Fig 1.17). Both rifampicin and desacetylrifampicin are partially excreted into bile, although only rifampicin can be reabsorbed by entero-hepatic recycling. Approximately 40 to 60% of an oral dose is excreted in the faeces (Dollery, 1998). A summary of the pharmacokinetic parameters of rifampicin are given in Table 1.3 (Peloquin *et al.*, 1997).

Rifampicin is not highly toxic on its own, however its ability to induce hepatic enzymes including CYP3A4 mediates a large potential for toxicity due to drug interactions (Girling, 1977). Otherwise rifampicin toxicity has been linked with rifampicin hypersensitivity which leads to symptoms including fever, rash, flu-like syndrome, acute renal failure, hemolytic anemia, thrombocytopenia, and anaphylactic events (Martinez *et al.*, 1999).

Table 1.3: Previously published pharmacokinetic parameters of rifampicin. Data from (Peloquin *et al.*, 1997) given as mean (range).

Cmax (μg/mL)	11.8 (9.7-25.0)
Tmax (hr)	1.5 (1.0-3.0)
$AUC_{0-\infty}$ (μg.hr/mL)	70.6 (47.4-142.7)
Half life ($t_{1/2}$) (hr)	3.33 (2.27-5.55)
Volume of distribution (L/kg)	0.49 (0.33-0.74)
Clearance (L/hr)	8.5 (4.2-12.7)

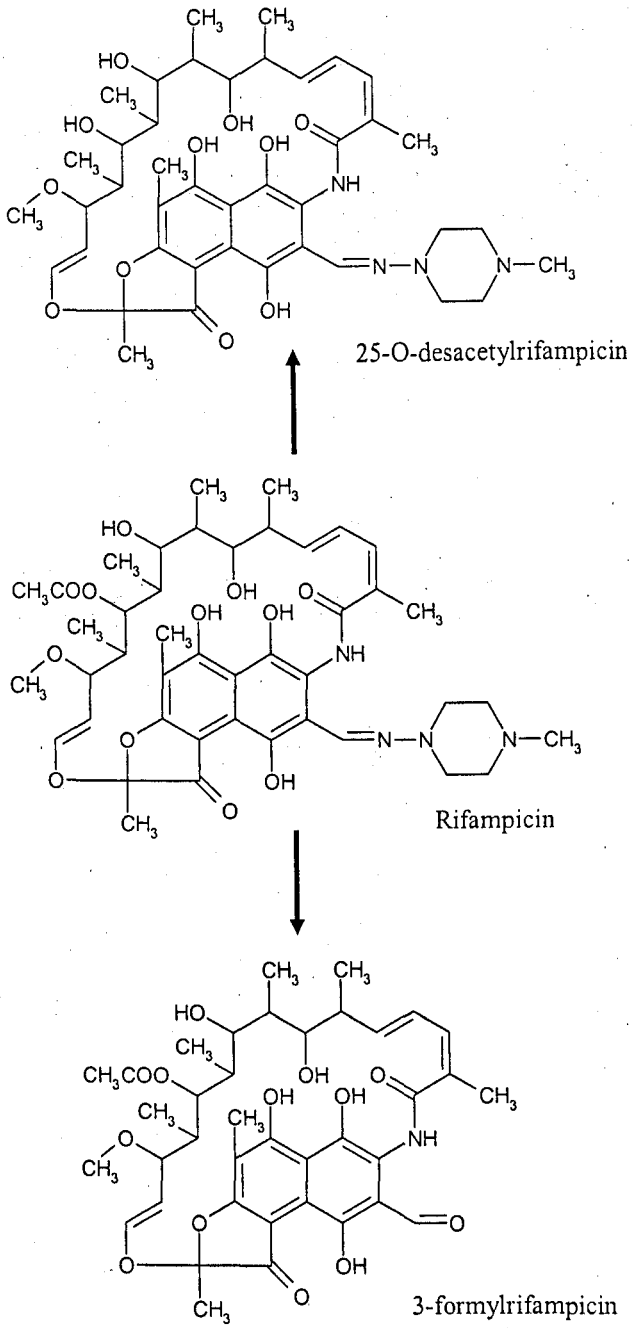

Figure 1.17: Hepatic rifampicin metabolism. Rifampicin is metabolised to 25-O-desacetylrifampicin by liver microsmal enzymes. In urine rifampicin can also spontaneously form formylrifampicin (Dollery, 1998).

1.2.4 Ethambutol

Ethambutol is a small hydrophilic compound that, similarly to isoniazid is thought to enter MTB through porins, although some evidence of active uptake exists (Lambert, 2002). It is the active S,S enantiomer of ethambutol that is bacteristatic to virtually all strains of actively growing mycobacteria including MTB.

Although the mechanism of action is not fully understood, ethambutol was shown to inhibit the synthesis of arabinogalactan (Takayama and Kilburn, 1989) with secondary effects on lipoarabingalactan (Deng *et al.*, 1995) and mycolic acids (Mikusova *et al.*, 1995), essential lipids in the MTB cell wall (Fig. 1.4). Later work shows that treatment of mycobacteria (*M. smegmatis*) with ethambutol leads to the build up of deca-prenyl-P-arabinose (Wolucka *et al.*, 1994) suggesting that ethambutol targets an arabinosyl transferase. By analysing the mutations associated with resistance to ethambutol, changes in *embB* (translates into a putative arabinosyl-transferase) were associated with 70 % of resistant strains (Sreevatsan *et al.*, 1997; Telenti *et al.*, 1997).

Following oral dosing of ethambutol, approximately 80 % is absorbed, with the remaining 20 % excreted in the faeces. Ethambutol concentrations peak 2 to 4 hr post dose and the elimination half life is 10 to 15 hr. Plasma protein binding is 10 to 40 % with a volume of distribution of around 3.9 L/kg (Dollery, 1998). Ethambutol has been found to accumulate in lung tissue (alveolar cells) (Conte *et al.*, 2001). Most of the ethambutol dose absorbed is excreted unchanged in the urine, while a small amount (approximately 15%) is metabolised by alcohol and aldehyde dehydrogenase to 2,2' (ethylenediamino)-dibutyric acid (EDBA) (Fig. 1.18) (Dollery, 1998).

The main toxicity observed with ethambutol is ocular toxicity (optic neuropathy) which occurs in <5% of patients taking the recommended daily dose (Leibold, 1966; Hadjikoutis *et al.*, 2005). Both ethambutol and EDBA are zinc chelators and it has been suggested that a decrease in intracellular or extracellular zinc levels plays a role in ocular toxicity (Campbell and Elmes, 1975). Further, allergic rashes and gastrointestinal disturbances have been reported in around 0.5% of patients (Dollery, 1998).

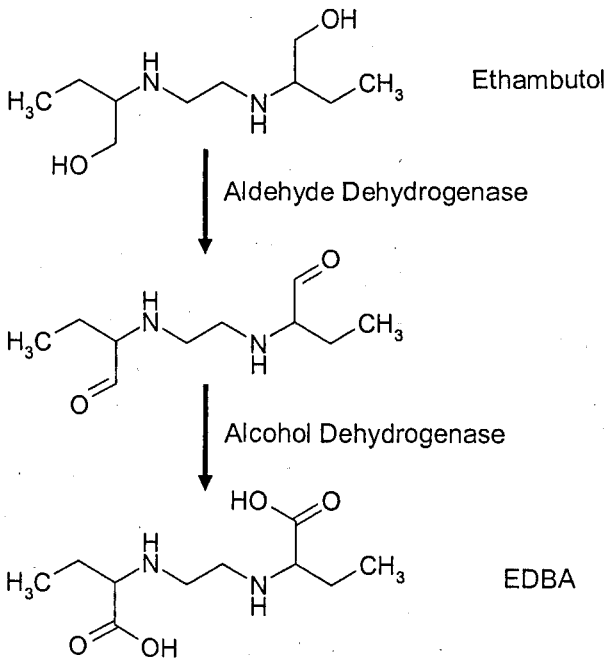

Figure 1.18: Ethambutol hepatic metabolism. Around 15% of ethambutol is metabolised to 2,2' (ethylenediamino)-dibutyric acid (EDBA) by alcohol and aldehyde dehydrogenase (Dollery, 1998).

1.2.5 Anti-microbial activity of the anti-tuberculosis drugs *in vivo*

Tuberculosis bacilli residing in susceptible patients exist in different distinct populations ('mixed population') that are differentially susceptible to the diverse anti-tuberculosis drugs used. Further, MTB bacilli are known to be present in extracellular space, inside macrophages and inside granulomas or cavities.

When looking at the rate of mycobacterial kill (drop in cfu/mL) over time in tuberculosis patients receiving rifampicin, isoniazid, pyrazinamide and ethambutol, it can be seen that there are two distinct pharmacodynamic phases. The first phase; known as early bactericidal activity (EBA), consists of a rapid decline in bacterial load over a period of 2 days. Following the first few days of therapy, mycobacteria killing declines at a slower rate during what is termed the 'sterilising phase'. The origin of the two phases is thought to be different drugs acting on different bacteria of the mixed population present in man (Mitchison, 2000; Jindani *et al.*, 2003).

Data suggests that the main drug responsible for bactericidal activity in the EBA phase is isoniazid (INH > EMB > RIF > PYR) (Mitchison, 2000; Jindani *et al.*, 2003). Interestingly, when given in combination, rifampicin, ethambutol, pyrazinamide and isoniazid did not enhance the EBA compared to isoniazid on its own (Fig. 1.19) (Jindani *et al.*, 1980).

In the second, sterilising phase, the overall rate of killing of tuberculosis decreases. This change in bactericidal activity is largely due to the decrease in bactericidal activity mediated through isoniazid (Mitchison, 2000; Jindani *et al.*, 2003). Isoniazid is thought to mainly target and kill rapidly growing extracellular bacilli during EBA.

The subsequent decrease of this MTB population therefore decrease isoniazid mediated killing. The other anti-bacterial drugs are thought to have a more general activity against both extracellular and intracellular bacteria. This is observed in the sterilising phase, where rifampicin (which has the greatest bactericidal activity in the sterilising phase) ethambutol and pyrazinamide determine the overall bactericidal activity. The differential rate of MTB killing by isoniazid over time was well demonstrated by (Jindani *et al.*, 2003) (Fig. 1.20). These data also show the constant activity of rifampicin and other drugs over the first 2 weeks of treatment.

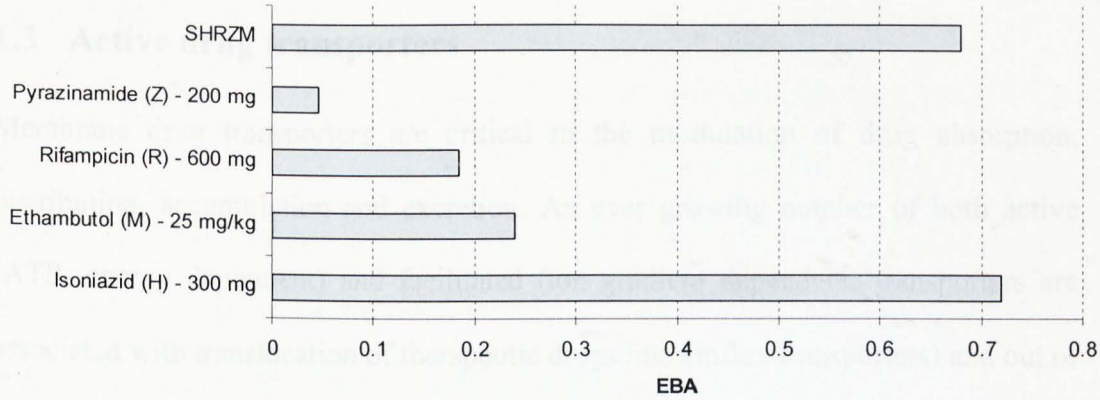

Figure 1.19: The early bactericidal (EBA) activity of various anti–tuberculosis drugs given alone or in combination, over the first two days of treatment in patients. Data from (Jindani *et al.*, 1980). S = streptomycin, H = isoniazid, R = rifampicin, Z = Pyrazinamide, M = ethambutol.

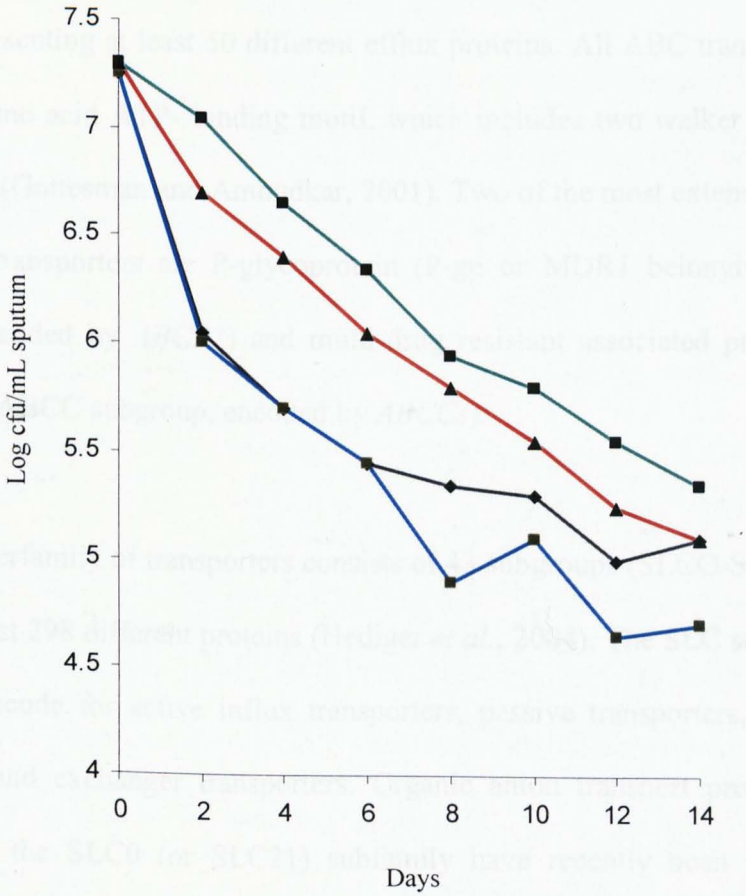

Figure 1.20: The rate at which bacterial load decreases in patients on isoniazid (—), rifampicin (—), isoniazid and rifampicin (—) and other drugs (—). Data taken from (Jindani *et al.*, 2003).

1.3 Active drug transporters

Membrane drug transporters are critical in the modulation of drug absorption, distribution, accumulation and excretion. An ever growing number of both active (ATP- energy dependent) and facilitated (ion gradient dependent) transporters are associated with translocation of therapeutic drugs into (influx transporters) and out of cells (efflux transporters). Drug transporters have recently been classified into active efflux proteins; which belong to the ABC (ATP- Binding Cassette) family, and influx transporters; which belong to the SLC (Solute Carrier) family (Owen *et al.*, 2005).

The ABC superfamily of drug efflux transporters contains seven subgroups (ABCA-ABCG) representing at least 50 different efflux proteins. All ABC transporters have a 90-110 amino acid ATP- binding motif, which includes two walker motifs and a linker region (Gottesman and Ambudkar, 2001). Two of the most extensively studied drug efflux transporters are P-glycoprotein (P-gp or MDR1 belonging to ABCB subgroup, encoded by *ABCB1*) and multi-drug resistant associated protein (MRPs belonging to ABCC subgroup, encoded by *ABCCs*).

The SLC superfamily of transporters consists of 43 subgroups (SLCO-SLC43) which include at least 298 different proteins (Hediger *et al.*, 2004). The SLC series includes genes that encode for active influx transporters, passive transporters, ion coupled transporters and exchanger transporters. Organic anion transport protein (OATP) belonging to the SLC0 (or SLC21) subfamily have recently been shown to be involved in broad spectrum active influx of xenobiotics.

1.3.1 P-glycoprotein (P-gp)

The most intensely studied of the drug transporters is P-glycoprotein (P-gp), which was first discovered for altering the efficacy of anti-cancer therapy by decreasing cellular accumulation (Juliano and Ling, 1976). P-gp is a 170 kDa membrane associated active efflux protein encoded by *ABCB1* (a.k.a. *MDR1*). It is 1280 amino acids long, comprising of two homologous halves linked by a 60 amino acid long linker protein (Chen *et al.*, 1986). Each half consists of 6 trans-membrane domains and a hydrophilic domain between them and at the carboxyl end, responsible for ATP binding (nucleotide binding domain; NBD) (See Fig 1.21).

In the presence of ATP, P-gp is able to translocate a broad spectrum of compounds to the extracellular fluid (amongst these are anticancer, immunosuppressive, antibiotic and antiretroviral drugs) (Borst *et al.*, 1993; Gottesman and Pastan, 1993). The method of translocation is uncertain, but it has been hypothesized that either drug is removed from the cytosol to the extracellular fluid through a pore in the transporter, or the transporter acts as a 'flipase', moving the drug from the inner leaflet of the membrane to the outer leaflet (Johnstone *et al.*, 2000).

As well as mediating the transport of anti-cancer drugs, P-gp has been found to translocate a wide diversity of compounds including calcium channel blockers, peptides, steroids, anti-histamines, and anti-retrovirals (Endicott and Ling, 1989; Gottesman and Pastan, 1993; Jones *et al.*, 2001c). Most molecules found to be substrates for P-gp are large, amphiphathic and aromatic compounds, though this is not always the case. With respect to anti-tuberculosis drugs there is some evidence

from work in mice, that rifampicin may be a substrate for P-gp (Schuetz *et al.*, 1996). No data are however available on the other first choice anti-tuberculosis drugs.

P-gp has a wide tissue distribution including both epithelial (liver, lung, intestine, brain etc.) (Johnstone *et al.*, 2000; Tan *et al.*, 2000) and non-epithelial cells such as lymphocytes (Lucia *et al.*, 1997). On epithelial cells, P-gp is always polarised to the apical membrane, so that it pumps drugs back into the intestine (decreasing absorption), into the bile (increasing biliary excretion) and back into the blood in the blood brain barrier (decreasing brain distribution) (See Fig. 1.22).

The potential impact of P-gp on drug pharmacokinetics is nicely demonstrated in mice where *mdr1a* (-/-) mice showed both a increase in drug (anti-HIV protease inhibitors) bioavailability and brain penetration compared to the wild-type *mdr1a* (+/+) mice (Kim *et al.*, 1998). Furthermore, cytochrome P450 3A4 (a major drug metabolising enzyme) and active efflux pumps show overlapping substrate specificity and may even work synergistically (to optimise the detoxification of drugs in cells whilst avoiding the saturation of the enzyme) (Benet *et al.*, 1999).

P-gp expression has been associated with a genetic polymorphism in exon 26 of *MDR1* (C3435T), correlating to an altered expression and function of P-gp levels in the intestine (Hoffmeyer *et al.*, 2000). The frequency of this mutation appears to show inter-ethnic variability, with a greater proportion of Caucasians carrying the mutant T allele compared to African populations where this mutation is relatively rare (Ameyaw *et al.*, 2001; Schaeffeler *et al.*, 2001). This may be relevant to

pharmacotharapy, due to widespread infection of MTB in Africa. Many other polymorphisms have been identified, although there impact is as yet unclear.

1.3.2 Multidrug resistance associated protein (MRP)

Multi-drug resistance associated proteins 1 (MRP1 encoded by ABCC1) is an active efflux protein that was first identified in doxorubicin selected multi-drug resistant cells that did not express P-gp (Cole *et al.*, 1992). MRP1 is a 190 kDa membrane protein consisting of 1531 amino acids and sharing 15% homology with P-gp (Huai-Yun *et al.*, 1998). Now, at least 12 MRP transporters (ABCC family) have been identified of which the most extensively studied are MRP1 to MRP5.

MRPs transport organic anions and neutral drug conjugated to acidic ligands such as glutathione and glucuronate (Borst *et al.*, 2000). MRP1-3 can also cause resistance to non-conjugated neutral organic drugs. MRP1-3 contains 17 trans-membrane domains, whilst MRP4 and 5 contain 12 trans-membrane domains (Fig. 1.21). As with P-gp, MRP transporters distribution is widespread with expression in both epithelial membranes and non-epithelial cells. On epithelial cells MRPs are polarized, either being expressed on the apical side like P-gp (MRP2, 4 and 5) or on the basolateral side (MRP1 and 3) (Fig. 1.22). MRP1 has been found to be expressed in the lung, kidney, intestine, liver as well as lymphocytes (Jones *et al.*, 2001b).

Rifampicin is an inducer of MRP2, 3 and 5, but not MRP1 (Fromm *et al.*, 2000; Schrenk *et al.*, 2001). There are however no data available on whether rifampicin or any of the other anti-tuberculosis drugs are substrates for any of the MRPs.

1.3.3 Organic anion transport protein (OATP)

Organic anion transport polypeptides (OATP) are active influx transporters that belong to the SLCO (old gene symbol SLC21) subfamily. The first member of the OATP family was identified in Rat (Oatp1) (Jacquemin *et al.*, 1994) and the SLCO subgroup now constitutes at least 11 members (Hediger *et al.*, 2004) in humans (Table 1.4).

OATPs are polarized to the basolateral membrane (Fig. 1.22) and have been shown to contain 12 transmembrane domains (Fig. 1.21). Originally OATPs were thought to only transport organic anions however, as with efflux transporters, OATPs are now known to transport a large number of endogenous and xenobiotic compounds including cationic, neutral, zwitterionic as well as anionic compounds (Kim, 2003). The fact that many OATPs share substrates with apical efflux transporters, suggests that they act synergistically to transport drugs across a membrane.

OATPs have a wide tissue distribution and are expressed in similar tissues to the ABC transporters; intestine, liver, kidney, lung and blood brain barrier. A comprehensive study of the distribution of some OATPs also shows the expression of OATP4A1 on lymphocytes (Tamai *et al.*, 2000), however the expression on other non-epithelial cell such as macrophages has as yet not been studied.

With respect to anti-tuberculosis drugs, rifampicin has been shown to be a substrate for both OATP1B1 and 1B3 (Vavricka *et al.*, 2002). It is however not known whether the other anti-tuberculosis drugs are substrates.

Table 1.4: Summary of nomenclature of the organic anion transporter polypeptide family (Su *et al.*, 2004)

New Gene Symbol	New Protein Symbol	Old Gene Symbol	Old Protein Symbol
SLCO1A2	OATP1A2	SLC21A3	OATP-A, OATP
SLCO1B1	OATP1B1	SLC21A6	OATP-C, LST-1, OATP-2
SLCO1B3	OATP 1B3	SLC21A8	OATP-8
SLCO1C1	OATP1C1	SLC21A14	OATP-F, OATP-RP5
SLCO2A1	OATP2A1	SLC21A2	hPGT
SLCO2B1	OATP2B1	SLC21A9	OATP-B, OATP-RP2
SLCO3A1	OATP3A1	SLC21A11	OATP-D, OATP-RP3
SLCO4A1	OATP4A1	SLC21A12	OATP-E, OATP-RP1
SLCO4C1	OATP4C1	SLC21A20	OATP-H
SLCO5A1	OATP5A1	SLC21A15	OATP-J, OATP-RP4
SLCO6A1	OATP6A1	SLC21A19	OATP-I, GST

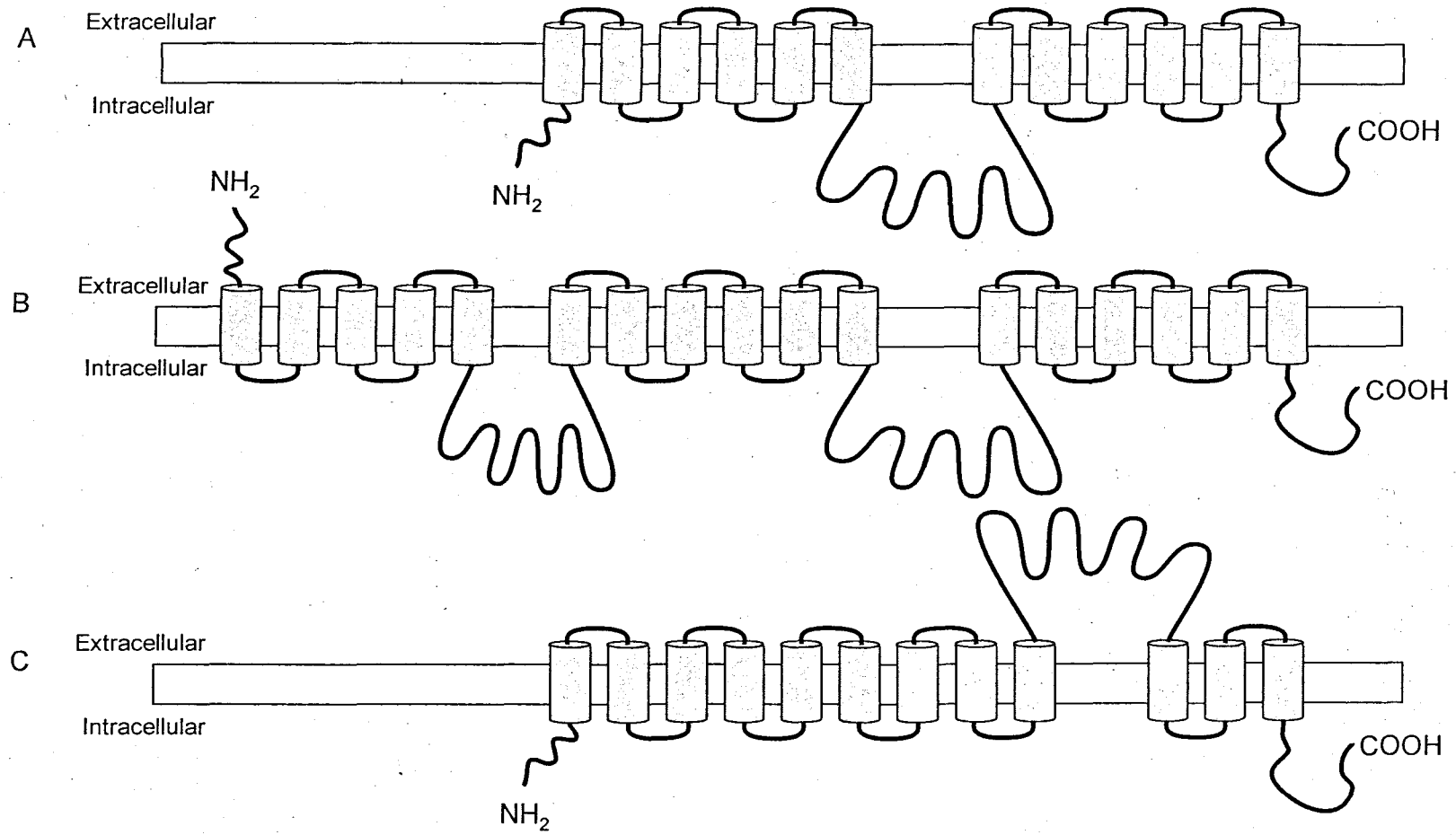

Figure 1.21: Topology of P-glycoprotein (A), MRP1-3 (B) and OATP (C)

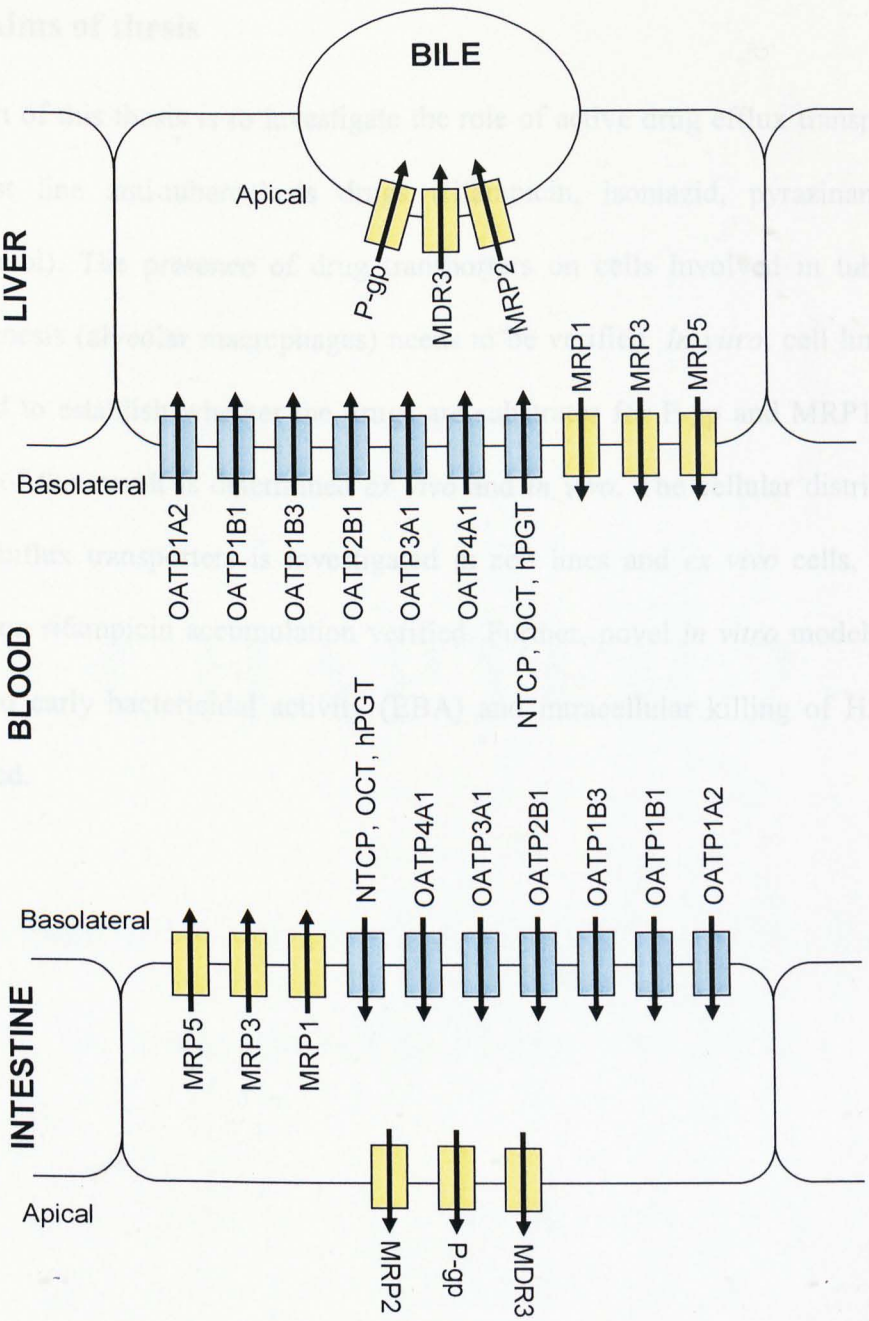

Figure 1.22: The polarised membrane distribution of the ABC efflux and SLC influx transporters on the intestinal wall and in the liver/bile. Modified from (Faber *et al.*, 2003)

1.4 Aims of thesis

The aim of this thesis is to investigate the role of active drug efflux transporters on the first line anti-tuberculosis drugs (rifampicin, isoniazid, pyrazinamide and ethambutol). The presence of drug transporters on cells involved in tuberculosis pathogenesis (alveolar macrophages) needs to be verified. *In vitro*, cell line models are used to establish whether the drugs are substrates for P-gp and MRP1, and the impact of this result is determined *ex vivo* and *in vivo*. The cellular distribution of OATP influx transporters is investigated in cell lines and *ex vivo* cells, and their impact on rifampicin accumulation verified. Further, novel *in vitro* models of drug mediated early bactericidal activity (EBA) and intracellular killing of H37Rv are examined.

CHAPTER 2

Effect of P-glycoprotein and MRP1 on the cellular accumulation of anti-tuberculosis drugs

2.1 Introduction 62

2.2 Methods 64

2.2.1 Materials 64

2.2.2 Cell lines and culture 65

2.2.3 Isolation of PBMC 65

2.2.4 Generation of MDM for confocal microscopy 65

2.2.5 Isolation of macrophages from BAL 66

2.2.6 Immunohistochemical analysis of P-glycoprotein expression on BAL 66

2.2.7 Confocal microscopic analysis of P-glycoprotein expression on MDM 67

2.2.8 Extraction of total RNA 67

2.2.9 Reverse transcription 68

2.2.10 Real time RT-PCR P-gp and MRP1 expression on Alveolar Macrophages 68

2.2.11 Validation of cell P-gp and MRP1 expression by flow cytometry 69

2.2.12 Validation of cellular P-gp and MRP1 expression by Western blot 70

2.2.13 Evaluation of the toxicity of anti-TB drugs on the CEM cell lines 72

2.2.14 Rifampicin accumulation in heat killed cells 73

2.2.15 Accumulation assays in CEM cell lines for rifampicin and isoniazid 74

2.2.16 MDCKII Transwell for rifampicin 75

2.2.17 Determining the impact of P-gp and MRP1 in PBMCs 76

2.2.18 PBMC P-gp and MRP1 expression vs rifampicin accumulation 77

2.2.19 Data handling and statistical analysis 77

2.3 Results 78

2.3.1 Macrophage Transporter expression 78

2.3.2 CEM cell line P-gp and MRP1 expression 78

2.3.3 Rifampicin accumulation in denatured cells 79

2.3.4 Differential drug toxicity in CEM cells 79

2.3.5 Differential drug accumulation in CEM cells 80

2.3.6 Rifampicin transport in MDCKII transwell assays 81

2.3.7 Modulation of rifampicin CAR in PBMCs by other drugs 82

2.3.8 Rifampicin accumulation vs transporter expression 82

2.3.9 Results Tables 83

2.3.10 Results Figures 87

2.4 Discussion 103

2.1 Introduction

Rifampicin, isoniazid, pyrazinamide and ethambutol remain first-line drugs for the treatment of *Mycobacterium* tuberculosis (MTB). Short course combination therapy for tuberculosis (TB) requires the drugs to be administered for at least 6 months in order to fully sterilise bacilli persisting in a non-replicating state within sanctuary sites. One of the sanctuary sites that MTB utilises to evade the human immune response is within phagosomes of alveolar macrophages (Fenhalls *et al.*, 2002; Mwandumba *et al.*, 2004). The accumulation of anti-tuberculosis drugs within alveolar macrophages may therefore be an important determinant of the effectiveness of therapy.

The two main groups of active drug efflux proteins; P-glycoprotein (P-gp) and Multi-drug resistance proteins (MRPs) have been widely associated with the drug disposition of a plethora of drugs in the liver and gut (Endicott and Ling, 1989; Kerb *et al.*, 2001). The impact of P-gp and MRPs on the cellular accumulation of drugs in non-epithelial cells has however been studied to a lesser extent. In HIV, numerous *in vitro* and *ex vivo* studies have demonstrated that active drug transporters can impact upon intracellular accumulation and activity of several anti-HIV protease inhibitors in CD4+ T-lymphocytes (Lee *et al.*, 1998; Jones *et al.*, 2001a; Owen *et al.*, 2004; Janneh *et al.*, 2005). Further, the expression of active drug transporters on mouse macrophage cell lines (J744) have been shown to modulate the accumulation of macrolide and quinolone antibiotics (Seral *et al.*, 2003; Michot *et al.*, 2004).

With the exception of rifampicin, no data are available on the impact of drug transporters on isoniazid, pyrazinamide or ethambutol, or vice versa. Rifampicin has

been shown to induce both intestinal (Greiner *et al.*, 1999) and lymphocyte (Asghar *et al.*, 2002) P-gp expression *in vivo*. Induction of MRP2, MRP3 and MRP5 by rifampicin in enterocytes has also been documented (Fromm *et al.*, 2000; Schrenk *et al.*, 2001). Furthermore, rifampicin modulates the cellular accumulation of vinblastine through P-gp inhibition (Fardel *et al.*, 1994) and the accumulation of calcein and vincristine through MRP inhibition (Courtois *et al.*, 1999). The only study that gives an indication that rifampicin is a substrate for active drug transporters is that the bioavailability of rifampicin in P-gp knockout mice was greater than that of wild-type mice (Schuetz *et al.*, 1996). However, cytochrome P450 (CYP) isoforms responsible for rifampicin metabolism are differentially expressed in the knockout and wildtype mouse (Schuetz *et al.*, 2000). It has thus not been categorically shown that rifampicin is a substrate for active drug transporters. Therefore, in this study the primary object was to determine *in vitro* whether rifampicin, isoniazid, pyrazinamide and ethambutol are substrates for P-gp and MRP1. In addition we examined alveolar macrophages for expression of both P-gp and MRP1 and, using *in vitro* cell models and *ex vivo* PBMCs screened the anti-TB drugs for their substrate affinity for both P-gp and MRP1 to determine the potential impact of the drug transporters on TB therapy.

2.2 Methods

2.2.1 Materials

[^{3}H]-rifampicin, [^{14}C]-isoniazid, [^{3}H]-saquinavir, [^{14}C]-diclofenac and [^{3}H]-methotrexate were purchased from Moravek Biochemicals (Brea, California, USA). Radiolabelled pyrazinamide and ethambutol were not commercially available. Tariquidar was kindly donated by Xenova Group Plc (Berkshire, UK). MK571 was kindly donated by Merck Frosst Canada Ltd (Kirkland, Quebec, Canada). Ultima-Gold scintillation fluid was purchased from Packard (Meriden, Connecticut, USA). All other chemicals were purchased from Sigma Chemicals Co (Poole, UK). MRPm5 was obtained from Kamiya Biomedical Company (Seattle, WA, USA), M2I-4 was obtained from Abcam Ltd (Cambridge, UK), peroxidase-conjugated secondary antibody from Amersham PLC (Buckinghamshire, UK), UIC2 and UIC2-rPE from Immunotech (Marseille, France), QCRL-1 from Merck Biosciences Ltd. (Nottingham, UK), IgG_{2A}, IgG_{2A}-rPE and IgG_1 isotype control from Serotec (Oxford, UK).

$MDCKII_{CTL}$, $MDCKII_{MDR1}$ (P-gp over-expressing) and $MDCKII_{MRP1}$ (MRP1 over-expressing) cells were a generous gift from Prof. P. Borst [Netherlands Cancer Institute (NKI), Amsterdam, the Netherlands]. CEM (parental), CEM_{VBL100} (P-gp over-expressing), CEM_{E1000} (MRP1 over-expressing) cells were gifts from Dr R. Davey, University of Queensland, Australia. All other materials were purchased from Sigma-Aldrich (Poole, UK).

2.2.2 Cell lines and culture

Parental Madin-Darby Canine Kidney cell lines ($MDCKII_{CTL}$), those transduced with P-gp ($MDCKII_{MDR1}$) and MRP1 ($MDCKII_{MRP1}$) were routinely cultured in Dulbecco's modified eagle's medium (DMEM) supplemented with 10% foetal calf serum (FCS). CEM (human T-lymphoblastoid cell line), CEM_{VBL100} (P-gp over-expressing) and CEM_{E1000} (MRP1 over-expressing) were routinely cultured in RPMI medium 1640 (RPMI) supplemented with 10 % FCS.

2.2.3 Isolation of PBMC

Peripheral blood mononuclear cells (PBMC) were isolated from blood samples obtained from healthy volunteer and buffy coats (obtained from the regional blood transfusion centre) by density gradient centrifugation on Ficoll-Hypaque (800 x g, 30 min) (ethics committee approval for blood sampling obtained).The central band containing the PBMCs was removed and diluted 3 fold in sterile phosphate buffered saline (PBS). PBMCs were then pelleted (800 x g, 6 min), counted using a NucleoCounter (Chemometric), and resuspended to the required concentration in the media of choice.

2.2.4 Generation of MDM for confocal microscopy

Monocyte derived macrophages (MDM) were generated by isolating PBMCs from whole blood and washing the cell pellet 3 times (800 x g, 6 min) in order to remove all the Ficoll-Hypaque. Cells were then resuspended in RPMI 1640 (without FCS, 2 x 10^6 cells/ml), transferred onto 35 mm glass based dishes (500 µL) (IWAKI, Asahi Technoglass, Japan). Monocytes were allowed to adhere to the glass (1 hr, 37°C and 5% CO_2) before all the remaining non-adherent cells were washed off with sterile

PBS. The remaining monocytes that adhered were matured into macrophages by culturing them in RPMI 1640 and 1% human serum (7 days, 37°C, 5%CO_2).

2.2.5 Isolation of macrophages from BAL

Alveolar macrophages were obtained from bronchoalveolar lavage (BAL) at the North West Lung Research Centre (South Manchester University Hospitals Trust, Manchester, UK). Briefly, a bronchoscope was wedged in an appropriate tertiary bronchus (usually the right middle lobe) and a BAL was carried out using normal pre-warmed saline (37°C, 50ml). Recovered BAL fluid (stored at 4°C) was then passed through a filter nylon cell strainer (100µm, BD Falcon) and centrifuged (300 x g, 10 min, 4°C). Alveolar macrophages were purified from the BAL using magnetic cell sorting (MACS technology) according to the manufacturer's instructions. Briefly, 2 x 10^7 cells were resuspended in 160 µL of MACS buffer (PBS, 0.5% BSA, 2mM EDTA, pH 7.2, 4°C) and mixed with 40 µL of CD14 microbeads (Miltenyi Biotec, Bergisch Gladbach, Germany). Cells were incubated (15 min, 4°C) and washed with MACS buffer (1mL, 300 x g, 10 min). The pellet was then resuspended in 500 µL of MACS buffer and added to an equilibrated LS separation column (Miltenyi Biotec, Bergisch Gladbach, Germany). Unlabelled cells were then eluted with buffer (3 x 3 ml). Labelled cells were subsequently eluted following removal of the LS separation column from the magnet, and pelleted (300 x g, 10 min)

2.2.6 Immunohistochemical analysis of P-glycoprotein expression on BAL

BAL cells were cytospun to glass slides and fixed (100% methanol, 10 min, 4°C) and incubated in hydrogen peroxide (10min) in order to remove any endogenous oxygen radicals. The slides were then probed with either isotype control antibody (IgG_{2A},

200μL of 250 ng/mL, 1hr) or an anti-P-gp antibody (UIC2; 200μL of 250 ng/mL, 1hr). Biotinylated goat anti-mouse IgG secondary antibody (Sigma: B7264, 200μL, 1:500 v/v, 1hr) was applied followed by peroxidase-conjugated streptavidin (200μl, 10 min). Detection was achieved using di-amino benzidene (DAB, 0.7 mg/mL, supplemented with 6 μL/mL H_2O_2) for 5min. Light nuclear staining was carried out using haematoxylin and cells visualised by light microscopy.

2.2.7 Confocal microscopic analysis of P-glycoprotein expression on MDM

MDM grown on a 35 mm glass base disk (see 2.2.4) were fixed (100% methanol, 10 min, 4°C). The MDMs were then probed with either r-phycoerythrin (rPE) conjugated isotype control antibody (IgG_{2A}-rPE, 200μL of 2.5 μg/mL, 1hr) or an rPE conjugated anti-P-gp antibody (UIC2-rPE; 200μL of 2.5 μg/mL, 1hr). MDM were washed with PBS and visualised by confocal microscopy set up to detect rPE (excitation 565, emission 575).

2.2.8 Extraction of total RNA

Total RNA was extracted from alveolar macrophages isolated from BAL using TRIzol according to manufacturer's instructions with minor modifications. Briefly, cell pellets (1 x 10^7 cells) were mixed thoroughly in TRIzol (1mL) and frozen (-80°C). Chloroform (200 μL) was then added to the thawed TRIzol mixtures; samples were thoroughly mixed, incubated (20°C, 3 min) and centrifuged (12000 x g, 15 mins). The aqueous phase was then removed and mixed with isopropanol (500 μL), incubated (20°C, 10 min) and centrifuged (12000 x g, 10mins). The supernatant was discarded and the RNA pellet washed in 75% ethanol (1 mL, 7500 x g, 5 min) and allowed to air dry before being resuspended in RNase free water (20 μL).

Concentration and purity of RNA obtained was determined using a spectrophotometer.

2.2.9 Reverse transcription

Reverse transcription of the extracted total RNA to cDNA was performed using TaqMan Reverse Transcription Reagents (Applied Biosystems, New Jersey, USA) by mixing 10× Taqman RT Buffer (10 µl, final conc. 1x), 25 mM $MgCl_2$ (22 µL final conc. 5.5mM), 2.5 mM dNTP mix (20 µL, final conc. 500 µM of each), 50 µM random hexamer primers (5 µL, final conc. 2.5µM), 20 U/µL RNase inhibitor (2µl, 0.4 U/µL), 50 U/µL Multiscribe reverse transcriptase (2.5 µL, total conc. 1.25 U/µl) and 50 ng/mL total RNA (20 µL final conc. 0.01 µg/µL) and RNase free water (18.5 µL). Reverse transcription thermal cycling (25°C, 10 min; 48 °C, 30 min; 95°C, 5 min; 4°C, ∞) was performed using a GeneAmp PCR System (Applied Biosystems, Warrington, UK). The resulting cDNA was frozen at -20°C until use.

2.2.10 Real time RT-PCR P-gp and MRP1 expression on Alveolar Macrophages

Quantification of mRNA transcripts for MDR1 and MRP1 was achieved by real-time polymerase chain reaction using an Opticon2 sequence detection system as described previously (Owen *et al.*, 2005). Glyceraldehyde-3-phosphate dehydrogenase (GAPDH) was used as the house-keeping gene. cDNA (40 ng) was combined with Universal master mix, sense and antisense primers (0.4 µM each), and oligonucleotide probe (0.2 µM) in a final volume of 25 µl. Amplification was carried out for 40 cycles with a combined annealing/extending temperature of 60°C. Primers and probes were obtained via the Assays-on-Demand Gene Expression products available through the Applied Biosystems (Foster City, CA) Web site (http://home.appliedbiosystems.com).

2.2.11 Validation of cell P-gp and MRP1 expression by flow cytometry

Assessment of P-gp expression: Cells were grown until confluent and counted by NucleoCounter (Chemometric). An appropriate number of cells were pelleted (800 x g, 6 min) and fixed (1 x 10^6 cells/mL in 1:10 CellFIX, 25min). 100 µL aliquots (2 x 10^5 cells) were then transferred to a 96 well plate (U bottom) and washed (200 µL PBS, 800 x g, 10 min). The cell pellet was then stained for P-gp using r-phycoerythrin conjugated mouse-anti-human P-gp antibody (UIC2-rPE: 50 µL of 2.5 µg/ml, 2 hr). Non-specific antibody binding was determined by staining cells with r-phycoerythrin conjugated mouse-anti-human IgG_{2A} isotype control (IgG_{2A}-rPE: 50 µL of 2.5 µg/ml, 2 hr). Cells were washed three times (200 µL PBS, 800 x g, 10 min), resuspended (300 µL of 1:10 CellFix) and transferred into 5 ml FACS tubes.

Flow cytometry was conducted on a Coulter epics XL-MCL. Forward scatter (FS: indicating cell size) and side scatter (SS: indicating cell granularity) were detected on a linear scale. The live cell population was electronically gated to exclude debris. Median fluorescence intensity values of the gated cells were obtained in FL2 (mean peak emission wavelenth 570 nm) and registered on a logarithmic scale against the number of events. P-gp expression was determined by the relative fluorescence units as shown below:

P-gp expression (RFU): Specific antibody FL2 fluorescence - isotype control FL-2 fluorescence

Assessment of MRP-1 expression: Following the counting and fixing of cells as described above, cells were permeabilised with saponin (100 µL, 0.1 $mg.ml^{-1}$, 30 min). The cell pellet was stained for MRP1 using primary mouse-anti-human MRP1 antibody (QCRL1: 50 µL of 2.5 µg/ml, 1 hr). Non-specific antibody binding was

determined by staining cells with mouse-anti-human IgG_1 isotype control (IgG_1: 50 µL of 2.5 µg/ml, 1 hr). Following 3 washes (200 µL, 0.1 $mg.ml^{-1}$ saponin in PBS, 800 x g, 10 min) cell pellets (both specific and isotype control stained cells) were stained with secondary goat-anti-mouse IgG conjugated to FITC (50 µL, 5 µg/ml, 1 hr). Following 3 washes (200 µL, 0.1 $mg.ml^{-1}$ saponin in PBS, 800 x g, 10 min) cell pellets were resuspended (300 µL of 1:10 CellFix) and transferred into 5 ml FACS tubes

The median fluorescence intensity values of the gated cells were obtained in FL1 (mean peak emission wavelength 530 nm) and registered on a logarithmic scale against the number of events. MRP1 expression was determined by the relative fluorescence units as shown below:

MRP1 expression (RFU): specific antibody FL1 fluorescence - isotype control FL-1 fluorescence

2.2.12 Validation of cellular P-gp and MRP1 expression by Western blot

Preparing cell homogenate: Western blot was used in order to determine P-gp, MRP1 and MRP2 expression on CEM, CEM_{VBL100}, CEM_{E1000}, MDCKII-MRP1 (positive control for MRP1 expression) and MDCKII-MRP2 (positive control for MRP2 expression). 1×10^7 cells were pelleted (800 x g, 6 min) and resuspended in 200 µL of Western lysis buffer (50mM NaCl, 10mM HEPES [pH 8], 0.5M sucrose, 1mM EDTA, 0.5mM spermidine, 0.15mM spermine, 0.2% triton X-100, containing 0.5µl ml^{-1} β-mercaptoethanol, 3µg ml^{-1} aprotinine, 2µg ml^{-1} leupeptin, 3µg ml^{-1} pepstain and 0.2mM PMSF). Following lysis for 20 min on ice, samples were frozen at –80°C in aliquots of 20 µL.

Protein Assay: The nuclei were removed from the cell homogenates by centrifugation (1100 x g for 5 min). Total protein concentration of the supernatant fraction was determined by the bicinchoninic acid protein assay as described by (Smith *et al.*, 1985). Briefly, 100 µL of bovine serum albumin (BSA) solution (100 – 1000 µg/ml in distilled water), and 100 µL of an appropriate cell homogenate dilution was added to a 96 well plate (flat bottom). Subsequently, 100 µL of working solution (2 % [v/v] reagent B: 4% copper sulphate pentahydrate ($CuSO_4.5H_2O$), 98% reagent A: 1% sodium bicinchominate, 2% sodium carbonate, 0.16% sodium tartate, 0.4% NaOH, 0.95% sodium bicarbonate, pH 11.25) was added to each well. Following incubation (60°C for 30 min) the plate was left to cool at room temperature and read at 570 nm on a spectrophotometer (Dynex. 2.0).

Electrophoresis: 50µg total protein was combined with an equal volume of NuPAGE LDS loading buffer (containing 10 % NuPAGE reducing agent). To linearise the proteins, the sample was heated (70 °C, 10 min) and cooled to 40 °C. The entire sample (50 µg protein) was then loaded on 3 - 12% tris-acetate gels (Invitrogen) and electrophoresed (160 V, 1 hr) (Invitrogen tris-acetate running buffer outside gasket; Invitrogen tris-acetate running buffer plus 2.5% v/v NuPAGE reducing agent inside gasket). 10µL pre-stained molecular weight markers were also loaded onto two wells per gel.

Transfer: Following electrophoresis, all apparatus for protein transfer [3-12% Tris-acetate gel, sponges, filter paper and nitrocellulose membrane (0.45 µm pore size)] was soaked in NuPAGE transfer buffer with 10% methanol for 30 min. Proteins were

then transferred electrophoretically to a nitrocellulose membrane (100 V, 1 hr: cooled with an ice block).

Staining: To block hydrophobic or non-specific sites the nitrocellulose membrane was incubated overnight at 4°C in blocking buffer (10% non-fat dried milk in tris-buffered saline (50 mM Tris and 150 mM NaCl) containing Tween 20 (TBS-T). Tween 20 concentration throughout the procedure was 0.3, 0.1 and 0.05% for the P-gp, MRP1 and MRP2 detection respectively.

The nitrocellulose membrane was briefly washed 4 times with TBS-T followed by 4 longer washes in TBS-T (5 min). The membranes were then incubated with mouse-anti-human monoclonal antibodies F4, MRPm5 and M2I-4 against P-gp, MRP1 and MRP2 respectively (1:2000 in TBS-T containing 2% non-fat dried milk, 2 hr). The membrane was washed as previously described and incubated with goat-anti-mouse IgG horseradish peroxidase-conjugated secondary antibody (1:10000 in TBS-T containing 2% non-fat dried milk, 1hr). The membrane was then washed as previously and visualisation of the protein-antibody conjugates was carried out using enhanced chemiluminescence reagent (ECL). Briefly, excess washing buffer was gently removed with tissue and 2 ml of 50 % (v/v) enhanced luminol reagent in oxidizing agent (PerkinElmer Life Sciences) was added to the membrane for 1 min. The membrane was subsequently exposed to ECL hyperfilm for between 10 sec and 4 min.

2.2.13 Evaluation of the toxicity of anti-TB drugs on the CEM cell lines

To determine the viability of the CEM, CEM_{VBL100} and CEM_{E1000} the MTT cytotoxicity assay was used. This assay uses mitochondrial viability as a marker for

cell viability and is based on the conversion of MTT (yellow coloured; 3-[4,5-dimethyl-thiazole-2-yl]-2,5-diphenyl tetrazolium bromide) into its reduced formazan form (which is blue) by viable mitochondria (Mosmann, 1983). Briefly, confluent CEM, CEM_{VBL100} and CEM_{E1000} were pelleted (800 x g, 6 min), and resuspended in RPMI-1640 (without phenol red, supplemented with 10% FCS). 100 µL of cells (2 x 10^5 cells/mL) were plated in a 96 well plate in the presence or absence of rifampicin (0 – 450 µM), isoniazid (0 – 100 mM), pyrazinamide (0 - 40 mM) and ethambutol (0 µM – 50 mM). For each drug concentration a cell free control was used to correct for background absorbance by the drug. Following incubation (37°C, 5% CO_2, 3 days), 20 µL of 5 mg/mL MTT was added to each well and cells were incubated (2 hr, 37°C, 5% CO_2). The MTT reaction was terminated by adding 100 µL of MTT lysis buffer (50% v/v N,N-dimethylformamide, 20% w/v sodium dodecyl sulphate) and incubation for a further 24 hr (37°C, 5% CO_2). The formation of the blue MTT formazan was determined spectrophotometricaly (absorbance at 570 nm). Cytotoxicity was expressed as the concentration of drug giving 50% cell death (EC50) as determined using Graphpad Prism v3.

For the drugs that showed significant differential toxicity in CEM_{VBL100} or CEM_{E1000} compared to parental CEM cells, experiments were repeated in the presence of the potent P-gp inhibitor tariquidar (1 µM) and the MRP1 inhibitor MK571 (100 µM).

2.2.14 Rifampicin accumulation in heat killed cells

Cellular accumulation ratios of ^{3}H-rifampicin were determined in CEM, CEM_{VBL100} and CEM_{E1000} cells as well as in buffy coat PBMCs (n = 4). Brifly, cells were pelleted (800 x g, 6 min) and re-suspended in RPMI 1640 without FCS (3 x 10^6 cells/mL). Following pre-incubation (10 min, 37°C in 5% CO^2) of 1 mL of the cell

suspension (3 x 10^6 cells) in a 1.5 mL microfuge tube, 10 µL of [^{3}H]-rifampicin (100 µM solution: 5 µCi/ml) was added (final concentration of 1µM). Following incubation (30 min, 37°C in 5% CO_2), cells were pelleted (2000 x g, 1 min, 4°C) and 100 µL of incubation media removed for radioactivity counting (extracellular count). Cell pellets were washed 3 times in phosphate buffered saline (PBS) (2000 x g, 1 min, 4°C) and lysed with tissue solubilising solution (hydrogen peroxide: glacial acetic acid: tissue solubiliser at 2.5:5:5 (v:v:v)) and counted for radioactivity (cell associated count). Cellular drug accumulation was expressed as the cellular accumulation ratio (CAR), being the ratio of cell associated drug, to media associated drug (based on a cell volume of 1 pL, (Jones *et al.*, 2001b)). The experiments were repeated with heat killed cells (Heat kill by: 30 min, 60°C, incubation at 37°C, 30 min).

2.2.15 Accumulation assays in CEM cell lines for rifampicin and isoniazid

The basal accumulation of [^{14}C]-isoniazid (1 µM, 0.05 µCi /ml) and [^{3}H]-rifampicin (1 µM, 0.05 µCi /ml) as well as [^{3}H]-saquinavir (positive control for P-gp, (Srinivas *et al.*, 1998; Jones *et al.*, 2001a; Dallas *et al.*, 2004), [^{3}H]-methotrexate (positive control for MRP1, (Hooijberg *et al.*, 1999; Zeng *et al.*, 2001) and [^{14}C]-diclofenac (a negative control for both transporters, unpublished observation) were assessed in CEM, CEM_{VBL100} and CEM_{E1000} cell lines. Cells were pelleted (800 x g, 6 min) and re-suspended in RPMI 1640 without FCS (3 x 10^6 cells/mL). Following pre-incubation (10 min, 37°C in 5% CO^2) of 1 mL of the cell suspension (3 x 10^6 cells) in a 1.5 mL microfuge tube, either 10 µL of [^{3}H]-rifampicin (100 µM solution: 5 µCi/ml), 10 µL of [^{14}C]-isoniazid (100 µM solution: 5 µCi/ml), 10 µL of [^{3}H]-saquinavir (100 µM solution: 5 µCi/ml), 10 µL of [^{3}H]-methotrexate (100 µM solution: 5 µCi/ml) or 10 µL of [^{14}C]-diclofenac (100 µM solution: 5 µCi/ml) was

added to the CEM, CEM_{VBL100} and CEM_{E1000} cell lines (final concentration of 1μM). Following 30 min incubation (37°C in 5% CO^2), CAR was determined as described in 2.2.14.

To determine optimal inhibitory concentrations of P-gp and MRP1 by tariquidar and MK571 respectively, concentration dependent effects were determined on saquinavir accumulation in CEM, CEM_{VBL100} and CEM_{E1000} cell lines. [^{3}H]-saquinavir accumulation studies were performed as described above with the exception that cell lines were pre-incubated with either tariquidar (0, 3, 10, 30, 100, 300 or 1000 nM) or MK571 (0, 1, 3, 10, 30 or 100 μM).

To evaluate differential rifampicin accumulation in CEM, CEM_{VBL100} and CEM_{E1000} cell lines, [^{3}H]-rifampicin accumulation was assessed in the absence and presence of tariquidar (0, 10, 100 and 1000 nM) and MK571 (1, 10 and 100 μM)

2.2.16 MDCKII Transwell for rifampicin

The MDCKII transport assays were performed as previously described (Huisman *et al.*, 2001). Briefly, polycarbonate filters (3.0 μm membrane pore size, 4.7 cm^2 growth area, 24 mm insert diameter; Transwell 3414; Costar) were pre-incubated with DMEM supplemented with 10% FCS (1 hr, 37°C, 5% CO_2). Following media aspiration, 2 mL of $MDCKII_{CTL}$, $MDCKII_{MDR1}$ and $MDCKII_{MRP1}$ cell suspensions (1×10^6 cells/mL) were added to the apical (AP) compartment and fresh media to the basolateral (BL) compartment. Cells were grown for 3 days with media replaced daily. 1 hr before the start of the experiment, media was aspirated from both compartments and replaced with DMEM (without FCS). Trans-epithelial resistance (TER) was then measured to confirm confluency (TER accepted above 150 Ω).

In order to perform transwell experiments, the rate of apically directed (basolateral to apical drug movement) and basolaterally directed (apical to basolateral drug movement) flux was assessed. Media was aspirated and replaced with 2 mL DMEM (without FCS) in one compartment and with 2 mL of DMEM (without FCS) containing 1μM [^{3}H]-rifampicin (0.5 μCi) with [^{14}C]-mannitol (0.2 μCi) in the other compartment. Mannitol does not cross intact MDCKII monolayers, therefore transport of [^{14}C]-mannitol across the monolayer is an indicator of leakage, and was tolerated up to 1 %/hr per well. Cells were incubated (37°C in 5% CO^{2}) and 100 μl aliquots of incubation media were taken from each compartment at hourly intervals, for 4 h and counted for radioactivity. Trans-epithelial transport was measured as the percentage of radioactivity appearing in the receiver compartment compared to provider compartment, per hour.

Transwell experiments were repeated in the presence of 1000 nM tariquidar (in $MDCKII_{MDR1}$) and 100 μM MK571 (in $MDCKII_{MRP1}$) to asses if differential transport was specific to P-gp and MRP1 respectively. Transwell studies were also performed with 1 μM [^{3}H]-saquinavir (in $MDCKII_{CTL}$ $MDCKII_{MDR1}$) and 1 μM [^{3}H]-methotrexate (in $MDCKII_{CTL}$ $MDCKII_{MRP1}$).

2.2.17 Determining the impact of P-gp and MRP1 in PBMCs

To determine the influence of P-gp and MRP1 expressed on PBMCs on ^{3}[H]-rifampicin accumulation, rifampicin CAR was determined in buffy coat derived PBMCs in absence and presence of tariquidar (1μM), MK571 (50 μM) and a combination of both. Further it was determined whether there was a significant drug interaction between rifampicin and other anti-TB drugs (100 μM isoniazid,

pyrazinamide and ethambutol), anti-HIV drugs (100 μM saquinavir, ritonavir and nelfinavir) and anti-malarial drugs (100 μM mefloquine and chloroquine).

2.2.18 PBMC P-gp and MRP1 expression vs rifampicin accumulation

PBMCs were isolated from 60 mL of blood taken from 12 healthy volunteers (2.2.3). Rifampicin CAR was determined in quadruplicate samples, and remaining cells were frozen down (-80°C) in FCS (10% DMSO), to be analysed for P-gp and MRP1 expression at a later date. Rifampicin CAR was then correlated with transporter expression.

2.2.19 Data handling and statistical analysis

Data are presented as mean ± SD. Data were checked for normality using a Shapiro-Wilk test. If data were found to be normally distributed a paired or unpaired T-test was used. If data were found to be non-normally distributed a Mann-Whitney test was used. For correlation analysis, data were tested for normality and a simple linear regression performed. $P<0.05$ was taken as indicative of significance. EC50s were calculated using GraphPad Prism 3.

2.3 Results

2.3.1 Macrophage Transporter expression

Both immnohistochemistry and confocal microscopy of BAL and MDM respectively showed greater P-gp specific UIC2 binding than isotype control binding (Fig. 2.1 and 2.2). Real time PCR for the detection of P-gp and MRP1 mRNA showed that all four alveolar macrophage mRNA extracts expressed both transporters, and that the products were of the correct amplicon size (P-gp: 79 bp, MRP-1: 107 bp) (Fig. 2.3).

2.3.2 CEM cell line P-gp and MRP1 expression

Using flow cytometry, a significant difference in P-gp expression was observed between CEM_{VBL100} (difference in FL2 fluorescence ± SD: 34.70 ± 4.32, $P < 0.05$) and CEM (0.29 ± 0.04). No difference was observed between the P-gp expression of CEM (0.29 ± 0.04) and CEM_{E1000} (0.33 ± 0.07) (Fig. 2.4 and 2.5). Both CEM_{E1000} (difference in FL1 fluorescence ± SD: 5.22 ± 0.87, $P < 0.05$) and CEM_{VBL100} (1.06 ± 0.26, $P < 0.05$) showed a significant increase in MRP1 expression compared to that of the parental CEM (0.22 ± 0.06) (Fig. 2.4 and 2.5).

Western blot analysis of the CEM cell lines (Fig. 2.6) showed basal P-gp expression in CEM and CEM_{E1000} and a much greater P-gp expression in the CEM_{VBL100}. MRP1 could only be detected in the CEM_{E1000} cells and the positive control $MDCK_{MRP1}$ cells. MRP2 was not detected in any of the CEM cell lines and was only seen in the $MDCKII_{MRP2}$ positive control.

2.3.3 Rifampicin accumulation in denatured cells

Rifampicin cellular accumulation was found to be significantly increased in CEM, CEM_{VBL100} $CEME_{1000}$ cells and buffy coat PBMCs when the cells were denatured by heat kill compared to controls (Fig 2.7, Table 2.1)

2.3.4 Differential drug toxicity in CEM cells

The cellular toxicity of rifampicin, isoniazid, pyrazinamide and ethambutol was determined in CEM, CEM_{VBL100} and CEM_{E1000} cell lines (Fig. 2.8 and 2.9, Table 2.2). No differential toxicity was observed for isoniazid and pyrazinamide in the three cell lines. Ethambutol toxicity was the same in CEM (Mean EC50 ± SD: 5.6 ± 0.7 mM) and CEM_{E1000} (4.3 ± 0.7 mM) cells but was significantly reduced in CEM_{VBL100} (15.0 ± 1.4 mM, $P<0.05$, n=4). Tariquidar was able to significantly increase CEM_{VBL100} toxicity (9.5 ± 1.0 mM) without affecting CEM toxicity (5.1 ± 0.7 mM) (Table 2.2).

Rifampicin toxicity was significantly decreased in CEM_{VBL100} (152 ± 4.1 μM, $P<0.05$, n=8) and CEM_{E1000} (115 ± 6.7 μM, $P<0.05$, n=8) compared to the parental CEM (104 ± 2.3 μM, n=8). Tariquidar (1 μM) reversed the EC50 of rifampicin in CEM_{VBL100} (103 ± 5.1 μM, $P>0.01$, n=4) to that of the parental CEM, but also caused a slight decrease in the EC50 measured in CEM cells (91.1 ± 6.7 μM, $P<0.05$, n=4). MK571 (100 μM) significantly decreased the rifampicin EC50 in CEM_{E1000} (72.4 ± 3.7, $P>0.01$, n=4) but also had a dramatic effect in CEM cells (61.0 ± 5.8, $P>0.01$, n=4) (Table 2.2). Both tariquidar (1 μM) and MK571 (100 μM) were not found to be toxic on their own.

2.3.5 Differential drug accumulation in CEM cells

The CAR of the control drugs; saquinavir, methotrexate and diclofenac, confirmed that CEM_{VBL100} effluxed saquinavir (a known P-gp substrate), CEM_{E1000} effluxed methotrexate (a known MRP1 substrate) and that diclofenac was not effluxed by either transporter (Table 2.3).

To determine optimal inhibitory concentrations of tariquidar and MK571, the effect was determined on [^{3}H]-saquinavir accumulation (Fig. 2.10 and 2.11). Saquinavir CAR in CEM_{VBL100} (mean ± SD; 12.3 ± 5.9) was significantly increased at tariquidar concentrations above 30 nM (69.8 ± 5.1, $P>0.05$) and was optimal above 100 nM (96.8 ± 3.8, $P>0.05$) (Fig. 2.10). Tariquidar showed no effect on saquinavir accumulation in the CEM or CEM_{E1000} cells. Saquinavir accumulation in CEM_{E1000} (78.9 ± 3.4) was significantly increased in the presence of 3 μM MK571 (101.3 ± 2.9, $P>0.05$) and was optimally inhibited at MK751 concentrations above 30 μM (135.5 ± 10.0, $P>0.05$) (Fig. 2.11). MK571 however also caused a significant increase in saquinavir accumulation in CEM cells above 3 μM.

The basal CAR of isoniazid in CEM, CEM_{VBL100} and CEM_{E1000} cell lines were similar (Fig. 2.12, Table 2.3). The CAR of [^{3}H]-rifampicin was significantly decreased in CEM_{VBL100} (mean ± SD: 3.19 ± 0.24, $P<0.05$) and CEM_{E1000} (3.77 ± 0.38, $P<0.05$) compared to the parental CEM cell line (5.19 ± 0.38) (Fig 12, Table 2.3).

1 μM Tariquidar caused a significant increase in rifampicin CAR in CEM_{VBL100} (4.06 ± 0.13, $P<0.05$) compared to the drug alone (3.19 ± 0.24). Tariquidar showed no

effect on rifampicin accumulation in CEM or CEM_{E1000} cells (Fig. 2.13, Table 2.3). 100 μM MK571 caused a significant increase in rifampicin CAR in CEM_{E1000} (4.71 ± 0.41, $P<0.05$) compared to controls (3.77 ± 0.38). However, 100 μM MK571 also caused a significant increase in the accumulation of rifampicin in CEM_{VBL100} cells (from 3.19 ± 0.24 to 3.95 ± 0.21, $P<0.05$) (Fig. 2.13, Table 2.3).

2.3.6 Rifampicin transport in MDCKII transwell assays

To confirm substrate affinity of rifampicin, $MDCKII_{CTL}$, $MDCKII_{MDR1}$ and $MDCKII_{MRP1}$ transwell studies were performed to evaluate the rate of basolaterally and apically directed translocation across the monolayer. In all cases the rate of apical or basal translocation of [^{14}C]-mannitol was less than 1 %/hr, indicating monolayer integrity. P-gp in $MDCKII_{MDR1}$ clones is located on the apical membrane whereas MRP1 in $MDCKII_{MRP1}$ is located on the basolateral membrane. Parental MDCKII cells express endogenous transporters that govern the basal translocation of rifampicin.

Apically directed rifampicin transport was increased in the $MDCKII_{MDR1}$ (12.1 ± 0.4 %/hr, $P<0.05$) (Fig. 2.14, Table 2.4) compared to the $MDCKII_{CTL}$ cells (8.9 ± 0.5 %/hr). $MDCKII_{MDR1}$ apically directed transport was reverted back to that of the $MDCKII_{CTL}$ by tariquidar (1μM) (8.1 ± 0.6 %/hr, $P<0.05$). The basolateral translocation of rifampicin was similar in the $MDCKII_{MRP1}$ (1.5 ± 0.1 %/hr) compared to the $MDCKII_{CTL}$ (1.1 ± 0.1 %/hr) and was also not influenced in the presence of 100 μM MK571 (Fig. 2.14, Table 2.4).

The positive control for P-gp, saquinavir showed significantly increased apical translocation in $MDCKII_{MDR1}$ (25.2 ± 1.78 %/hr, $P<0.05$) compared to $MDCKII_{CTL}$ (13.6 ± 2.14 %/hr). However, basolateral translocation of the MRP1 substrate methotrexate was not significantly different between the $MDCKII_{CTL}$ (0.50 ± 0.11 %/hr) and the $MDCKII_{MRP1}$ (0.42 ± 0.13 %/hr).

2.3.7 Modulation of rifampicin CAR in PBMCs by other drugs

Rifampicin CAR in buffy coat derived PBMCs (n=6) was not affected by P-gp and/or MRP1 inhibition, or by the co-incubation with anti-TB drugs (100 μM isoniazid, pyrazinamide and ethambutol), anti-HIV drugs (100 μM saquinavir, ritonavir and nelfinavir) or anti-malarial drugs (100 μM mefloquine and chloroquine) (Fig. 2.15).

2.3.8 Rifampicin accumulation vs transporter expression

Rifampicin CAR in PBMCs derived from 12 healthy volunteers did not correlate with the P-gp or MRP1 expression of those PBMCs (Fig. 2.16). There was however a significant positive linear correlation between the PBMC P-gp and MRP1 expression ($r^2 = 0.37$, $P<0.05$) (Fig. 2.16).

2.3.9 Results Tables

Table 2.1: Rifampicin CAR in CEM, CEM_{VBL100}, CEM_{E1000} and buffy coat PBMCs alone, and in heat killed denatured cells. Data mean ± SD ($n \geq 4$), * $P<0.05$ compared to control conditions.

	Rifampicin Cellular Accumulation Ratio (CAR) mean ± SD	
	Control	**Denatured cells**
CEM	5.54 ± 0.21	7.58 ± 1.28*
CEM_{VBL100}	3.40 ± 0.14	6.66 ± 0.86*
CEM_{E1000}	4.63 ± 0.34	7.44 ± 1.56*
PBMC	5.96 ± 0.80	8.41 ± 1.21*

Table 2.2: EC50 values of rifampicin (RIF), isoniazid (INH), pyrazinamide (PZA) and ethambutol (EMB) in CEM, CEM_{VBL100} and CEM_{E1000}. For rifampicin and ethambutol, experiments were conducted alone and in the presence of tariquidar (1 μM) or MK571 (100 μM). Data are mean ± SD (n = 4). $^{+++}$ $P < 0.001$ (compared to CEM), * $P < 0.05$, ** = $P < 0.01$ (compared to drug alone).

Cell Line	EC50 values						
	Isoniazid (mM)	Pyrazinamide (mM)	Ethambutol (mM)		Rifampicin (μM)		
	Drug Alone	Drug Alone	Drug Alone	+ Tariquidar	Drug Alone	+ Tariquidar	+ MK571
CEM	16.6 ± 4.2	12.6 ± 1.3	5.6 ± 0.7	5.1 ± 0.7	104 ± 2.3	91.1 ± 6.7	61.0 ± 5.8**
CEM_{VBL100}	13.4 ± 1.9	11.4 ± 2.7	15.0 ± 1. 4^{+++}	9.5 ± 1.0*	152 ± 4.1^{+++}	103 ± 5.1**	N/A
CEM_{E1000}	13.3 ± 3.2	9.9 ± 0.5	4.3 ± 0.7	N/A	115 ± 6.7^{+++}	N/A	72.4 ± 3.7**

Table 2.3:. The CAR of 1 μM [^{3}H]-rifampicin and 1 μM [^{14}C]-isoniazid in CEM, CEM_{VBL100} and CEM_{E1000} cells. The accumulation of 1 μM [^{3}H]-saquinavir (P-gp substrate control), [^{3}H]-methotrexate (MRP1 substrate control) and [^{14}C]-diclofenac (negative control for both transporters) is also given. Data are mean ± SD (n = 4). $^{+++}$ $P < 0.001$ (compared to CEM), * $P < 0.05$, ** = $P < 0.01$ (compared to drug alone).

Cell Line	Cellular Accumulation Ratio (CAR)						
	Rifampicin			Isoniazid	Saquinavir	Methotrexate	Diclofenac
	Drug Alone	+ Tariquidar	+ MK571	Drug Alone	Drug Alone	Drug Alone	Drug Alone
CEM	5.19 ± 0.38	5.08 ± 0.29	5.34 ± 0.42	0.27 ± 0.08	123.7 ± 19.9	1.19 ± 0.23	9.25 ± 1.51
CEM_{VBL100}	3.19 ± 0.24^{+++}	4.18 ± 0.13**	3.95 ± 0.21*	0.23 ± 0.05	7.76 ± 1.9**	N/A	8.17 ± 0.48
CEM_{E1000}	3.77 ± 0.38^{+++}	3.69 ± 0.53	4.71 ± 0.41*	0.25 ± 0.04	N/A	0.81 ± 0.10*	9.22 ± 1.18

Table 2.4: Rate of apically and basolaterally directed transport of rifampicin, saquinavir and methotrexate in $MDCKII_{CTL}$, $MDCKII_{MDR1}$ and $MDCKII_{MRP1}$. Rifampicin transport is also repeated in the presence of the P-gp inhibitor tariquidar (1 μM) and the MRP1 inhibitor MK571 (100 μM). Data are mean ± SD (n = 4). * $P < 0.05$ (compared to $MDCKII_{CTL}$), $^{+}$ $P < 0.05$ (compared to drug alone).

Cell Line	Transport Direction	Rate of directional transport (%/hr)				
		Rifampicin (μM)			Saquinavir	Methotrexate
		Drug Alone	+ Tariquidar	+ MK571	Drug Alone	Drug Alone
$MDCKII_{CTL}$	Apical → Basal	1.1 ± 0.1	1.1 ± 0.1	N/A	0.21 ± 0.09	0.50 ± 0.11
	Basal → Apical	8.9 ± 0.5	8.6 ± 0.3	N/A	13.6 ± 2.14	0.65 ± 0.12
$MDCKII_{MDR1}$	Apical → Basal	0.6 ± 0.1	1.3 ± 0.0	N/A	0.77 ± 0.34	N/A
	Basal → Apical	12.1 ± 0.4 *	8.1 ± 0.6^{+}	N/A	25.2 ± 1.78 *	N/A
$MDCKII_{MRP1}$	Apical → Basal	1.5 ± 0.1	N/A	2.8 ± 0.5	N/A	0.42 ± 0.13
	Basal → Apical	2.4 ± 0.2	N/A	3.0 ± 0.1	N/A	0.57 ± 0.16

2.3.10 Results Figures

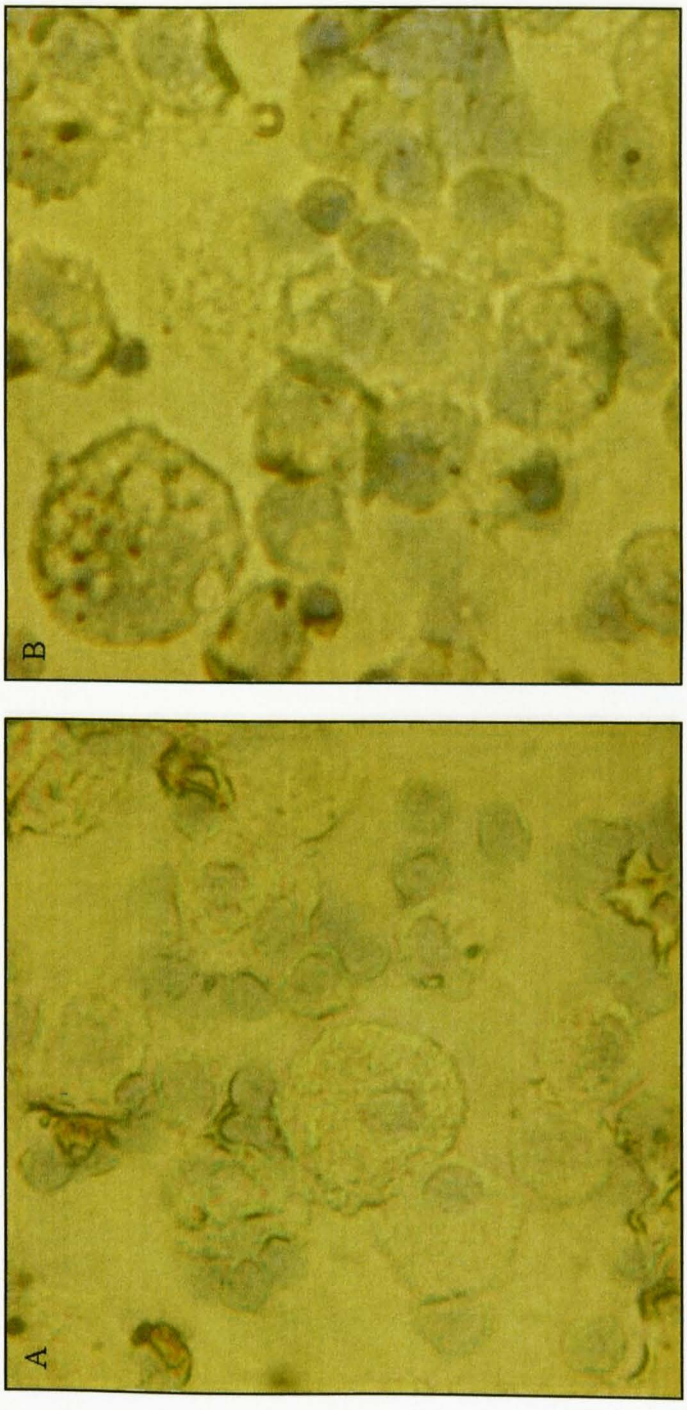

Figure 2.1: Immunohistochemical detection of P-glycoprotein in BAL cells stained with (A) isotype control antibody (IgG_{2A}) and (B) P-gp specific UIC2 antibody.

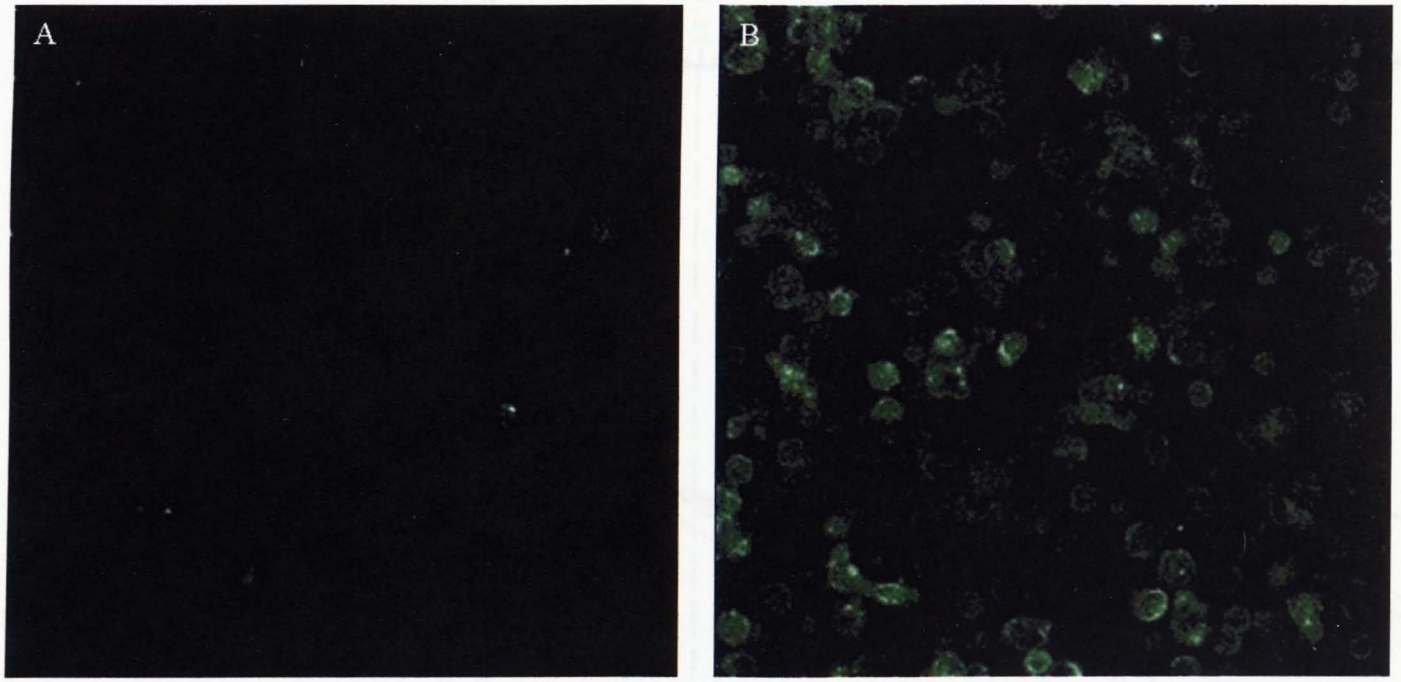

Figure 2.2: Confocal microscopy detection of P-glycoprotein in MDM cells stained with (A) rPE conjugated isotype control antibody (IgG_{2A}-rPE) and (B) rPE conjugated P-gp specific antibody. (UIC2-rPE)

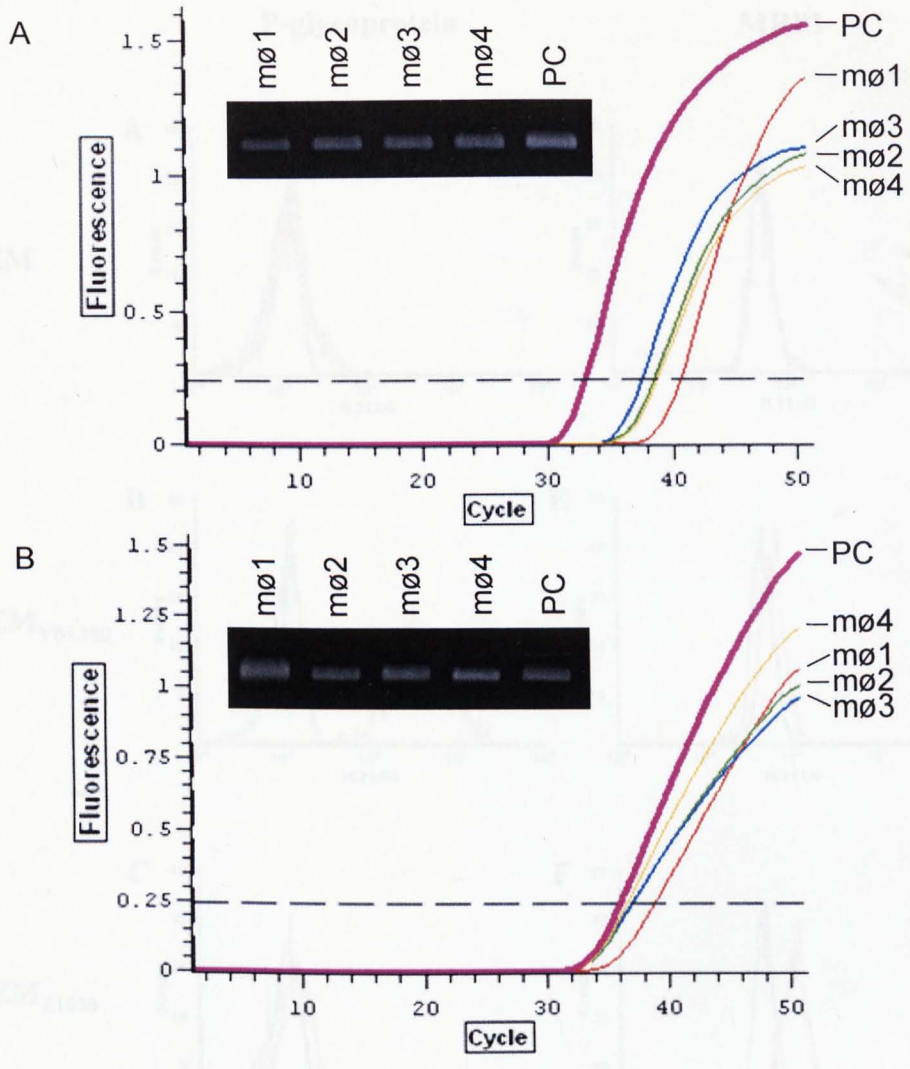

Figure 2.3: Real-time RT-PCR for the detection of (A) P-gp and (B) MRP1 in human liver cDNA (positive control) and alveolar macrophage cDNAs (mø1-4) purified from 4 BAL samples. Top left of each trace shows the PCR products of the appropriate size on a 3% agarose gel.

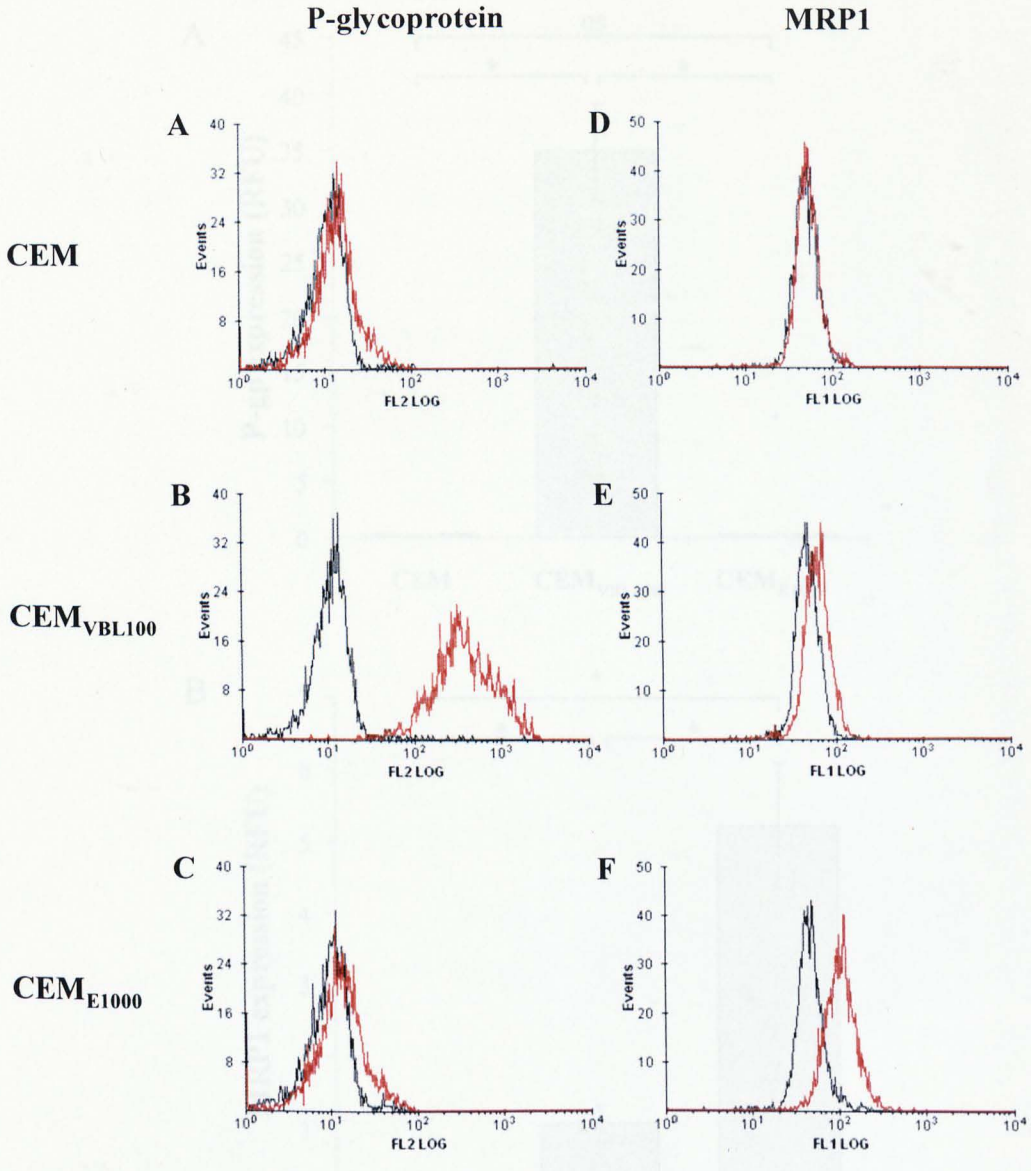

Figure 2.4: Representative flow cytometric histograms depicting the expression of P-gp (A, B, C) and MRP1 (D, E, F) in CEM (A, D), CEM_{VBL100} (B, E) and CEM_{E1000} (C, F) cell lines. Black lines (——) represent isotype control antibody binding and red lines (——) represent specific antibody binding. The difference in the mean fluorescence of the specific vs non-specific binding is used as a measure of antibody expression.

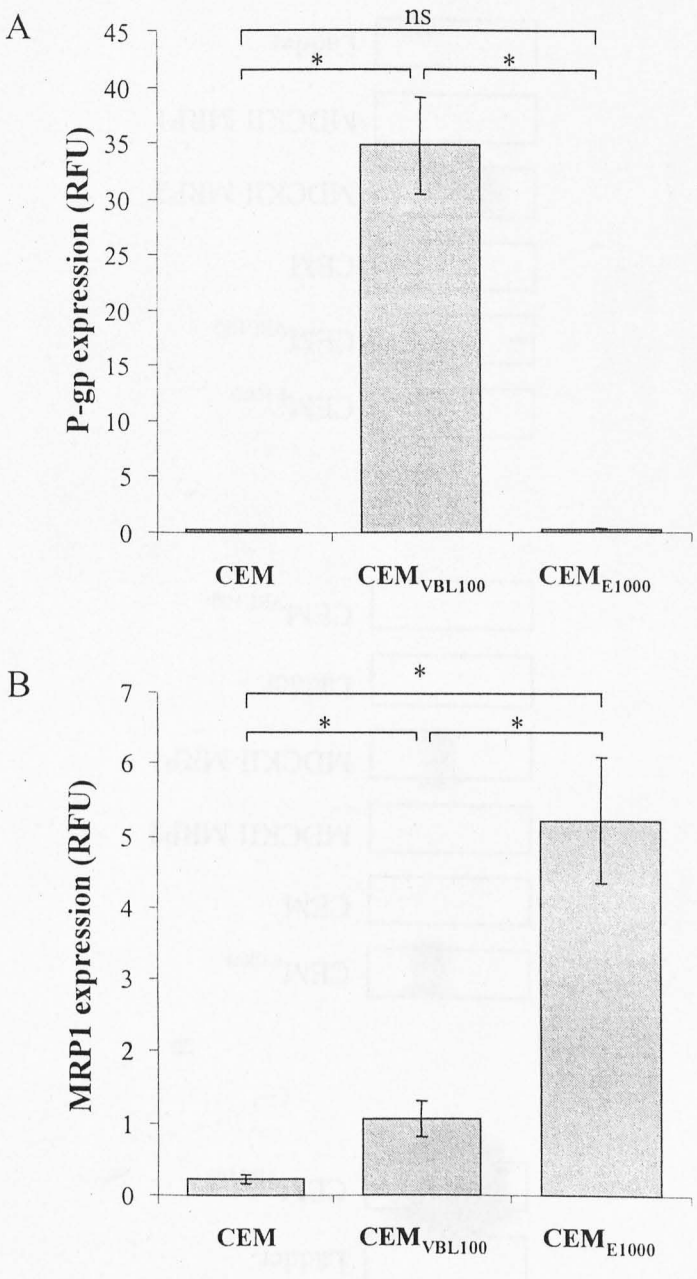

Figure 2.5: Expression of (A) P-gp and (B) MRP1 in CEM cell lines as measured by flow cytometry. Data are expressed as a mean difference in median fluorescence of the specific antibody binding to that of the non-specific antibody and are the mean of 4 independent replicates ± SD. *P < 0.05, Mann Whitney)

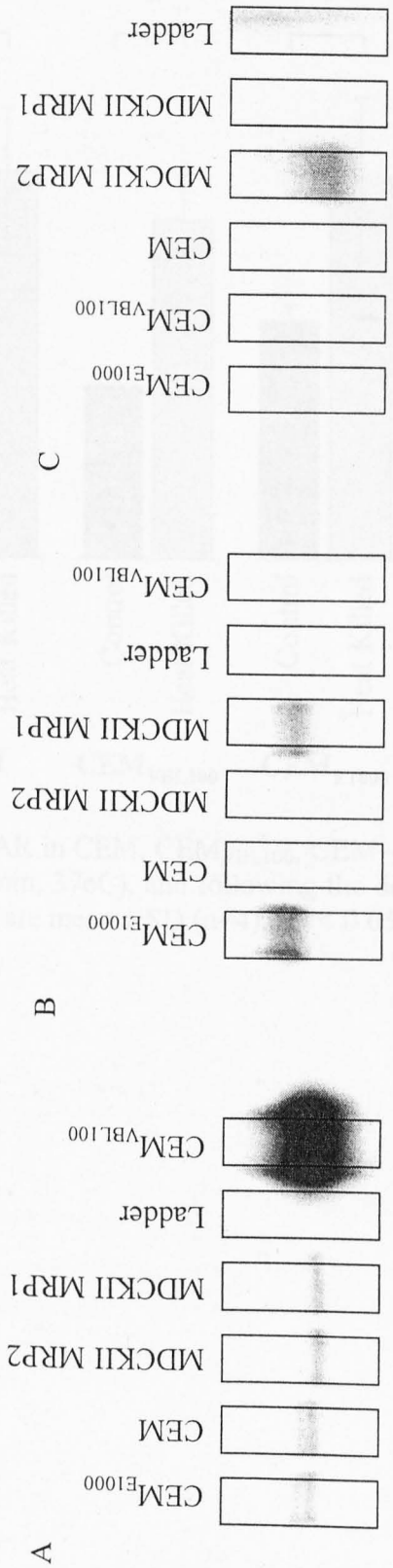

Figure 2.6: Representative western blots of P-gp (A) MRP1 (B) and MRP2 (C) expression in CEM, CEM_{VBL100}, CEM_{E1000}, $MDCKII_{MRP1}$ and $MDCKII_{MRP2}$.

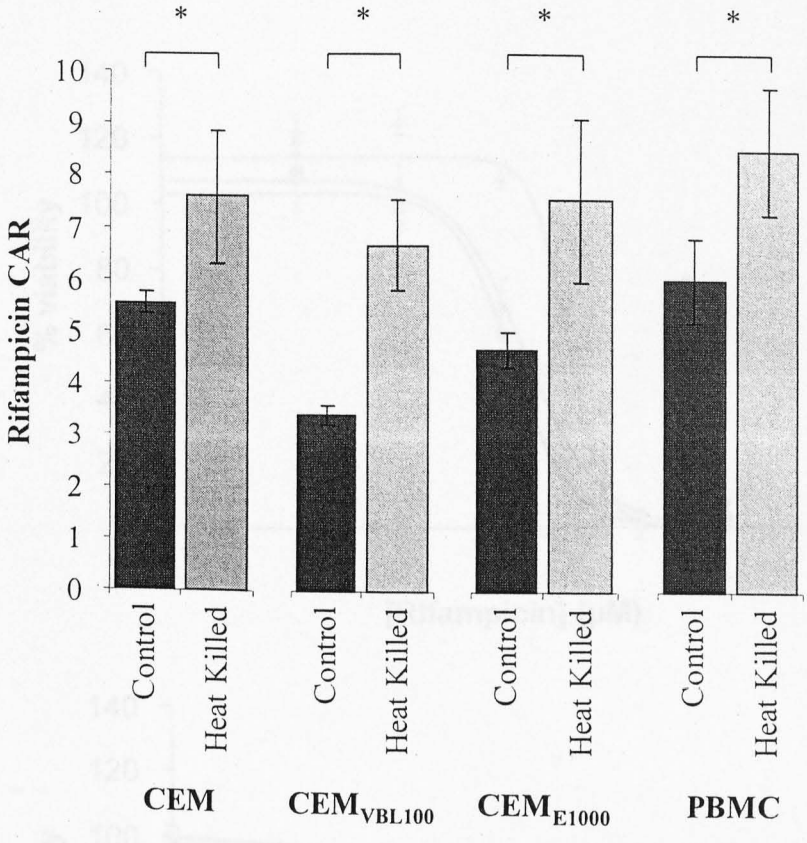

Figure 2.7: Rifampicin CAR in CEM, CEM$_{VBL100}$, CEM$_{E1000}$ and buffy coat PBMCs in control conditions (30 min, 37oC), and following the denaturing of the cells (heat kill at 60°C, 30 min). Data are mean ± SD (n=4), *P < 0.05, Mann Whitney.

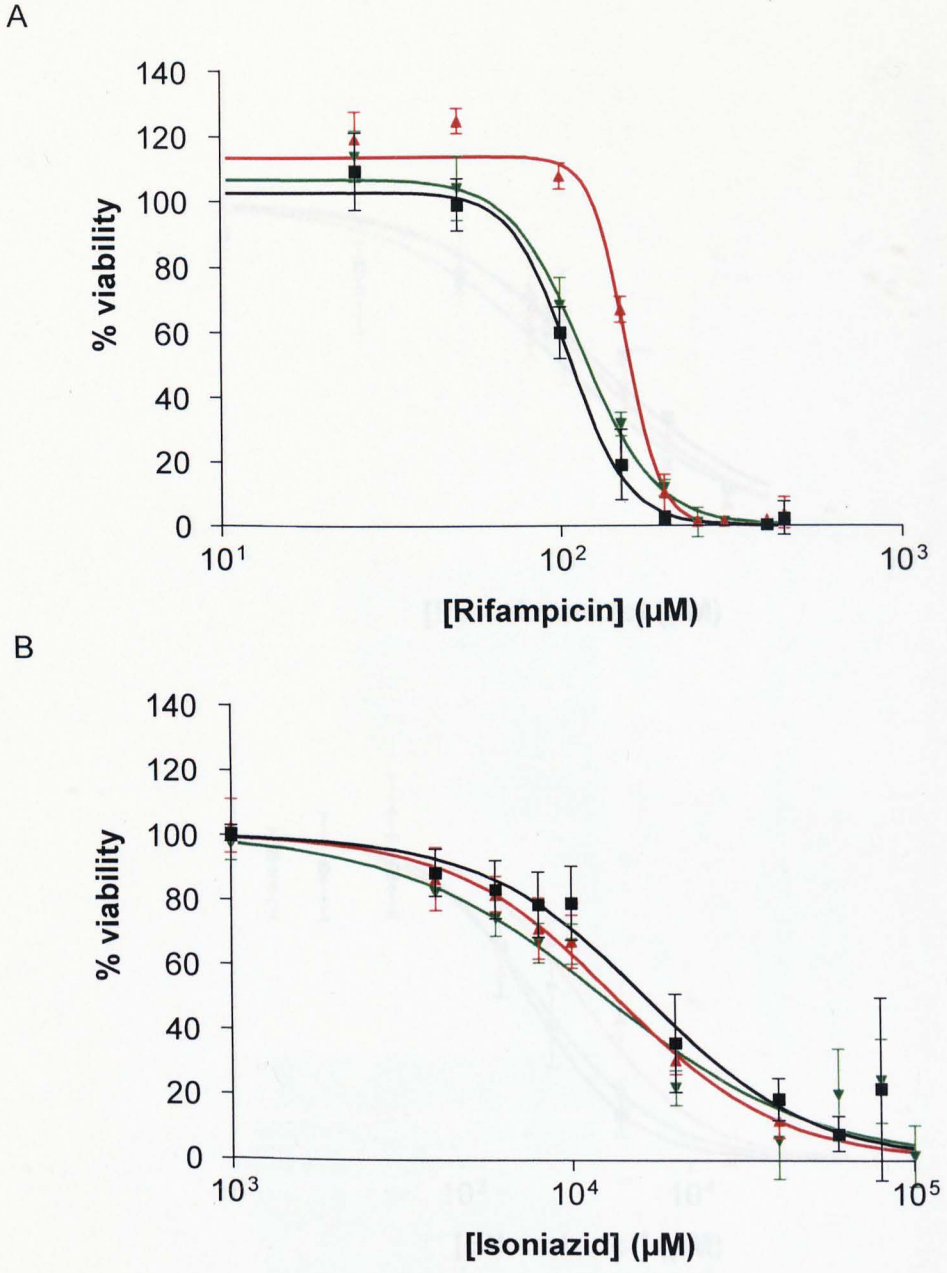

Figure 2.8: Toxicity profile of rifampicin (A) and isoniazid (B) in CEM (—■—), CEM_{VBL100} (—▲—) and CEM_{E1000} (—▼—). Results are expressed as a mean % cell viability ± SD (n = 4).

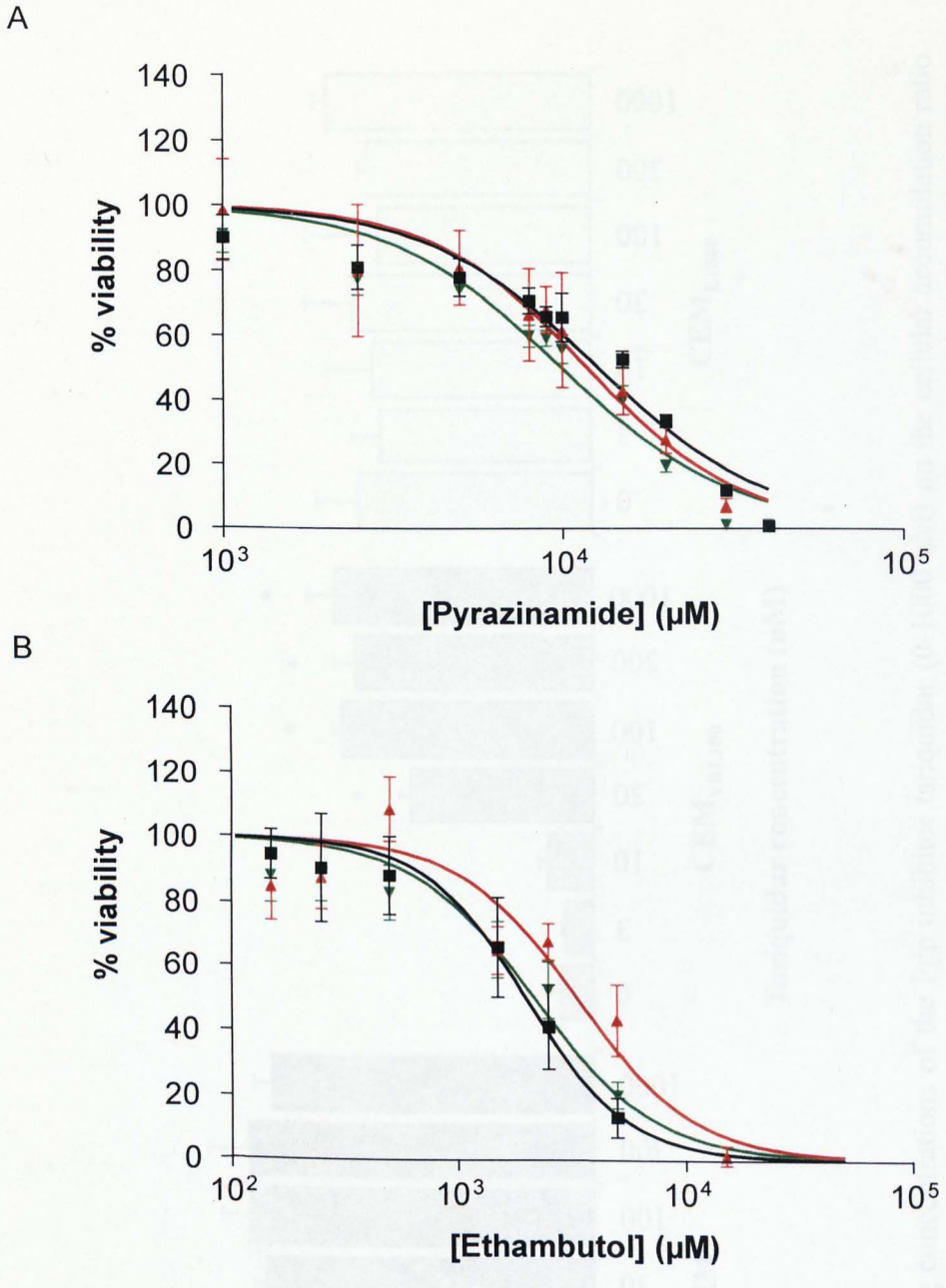

Figure 2.9: Toxicity profile of pyrazinamide (A) and ethambutol (B) in CEM (—■—), CEM_{VBL100} (—▲—) and CEM_{E1000} (—▼—). Results are expressed as a mean % cell viability ± SD (n = 4).

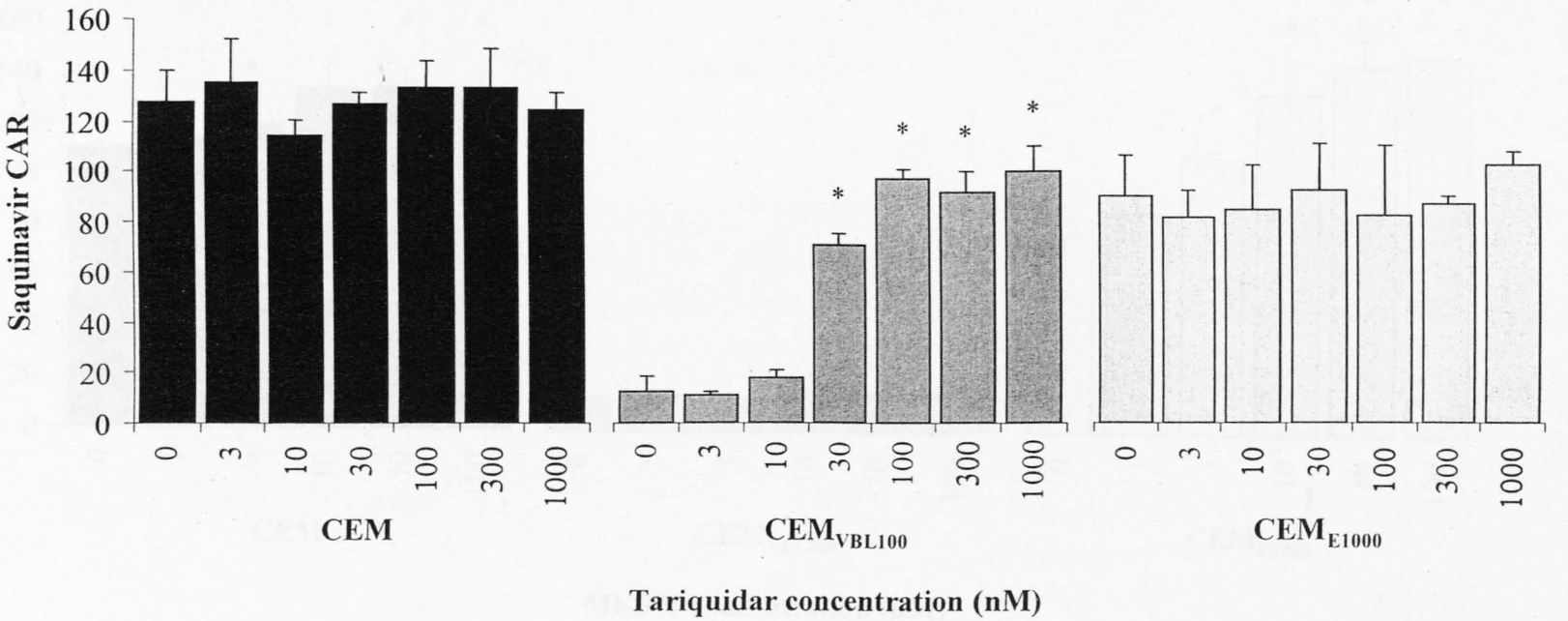

Figure 2.10: The effect of increasing concentrations of the Pgp inhibitor tariquidar (0-1000 nM) on the cellular accumulation ratio (CAR) of 10 μM saquinavir in CEM, CEM_{VBL100} and CEM_{E1000}. Saquinavir is uded as a paradigm substrate for both P-gp amd MRP1. Data are mean ± SD (n = 4). *P < 0.05, Mann Whitney

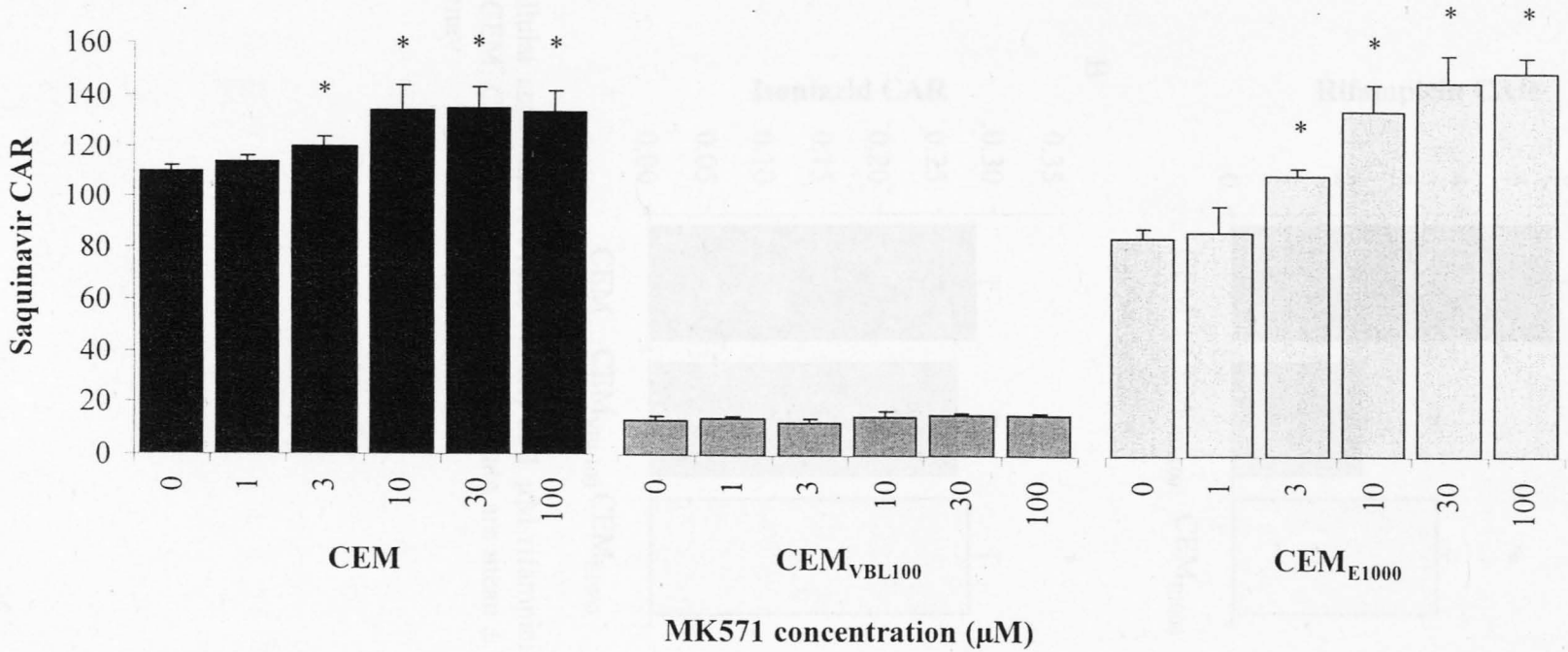

Figure 2.11: The effect of increasing concentrations of the MRP1 inhibitor MK571 (0-100 μM) on the cellular accumulation ratio (CAR) of 10 μM saquinavir in CEM, CEM_{VBL100} and CEM_{E1000}. Data are mean ± SD (n = 4). *P < 0.05, Mann Whitney

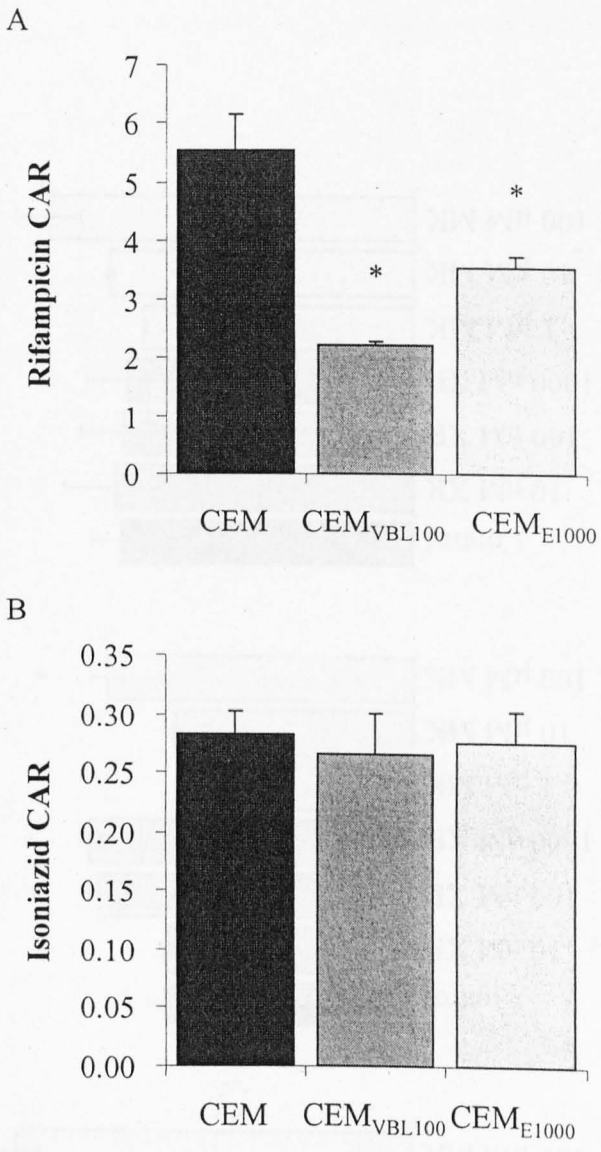

Figure 2.12: Cellular accumulation ratio (CAR) of 1 μM rifampicin (A) and 1 μM isoniazid (B) in CEM, CEM$_{VBL100}$ and CEM$_{E1000}$. Data are mean ± SD (n = 4) *P < 0.05, Mann Whitney

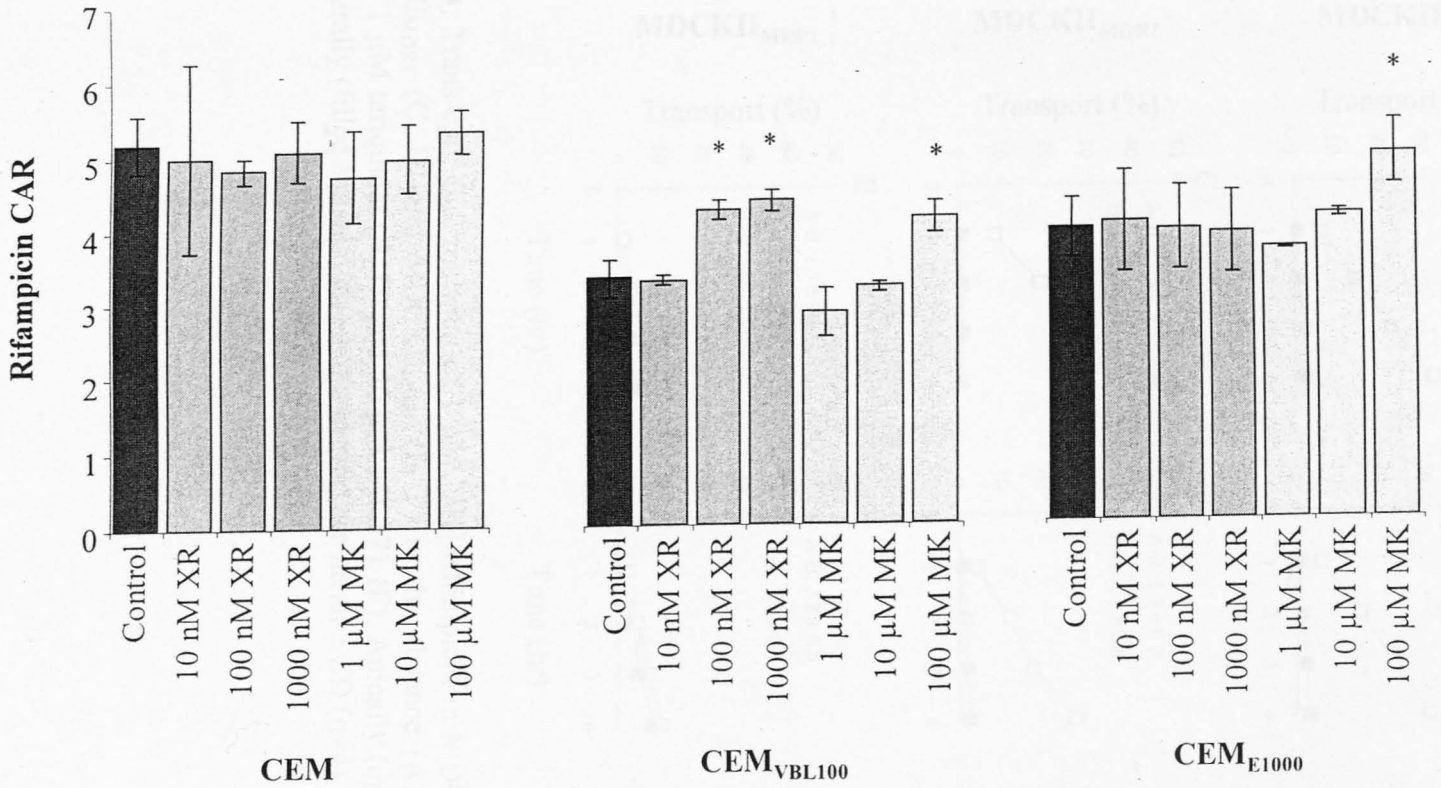

Figure 2.13: The effect of increasing concentrations of the P-gp inhibitor tariquidar (XR: 10, 100 and 1000 nM) and the MRP1 inhibitor MK571 (1, 10 and 100 μM) on the cellular accumulation ratio (CAR) of 1 μM rifampicin in CEM, CEM$_{VBL100}$ and CEM$_{E1000}$. Data are mean ± SD (n = 4). *P < 0.05, Mann Whitney

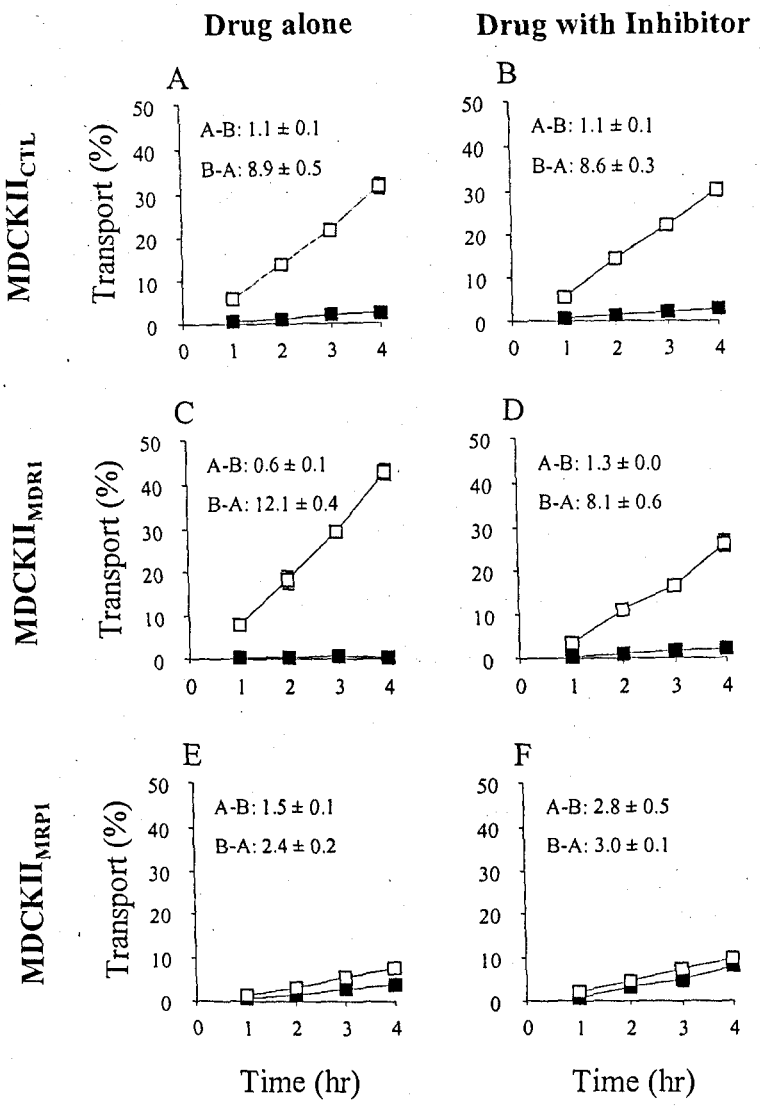

Figure 2.14: Trans-epithelial transport of 1 μM [3H]-rifampicin in MDCKII$_{CTL}$ (A, B) MDCKII$_{MDR1}$ (C, D) and MDCKII$_{MRP1}$ (E, F) in the absence (A, C, E) and presence of 1 μM tariquidar (B, D) and 50 μM MK571 (F). Apically (open squares) and basolaterally (filled squares) directed transport are mean ± SD (n=4).

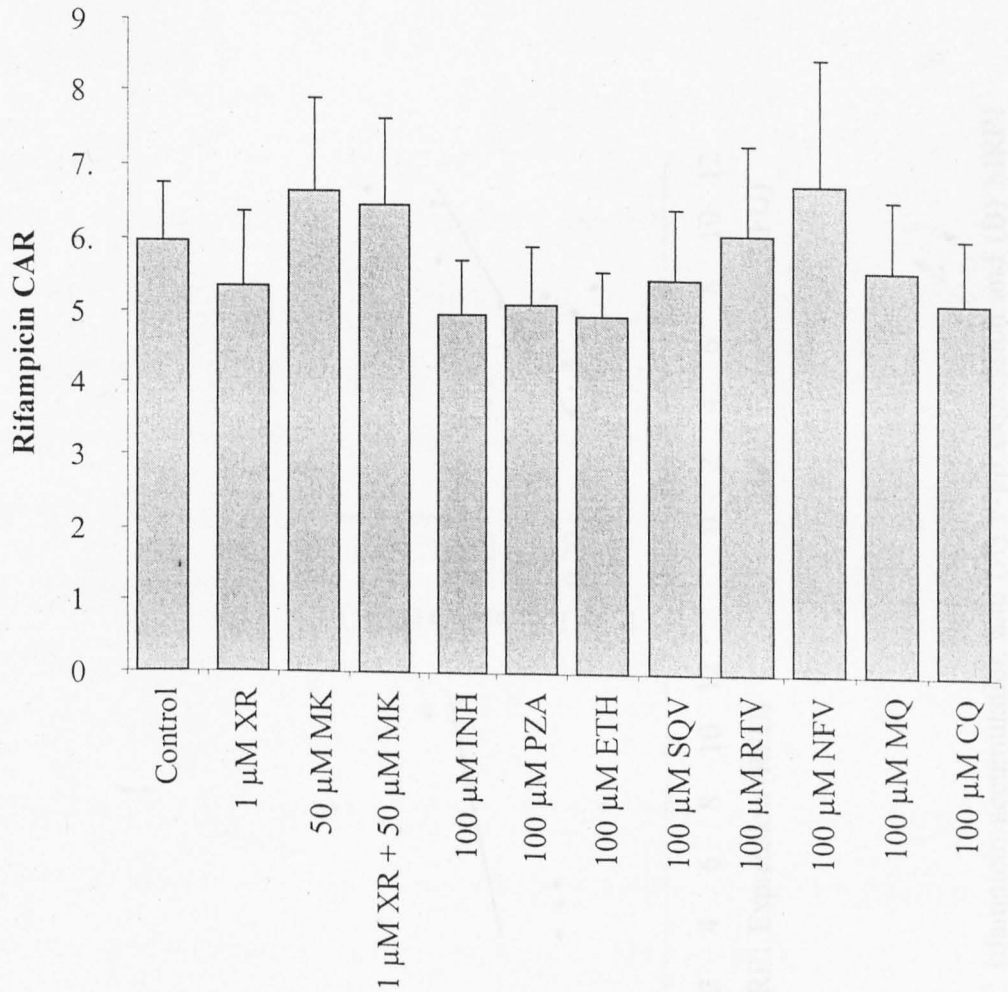

Figure 2.15: Rifampicin CAR in buffy coat PBMCs under control conditions (30 min, 37°C), and following pre-incubation of cells with tariquidar (XR), MK571 (MK), isoniazid (INH), pyrazinamide (PZA), ethambutol (ETH), saquinavir (SQV), ritonavir (RTV), nelfinavir (NFV), mefloquine (MQ) and chloroquine (CQ). Data are mean ± SD (n=6).

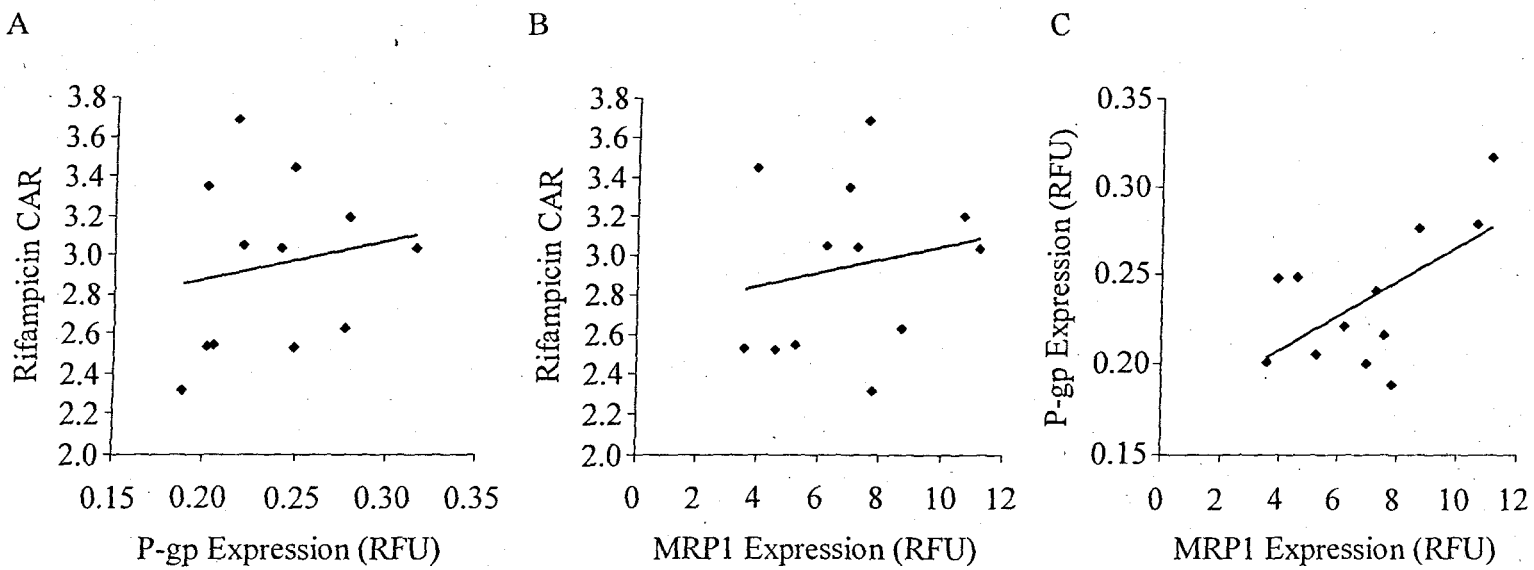

Figure 2.16: Correlation between *ex vivo* healthy volunteer PBMC rifampicin accumulation and (A) P-gp expression and (B) MRP1 expression as measured by flow cytometry. In both cases the correlation is weak ($r^2 = 0.031$ and 0.035 respectively) and non-significant. There was a significant positive relationship between basal healthy volunteer P-gp and MRP1 expression (C) ($P < 0.05$).

2.4 Discussion

Confocal, immunohistochemical and real time RT-PCR identified the presence of P-gp and MRP1 protein and mRNA transcripts in alveolar macrophages and MDMs. The presence of these active drug transporters may impact on the treatment of any pathogens surviving within macrophages, such as tuberculosis and HIV. A large number of studies have looked at the impact of these drug transporters on HIV drugs, however assessment of their impact on anti-tuberculosis drug accumulation has been limited.

Currently no human macrophage cell line is readily available to test the hypothesis that transporters may modulate the cellular accumulation of anti-TB drugs, thereby impacting upon their activity against intracellular MTB. Instead two well established methods used to determine the substrate specificity of protease inhibitors (Jones *et al.*, 2001b; Huisman *et al.*, 2002), have been utilised to determine whether the anti-TB drugs are substrates for P-gp and/or MRP1. These include using human T-lymphoblastoid cell lines (CEM) that overexpress P-gp (CEM_{VBL100}) and MRP1 (CEM_{E1000}) as well as Madin-Darby Canine Kidney cell lines (MDCKII) that overexpress P-gp ($MDCKII_{MDR1}$) and MRP1 ($MDCKII_{MRP1}$).

Initial screening of rifampicin, isoniazid, pyrazinamide and ethambutol substrate specificity for P-gp and MRP1 was performed by determining their differential toxicity in the CEM cell lines. Screening of the CEM cell lines by flow cytometry and western blot confirmed the expected P-gp and MRP1 expression profiles. Data demonstrated that CEM_{VBL100} are protected against the toxicity of rifampicin and

ethambutol compared to the parental CEM cells. Furthermore, inhibition of P-gp by tariquidar is able to fully reverse, or partially reverse the EC50 of rifampicin and ethambutol respectively to that of CEMs. The decrease in rifampicin EC50 in CEMs by tariquidar may be due to inhibition of basal P-gp mediated rifampicin transport, whilst the partial reversal of the ethambutol EC50 in CEM_{VBL100} by tariquidar suggests the influence of other transporters expressed on CEM_{VBL100} that can mediate ethambutol accumulation. This data suggests that both rifampicin and ethambutol are substrates for the P-gp, and are able to be modulated sufficiently to alter toxicity profiles.

Data showed that CEM_{E1000} were also protected against rifampicin toxicity compared to parental CEMs. However, inhibition of MRP1 by MK571 did not specifically reverse this but instead dramatically influenced rifampicin toxicity in both CEM and CEM_{E1000} cells. These data therefore suggest that the reason for the differential toxicity may be, partly caused by MRP1 overexpression. CEM_{E1000} cells were generated from CEM cells by the gradual selection in the MRP1 substrate; epirubicin. This selection process may have also altered the expression profile of other influx or efflux transporters that may influence rifampicin accumulation.

The lack of differential toxicity for isoniazid and pyrazinamide on these cells suggests that the overexpression of P-gp and MRP1 does not influence the intracellular concentrations of these drugs. However, it must be noted that both isoniazid and pyrazinamide are only toxic at very high concentrations at which the transporters might be saturated and therefore are unable to affect intracellular concentrations.

At present there is no readily available radiolabelled ethambutol and pyrazinamide, hence, we could not study their accumulation profiles in the CEM cell lines. The CAR of the control drugs saquinavir, methotrexate and diclofenac, agree with previous observations that saquinavir is a P-gp substrate (Srinivas *et al.*, 1998; Jones *et al.*, 2001a; Dallas *et al.*, 2004), methotrexate is a MRP1 substrate, (Hooijberg *et al.*, 1999; Zeng *et al.*, 2001) and diclofenac is not a substrate for these transporters.

Inhibition of P-gp and MRP1 by tariquidar and MK571 respectively was optimised using saquinavir accumulation as a reference. Tariquidar mediated inhibition of P-gp was found to be optimal above 100 nM and specific for P-gp (in agreement with (Mistry *et al.*, 2001). On the other hand, MK571 was able to optimally affect saquinavir accumulation in CEM_{E1000} above 30 μM, but at these concentrations also affected the accumulation in the parental CEM cells, suggesting a lack in specificity.

No differential accumulation was observed for isoniazid, which is in agreement with the isoniazid toxicity data, suggesting that isoniazid is not a substrate for P-gp or MRP1. Also in agreement with the toxicity data discussed above, P-gp and MRP1 are able to reduce the cellular accumulation of rifampicin in $CEM_{VBL1000}$ and CEM_{E1000} compared to the CEM. Tariquidar at 100 and 1000 nM was able to largely reverse this accumulation without altering the accumulation in CEM or CEM_{E1000} cells. MK571 was able to modulate rifampicin accumulation in CEM_{E1000}, however inhibition of rifampicin accumulation in CEM_{VBL100} by MK571 put into question whether rifampicin is a MRP1 substrate. Increased accumulation of rifampicin in CEM_{VBL100} may be due to the inhibition of basal MRP1 in CEM_{VBL100} (which is

higher than in CEMs, Fig. 2.5). However, as with the toxicity data, changes seen may indicate the inhibition of, as yet unknown transporters that influence rifampicin accumulation by MK571. No differential accumulation was observed for isoniazid, which again suggests that it is not a substrate for P-gp or MRP1.

In order to investigate if the observations generated in the CEM cell lines could be replicated in other cell types, we studied trans-epithelial transport of rifampicin and control drugs in MDCKII cell lines. As with the positive control P-gp substrate; saquinavir (Huisman *et al.*, 2002), the overexpression of P-gp in $MDCKII_{MDR1}$ (expressed apically) caused an increase in apically directed drug transport compared to the parental $MDCKII_{CTL}$ cell line. In the case of rifampicin, tariquidar was also able to completely revert transport back to that of the parental $MDCKII_{CTL}$ by tariquidar. These findings supports the data generated in the CEM cells showing that rifampicin is a P-gp substrate.

Although routine characterisation of the MDCKII cell lines by Western blot for human P-gp and MRP1 established that there was no loss of the transfected transporters (Owen *et al.*, 2003), no difference was observed in the basolateral translocation of the MRP1 positive control substrate methotrexate (Hooijberg *et al.*, 1999; Zeng *et al.*, 2001) in $MDCKII_{MRP1}$ cells compared to $MDCKII_{CTL}$. The unchanged basolaterally directed transport of rifampicin between $MDCKII_{MRP1}$ and $MDCKII_{CTL}$ cells therefore is unable to clarify whether or not rifampicin is an MRP1 substrate. Previous studies with $MDCKII_{MRP1}$ cell lines have also produced conflicting results, indicating that the antiretroviral, saquinavir, was not an MRP1 substrate (Huisman *et al.*, 2002), whilst saquinavir has been shown to be a substrate

for MRP1 by other MRP1 systems (Srinivas *et al.*, 1998; Jones *et al.*, 2001a; Dallas *et al.*, 2004).

As cell line models with high transporter expression have been utilised to determine drug substrates affinities for P-gp and MRP1, one cannot draw direct conclusions on the role of drug transporters on the modulation of anti-TB drugs in alveolar macrophages. Data looking at the modulation of rifampicin accumulation in buffy coat derived PBMCs (Fig. 2.15) however, show that basal expression of drug transporters has little effect on the rifampicin accumulation. Further, other drugs that are likely to be co-administered with rifampicin; other anti-tuberculosis drugs, anti-retrovirals and anti-malarials, had no impact on cellular rifampicin accumulation. No correlation was also found between the expression of basal P-gp and MRP1 and the rifampicin CAR. Even though transporter expression is not directly a marker of transporter activity, data does suggest that the modulation of rifampicin by basal levels of P-gp and MRP1 is limited. It must be remembered that rifampicin itself is an inducer of P-gp and may therefore be able to modulate its own efflux when P-gp expression increases.

Further studies on the role of drug transporters on rifampicin and ethambutol accumulation in alveolar macrophages are required to understand their *in vivo* role.

In summary, using these cell systems, conclusive evidence has been provided to show that rifampicin is a P-gp substrate. This adds to the original observations by (Schuetz *et al.*, 1996), that P-gp knockout mice have increased rifampicin bioavailabilty compared to the wild-type. Further, it has been demonstrated that

ethambutol is a P-gp substrate but isoniazid and pyrazinamide are not substrates for P-gp or MRP1. To understand the full contribution of the active drug transporter on the drug accumulation and anti-bacterial activity of rifampicin and ethambutol, similar studies need to be performed in alveolar macrophages of tuberculosis patients with induced P-gp.

CHAPTER 3

Characterisation of the time and concentration dependent bacteriostatic activity of anti-tuberculosis drugs on extracellular H37Rv

3.1 Introduction 111

3.2 Methods 113

3.2.1 Materials 113

3.2.2 Preparation of H37Rv suspensions 113

3.2.3 Quantification of bacterial concentrations in liquid suspensions 113

3.2.4 Determination of H37Rv sterilisation method 114

3.2.5 Determination of the lower limit of sensitivity of MTT and Alamar blue 115

3.2.6 Determination of the upper limit of sensitivity of Alamar blue 115

3.2.7 Microplate Alamar Blue Assay (MABA) 116

3.2.8 Paraformaldehyde mediated H37Rv kill by MABA 117

3.2.9 Time and drug concentration dependent kill of extracellular H37Rv 117

3.2.10 Rifampicin susceptibility of isoniazid tolerant H37Rv 118

3.2.11 Generation and assessment of rifampicin and isoniazid tolerant H37Rv strains 118

3.2.12 Data handling and statistical analysis: 119

3.3 Results 120

3.3.1 H37Rv sterilisation method: 120

3.3.2 H37Rv detection by Alamar blue and MTT 120

3.3.3 Time dependent drug kill 121

3.3.4 Rifampicin kill of isoniazid tolerant remaining H37Rv suspension 122

3.3.5 Characterisation of generated H37Rv strains 122

3.3.6 Results Tables 124

3.3.7 Results Figures 126

3.4 Discussion 135

3.1 Introduction

With the need for long term drug therapy to fully eradicate TB from a patient's body, it is important to understand the pharmacology of the anti-TB drugs on *Mycobacterium tuberculosis* (MTB) over time. Targeting extracellular bacilli is an important component at the beginning of TB therapy (early bactericidal activity: EBA). Numerous assays have previously been employed to examine a 'snap-shot' determination of the drug concentration dependent sterilisation activity of extracellular MTB. Limited data are however available on the effect of both drug concentration and exposure time on the sterilisation of extracellular bacilli.

Traditional culture methods for extracellular MTB drug susceptibility testing is by the proportion method, performed on solid media (middlebrook 7H10/7H11 agar or Lowenstein-Jensen slopes). However, solid media culture experiments are very time consuming (at least 3 weeks) because MTB grows more slowly on solid media than in liquid culture (Cheng *et al.*, 1994). In the search for high throughput methods to assess multi-drug resistant tuberculosis, many new screening methods have been developed involving liquid culture. In addition to assessing bacterial strain resistance, these novel methods can also be utilised to increase the understanding of the anti tuberculosis activity of current drugs.

The two main colourimetric methods developed for quantifying MTB drug susceptibility are the microplate based MTT assay (MMA) and the microplate based Alamar blue assay (MABA). MTT and Alamar blue are the two respective indicator dyes used by these methods to determine MTB viability in the presence of drugs. Both the MMA and the MABA assay have been routinely used in determining drug

sensitivity and susceptibility (Collins and Franzblau, 1997; Abate *et al.*, 1998; Franzblau *et al.*, 1998; Mshana *et al.*, 1998; De Logu *et al.*, 2001; Caviedes *et al.*, 2002; Foongladda *et al.*, 2002; Luna-Herrera *et al.*, 2003; Abate *et al.*, 2004; Reis *et al.*, 2004).

More sophisticated liquid culture drug susceptibility assays such as the BACTEC system can also be used which relies on the determination of the rate of ^{14}C-labeled CO_2 as an indicator of MTB viability (Collins and Franzblau, 1997; Jayaram *et al.*, 2003; Jayaram *et al.*, 2004). Further, the Green Fluorescent Protein microplate assay (GFPMA) can be used to measure drug susceptibility by utilising an H37Rv MTB strain containing a transfected green fluorescent protein reporter gene (H37Rv *gfp*) (Changsen *et al.*, 2003).

In this study the MABA assay has been developed to characterise the time and concentration dependent bacteriostatic activity of rifampicin, isoniazid, ethambutol and pyrazinamide on H37Rv grown in liquid culture. Further, we examined the emergence of drug resistance and tolerance by MTB over time in the MABA.

3.2 Methods

3.2.1 Materials

Middlebrook 7H9, Middlebrook 7H11, and the oleic acid, albumin, dextrose mix (OADC) were purchased from Becton Dickinson, Oxford, UK. Alamar blue was obtained from Serotec, Oxford, UK. The *Mycobacterium tuberculosis* reference strain (H37Rv) was obtained from the American Type culture Collection (ATCC, Rockville, MD). All other materials were purchased from Sigma-Aldrich (Poole, UK).

3.2.2 Preparation of H37Rv suspensions

To obtain log-phase bacterial suspensions, H37Rv was grown on Lowenstein Jensen slopes (37°C, 2 weeks). Individual colonies were then transferred to a 28 ml McCartney bottle containing around 20 borosilicate solid glass beads (2 mm diameter) and 5 ml of Middlebrook 7H9 broth (Becton Dickinson, Oxford, UK) supplemented with 0.2 % (v/v) Glycerol, 0.05 % (v/v) Tween 80 and 10 % (v/v) OADC (oleic acid, albumin, dextrose, catalase; Becton Dickinson, Oxford, UK)(7H9GT). The suspension was vortexed to break up clumps and allowed to grow (1 week, 37°C).

3.2.3 Quantification of bacterial concentrations in liquid suspensions

McFarland standards were used to standardise the approximate number of bacteria in a liquid suspension by comparing their turbidity at 600 nm (Ab600) to that of the McFarland standards (McFarland, 1907). McFarland standards were prepared by thoroughly mixing 1% (w/v) $BaCl_2$ and 1% (w/v) H_2SO_4 as shown in Table 3.1. A standard curve was generated by measuring the Ab600 (Biowave CO8000 cell

density meter, Jencons-PLS, Bedfordshire, UK) of each standard (500 µL) and plotting it against their representative bacterial concentrations (McFarland No 1 is approximately 3 x 10^8 cfu/ml). Prior to each experiment, H37Rv suspensions were vortexed thoroughly and clumps left to settle (10 min). The turbidity was then measured (Ab600) and bacterial concentration estimated of the standard curve.

Table 3.1: Representative bacterial concentrations for the different McFarland standards, and the proportion of 1% $BaCl_2$ and 1% H_2SO_4 needed to produce them.

McFarland Standard No.	Bacterial concentration (CFU/ml)	1% $BaCl_2$ Volume (µL)	1% H_2SO_4 Volume (µL)
0	0	0	10000
0.5	1.5 x 10^8	50	9950
1	3 x 10^8	100	9900
1.5	4.5 x 10^8	150	9850
2	6 x 10^8	200	9800
2.5	7.5 x 10^8	250	9750
3	9 x 10^8	300	9700

3.2.4 Determination of H37Rv sterilisation method

To allow for the analysis of experimental procedures outside the category 3 facility it was essential to determine a suitable method to sterilise H37Rv suspensions. H37Rv suspensions were diluted to 1 x 10^7 CFU/ml in 7H9GT broth and aliquoted into a 96 well plate (100 µL). To respective wells, either Alamar blue working solution (30 µL, 2:1 (v/v) Alamar blue, 10 % Tween 80), MTT working solution (20 µL, 5 mg/ml MTT) or 7H9GT (30 µL) was added. Following incubation (37°C, 24 hr), 100 µL of the following potential sterilising solutions was added to the wells with and without the added dyes: 7H9GT (Control), 20% SDS 50% dimethylformamide (MTT lysis buffer), 0.1 N HCl in isopropanol, 1 % paraformalydehyde, 2 % paraformalydehyde, 4 % paraformalydehyde and 8 % paraformalydehyde.

Following incubation (24 hr, 37°C), samples were transferred to screwcap tubes and washed 3 times (1 ml sterile PBS, 2000 x g, 10 min). The H37Rv pellets were then resuspended (100 µL 7H9GT) and transferred onto Middlebrook 7H11 plates (supplemented with 0.2 % (v/v) Glycerol, 0.05 % (v/v) Tween 80 and 10 % (v/v) OADC). Plates were then incubated (8 weeks, 37 °C) before being scored for H37Rv colony growth (culture positive or negative).

3.2.5 Determination of the lower limit of sensitivity of MTT and Alamar blue

Stock H37Rv suspensions were quantified (n=4) and serially diluted (1 in 3) in 7H9GT (1 x 10^7 to 1 x 10^3 cfu/ml). 100 µL of each H37Rv concentration was added to a 96 well plate (8 wells per plate, in duplicate) as well as 100 µL of media (negative control). 20 µL of MTT (5mg/mL) or 30 µL of Alamar blue (2:1 (v/v) Alamar blue: 10% Tween 80) was added to all the wells of paired plates. Following incubation (24 hr, 37°C) 100 µL of MTT lysis buffer (100µL, 20% SDS 50% dimethylformamide) was added to the MTT plates and 8 % paraformaldhyde to the Alamar blue plates. Following further incubation (24 hr, 37 °C), H37Rv MTT formazan (MTT metabolite) formation was measured at an absorbance of 570 nm, while the Alamar blue reduction was measured by a fluorescence spectrophotometer (excitation 530 nm, emission 590 nm). Data were expressed as percentage increased fluorescence or absorbance compared to the H37Rv free control.

3.2.6 Determination of the upper limit of sensitivity of Alamar blue

The experiment was performed as described above but with a H37Rv concentration ranging from 1 x 10^8 to 1 x 10^5 cfu/ml. Alamar blue was used to measure H37Rv viability.

3.2.7 Microplate Alamar Blue Assay (MABA)

This assay was set up as described by (Collins and Franzblau, 1997) with certain modifications. Briefly, 96 well microplates were set up as in Fig 3.1. Sterile PBS (200 µl) was added to the outside two wells of a 96 well plate to reduce later evaporation from the inner wells. Serial drug dilutions were made up in 7H9GT (at two times the desired concentration) and added to the columns (50 µL) of a 96 well plate (leaving one column as a drug free control: 7H9GT only). 50 µL of 7H9GT was then added to the top row (H37Rv free, drug only control). Stock H37Rv suspension concentrations were determined, diluted (2 x 10^7 cfu/ml in 7H9GT) and added to the bottom 3 rows (50 µL). The plate was then returned to the incubator (37 °C) for the desired amount of time.

Figure 3.1: Representation of the layout of the MABA microplate. Blue wells represent PBS to reduce sample evaporation.

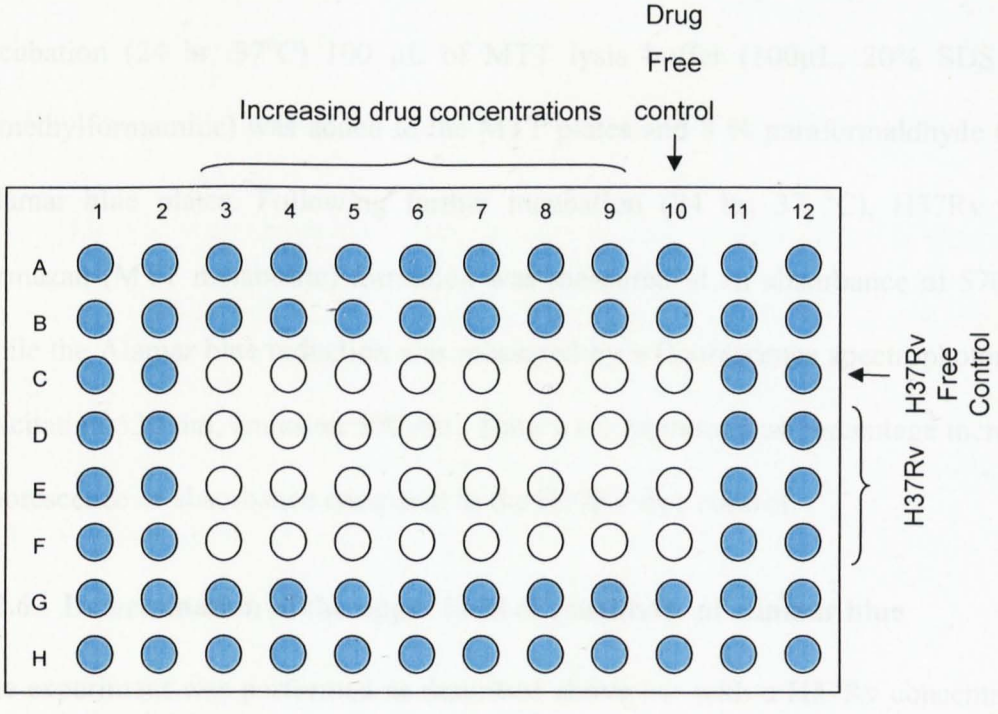

Following the incubation, 30 µL of Alamar blue (2:1 (v:v) Alamar blue: Tween 80) was added to the test wells to determine H37Rv viability. Following incubation (24

hr, 37 °C) the plate was sterilised by the addition of 8 % paraformaldhyde (100 µL) and the Alamar blue plates were read by a fluorescence spectrophotometer (excitation 530 nm, emission 590 nm). Data was presented as background (H37Rv free) corrected fluorescence or absorbance units.

3.2.8 Paraformaldehyde mediated H37Rv kill by MABA

To investigate the paraformaldehyde concentration dependent sterilisation of H37Rv, MABA was used. Serial 2 fold dilutions of paraformaldehyde (10%) were performed and 50 µL added to each column of a 96 well plate (n=4). Stock H37Rv suspensions were quantified, diluted to 3 x 10^8 cfu/ml (McFarland standard No 1), and 50 µL added to each well (n=4). Following incubation (24hr, 37°C), 30 µL of Alamar blue working solution (2:1 (v/v) Alamar blue: 10% Tween 80) was added to each well (24hr, 37°C). 100 µL of 8% paraformaldehyde was then added (24hr, 37°C) and H37Rv viability assessed as described before in section 3.2.7.

3.2.9 Time and drug concentration dependent kill of extracellular H37Rv

To determine the concentration and time dependent kill of H37Rv, 4 quadruplicate rifampicin (final conc. 0.23 – 166 ng/mL), isoniazid (6.9 – 5000 ng/mL), ethambutol (69 – 50000 ng/mL) and pyrazinamide (69 – 50000 ng/mL) MABA plates were set up with a final bacterial concentration of approximately 1 x 10^7 cfu/ml. H37Rv viability was determined at day 0, 7, 14 and 21.

Simultaneously, one 96 well plate was prepared containing the same drug concentrations as above, but with a bacterial mixture of the 4 stock H37Rv mixtures (final concentration of approx. 1 x 10^7 cfu/ml). The full 100 µL of each well was

then transferred onto a 7H11GT agar plate made to the same drug concentration as the sample. 7H11GT agar plate were incubated (3 weeks, 37°C) and H37Rv colony growth assessed.

3.2.10 Rifampicin susceptibility of isoniazid tolerant H37Rv

At bacterial concentrations above 1 x 10^7 cfu/ml, isoniazid exposure (up to 5000 ng/mL for 7 days) is unable to prevent H37Rv mediated Alamar blue turnover. In order to determine if this phenomenon is due to viable, isoniazid tolerant bacteria, the bacterial population was tested for its rifampicin susceptibility. For this experiment one MABA plate was set up with an isoniazid curve (final conc.: 6.9 – 5000 ng/mL), and another with all wells containing 5000 ng/ml isoniazid. Both plates contained 50 µL of drug and 50 µL of H37Rv (final conc. 3 x 10^7 cfu/mL). Following incubation (7 days, 37°C), 50 µL of rifampicin (0 – 500 ng/mL, final conc. 0 – 166 ng/mL) was added to the plate containing the H37Rv bacteria in 5 µg/ml isoniazid. Following further incubation (7 days, 37°C) both plates were analysed for H37Rv viability.

3.2.11 Generation and assessment of rifampicin and isoniazid tolerant H37Rv strains

Middlebrook 7H11 agar plates (Becton Dickinson, Oxford, UK) supplemented with 0.2 % (v/v) Glycerol, 0.05 % (v/v) Tween 80 and 10 % (v/v) OADC (oleic acid, albumin, dextrose, catalase; Becton Dickinson, Oxford, UK)(7H11GT) were made containing isonaizid (5000 ng/mL) or rifampicin (166 ng/mL). H37Rv suspensions were then diluted (to: 3 x 10^8, 3 x 10^7, 3 x 10^6 and 3 x 10^5 cfu/ml) and 100 µL spread over 7H11GT plates. Following incubation (3 weeks, 37°C) single colonies were selected from the 7H11GT plates containing isoniazid ($H37Rv_{INH}$) or rifampicin ($H37Rv_{RIF}$) and split into either 7H9GT ($H37Rv_{RIF/MEDIA}$ and $H37Rv_{INH/MEDIA}$) or in

7H9GT containing 5000 ng/mL isoniazid ($H37Rv_{INH/INH}$) or 166 ng/mL rifampicin ($H37Rv_{RIF/RIF}$). H37Rv strains were grown up and split in their respective medias (3 weeks, 37°C) to allow for reversal of tolerance.

To determine whether the developed drug tolerance was reversible or permanent, 7 day isoniazid susceptibility curves (6.9 – 5000 ng/mL) were performed on the original parental H37Rv, $H37Rv_{INH/MEDIA}$ and $H37Rv_{INH/INH}$ strains, and a rifampicin susceptibility curve (0.23 – 166 ng/mL) on the parental H37Rv, $H37Rv_{RIF/MEDIA}$ and $H37Rv_{RIF/RIF}$. Also an ethionamide susceptibility curve was run on the parental H37Rv, $H37Rv_{INH/MEDIA}$ and $H37Rv_{INH/INH}$ strains.

To determine the level of growth fitness of the generated H37Rv strains their growth rate was determined. Serial (1 in 3) dilutions of the H37Rv strains (in 7H9GT) were made ($0 – 1 \times 10^8$) and 100 µL added to 96 well plate (quadruplicate). Following 0, 2, 4, 7 and 9 day incubation (37°C) Alamar blue was added to the wells (24 hr, 37°C) and terminated (24 hr, 37°C). The rate of growth for each H37Rv concentration was determined when growth was linear (linear part of sigmoidal growth curve).

3.2.12 Data handling and statistical analysis:

EC50 and EC90 data were measured using Graphpad Prism (3.0). Analysis for statistical significance of the change in EC50 over time was measured by Paired T-test analysis.

3.3 Results

3.3.1 H37Rv sterilisation method:

Following the one day incubation of H37Rv in the presence of MTT or Alamar blue all wells displayed colour change. Following a subsequent 24 hr exposure to proposed killing solutions, bacterial viability was assessed by 8 week culture positivity. Results indicate that neither MTT nor Alamar blue alone affected H37Rv viability, while all the sterilising solutions tested did result in culture negative 7H11GT plates after 8 weeks (Table 3.2). It was noted however that 0.1 N HCL isopropanol caused a colour change to the MTT formazan and the reduced Alamar blue. Further, paraformaldehyde did not solublise MTT formazan and could therefore not be used for the MTT assay. Concentration dependent sterilisation of H37Rv using the MABA showed that concentrations of paraformaldehyde above 0.5 % for 24hr prevented H37Rv mediated Alamar blue turnover (Fig. 3.2).

3.3.2 H37Rv detection by Alamar blue and MTT

Both Alamar blue and MTT were good surrogate markers for H37Rv viability. However, Alamar blue (lower limit of sensitivity around 1 x 10^5 cfu/ml, 1 x 10^4 cfu/well) was around 10 fold more sensitive than MTT (lower limit of sensitivity around 1 x 10^6 cfu/ml, 1 x 10^5 cfu/well) in measuring H37Rv viability (Fig. 3.3). Alamar blue turnover saturates at around 2 x 10^7 cfu/ml (Fig. 3.4).

3.3.3 Time dependent drug kill

Differential day 0 H37Rv mediated Alamar blue turnover between the individual replicates (Fig. 3.5A, 3.6A, 3.7A and 3.8A) illustrate variation in the initial inoculum (n=2 > n=4 > n=1 > n=3).

Rifampicin concentration viability curves (Fig. 3.5) show that there is a gradual increase in the EC50 from 1.55 ng/mL (day 7) to 24.7 ng/mL (day 21) (Table 3.3). Further, rifampicin eliminates the basal level of Alamar blue turnover (Day 0), within 7 days. All the samples that were placed on rifampicin containing 7H11GT were positive (with at least 100 colonies per plate) (Table 3.4).

Isoniazid concentration viability curves show a dramatic increase in the EC50 over time (Fig. 3.6) (Table 3.3). Day 7 H37Rv susceptibility to isoniazid is relatively consistent at 47.6 ± 7.78 ng/mL (mean ± SD, n=4). At day 14, 2 of the four independent replicates show full isoniazid tolerance (at 5000 ng/mL), whilst the other 2 show increased EC50. At day 21, 3 of the four independent replicates show full isoniazid tolerance. Further, isoniazid caused an increase (not decrease) in the basal (day 0) Alamar blue turnover, over the course of the 3 weeks. Samples that were placed on isoniazid containing 7H11GT were positive (with at least 100 colonies per plate) at concentrations below 61.7 ng/mL. At and above this concentration (5000 ng/mL) a small number of colonies were able to persist (Table 3.4).

Ethambutol concentration dependent decrease in H37Rv viability remained unchanged over the 3 week period (Fig. 3.7) (Table 3.3). Ethambutol caused a time

dependent decrease of the basal level (Day 0) of Alamar blue turnover, taking at least 2 weeks to eliminate detectable turnover. Samples that were placed on ethambutol containing 7H11GT were positive (with at least 100 colonies per plate) at concentrations below 617 ng/mL. At 617 ng/mL there was a sharp reduction in cfu to 4, and at higher concentration there were no cfu at all (Table 3.4).

Pyrazinamide in this MABA model showed no apparent anti-tuberculosis activity at concentrations below 50 µg/ml (Fig. 3.8) (Table 3.3). All samples that were placed on pyrazinamide containing 7H11GT were also positive (Table 3.4).

In order to compare the results with those published by other sources, EC90 data were also calculated as an indicator of the MIC (Table 3.3)

3.3.4 Rifampicin kill of isoniazid tolerant remaining H37Rv suspension

Following 14 day incubation of H37Rv in isoniazid concentrations, on average the remaining bacillary load was still able to turnover Alamar blue (14 day isoniazid EC50: 52.0 ng/mL isoniazid). This remaining Alamar blue turnover by H37Rv could however be eliminated by rifampicin (14 day isoniazid + 7 day rifampicin EC50: 5.66 ng/mL rifampicin) (Fig. 3.9).

3.3.5 Characterisation of generated H37Rv strains

$H37Rv_{RIF/RIF}$, was resistant to all concentrations of rifampicin (below 166 ng/mL), whilst $H37Rv_{RIF/MEDIA}$ rifampicin susceptibility (mean EC50 ± SD: 3.86 ± 0.30 ng/mL) reverted to that of the wildtype H37Rv (EC50: 3.69 ± 0.24 ng/mL) (Fig.

3.10). The $H37Rv_{INH/INH}$ was resistant to all concentrations of isoniazid (below 5000 ng/mL). $H37Rv_{INH/MEDIA}$ was also fully isoniazid tolerant and did not revert back to the isoniazid susceptible parental H37Rv (EC50: 52.7 ± 1.55 ng/mL) (Fig. 3.11). Ethionamide concentration, H37Rv viability curves showed no difference in the EC50 between wildtype (3081 ± 824 ng/mL) and $H37Rv_{INH}$ strains ($H37Rv_{INH/INH}$: 3064 ± 778, $H37Rv_{INH/MEDIA}$: 2655 ± 1003 ng/mL). Analysis of the growth rates of the different H37Rv strains indicated no differential growth rate in 7H9GT (Table 3.5).

3.3.6 Results Tables

Table 3.2: The sterilising effect of various agents on H37Rv suspensions at 1 x 10^8 cfu/ml. H37Rv was first grown for 24hr in the presence or absence of the viability dyes (Alamar blue or MTT) followed by 24 hrs of different killing solutions. H37Rv viability is assessed by culture positivity of plates at 8 weeks (n=4).

	8 week H37Rv colony growth		
Killing Solution	**Control**	**Alamar Blue**	**MTT**
7H9GT	+ ve	+ ve	+ ve
20% SDS 50% dimethylformamide	- ve	- ve	- ve
0.1 N HCl in isopropanol	- ve	- ve	- ve
1 % paraformalydehyde	- ve	- ve	- ve
2 % paraformalydehyde	- ve	- ve	- ve
4 % paraformalydehyde	- ve	- ve	- ve
8 % paraformalydehyde	- ve	- ve	- ve

Table 3.3: EC50 and EC90 values for the drug concentration vs H37Rv viability curves after 7, 14 and 21 days of drug exposure. Data are presented as mean (range) (n=4), * $p \leq 0.05$, paired T-test (compared to day 7 data).

	MIC/EC90	Mean EC50 (range) ng/mL		
Drug	**Mean ± STD**	**Day 7**	**Day 14**	**Day 21**
Rifampicin	2.2 ± 0.2	1.55 (0.70-1.96)	7.38 (2.02-17.8)*	24.7 (5.60-45.3)*
Isoniazid	60 ± 11	47.6 (36.7-54.7)	53.2 (35.3-71.0)*	>5000 (61.3->5000)*
Ethambutol	634 ± 198	390 (211-591)	514 (494-531)	574 (393-673)
Pyrazinamide	>50000	>50000	>50000	>50000

Table 3.4: Number of H37Rv colonies 3 weeks after approximately 1 x 10^6 cfu were added to drug containing 7H11GT plates. Colony counting was performed when plates contained less than 100 colonies.

Rifampicin		Isoniazid		Ethambutol		Pyrazinamide	
(ng/mL)	CFU	(ng/mL)	CFU	(ng/mL)	CFU	(ng/mL)	CFU
0	>100	0	>100	0	>100	0	>100
0.23	>100	6.86	>100	68.6	>100	68.6	>100
0.69	>100	20.6	>100	206	>100	206	>100
2.06	>100	61.7	5	617	4	617	>100
6.17	>100	185	6	1852	0	1852	>100
18.5	>100	556	3	5555	0	5555	>100
55.5	>100	1667	4	16666	0	16666	>100
166	>100	5000	2	50000	0	50000	>100

Table 3.5: The growth rate of the H37Rv strains. Data are expressed as the mean increase in fluorescence units per day ± SD.

H37Rv strain	Growth Rate (Increase in Fluorescence units/ day)
H37Rv	726 ± 90
$H37Rv_{INH/MEDIA}$	752 ± 120
$H37Rv_{INH/INH}$	687 ± 73
$H37Rv_{RIF/MEDIA}$	621 ± 70
$H37Rv_{RIF/RIF}$	709 ± 106

3.3.7 Results Figures

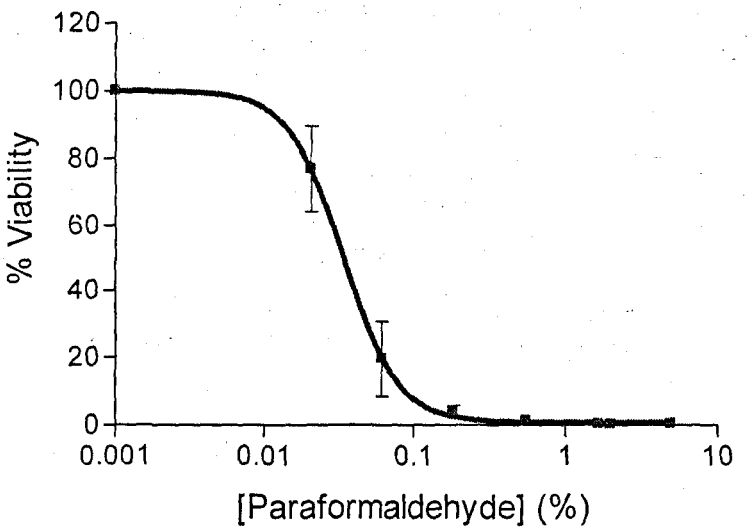

Figure 3.2: H37Rv viability after 24 hr exposure to increasing concentrations of paraformaldehyde. H37Rv viability expressed as percentage Alamar blue turnover compared to paraformaldehyde free control ± SD (n=4).

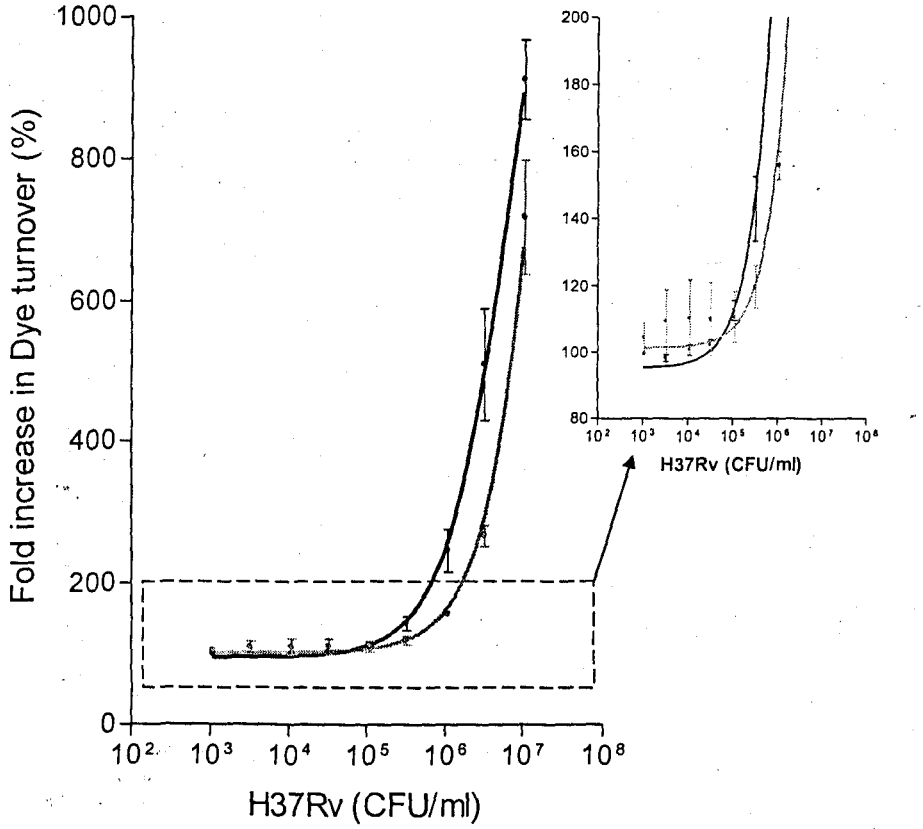

Figure 3.3: Lower limit of detection: H37Rv inocculum versus fold increase in Alamar blue (—) or MTT (—) turnover (compared to H37Rv free control). The magnified insert represents a close-up of the dye turnover at the lower limit of sensitivity. Data expressed as mean ± SD (n=4).

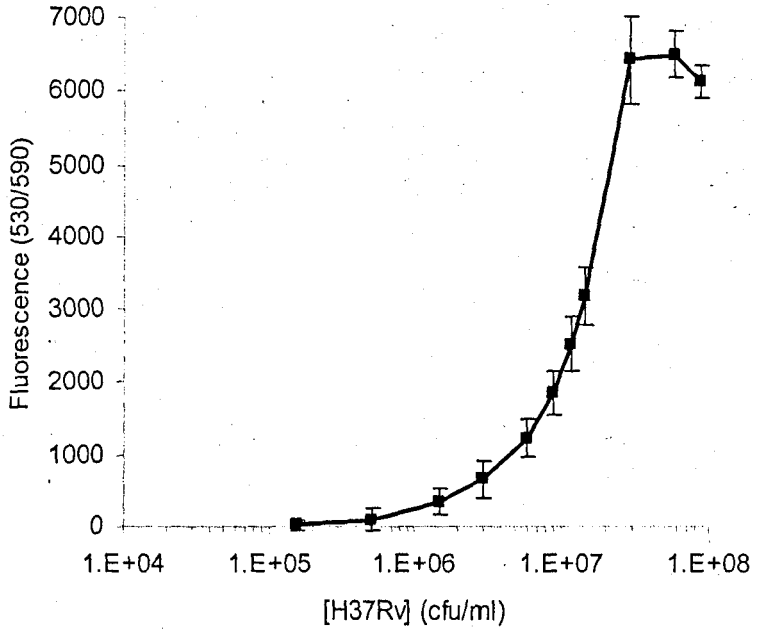

Figure 3.4: H37Rv inoculum versus Alamar blue turnover (background corrected fluorescence). Data are mean ± SD (n=4).

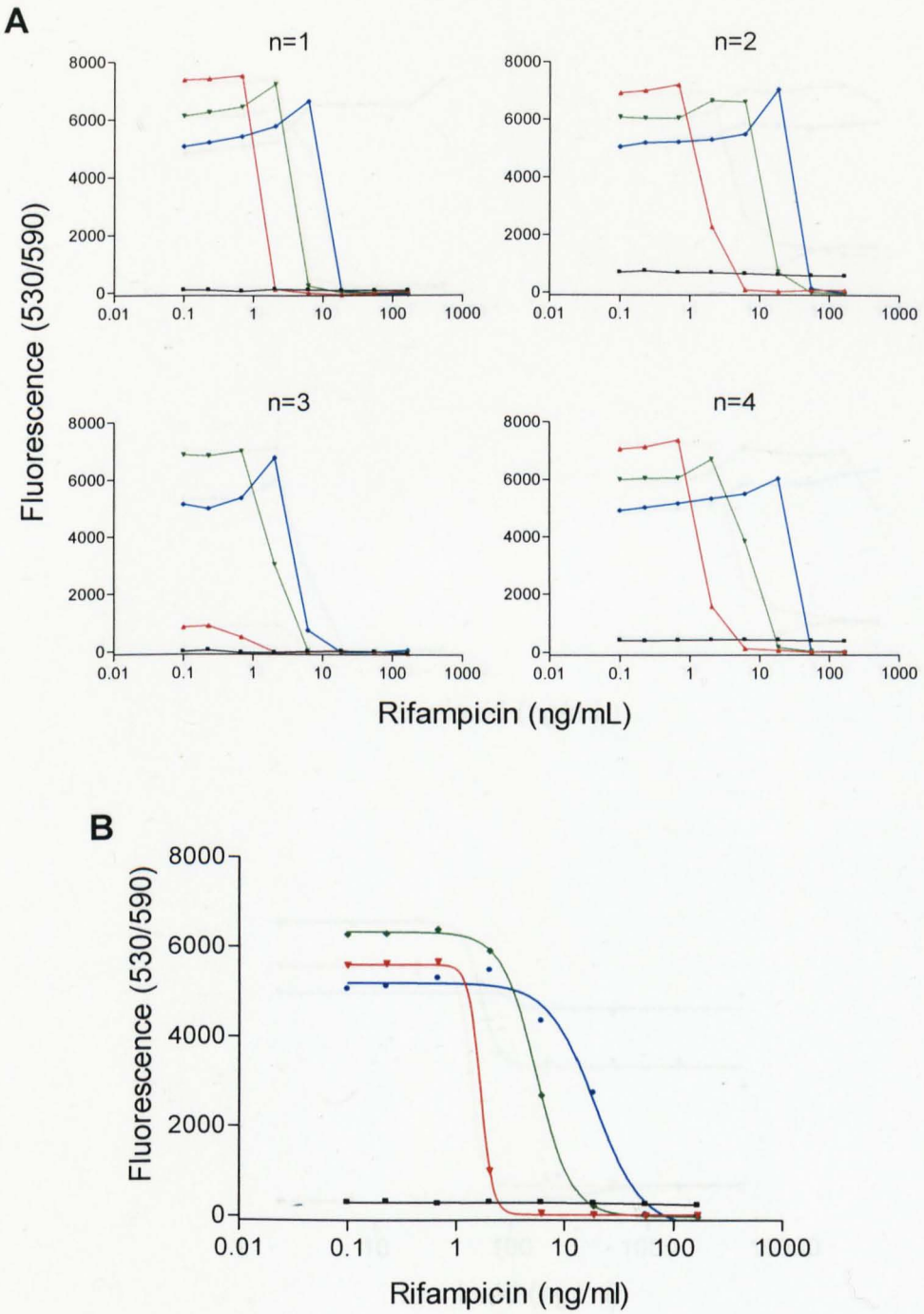

Figure 3.5: Individual (A) and mean (B) concentration dependent H37Rv viability curves following 0 (—), 7 (—), 14 (—) and 21 (—) day drug exposure to rifampicin as measured by background corrected Alamar blue fluorescence.

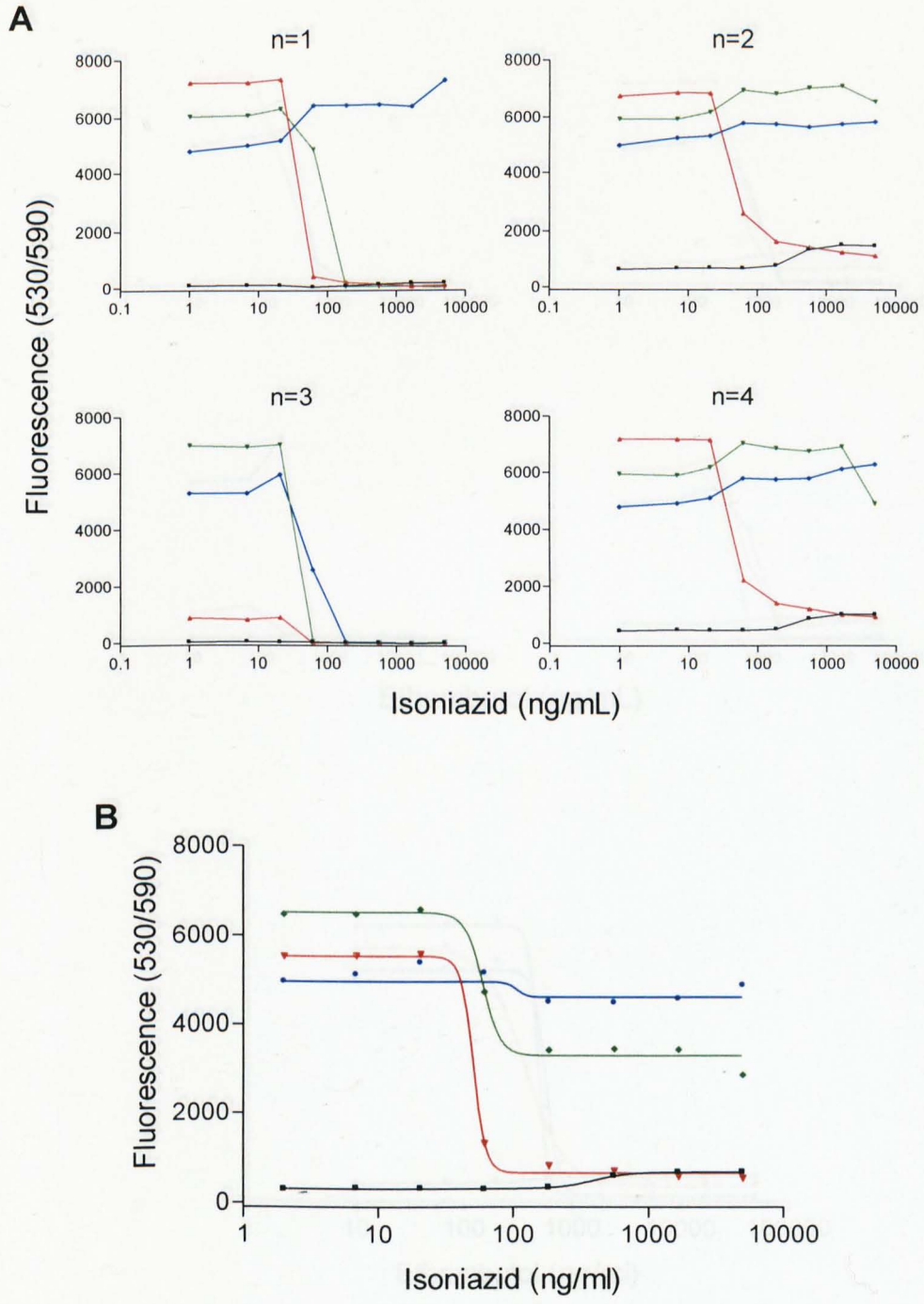

Figure 3.6: Individual (A) and mean (B) concentration dependent H37Rv viability curves following 0 (—), 7 (—), 14 (—) and 21 (—) day drug exposure to isoniazid as measured by background corrected Alamar blue fluorescence.

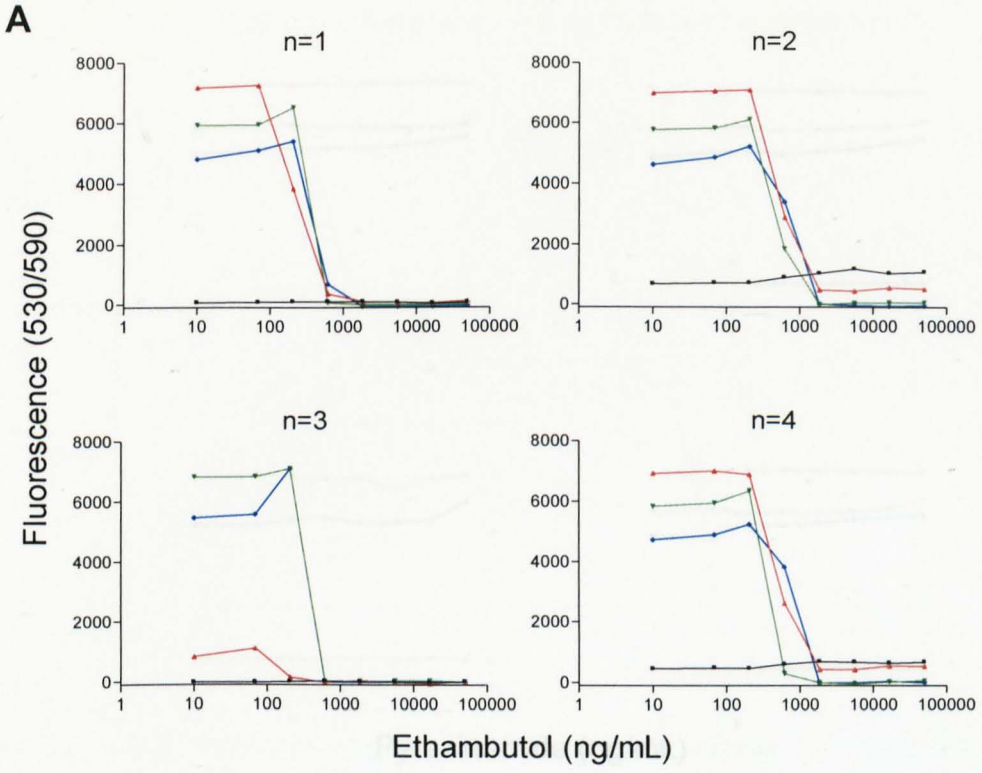

Figure 3.7: Individual (A) and mean (B) concentration dependent H37Rv viability curves following 0 (—), 7 (—), 14 (—) and 21 (—) day drug exposure to ethambutol as measured by background corrected Alamar blue fluorescence.

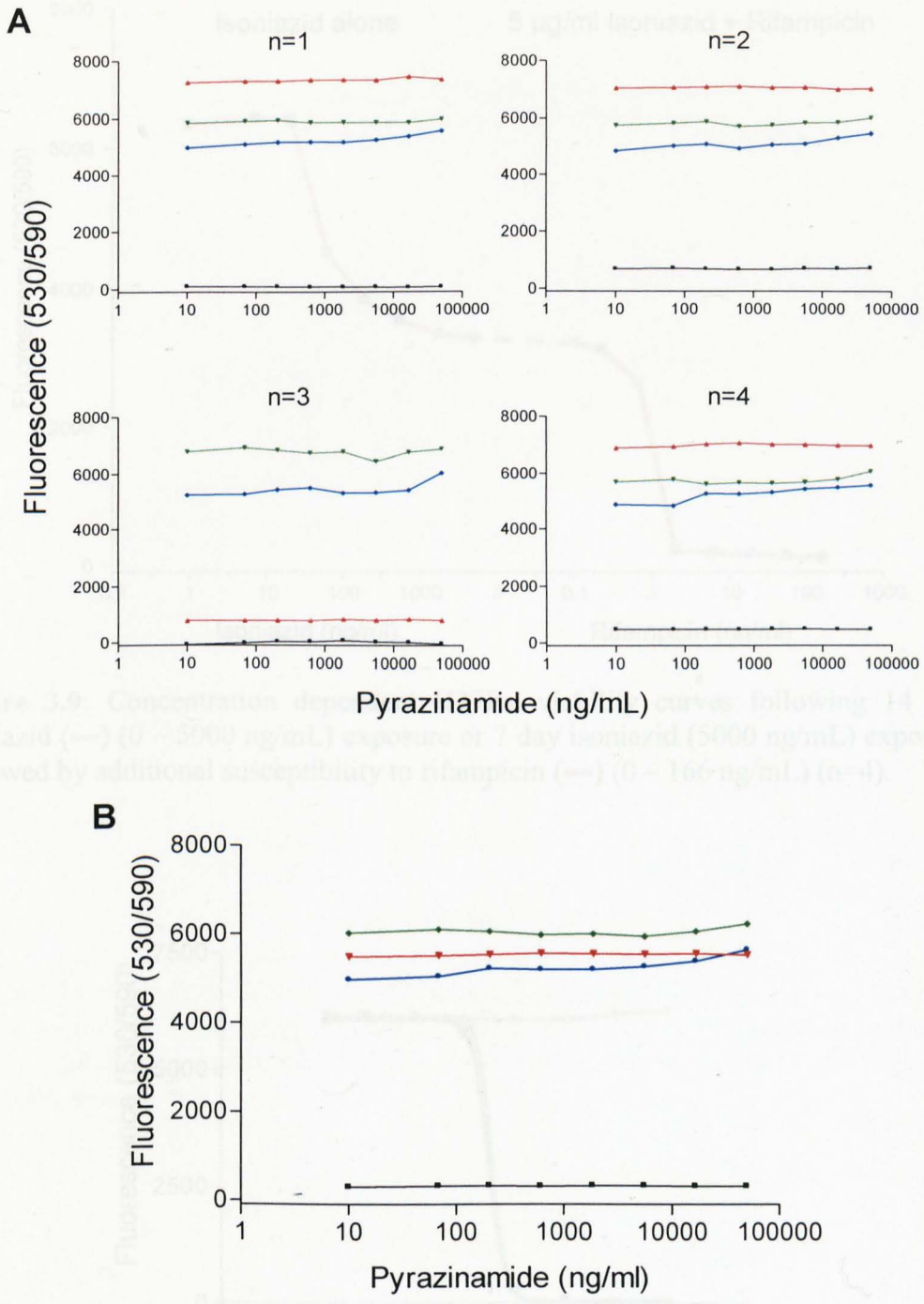

Figure 3.8: Individual (A) and mean (B) concentration dependent H37Rv viability curves following 0 (—), 7 (—), 14 (—) and 21 (—) day drug exposure to pyrazinamide as measured by background corrected Alamar blue fluorescence.

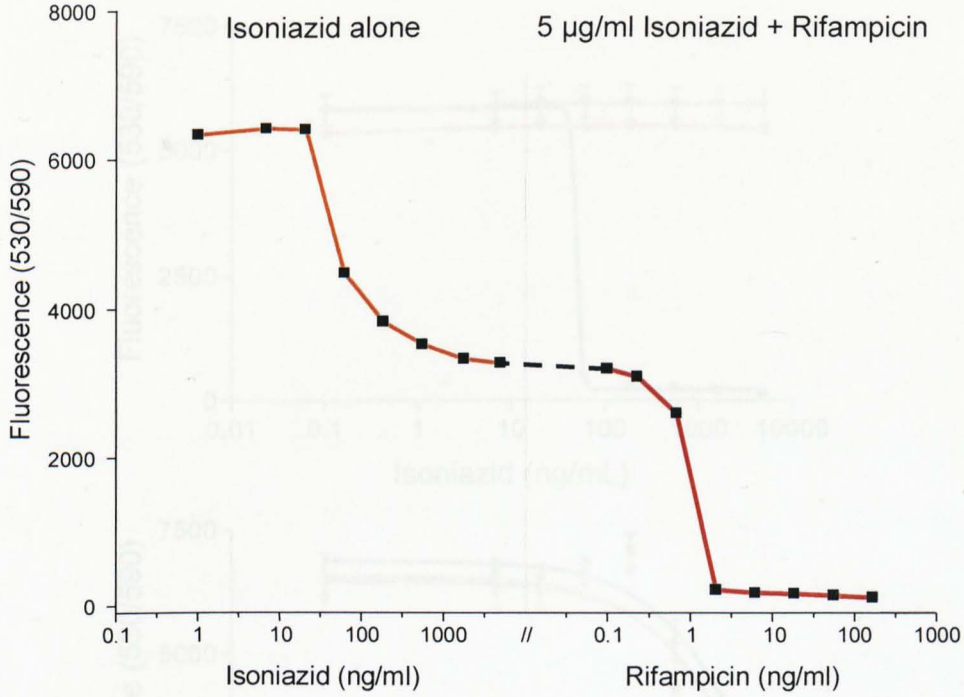

Figure 3.9: Concentration dependent H37Rv viability curves following 14 day isoniazid (—) (0 – 5000 ng/mL) exposure or 7 day isoniazid (5000 ng/mL) exposure followed by additional susceptibility to rifampicin (—) (0 – 166 ng/mL) (n=4).

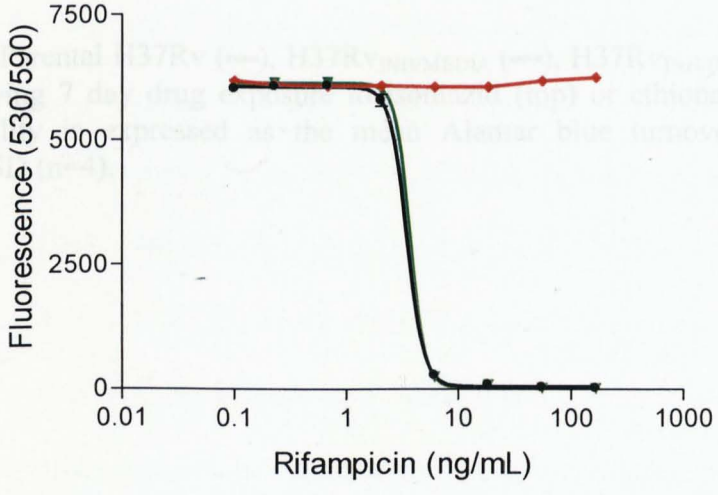

Figure 3.10: Parental H37Rv (—), H37Rv$_{RIF/MEDIA}$ (—), H37Rv$_{RIF/RIF}$ (—) viability curves following 7 day drug exposure to rifampicin. H37Rv viability is expressed as the mean Alamar blue turnover (background corrected) ± SD (n=4).

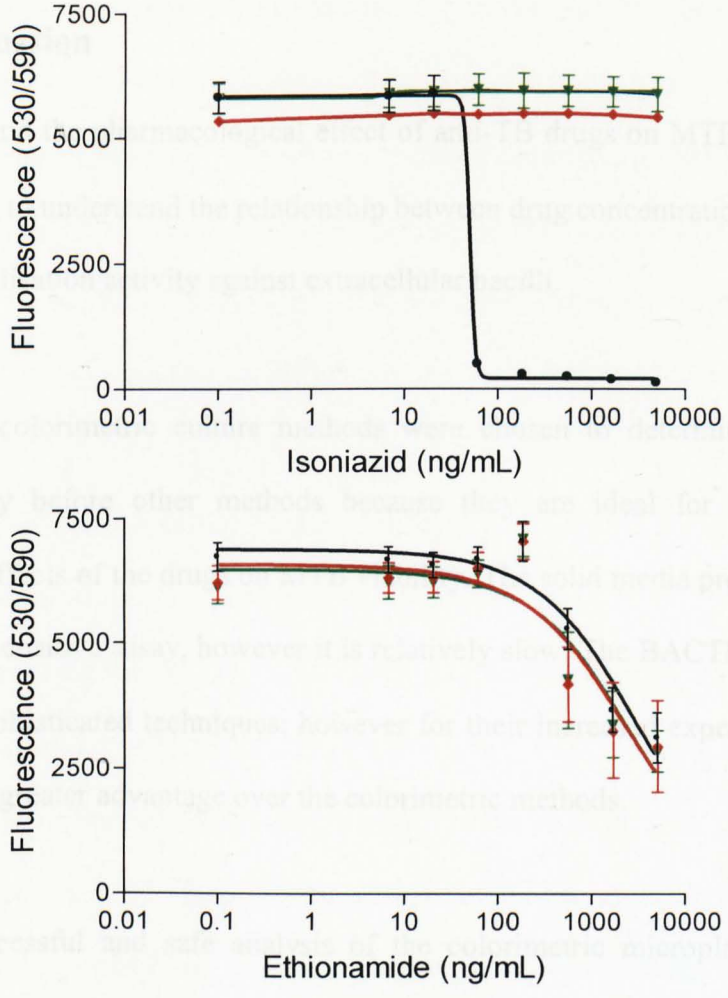

Figure 3.11: Parental H37Rv (—), H37Rv$_{INH/MEDIA}$ (—), H37Rv$_{INH/INH}$ (—) viability curves following 7 day drug exposure to isoniazid (top) or ethionamide (bottom). H37Rv viability is expressed as the mean Alamar blue turnover (background corrected) ± SD (n=4).

3.4 Discussion

To understand the pharmacological effect of anti-TB drugs on MTB during EBA, it is important to understand the relationship between drug concentrations and exposure and the sterilisation activity against extracellular bacilli.

Microplate colorimetric culture methods were chosen to determine H37Rv drug susceptibility before other methods because they are ideal for measuring time dependent effects of the drugs on MTB viability. The solid media proportion method is the most sensitive assay, however it is relatively slow. The BACTEC and GFPMA are more sophisticated techniques; however for their increased expense, they do not provide any greater advantage over the colorimetric methods.

For the successful and safe analysis of the colorimetric microplates outside the category 3 facility it was important to determine a safe MTB sterilising method to decontaminate the microplates. Paraformaldehyde, MTT lysis buffer and acidified isopropanol have previously been used to sterilise H37Rv (Abate *et al.*, 1998; Mshana *et al.*, 1998; Moore *et al.*, 1999; De Logu *et al.*, 2001; Schwebach *et al.*, 2001; Foongladda *et al.*, 2002). These sterilisation methods have however not been used in conjunction with the MABA, and as suggested by Blackwood *et al.*, (2005) all sterilisation methodologies, new and old should be investigated for their safety by the individual laboratories to validate the safe removal of material derived from MTB from the category 3 facility. Further, it was thought essential that 8 week cultures should be used as an indicator of H37Rv viability rather than the more conventional 3 week cultures to allow for increased sensitivity.

Results indicate that neither of the cell viability indicators (Alamar blue or MTT) are by themselves able to sterilise H37Rv. 24 hr exposure to the tested concentrations of paraformaldehyde; MTT lysis buffer and acidified isopropanol were however all able to sterilise H37Rv. It was decided that the use of 8% paraformaldehyde and MTT lysis buffer for sterilisation in the MABA and MMA methods respectively allowed for safe and effective analysis of MTB viability.

Data provided show that the MMA and MABA protocols are both effective at measuring MTB viability. Alamar blue is however around 10 fold more sensitive than MTT at measuring MTB viability. It must however be noted that lack of Alamar blue turnover indicates MTB concentration below 1 x 10^5 cfu/ml (1 x 10^4 cfu/well) rather than zero. Further, Alamar blue turnover saturates at 2 x 10^7 cfu/ml, above which an apparent decrease in Alamar blue reduction occurs due to the occlusion of light through the microplate by the MTB itself, thereby decreasing the fluorescent measurement.

MABAs are set up with a low bacterial load, and are mainly indicators of bacteriostatic drug activity. A decrease in MTB viability over time compared to day 0, can be used as an indicator of bactericidal activity, and may be improved if the assay is set up with a high bacterial load. However, both for ethambutol and isoniazid, a concentration dependent increase in dye turnover, that is as yet not understood, prevents this assay from being effective (data not shown).

MABA, BACTEC and GFPMA all generate concentration viability curves from which it is very difficult to actually measure an MIC. Previously published data have therefore defined the MIC as an EC90 (Collins and Franzblau, 1997; Changsen *et al.*, 2003) or EC99 (Luna-Herrera *et al.*, 2003) (Table 3.6). Data analysed here have used the EC50 as a marker of MTB viability, however in order to be able to compare data, EC90 values were also calculated (Table 3.3). The data on ethambutol are similar to those previously published. However, there is a greater discrepancy in regard to the EC90 for isoniazid (the present values are higher) and rifampicin (the present values are lower) compared to previously published data. This difference could be due to the time dependent kill of MTB by the drugs, therefore making the time when the MIC is measured important.

As has been observed in many in vitro assays, pyrazinamide exhibited no anti-TB activity at physiological pH (Zhang and Mitchison, 2003). H37Rv viability in the presence of ethambutol remained relatively unchanged between 1 and 3 weeks suggesting no time dependent generation of ethambutol tolerance by H37Rv. When looking at H37Rv in the presence of 50 μg/ml ethambutol (Fig. 3.7) there does seem to be a time dependent decrease in the baseline viability, suggesting some slow bactericidal activity. However, further experiments are needed to confirm this possible time dependent bactericidal activity.

Data on the H37Rv exposure to rifampicin suggest that over time there is an increased ability for the H37Rv strain to grow at higher concentrations (Table 3.3) illustrated by the shift in the H37Rv viability curves to the right (Fig. 3.5). When looking at the different individual curves for rifampicin it can also been seen that the

rate of tolerance generated by H37Rv is dependent on the initial inoculum of H37Rv (n=2 > n=4 > n=1 > n=3). Data from solid medium spiked with a rifampicin curve also suggest that over the course of three weeks H37Rv colonies are able to survive up to 166 ng/mL (Table 3.2). Previous work by Jayaram *et al.*, (2003) using the BACTEC system to look at time dependent activity of rifampicin on extracellular MTB, showed that there was an exposure dependent killing effect of rifampicin up to 9 days. This study did however not continue long enough to determine the emergence of drug tolerant MTB growth.

A similar, but more dramatic increase can be seen with H37Rv exposure to isoniazid, where over the course of 3 weeks the H37Rv strain seems to tolerate isoniazid concentrations equivalent to maximum plasma concentrations (5 μg/mL) (Table 3.3, Fig. 3.6). Again, as seen with rifampicin, it appears that the rate at which H37Rv develops an ability to survive high isoniazid concentrations is dependent on the initial inoculum. Data also suggest that this inoculum dependent tolerance to high concentrations of isoniazid can be seen as early at day 7, where high dose isoniazid is incapable of preventing H37Rv mediated Alamar blue turnover (Fig. 3.6). Confirmation that this population is isoniazid tolerant and viable is provided by showing that it remains rifampicin susceptible (Fig. 3.9).

Data obtained from the solid media spiked with isoniazid showed an isoniazid concentration dependent kill; however survival of certain H37Rv colonies at the higher isoniazid concentrations was observed (Table 3.4). This is in agreement with data by Jayaram *et al.*, (2004) that used the BACTEC system followed by solid media to study time dependent activity of isoniazid on extracellular MTB which also

showed incomplete killing of all bacteria by isoniazid. The growth of the surviving H37Rv population in liquid 7H9GT media most probably explains the increase in Alamar blue turnover over time.

One of the possible explanations for the rifampicin and isoniazid tolerance is the selection of MTB bacilli that have spontaneously mutated to their drug resistant forms. According to (David, 1970) the highest proportion of mutants in an unselected population of MTB that are resistant to 1 µg/mL isoniazid, 1 µg/mL rifampicin and 5 µg/mL ethambutol are 2.56×10^{-8}, 2.25×10^{-10} and 1.0×10^{-7} mutations per bacterium per generation. The MABA assay however is set up with around 1×10^{6} cfu/well, and therefore it would be highly unlikely for the observed tolerance to be due to pre-existing resistance. Further, if this were to be a likely explanation, results would show marked ethambutol tolerance over time, which was not observed. Also, the high proportion of isoniazid tolerant H37Rv at 7 days would suggest a relatively large isoniazid resistant population at day 0 for it to be detectable by day 7.

To investigate the nature of the increased tolerance of H37Rv to rifampicin and isoniazid, individual colonies were selected from rifampicin and isoniazid spiked solid media plates. Similar growth rates of the $H37Rv_{INH}$ and $H37Rv_{RIF}$ compare to the parental H37Rv suggest that the developed tolerance to isoniazid and rifampicin did not lead to an altered growth rate. It was then determined if the phenotypically tolerant $H37Rv_{RIF}$ and $H37Rv_{INH}$ strains reverted back into their wildtype phenotype or remained tolerant in the absence of drug pressure. Data suggest that $H37Rv_{RIF}$ that were grown in the absence of drug pressure ($H37Rv_{RIF/MEDIA}$) phenotypically resembled the parental H37Rv, while the $H37Rv_{RIF}$ culture under drug pressure

($H37Rv_{RIF/RIF}$) remained tolerant to rifampicin. This suggests that the rifampicin tolerance is a time dependent adaptive response by H37Rv to the presence of rifampicin that allowed it to remain viable.

$H37Rv_{INH}$ strains grown in the absence of isoniazid ($H37Rv_{INH/MEDIA}$) however did not phenotypically revert their isoniazid susceptibility to that of the parental H37Rv. Instead it remained fully tolerant to isoniazid (up to 5 μg/mL) and showed the same phenotype as the $H37Rv_{INH}$ strain grown in the presence of isoniazid ($H37Rv_{INH/INH}$). These data suggest that the $H37Rv_{INH}$ has undergone a mutation that has left it resistance to isoniazid. This is in agreement with data by Wallis *et al.*, (1999) using the BACTEC system showing that culture with 100 ng/mL isoniazid resulted in the emergence of isoniazid resistant MTB. It is however not known whether the isoniazid resistance mutants were present in the parental H37Rv population and positively selected for by the drug pressure, or whether the drug pressure has facilitated the formation of isoniazid resistant H37Rv strains. Drug pressure has been shown to alter the mRNA expression profile of MTB (Wilson *et al.*, 1999), and it may therefore be possible that this might facilitate the emergence of genetic drug resistance.

To identify the protein responsible for the isoniazid resistance, $H37Rv_{INH}$ ethionamide susceptibility tests were performed. Ethionamide is a "second-line" anti-tuberculosis drug that is a structural analogue of isoniazid. Both these drugs target InhA, however isoniazid requires bioactivation through a catalase-peroxidase (KatG), while it is thought that ethionamide is activated through EthA. High-level isoniazid resistance is mainly due to mutations in KatG, which results in no change

to ethionamide susceptibility (DeBarber *et al.*, 2000; Lee *et al.*, 2000; Morlock *et al.*, 2003). $H37Rv_{INH}$ susceptibility to ethionamide showed no change in its bacteriostatic activity between $H37Rv_{INH/MEDIA}$, $H37Rv_{INH/INH}$ and the parental H37Rv strain. These data therefore suggest that the emergence of isoniazid tolerance is due to a mutation in *KatG*. Sequencing of *KatG* would however be required to confirm this finding.

In vivo, the current understanding of TB therapy pharmacodynamics indicates that there are at least two phases of drug dependent kill. The initial EBA phase is thought to be mainly a result of isoniazid dependent kill, while the role of isoniazid in the second sterilising phase is limited (Jindani *et al.*, 2003). Traditional beliefs are that this is due to the presence of different bacterial populations, each differentially susceptible to isoniazid, however data shown here indicate that the bacterial population may be able to adapt quickly in the presence of isoniazid pressure and thereby evade its bactericidal activity. Data also indicated that the pharmacodynamics of rifampicin is a time and inoculum dependent factor and both need to be used to determine the actual MIC.

Table 3.6: Previously published H37Rv MIC data on rifampicin, isoniazid and ethambutol.

Drug	MIC (ng/mL) as measured by:			Reference
	BACTEC	MABA	GFPMA	
Rifampicin	25-200	50-200		(Collins and Franzblau, 1997)
		23-47	23-47	(Changsen *et al.*, 2003)
		>62		(Luna-Herrera *et al.*, 2003)
Isoniazid	25-50	50		(Collins and Franzblau, 1997)
		23	23	(Changsen *et al.*, 2003)
		>21		(Luna-Herrera *et al.*, 2003)
Ethambutol	940-1880	940-1880		(Collins and Franzblau, 1997)
		1875-3750	469-938	(Changsen *et al.*, 2003)
		>500		(Luna-Herrera *et al.*, 2003)

CHAPTER 4

Intracellular anti-tuberculosis activity and the influence of P-glycoprotein

4.1 Introduction 145

4.2 Methods 146

4.2.1 Materials 146

4.2.2 Cell culture 146

4.2.3 Determination of H37Rv MOI required to kill A-THP1 146

4.2.4 Intracellular MABA 148

4.2.5 Extracellular MABA 148

4.2.6 THP1 and A-THP1 P-glycoprotein expression 149

4.2.7 THP1 and A-THP1 rifampicin cellular accumulation ratio 149

4.2.8 Data handling and statistical analysis: 149

4.3 Results 150

4.3.1 H37Rv concentration versus A-THP1 viability 150

4.3.2 Intracellular vs extracellular H37Rv kill and the effect of p-glycoprotein 150

4.3.3 THP1 and A-THP1 P-glycoprotein expression 150

4.3.4 Rifampicin accumulation in THP1 and A-THP1 151

4.3.5 Results Tables 152

4.3.6 Results Figures 153

4.4 Discussion 157

4.1 Introduction

Alveolar macrophages are generally thought of as the first line of defence against MTB entering the body (Henderson *et al.*, 1963). Bacilli that are phagocytosed by the alveolar macrophages and survive the immune response are able to start replicating in the phagosomes, until they outgrow and kill their host cells (Bermudez and Goodman, 1996; Mehta *et al.*, 1996). As the MTB bacilli are able to survive within the macrophages, they are an important pharmacological target for drugs against tuberculosis. However, although much work has been performed in determining the MIC of drugs acting on extracellular MTB bacilli, limited work has been done to evaluate drug activity on intracellular bacilli. Specifically there are limited data on rifampicin (Carlone *et al.*, 1985; Mor *et al.*, 1995; Jayaram *et al.*, 2003; Duman *et al.*, 2004) and isoniazid (Jayaram *et al.*, 2004) mediated intracellular kill, with no data available on ethambutol. Further, it has not been determined if the drugs transporter P-glycoprotein is able to modulate the bactereriostatic activity of the anti-TB drugs.

This chapter aims to introduce a relatively time efficient, high throughput, novel assay to determine the concentration dependent bacteriostatic activity of anti-TB drugs against intracellular MTB. Further, the impact of P-glycoprotein is assessed on the intracellular kill by the anti-TB drugs.

4.2 Methods

4.2.1 Materials

The human monocytic leukaemia cell line THP1 was purchased from the European collection of cell culture (ECACC No. 88081201). Tariquidar was kindly donated by Xenova Group PLC (Berkshire, UK). All other materials were obtained from Sigma-Aldrich (Poole, UK)

4.2.2 Cell culture

THP1 cells were routinely cultured in RPMI 1640 supplemented with 10 % FCS (37°C, 5% CO_2). THP1 cells were activated into macrophage like cells (A-THP1) by addition of 100 nM Phorbol 12-myristate 13-acetate (PMA) to the culture medium (3 days).

4.2.3 Determination of H37Rv MOI required to kill A-THP1

The methodology for infection of A-THP1 cells was based on the work of (Stokes and Doxsee, 1999; Theus *et al.*, 2004). 500 µL of THP1 cells (1 x 10^6 cells/mL, 5 x 10^5 cells/well) were activated (100 nM PMA) and added to the wells of the bottom 4 rows of a 48 well plate. A-THP1 cells were allowed to adhere and differentiate into macrophage like cells (3 days, 37°C, 5% CO_2). Media was then aspirated and cells washed (2 times 500 µL) with binding media (138 mM NaCl, 8.1 mM Na_2HPO_4, 1.5 mM KH_2PO_4, 2.7 mM KCL, 0.6 mM $CaCl_2$, 1 mM $MgCl_2.6H_2O$, 5.5 mM D-glucose) supplemented with 1 % pooled human serum. Following aspiration of the media, 250 µL of binding media (supplemented with 1 % pooled human serum and 100 nM PMA) was added to each well to allow the A-THP1 to acclimatise (10 min, 37°C, 5% CO_2).

Stock H37Rv liquid cultures were routinely cultured in log phase in Middlebrook 7H9GT media as described in section 3.2.2. Following the quantification of H37Rv density (Absorbance at 600 nm), serial 2 fold dilutions were performed (between 1 x 10^8 and 8 x 10^5 cfu/ml) in binding media (supplemented with 1 % pooled human serum and 100 nM PMA). 250 µL of bacterial suspension (2.5 x 10^7 and 2 x 10^5 cfu/well; multiplicity of infection (MOI) between 50 and 0.4) was then added to the middle 4 rows of the 48 well plates. 250 µL of binding media (supplemented with 1 % pooled human serum and 100 nM PMA) was added to the top row (no A-THP1, no bacterial, background control) and bottom row (A-THP1, no bacteria, 100% A-THP1 viable positive control). Following incubation (3 hr, 37°C) all the wells were washed thoroughly with 500 µL binding media (using a thin tip Pasteur pipette) and incubated in 500 µL of RPMI 1640 (10% FCS and 100 nM PMA).

Following incubation of plates (1 week, 37°C, 5% CO_2), the wells were washed with binding media. 300 µL of RPMI 1640 (10% FCS) was added to the wells, with 100 µL Alamar blue: Tween 80 (2:1) to assess A-THP1 viability. Following incubation (24 hr, 37°C, 5% CO_2), 200 µL of 10 % paraformaldehyde was added to terminate the reaction. Following further incubation (24 hr, 37°C, 5% CO_2), the plates were removed from the category 3 facility and fluorescence measured (excitation 530: emission 590). A-THP viability was calculated as the percentage background corrected fluorescence of the test well compared to the 100% A-THP1 viable positive control fluorescence.

4.2.4 Intracellular MABA

Determining the kill of intracellular MTB bacilli by anti-tuberculosis drugs is based on the ability of that drug to protect the A-THP1 cells from being killed by H37Rv. Similar to the methodology described in section 4.2.3, THP-1 cells were seeded in 48 wells plates (5 x 10^5 cfu/well) and activated (100 nM PMA). Following incubation (3 days) and washing of the wells with binding media (supplemented with 1 % pooled human serum and 100 nM PMA), all wells were incubated with H37Rv (3 hr, 5% CO_2, 37°C, 250 µL of 2 x 10^7 cfu/mL, MOI = 10). This was followed by 3 thorough washes of the wells with binding media, 450 µL of RPMI 1640 (10 % FCS, 100 nM PMA).

3 fold drug dilutions were made-up (in RPMI, 10% FCS, 100 nM PMA) at 10 fold the desired concentrations (rifampicin: 0-10 µg/mL, isoniazid: 0-100 µg/mL, ethambutol, 0-1000 µg/mL) and 50 µL added along the plates (final conc.: rifampicin: 0-1 µg/mL, isoniazid: 0-10 µg/mL, ethambutol, 0-100 µg/mL). The plates were then incubated (1 week, 37°C, 5% CO_2) and A-THP1 viability measured as described in section 4.2.3. Experiments were repeated in the presence of 1 µM tariquidar (P-gp inhibitor).

4.2.5 Extracellular MABA

To asses the potential difference in H37Rv drug susceptibility when grown in a CO_2 incubator (as used for intracellular MABA) compared to a non-CO_2 incubator (as in chapter 3), extracellular MABA was repeated as described in section 3.2.7 but in a 5% CO_2 incubator. Experiments were also repeated in the presence of 1 µM tariquidar.

4.2.6 THP1 and A-THP1 P-glycoprotein expression

A-THP1 cells were generated by activating THP1 cells (4 x 10^6 cells, 100 nM PMA, 3 days). The adherent A-THP1 cells were then trypsinised and fixed before P-glycoprotein expression was assessed by flow cytometry as described in section 2.2.11.

4.2.7 THP1 and A-THP1 rifampicin cellular accumulation ratio

The cellular accumulation ratio (CAR) of ^{3}H-rifampicin in THP1 cells (3 x 10^6 cells, 37°C, 30 min) was assessed as described in section 2.2.15. To determine the ^{3}H-rifampicin accumulation in A-THP1 cells, THP1 (3 x 10^6 cells) were activated (100 nM PMA, 3 days) in a 24 well plate. Following activation, the adherent A-THP1 cells were washed and cultured in the presence of ^{3}H-rifampicin (1 µM, 500 µL, 0.1 µCi, 30 min, 37°C). Cells were then thoroughly washed (3 times, 2 ml of PBS), freeze-thawed (-80°C) and solubilised (1 ml of Ultima-Gold scintillation liquid) and transferred into scintillation vials, before being analysed as standard. ^{3}H-rifampicin accumulation in both the THP1 and A-THP1 cells was also measured in the presence of 1 µM tariquidar. ^{3}H-rifampicin cellular accumulation was calculated as the intracellular dpm (per million cells) as a fraction of the extracellular dpm (in 100 µL).

4.2.8 Data handling and statistical analysis:

EC50 data were generated using Graphpad Prism (3.0). Analysis for statistical significance of the influence of tariquidar on the EC50 and drug accumulation was by paired T-test.

4.3 Results

4.3.1 H37Rv concentration versus A-THP1 viability

A-THP1 cell viability following infection by different H37Rv concentrations and 7 day culture shows a sigmoidal relationship (Fig. 4.1). At 1 bacteria/A-THP1 cell (MOI = 1) A-THP1 viability remained largely unaffected, while 10 bacteria/A-THP1 cell (MOI = 10) caused near to 100% cell death. An MOI of 10 was therefore usd in the subsequent experiments.

4.3.2 Intracellular vs extracellular H37Rv kill and the effect of p-glycoprotein

Drug mediated extracellular H37Rv bacteriostatic activity of rifampicin (mean EC50 ± SD: 1.27 ± 0.02 ng/ml), isoniazid (57.2 ± 2.5 ng/ml) and ethambutol (363 ± 12 ng/ml) was measured following 7 day incubation in a CO_2 incubator (Fig 4.2, Table 4.1). 1 μM tariquidar did not influence the extracellular kill of H37Rv by the drugs (Table 4.1).

Drug mediated intracellular H37Rv bacteriostatic activity of rifampicin (mean EC50 ± sd: 148 ± 32 ng/ml), isoniazid (36.7 ± 2.2 ng/ml) and ethambutol (243 ± 95 ng/ml) was measured as the ability to protect THP-1 cells from the killing effect of H37Rv over a 7 day incubation (Fig. 4.2, Table 4.1). Tariquidar was able to significantly reduce the EC50 of both rifampicin (119 ± 31 ng/mL, P>0.001) and ethambutol (144 ± 83 ng/mL, P>0.001), while not affecting isoniazid (Fig. 4.3, Table 4.1).

4.3.3 THP1 and A-THP1 P-glycoprotein expression

Dot plots (Fig. 4.4) show that there is a clear change in the morphology between the parental THP1 and its activated form; A-THP1, with both an increase in the side

scatter (SS, representative of granularity) and forward scatter (FS, representative of cell size). Further, there is a significant increase in the P-gp expression between the parental THP1 cells (RFU: 0.34 ± 0.08) and the activated A-THP1 cells (RFU: 1.58 ± 0.11, $P<0.05$) as measured by the difference between isotype control and specific UIC2 FL2 fluorescence (Fig. 4.4).

4.3.4 Rifampicin accumulation in THP1 and A-THP1

1 μM rifampicin CAR for the parental THP1 (mean ± SD: 5.70 ± 0.70 dpm per million cells / dpm in extracellular media) cells remained unchanged in the presence of the P-gp inhibitor tariquidar (5.69 ± 0.56). A-THP1 CAR (4.53 ± 0.19) was however significantly increased by approximately 18% in the presence of tariquidar (5.36 ± 0.10, $P<0.05$) (Fig. 4.5).

4.3.5 Results Tables

Table 4.1: Intracellular and extracellular bacteriostatic EC50 values for rifampicin isoniazid and ethambutol in the absence and presence of 1 μM Tariquidar. Data are mean ± SD (n=4), ** P<0.001 compared to drug alone (Paired T-Test).

	Intracellular MABA		Extracellular MABA	
	Alone	1μM Tariquidar	Alone	1μM Tariquidar
Rifampicin	148 ± 32	119 ± 31**	1.27 ± 0.02	1.29 ± 0.03
Isoniazid	36.7 ± 2.2	34.8 ± 7.0	57.2 ± 2.5	55.4 ± 3.9
Ethambutol	243 ± 95	144 ± 83**	263 ± 12	294 ± 44

4.3.6 Results Figures

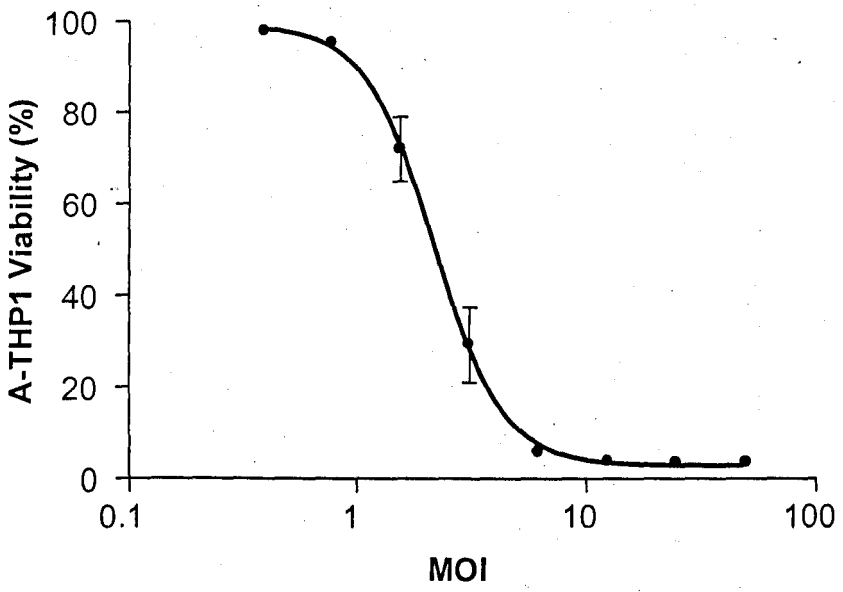

Figure 4.1: Percentage A-THP1 viability following 3 hr infection with different concentrations of H37Rv and subsequent 7 day culture. Data represent the mean ± SD (n=4).

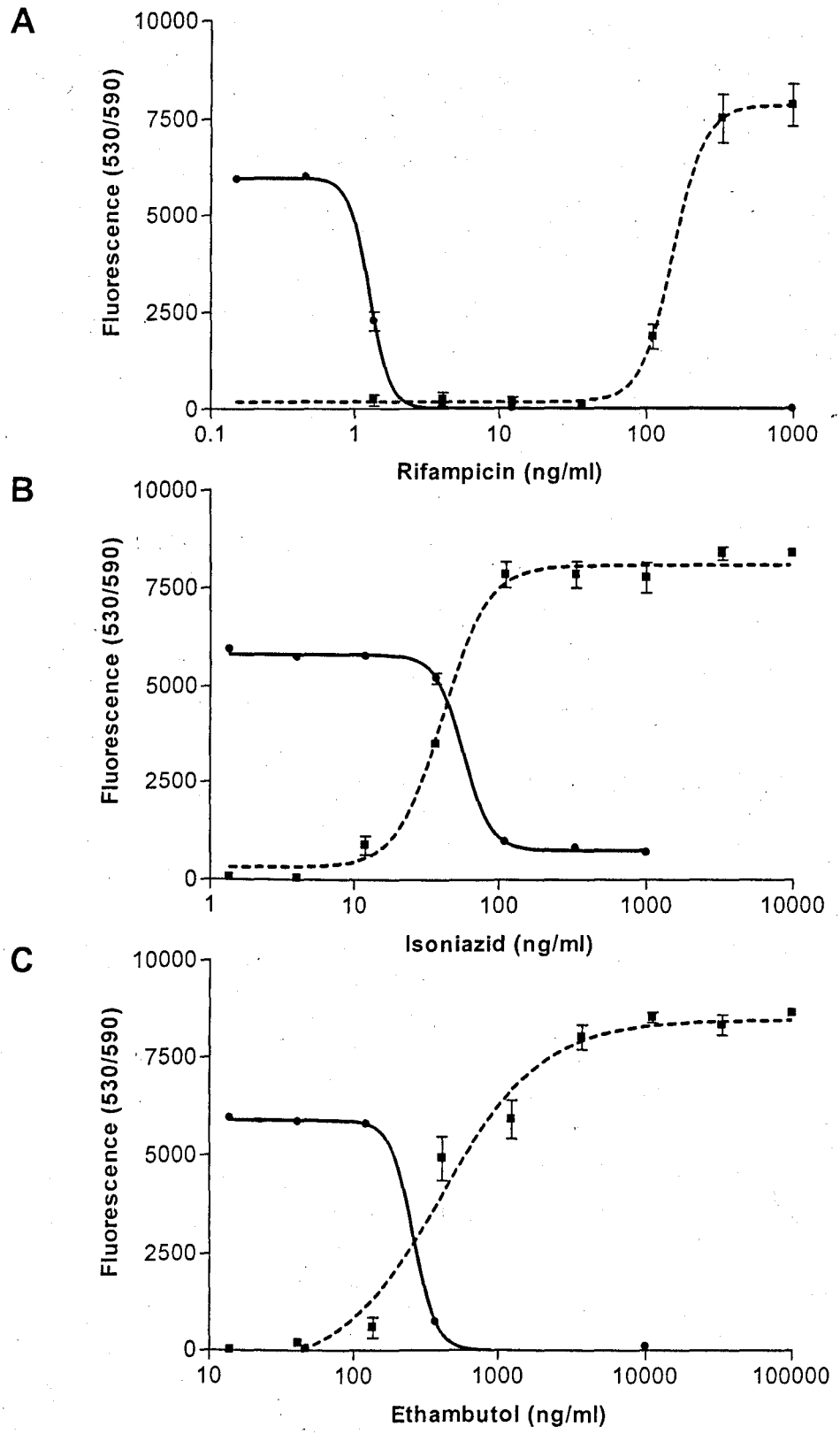

Figure 4.2: A-THP1 viability following H37Rv infection (MOI = 10) (▪▪▪▪▪) and extracellular H37Rv viability (——) versus the media concentrations of rifampicin (A), isoniazid (B) and ethambutol (C) as derived from their respective MABA assays. Data represent mean ± SD (n=4).

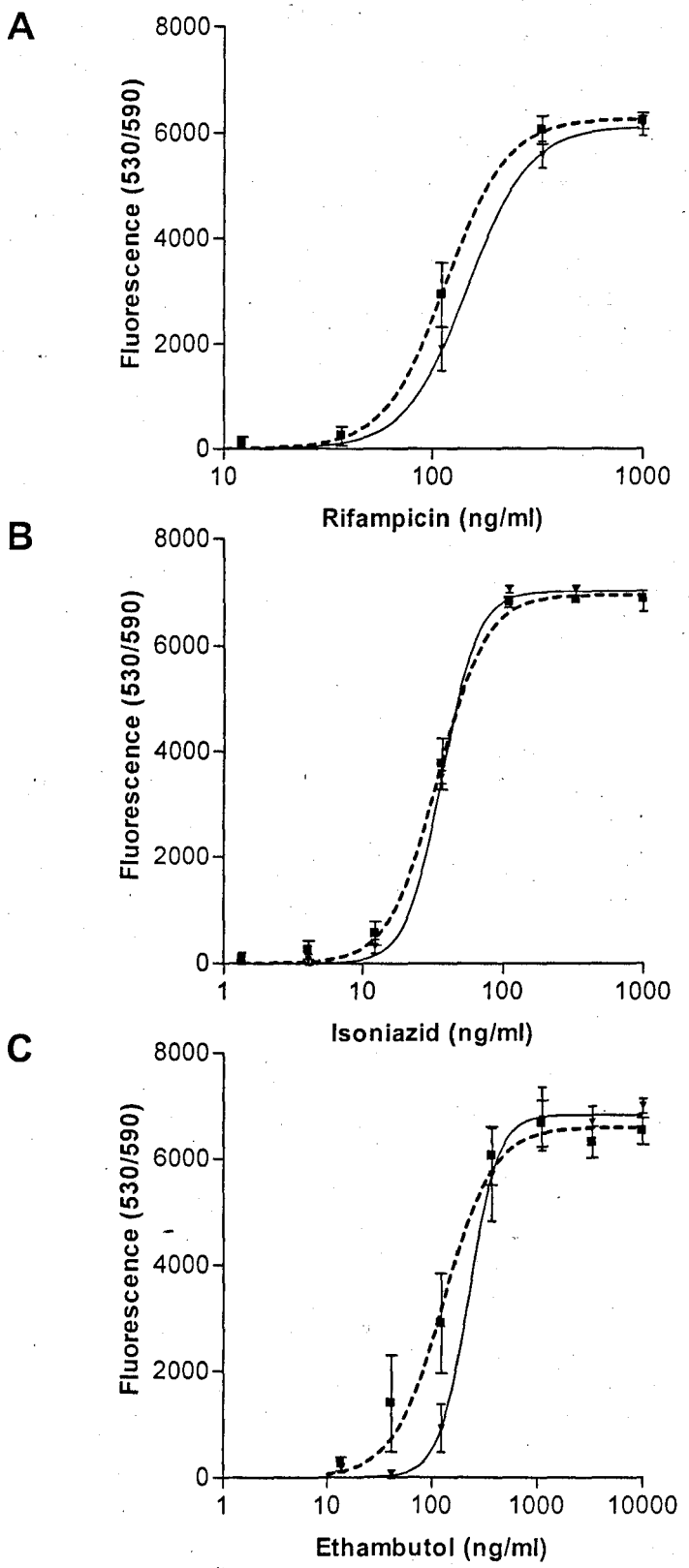

Figure 4.3: A-THP1 viability following H37Rv infection (MOI = 10) versus the media concentration of rifampicin (A), isoniazid (B) and ethambutol (C) in the presence (▪▪▪▪▪) and absence (——) of 1 μM tariquidar. Data represent mean ± SD (n=4).

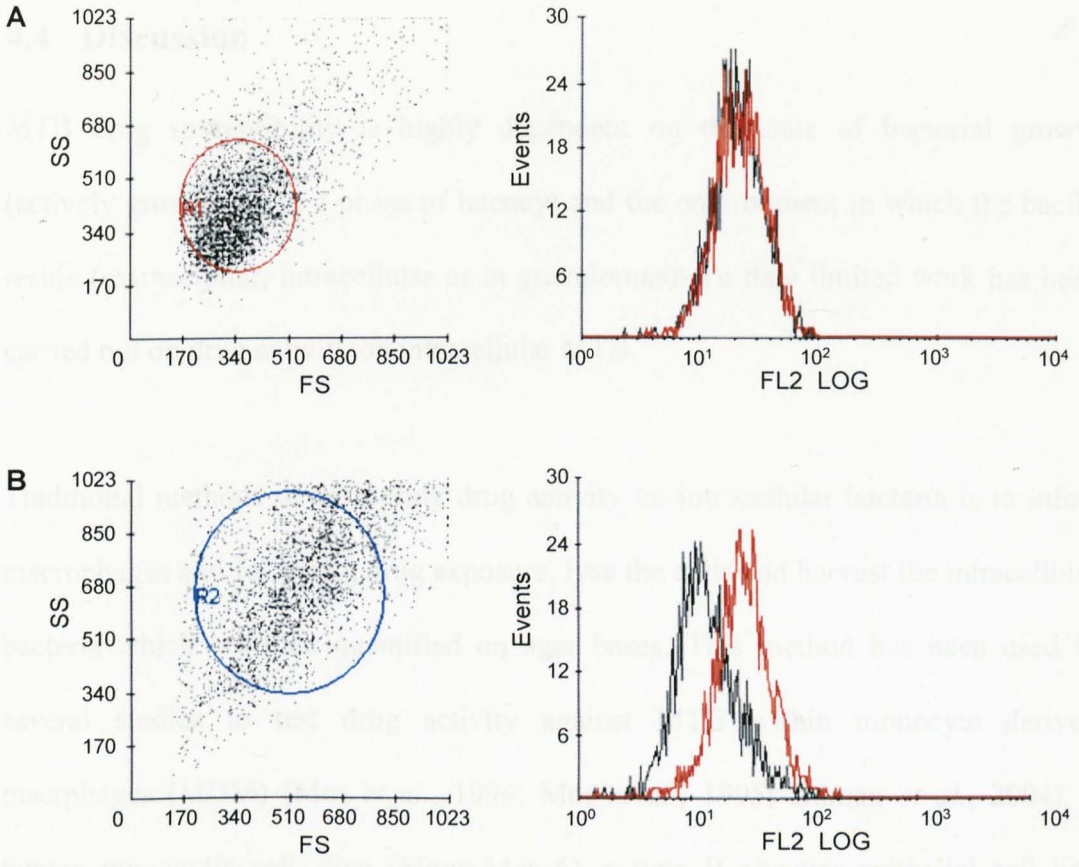

Figure 4.4: A representative dot-plot (left) of THP1 (A) and A-THP1 cells (B). The right hand side are histograms of the isotype control FL2 fluorescence (—) and the anti- P-gp; (UIC2) FL2 fluorescence (—).

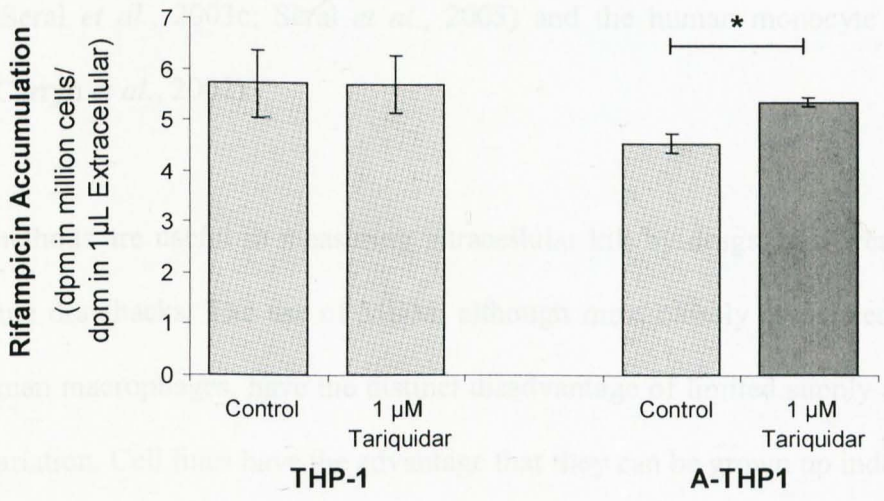

Figure 4.5: The effect of 1 µM tariquidar on the cellular accumulation ratio of 1 µM ^{3}H-rifampicin in parental THP-1 cells and A-THP1 cells. Data are mean ± SD, (n=4), * $P < 0.05$ (paired T-test).

4.4 Discussion

MTB drug susceptibility is highly dependent on the state of bacterial growth (actively growing or in a phase of latency) and the environment in which the bacilli reside (extracellular, intracellular or in granulomas). To date limited work has been carried out on drug activity on intracellular MTB.

Traditional methods of measuring drug activity on intracellular bacteria is to infect macrophages and following drug exposure, lyse the cells and harvest the intracellular bacteria which are then quantified on agar bases. This method has been used in several studies to test drug activity against MTB within monocyte derived macrphages (MDM) (Mor *et al.*, 1994; Mor *et al.*, 1995; Duman *et al.*, 2004), a human monocytic cell line (Mono-Mac 6), a type II alveolar epithelial cell line (A549) (Sato *et al.*, 2003) and in mouse macrophage cell lines (J744) (Jayaram *et al.*, 2003; Jayaram *et al.*, 2004). Similar models have also been used when investigating drug activity against intracellular *listeria monocytogenes* in J744 cells (Seral *et al.*, 2003a; Seral *et al.*, 2003c; Seral *et al.*, 2005) and the human monocyte cell line THP1 (Carryn *et al.*, 2002).

These methods are useful in measuring intracellular kill by drugs; however they do have some drawbacks. The use of MDM, although most closely associated with in vivo human macrophages, have the distinct disadvantage of limited supply and inter donor variation. Cell lines have the advantage that they can be grown up indefinitely; however J744 is a mouse macrophage cell line and may act differently to human macrophages while Mono-Mac 6 and THP1 cells are human monocyte cell lines, that although 'macrophage like', are not fully differentiated into macrophages.

PMA mediated activation of THP1 cells and their infection in the presence of 1% non-heat inactivated human serum has been found to be a good alternative to MDM (Stokes and Doxsee, 1999; Theus *et al.*, 2004). Association between MTB and A-THP1 or MDM was found to be comparable; comprising of opsonic as well as CR3, mannan and glucan mediated binding (Stokes and Doxsee, 1999). Further, it was shown that intracellular MTB grows progressively in infected A-THP1. The comparable nature of A-THP1 infection to that of MDM by MTB, and the capacity for an indefinite supply of the parental THP-1 cell, suggest that this cell system is ideal for high throughput intracellular drug activity measurements.

Data presented here introduces a novel method for analysing the intracellular activity of anti-TB drugs. In a similar way to that in which MT4 cells are used to determine anti-HIV activity following *in vitro* infection with HIV (Pauwels *et al.*, 1987; Owen *et al.*, 2005), A-THP1 cell viability has here been used as an indicator of intracellular MTB viability within the cells. 7 day culture of A-THP1 cells following a lethal dose of H37Rv (MOI of 10) ordinarily leads to the killing of all A-THP1 cells. The presence of bacteriostatic or bactericidal concentrations of anti-TB drugs in the media is however able to protect the A-THP1 cells and thereby A-THP1 viability may be indirectly used as an indicator of intracellular MTB viability.

Data presented by (Danelishvili *et al.*, 2003) demonstrate that infection of a monocytic cell line (U937) with H37Rv (MOI of 10) results in both necrosis and apoptosis; the rate of which is time dependent. Extrapolated data from this study

would suggest near to 100 % cell death at 7 days following infection (MOI of 10), similar to that seen with the infected A-THP1 cells.

There are numerous advantages to using A-THP1 viability as a marker of intracellular viability compared to the traditional cell lysis and bacterial growth on solid media. Firstly; this assay is much less time consuming, only requiring adequate time for alamar blue turnover and sterilisation (2 days) to analyse the results, compared to at least 3 weeks of bacterial growth on solid media. Secondly; extracellular binding of MTB to the wells or the cell membranes (which would be measured on solid media) does not compromise this assay because only intracellular MTB affects A-THP1 viability. Potential disadvantages to the assay are that one cannot differentiate between bactericidal and bacteriostatic activity inside the cells.

MTB drug susceptibility may be altered depending on the metabolic state of the bacilli (Herbert *et al.*, 1996). Data however indicate that the presence of CO_2 has no influence on the extracellular H37Rv kill by rifampicin, isoniazid and ethambutol (Table 3.3). Further, incomplete 7 day bacteriostatic activity of isoniazid is observed once again as seen and discussed in chapter 3.

Isoniazid data show no difference in the intra- and extracellular bacteriostatic activity. This is a similar finding to (Jayaram *et al.*, 2004) who found that intracellular H37Rv bacteriostasis occurs at a drug concentration equal to the extracellular MIC in broth, but that the bactericidal activity of isoniazid was drastically diminished.

Data show that the intracellular H37Rv bacteriostatic activity of rifampicin was dramatically reduced compared to the extracellular kill. This is a greater difference compared with previous data that showed a 2 fold increase in the MIC from 0.12 to 0.25 μg/mL (Mor *et al.*, 1995). This large difference observed may be partially accounted for by differential protein binding. Extracellular MABA assays and the intracellular assay contain different amounts and types of protein. As rifampicin *in vivo* is approximately 80% protein bound, differential protein binding could partially account for the different EC50 (Acocella *et al.*, 1971). Another contributing factor may be accumulation of rifampicin in alveolar macrophages which has been reported as being as high as 16 (Ziglam *et al.*, 2002). Further, the sub localisation of the drug within the macrophage, and more importantly the bacilli containing phagosome is unknown. Rifampicin is also believed to accumulate in MTB bacilli (Piddock *et al.*, 2000); however it is not known if this accumulation also occurs when the bacilli are confined intracellularly. Also, changes in the phagosome pH as well as transcriptional adaptation of H37Rv during phagocytosis (Schnappinger *et al.*, 2003) may also influence the bacteriostatic activity of the anti-tuberculosis drugs.

No difference was found between the intracellular and extracellular ethambutol mediated EC50 bacteriostatic activity. However, when analysing the individual curves it can be seen that the concentration at which there is more or less 100 % H37Rv death is around 10 fold lower than the concentration that provides 100 % A-THP1 viability. This difference may be due to protein binding differences with ethambutol being approximately 20% to 30% protein bound (Lee *et al.*, 1977).

The dramatic decrease in the susceptibility of MTB to rifampicin may be an important factor in the treatment of tuberculosis. Rifampicin trough (Cmin) concentrations during therapy fall below the intracellular MIC of rifampicin. This may allow intracellular bacilli to recover and survive for longer inside macrophages, thereby contributing to the long length of TB therapy.

Previous data have shown that mouse J774 macrophages have been known to express active drug efflux pumps such as P-glycoprotein and MRP that can be modulated to alter macrolide and quinolone accumulation (Seral *et al.*, 2003a; Seral *et al.*, 2003b; Michot *et al.*, 2004; Michot *et al.*, 2005). Further, studies have shown that PMA is able to induce P-glycoprotein and thereby alter doxorubicin accumulation in MCF-7 cells (Ahn *et al.*, 1996). In this study we demonstrate that 100 nM PMA mediates induction of P-glycoprotein on A-THP1 cells, which when blocked by tariquidar results in a small but significant 18 % increase of rifampicin accumulation. These data are in keeping with data from chapter 2 in which rifampicin accumulation was manipulated by blocking P-gp in CEM_{VBL100} cells. Interestingly, inhibition of P-glycoprotein in the intracellular rifampicin MABA model results in a significant decrease in the EC50 of A-THP1 of 20%. This decrease is of the same magnitude as that observed for the change in cellular accumulation.

Since radiolabelled ethambutol was not commercially available, the influence of blocking P-gp on A-THP1 cells on the drug accumulation cannot be determined. However, the intracellular ethambutol MABA shows that tariquidar mediates a significant 40 % decrease in the A-THP1 viability EC50. This is again in agreement

with data presented in chapter 2, showing that ethambutol toxicity in CEM_{VBL100} cells increases when P-gp is inhibited.

The intracellular H37Rv bacteriostatic assay described here is a novel method that is relatively fast, effective and provides quantifiable concentration dependent anti-TB activity relationships. This assay could easily be modified into a 96 well format and be useful in high throughput automated screening of drugs. Further, this assay may be useful in the analysis of the role of cellular proteins (following the cloning of proteins in THP1 cells) on the cellular defence mechanisms against intracellular TB and drug pharmacodynamics. The data presented here are also consistent with the findings in chapter 2, suggesting that both rifampicin and ethambutol are substrates for P-gp.

CHAPTER 5

Characterisation of OATP expression and function in cell lines and alveolar macrophages

5.1 Introduction 165

5.2 Methods 167

5.2.1 Materials 167

5.2.2 Cell culture 167

5.2.3 Human liver, PBMC and alveolar macrophage sample collection 167

5.2.4 Rifampicin cellular accumulation at 4°C 168

5.2.5 Extraction of total RNA 169

5.2.6 Reverse transcription 169

5.2.7 Detection of OATP expression by Hotstart Touchdown PCR 170

5.2.8 E-3-S modulation of rifampicin uptake in CEM cell lines and PBMCs 170

5.2.9 Data handling and statistical analysis 171

5.3 Results 173

5.3.1 Rifampicin accumulation at 4°C and in heat killed cells 173

5.3.2 Optimisation of OATP Hot-start Touchdown PCR conditions 173

5.3.3 Cell screening of OATP mRNA expression 173

5.3.4 E-3-S modulation of rifampicin CAR 174

5.3.5 Results Tables 175

5.3.6 Results Figures 176

5.4 Discussion 181

5.1 Introduction

During initial treatment, rifampicin has been shown to induce hyperbilirubinemia (Acocella *et al.*, 1965; Laudano, 1972), reduce the elimination of sulfobromophthalein (BSP) and increase serum bile acid concentrations (Galeazzi *et al.*, 1980; Berg *et al.*, 1984). Organic anions such as BSP and bilirubin enter hepatocytes through organic anion transporting peptides (OATP) and therefore inhibition of this uptake system seemed a plausible mechanism (Kullak-Ublick *et al.*, 1995; Abe *et al.*, 1999; Konig *et al.*, 2000; Cui *et al.*, 2001; Kullak-Ublick *et al.*, 2001). Studies on rat hepatic Oatp1a1 and Oatp1a4 showed that rifampicin was an inhibitor of these uptake systems (Fattinger *et al.*, 2000). Following this data it was found that in complementary RNA injected Xenopus *Laevis* oocytes, rifampicin inhibited SLCO1B3 and to a lesser extend SLCO1A2, SLCO1B1 and SLCO2B1 (Vavricka *et al.*, 2002) (for table of OATP/SLC0 nomenclature ref back to table 1.4). Further, it was also found that rifampicin was a substrate for SLCO1B1 and SLCO1B3 (Cui *et al.*, 2001; Vavricka *et al.*, 2002; Tirona *et al.*, 2003; Spears *et al.*, 2005), and that some naturally occurring SLCO1B1 allelic variants markedly reduced rifampicin accumulation (Tirona *et al.*, 2003).

The tissue distribution of OATPs has mainly been performed in human epithelial cells (liver, brain, intestine, lung, kidney and other major organs) (Kullak-Ublick *et al.*, 2001; Tirona and Kim, 2002; Kim, 2003). Further, it has been demonstrated that PBMCs do not express any of SLCO1A2, SLCO1B1, SLCO2B1 or SLCO4A1, but do express SLCO3A1 (Tamai *et al.*, 2000; Kullak-Ublick *et al.*, 2001). However, limited work has been performed on the expression of OATPs on other non-epithelial cells such as alveolar macrophages, which are an important sanctuary site for MTB,

and therefore a target cell for rifampicin. Current knowledge regarding the expression of OATPs in liver, lung and PBMCs in summarised in Table 5.3

Rifampicin accumulation in CEM cells and PBMCs have been found to be approximately 5 to 6 fold higher than in the plasma (Chapter 2). However, a 16 fold increase in cellular to plasma rifampicin has been found in alveolar macrophages (Ziglam *et al.*, 2002), suggesting that a cellular uptake mechanism may be responsible for the increased rifampicin accumulation in alveolar macrophages.

The aim of this study is to determine the mRNA expression of the main OATPs (SLCO1A2, SCLO1B1, SLCO1B3, SLCO2B1, SLCO3A1 and SLCO4A1) in both epithelial (liver and lung cells) and in non-epithelial cell lines (PBMCs and alveolar macrophages). Further, the impact of OATPs on the accumulation of rifampicin in CEM cell lines and PBMCs is determined.

5.2 Methods

5.2.1 Materials

Tariquidar was kindly donated by Xenova Group Plc (Berkshire, UK).

CEM (parental) and CEM_{VBL100} (P-gp over-expressing) cells were gifts from Dr R. Davey (University of Queensland, Australia). THP1 (ECACC: 88081201) and A549 (ECACC: 86012804) were obtained from the European Collection of Cell Cultures (ECACC). ^{3}[H]-rifampicin was purchased from Moravek Biochemicals (Brea, California, USA). All other materials were purchased from Sigma-Aldrich (Poole, UK).

5.2.2 Cell culture

The T-lymphoblastoid cell line; CEM, CEM_{VBL100} and CEM_{E1000} and the human monocytic cell line THP1 were routinely cultured in RPMI 1640 (supplemented with 10% FCS). The human epithelial lung cell line A549 was routinely cultured in DMEM (supplemented with 10% FCS).

5.2.3 Human liver, PBMC and alveolar macrophage sample collection

Human liver samples were obtained from histologically normal livers from Caucasian donors (n = 4). Liver samples were portioned, frozen in liquid nitrogen and stored (-80°C) within 30 min of the donors death (in all cases certified death was traumatic injury due to road traffic accident). Approval was granted by the Liverpool local research ethics committee and prior consent was obtained from the donors, relatives.

PBMC samples were obtained from healthy volunteers (n = 4) and Buffy coats (Regional Blood Transfusion Centre, Liverpool). Briefly, heparinised peripheral blood was layered onto Ficoll-Paque Plus (Amersham Biosciences) and centrifuged (800 x g, 30 min, 4°C), the PBMC layer was then removed and washed 3 times in PBS (800 x g, 6 min, 4°C).

Alveolar macrophages were obtained from bronchoalveolar lavage (BAL) at the North West Lung Research Centre (South Manchester University Hospitals Trust, Manchester, UK). Briefly, a bronchoscope was wedged in an appropriate tertiary bronchus (usually the right middle lobe) and a BAL was carried out using normal pre-warmed saline (37°C, 50ml). Recovered BAL fluid (stored at 4°C) was then passed through filter nylon cell strainer (100μm, BD Falcon) and centrifuged (300 x g, 10 min, 4°C). Alveolar macrophages were purified from the BAL using magnetic cell sorting (MACS technology) according to the manufacturer's instructions. Briefly, 2 x 10^7 cells were resuspended in 160 μL of MACS buffer (PBS, 0.5% BSA, 2mM EDTA, pH 7.2, 4°C) and mixed with 40 μL of CD14 microbeads (Miltenyi Biotec, Bergisch Gladbach, Germany). Cells were incubated (15 min, 4°C) and washed with MACS buffer (1mL, 300 x g, 10 min). The pellet was then resuspended in 500 μL of MACS buffer and added to an equilibrated LS separation column (Miltenyi Biotec, Bergisch Gladbach, Germany). Unlabelled cells were then eluted with buffer (3 x 3 ml). Labelled cells were subsequently eluted following removal of the LS separation column from the magnet, and pelleted (300 x g, 10 min).

5.2.4 Rifampicin cellular accumulation at 4°C

Cellular accumulation ratios of ^{3}H-rifampicin (25 nM, 0.1μCi) were determined in CEM, CEM_{VBL100} and CEM_{E1000} cells as well as in buffy coat PBMCs (n = 4) as

described in section 2.2.15. The experiments were repeated on ice (30 min) to determine the influence of influx transporters.

5.2.5 Extraction of total RNA

Total RNA was extracted using TRIzol according to manufacturer's instructions with minor modifications, Briefly, cell pellets (1 x 10^7 cells of PBMC, CEM, CEM_{VBL100}, CEM_{E1000}, THP1 and A549) and homogenised human liver (100 mg using a glass-teflon homogeniser) were mixed thoroughly in TRIzol (1mL) and frozen (-80°C). Chloroform (200 µL) was then added to the thawed TRIzol mixtures; samples were thoroughly mixed, incubated (20°C, 3 min) and centrifuged (12000 x g, 15mins). The aqueous phase was then removed and mixed with isopropanol (500 µL), incubated (20°C, 10 min) and centrifuged (12000 x g, 10mins). The supernatant was discarded and the RNA pellet washed in 75% ethanol (1 mL, 7500 x g, 5 min) and allowed to air dry before being resuspended in RNase free water (20 mL). Concentration and purity of RNA was determined using a spectrophotometer.

5.2.6 Reverse transcription

Reverse transcription of the extracted total RNA to cDNA was performed using TaqMan Reverse Transcription Reagents (Applied Biosystems, New Jersey, USA) by mixing 10× Taqman RT Buffer (10 µl, final conc. 1x), 25 mM $MgCl_2$ (22 µL final conc. 5.5mM), 2.5 mM dNTP mix (20 µL, final conc. 500 µM of each), 50 µM random hexamer primers (5 µL, final conc. 2.5µM), 20 U/µL RNase inhibitor (2µl, 0.4 U/µL), 50 U/µL Multiscribe reverse transcriptase (2.5 µL, total conc. 1.25 U/µl) and 50 ng/mL total RNA (20 µL final conc. 0.01 µg/µL) and RNase free water (18.5 µL). Samples were then incubated at 25°C (10 min), 48°C (30 min) and 95°C (5 min)

in a GeneAmp PCR System (Applied Biosystems, Warrington, UK). The resulting cDNA was frozen at -20°C until use.

5.2.7 Detection of OATP expression by Hotstart Touchdown PCR

The primers for the OATP were designed on the basis of the published sequences from NCBI-UniGene using FastPCR (1998-2006 v.3.8 for Windows) (Table 5.1) and purchased from Sigma-Genosys (Poole, UK). Primer sequences were screened against the human genome and found to be specific for the genes of interest. PCR reaction mixtures were made by mixing 10x $MgCl_2$ (5μL, final conc. 1x), 2.5 mM dNTPs (4 μL, final conc. 200 μM of each), forward and reverse primers (1 μL, concentrations to be optimised), cDNA (5 μL) and RNase free water (33 μL). Hot-start PCR was then started by inserting the samples into a GeneAmp PCR System (Applied Biosystems, Warrington, UK) and heating them to 95°C, at when 1 μL of Expand Taq polymerase was added (Roche, Indianapolis, USA). PCR touchdown thermo-cycling then followed (Fig. 5.1). PCR conditions were optimised by altering forward and reverse primer concentrations (1, 10 and 100 μM) for OATP expression in A549 and liver cDNA. PCR for the detection of OATP cDNA for the human liver and PBMC samples was performed on a heterologous mixture of the 4 cDNA samples. PCR products were run on a 1% agarose gel (containing ethidium bromide) along with a 100 base pair DNA molecular weight marker XIV (Roche, Indianapolis, USA). Gels were photographed on a UV transilluminator and the cDNA of interest identified by the amplicon size.

5.2.8 E-3-S modulation of rifampicin uptake in CEM cell lines and PBMCs

Rifampicin (25 nM, 0.1μCi) cellular accumulation ratios were determined in CEM, CEM_{VBL100} and CEM_{E1000} cells as well as in buffy coat PBMCs (n = 4) as described

in section 2.2.15. Experiments were repeated following a pre-incubation of the cells with estrone-3-sulphate (E-3-S, 100 μM). The modulation of rifampicin CAR by E-3-S was also determined in CEM_{VBL100} pre-incubation in tariquidar (1 μM, 10 min).

5.2.9 Data handling and statistical analysis

CAR data are presented as mean ± SD. Data were checked for normality using a Shapiro-Wilk test and found to be non-normally distributed. For subsequent analyses a Mann-Whitney test was applied with a $P < 0.05$ taken as indicative of significance.

Table 5.1: Forward (FP) and reverse primers (RP) for the RT-PCR detection of OATP cDNA and the product fragment size.

OATP	Forward and reverse primer		Amplicon size	Accession number
SLCO1A2	FP:	CTG ACA CTC GTT GGG TCG	471	NM_005075
	RP:	CCA ACA TCC TAT GTG GGC AG		
SLCO1B1	FP:	TCT CGA TGG GTT GGA GCT TGG	358	AB026257
	RP:	AGG CTG ACC ATA CTG TTG CTC		
SLCO1B3	FP:	CAT TCC TAC GGT TGC AAC TGG	286	HSA251506
	RP:	TTG TTC CCA CAG ACT GGT TCC		
SLCO2B1	RP:	TGC TTG TCA TCC ATG GCT G	453	AB026256
	RP:	CTG TTG TCC AGA GCA TCC TG		
SLCO3A1	FP:	TGA TCC CGA AGG TCA C	557	AB031050
	RP:	ACG GTT GCG TTC TCA G		
SLCO4A1	FP:	TGA GTG CCT CAG AAG CTG C	468	AB031051
	RP:	AGT GCA TTT CCC TGC AGT G		

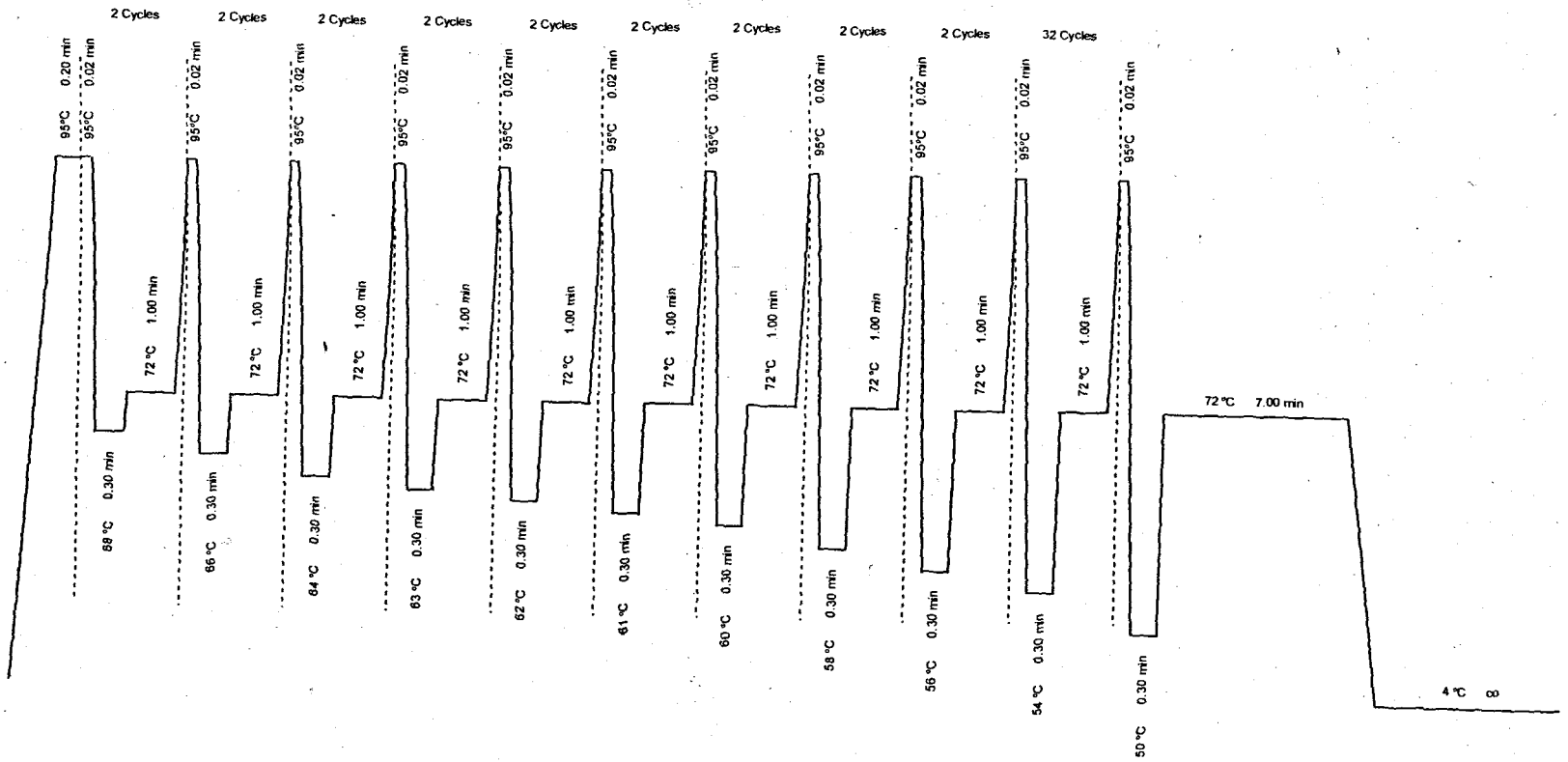

Figure 5.1.: Hot-Start Touchdown PCR thermocycle conditions. 1 µL of Expand Taq polymerase was added when samples were initially heated up to 95°C (Hotstart) for optimum activity.

5.3 Results

5.3.1 Rifampicin accumulation at 4°C and in heat killed cells

Basal rifampicin CAR in CEM, CEM_{VBL100}, CEM_{E1000} and buffy coat PBMCs were significantly increased when they were denatured (heat killed) and significantly decreased when CAR was determined at 4°C (Table 5.2).

5.3.2 Optimisation of OATP Hot-start Touchdown PCR conditions

Human lung epithelial cell line, A549 was found to express levels of all the OATP mRNA investigated, and was therefore used to optimise the primer concentrations for Hot-start Touchdown PCR conditions. All primers designed were able to detect the correctly sized cDNA amplicons in A549 cDNA by Hot-start Touchdown PCR. Optimal primer concentrations were found to be 10 μM for SLCO1A2, SLCO1B1, SLCO3A1, and SLCO1B3 and 100 μM for SLCO2B1 and SLCO4A1 (Fig. 5.2). In all cases 1 μM primer concentrations did not produce any visible bands (data not shown).

5.3.3 Cell screening of OATP mRNA expression

Heterologous liver (mixture of 4 individuals), heterologous PBMC (mixture of 4 individuals) and human cell line cDNA were screened for expression of OATP mRNA (Fig. 5.3). Positive control A549 cDNA expressed all tested OATP transcripts. Heterologous liver cDNA was found to express SLCO1A2, SLCO1B1, SLCO1B3, SLCO3A1 and SLCO2B1 but not SLCO4A1. Heterologous PBMC cDNA was found to only express SLCO3A1. CEM, CEM_{VBL100}, CEM_{E1000} were

found to have similar OATP mRNA expression (SLCO3A1 and SLCO4A1), however CEM_{VBL100} expressed SLCO1A2 which was not expressed in CEM and CEM_{E1000} cells. THP1 cells were found to express SLCO2B1, SLCO3A1 and SLCO4A1 (Fig. 5.3). Alveolar macrophages purified from BAL were found to express SLCO3A1 and SLCO1B3 (Fig. 5.4).

5.3.4 E-3-S modulation of rifampicin CAR

100 μM E-3-S had no significant effect on the CAR of rifampicin in CEM and CEM_{VBL100}. However, following inhibition of P-gp mediated rifampicin efflux in CEM_{VBL100} by tariquidar; E-3-S was able to significantly decrease the rifampicin CAR (Fig. 5.5). In buffy coat PBMCs, E-3-S was able to significantly decrease rifampicin CAR in 3 of the 4 samples (Fig. 5.6).

5.3.5 Results Tables

Table 5.2: Rifampicin CAR in CEM, CEM_{VBL100}, CEM_{E1000} and buffy coat PBMCs at 37°C and at 4°C. Data mean ± SD ($n \geq 4$), * $P<0.05$ compared to control conditions.

	Rifampicin Cellular Accumulation Ratio (CAR) mean ± SD	
	Control (37°C)	At 4°C
CEM	5.54 ± 0.21	2.56 ± 0.17*
CEM_{VBL100}	3.40 ± 0.14	2.23 ± 0.41*
CEM_{E1000}	4.63 ± 0.34	2.77 ± 0.36*
PBMC	5.96 ± 0.80	3.55 ± 0.49*

5.3.6 Results Figures

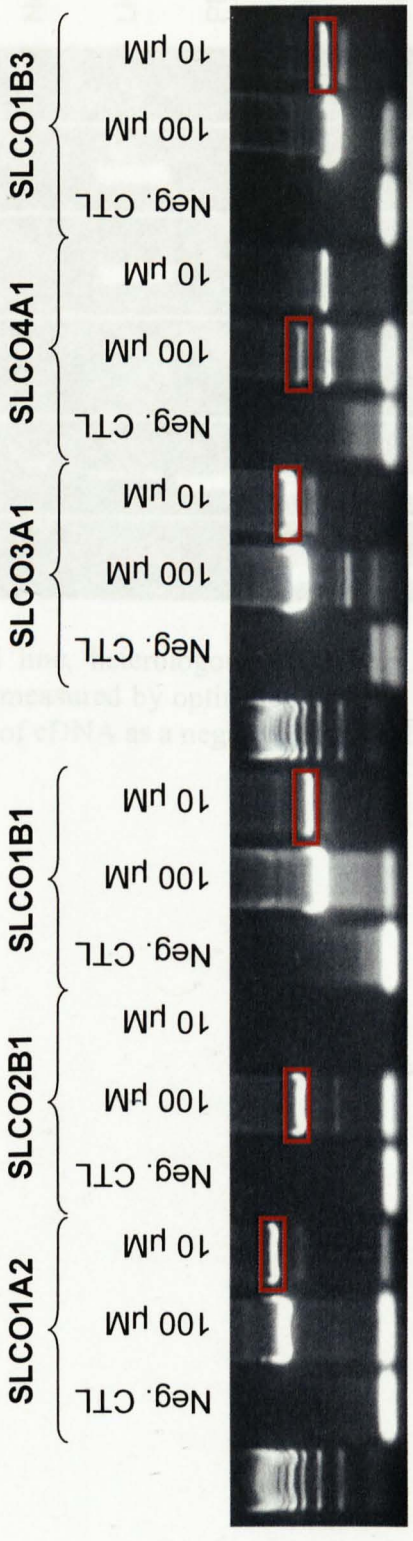

Figure 5.2.: PCR primer concentration optimisation for the Hotstart Touchdown detection of OATPs in A549 cDNA. Primer opimistaion was performed using 1, 10 and 100 µM forward and reverse primers. 1 µM primers produced no PCR products (data not shown). The appropriate PCR amplicon for the optimum PCR condition for each OATP is highlighted with a red box. RNase free water was used instead of cDNA as a negative control (Neg. CTL)

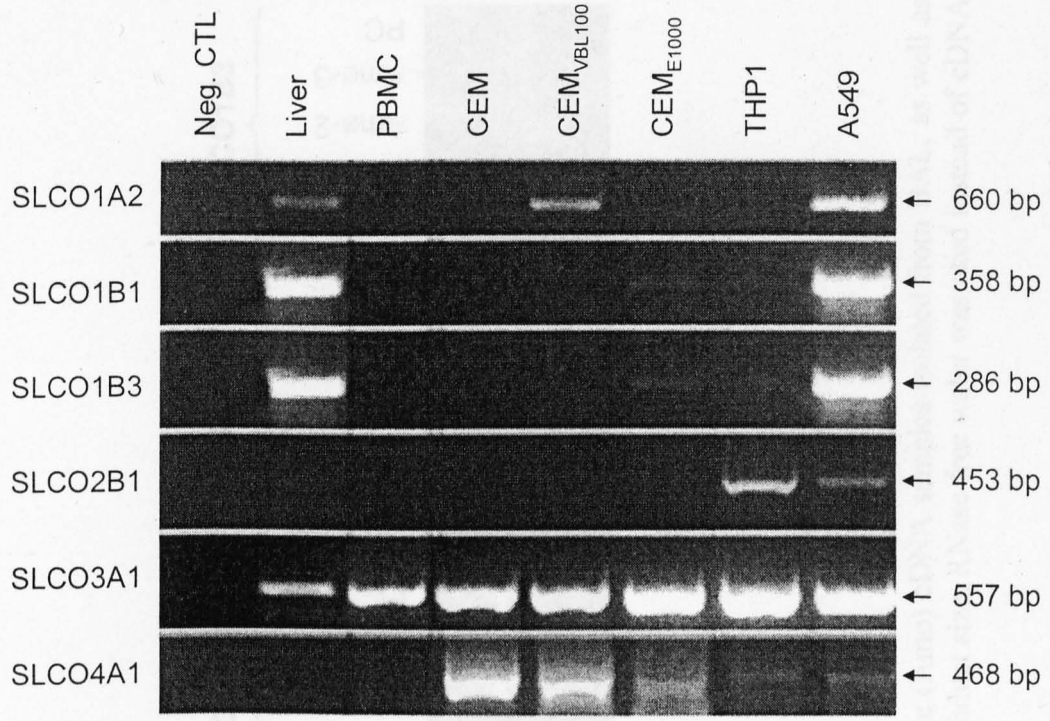

Figure 5.3: Cell line, heterologous PBMC and heterologous liver expression of OATP cDNA as measured by optimised hotstart touchdown PCR. RNase free water was used instead of cDNA as a negative control (Neg. CTL)

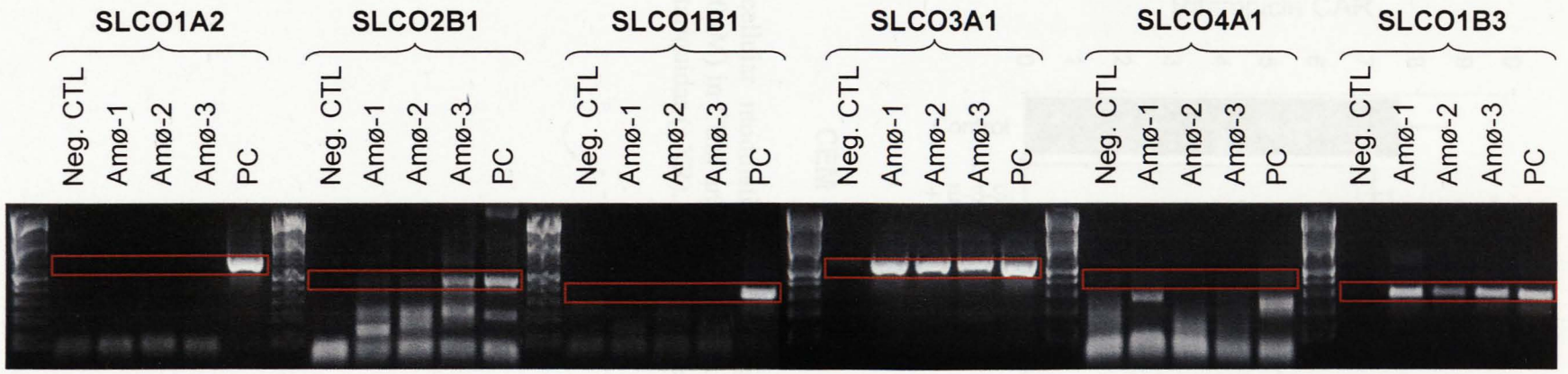

Figure 5.4.: The OATP mRNA expression measured in 3 alveolar macrophage (Amø) cDNA samples isolated from BAL, as well as in A549 cDNA (positive control, PC). Red boxes indicate the predicted OATP product size. RNase free water was used instead of cDNA as a negative control (Neg. CTL)

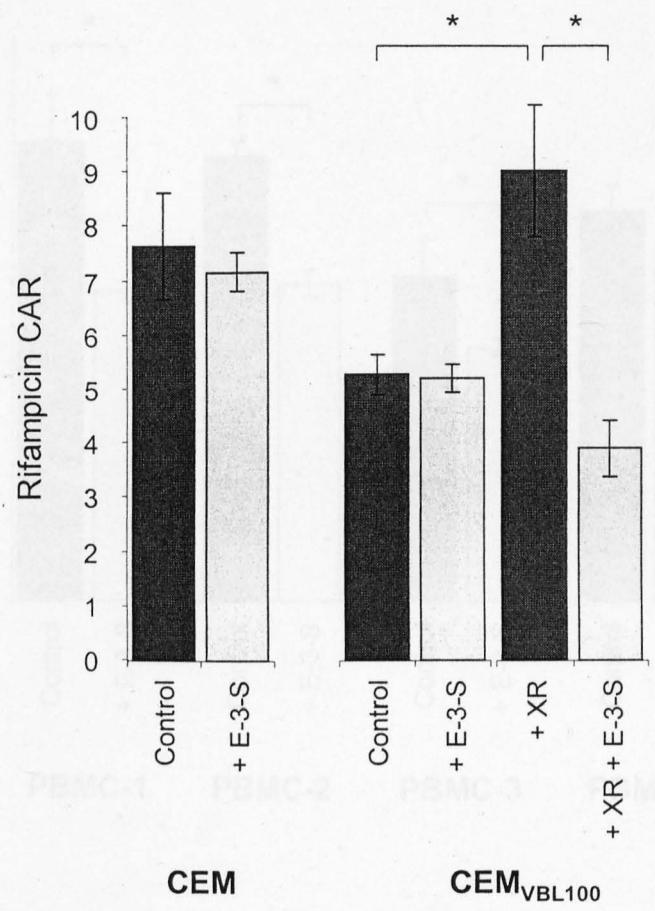

Figure 5.5: The cellular modulation of rifampicin accumulation by estrone-3-sulphate (E-3-S, 100μM) in CEM and CEM_{VBL100} and in CEM_{VBL100} pre-treated with the P-gp inhibitor; tariquidar (+XR). Data are presented as a mean ± SD (n = 4), * $P < 0.05$.

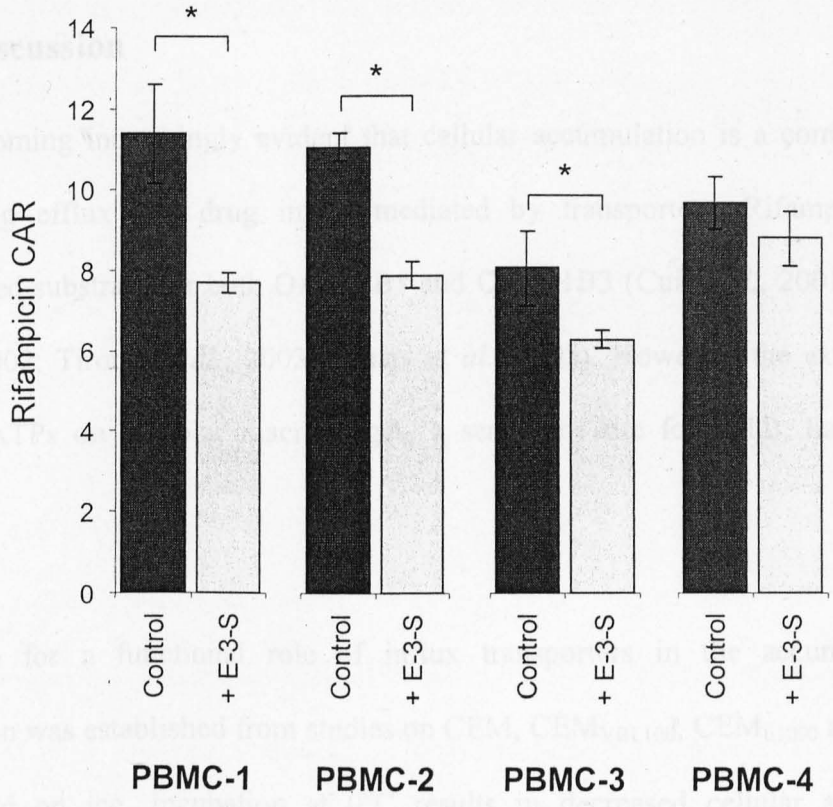

Figure 5.6: The cellular accumulation of rifampicin in PBMCs isolated from 4 buffy coats in the absence and presence of estrone-3-sulphate (E-3-S). Data are presented as a mean ± SD (n = 4), * $P < 0.05$.

5.4 Discussion

It is becoming increasingly evident that cellular accumulation is a composition of both drug efflux and drug influx mediated by transporters. Rifampicin is an established substrate for both OATP1B1 and OATP1B3 (Cui *et al.*, 2001; Vavricka *et al.*, 2002; Tirona *et al.*, 2003; Spears *et al.*, 2005). However, the expression of these OATPs on alveolar macrophages, a sanctuary site for MTB, has not been assessed.

Evidence for a functional role of influx transporters in the accumulation of rifampicin was established from studies on CEM, CEM_{VBL100}, CEM_{E1000} and PBMCs performed on ice. Incubation at 0°C results in decreased cellular activity and therefore shut down of active drug transport (both influx and efflux), suggesting that the observed accumulation of rifampicin is at least partially due to active uptake. However, it must be noted that performing an uptake experiment at 4°C has its limitations because the low temperature can leads to a change in membrane morphology and fluidity. This additional change may also influence the rate of passive and facilitated drug movement as well as influencing active transport. These data are therefore not conclusive evidence for the presence of active influx.

Overall there is a consensus between previous publications over the tissue distribution of the OATPs in the liver, lung and in leukocytes (Table 5.2). However, there are conflicting reports with respect to the tissue distribution of SLCO1A2 (in lung samples), SLCO3A1 (in liver and leukocytes samples) and SLCO4A1 (in liver samples). In this study liver OATP expression (Fig. 5.3) was found to be largely similar to that published previously, showing that that SLCO3A1 is expressed and

that SLCO4A1 is not expressed (Tamai *et al.*, 2000; Schiffer *et al.*, 2003). The fact that we only showed the expression of SLCO3A1 in heterologous PBMC cDNA is also in agreement with previous work (Tamai *et al.*, 2000).

With the exception of SLCO3A1 in A549 (Adachi *et al.*, 2003), SLCO expression has not previously been assessed in T-lymphocyte (CEM, CEM_{VBL100}, CEM_{E1000}), monocytic (THP1) and lung epithelial cell line (A549). A549 cells were found to also express the other OATP mRNAs tested, which is different to the lung tissue expression (Table 5.2) from which it was originally derived. The CEM and THP1 cell line have also undergone changes in their OATP expression compared to PBMC with CEM cells also expressing SLCO4A1 and THP-1 cells also expressing both SLCO4A1 and SLCO2B1.

The expression of SLCO1A2 by CEM_{VBL100}, but not the parental CEM cell line was unexpected. CEM_{VBL100} cells were originally generated by the stepwise selection of parental CEM cells up to 100 ng/ml of vinblastine in order to obtain a P-gp overexpressing cells (Beck *et al.*, 1979). This process could however also have led to the selection of SLCO1A2 expressing cells. To further verify the presence of functional OATP1A2 protein, active influx of rifampicin in CEM_{VBL100} was evaluated and modulated using the universal OATP substrate and therefore competitive inhibitor, E-3-S (Su *et al.*, 2004). Incubation with E-3-S had no effect on rifampicin CAR in CEM and CEM_{VBL100}, suggesting that rifampicin is not a substrate for OATP3A1 or OATP4A1 (also seen by (Tirona *et al.*, 2003)) (Fig. 5.5). As rifampicin is also a substrate for P-gp, which is overexpressed in CEM_{VBL100}, the full extent of influx could only be determined if P-gp was blocked. In the presence of a

P-gp inhibitor it could be seen that E-3-S did modulate rifampicin influx into CEM_{VBL100}, indicating that functional OATP1A2 was expressed (Fig. 5.5). Therefore, in non-epithelial CEM_{VBL100} cells it seems that rifampicin accumulation is regulated by both an active influx transporter (OATP1A2) and an active efflux transporter (P-gp), although the efflux system appears to be more efficient. In contrast to polarised cells the transporters would act in conjunction to facilitate trans-epithelial transport, with active influx on the basal membrane and active efflux on the apical membrane. The differential expression of SLCO1A2 by CEM_{VBL100} and the parental CEM cells therefore provides a useful tool to determine if drugs are substrates for OATP1A2.

Rifampicin accumulation in PBMCs was found to decrease at 4°C, and importantly could be modulated by E-3-S indicating the presence of an influx system. However PBMCs were found to only express SLCO3A1, a transporter also expressed in CEM cells (rifampicin accumulation was not modulated by E-3-S). E-3-S is however transported into cells by a plethora of influx transporters (OATP, NTCP- sodium dependent taurocholate transporter peptide, OAT- organic anion transporter), all of which can competitively inhibit if concentrations are sufficiently high (Kullak-Ublick *et al.*, 2001; Chandra and Brouwer, 2004). Previous work has however shown that rifampicin is not a substrate for NTCP, OATs (OAT1, OAT3) or organic cation transport (OCT1, OCT2) (Tirona *et al.*, 2003). The future development of more specific inhibitors of influx transporters will clarify the mechanism by which E-3-S modulates rifampicin accumulation in buffy coat PBMC.

As in PBMC, alveolar macrophages were found to express SLCO3A1 (Fig. 5.4). Interestingly, alveolar macrophages were also found to express SLCO1B3 for which rifampicin is a substrate (Cui *et al.*, 2001; Vavricka *et al.*, 2002; Tirona *et al.*, 2003; Spears *et al.*, 2005). The presence of OATP1B3 protein could not be verified because of the lack of specific commercially available antibodies. Further, limited alveolar macrophage yield form BAL and the lack of specific OATP1B3 substrates or inhibitors hinders the phenotypic characterisation of rifampicin influx into alveolar macrophages.

In summary, data shown here illustrate that CEM and CEM_{VBL100} can be used to screen for OATP1A2 substrates, and that the presence of the influx protein must be taken into consideration when the cells are used to screen for P-gp substrates. Further, the expression of SLCO1B3 by alveolar macrophages indicates that drug accumulation in epithelial and non-epithelial cells should be considered not only in terms of efflux but also influx. Further studies are now required to elucidate whether OATP1B3 mediates the influx of rifampicin in alveolar macrophage and whether this is related to intracellular TB kill.

Table 5.3: Published OATP tissue distribution in the liver, lung and in PBMCs as determined by mRNA RT-PCR expression[1] and Northern blots[2]. Dashes (-) indicate that expression has not been assessed.

Tissue	OATP Tissue Expression						Reference
	SLCO1A2	SLCO1B1	SLCO1B3	SLCO2B1	SLCO3A1	SLCO4A1	
Liver	Yes[1]	Yes[1]	-	-	-	-	(Su *et al.*, 2004)
	Yes[1]	Yes[1]	-	Yes[1]	Yes[1]	No[1]	(Schiffer *et al.*, 2003)
	-	Yes[2]	Yes[2]	-	-	-	(Cui *et al.*, 2003)
	Yes[1]	Yes[1]	Yes[1]	Yes[1]	Yes[1]	Yes[1]	(Tamai *et al.*, 2000)
	Yes[2]	-	-	-	-	-	(Kullak-Ublick *et al.*, 1995)
	-	Yes[2]	-	-	-	-	(Konig *et al.*, 2000)
	-	Yes[2]	-	-	-	-	(Hsiang *et al.*, 1999)
	-	-	-	Yes[2]	-	-	(Kullak-Ublick *et al.*, 2001)
	-	-	-	-	No[2]	-	(Adachi *et al.*, 2003)
Lung	No[1]	No[1]	No[1]	Yes[1]	Yes[1]	Yes[1]	(Tamai *et al.*, 2000)
	Yes[2]	-	-	-	-	-	(Kullak-Ublick *et al.*, 1995)
	-	No[2]	-	-	-	-	(Konig *et al.*, 2000)
	-	No[2]	-	-	-	-	(Hsiang *et al.*, 1999)
	-	-	-	Yes[2]	-	-	(Kullak-Ublick *et al.*, 2001)
	-	-	-	-	Yes[2]	-	(Adachi *et al.*, 2003)
PBMC	No[1]	No[1]	No[1]	No[1]	Yes[1]	No[1]	(Tamai *et al.*, 2000)
	No[2]	-	-	-	-	-	(Kullak-Ublick *et al.*, 1995)
	-	No[2]	-	-	-	-	(Konig *et al.*, 2000)
	-	No[2]	-	-	-	-	(Hsiang *et al.*, 1999)
	-	-	-	No[2]	-	-	(Kullak-Ublick *et al.*, 2001)
	-	-	-	-	No[2]	-	(Adachi *et al.*, 2003)

CHAPTER 6

Method Development for the Quantitative Analysis of Plasma Rifampicin, Isoniazid and Pyrazinamide by HPLC, HPLC-MS and HPLC-MS/MS

6.1 Introduction 188

6.2 Materials and Methods 189

6.2.1 Chemicals 189

6.2.2 HPLC and Mass Spectrometry apparatus 189

6.2.3 Rifampicin HPLC Method 190

6.2.4 Pyrazinamide HPLC Method 192

6.2.5 Isoniazid and acetylisoniazid HPLC Method 193

6.2.6 Rifampicin HPLC-MS Method 196

6.3 Results 199

6.3.1 Detection and chromatography: 199

6.3.2 Validation of all assays quality control samples 199

6.3.3 Rifampicin stability 200

6.3.4 Results Tables 201

6.3.5 Results Figures 206

6.4 Discussion 213

6.1 Introduction

Rifampicin, isoniazid and pyrazinamide are the primary drugs used in the chemotherapy of tuberculosis. Pharmacokinetic studies are an important tool that can be used to determine potential drug-drug interactions and the effect of protein induction. This is especially true for rifampicin and isoniazid that are taken for a long period of time, often co-prescribed with other drugs such as anti-retrovirals.

Criteria for the development of assays to quantify plasma drug concentrations are that they are specific, accurate and precise. Further, methods should be sensitive enough to measure full concentration ranges expected in a pharmacokinetic profile by preferably using a small sample volume.

Numerous assays have been published for the detection of rifampicin (Smith *et al.*, 1999; Mohan *et al.*, 2003; Calleja *et al.*, 2004), pyrazinamide (Yamamoto *et al.*, 1987; Gaitonde and Pathak, 1990; Revankar *et al.*, 1994; Walubo *et al.*, 1994; Kraemer *et al., 1998;* Conte *et al., 2000)* and isoniazid (Hutchings *et al.*, 1983; Delahunty *et al.*, 1998; Moussa *et al.*, 2002). However, no methods were available within our institution for the quantification of rifampicin, pyrazinamide and isoniazid.

Work shown here describes the development and validation of novel improved HPLC and HPLC-MS methods for the quantification of rifampicin. Further, HPLC methods have been developed and validated for the quantification of pyrazinamide and isoniazid based on previously published methods by (Conte *et al.*, 2000) and (Hutchings *et al.*, 1983) respectively.

6.2 Materials and Methods

6.2.1 Chemicals

Ammonium formate was purchased from Fisher Scientific (Loughborough, UK). HPLC grade acetonitrile (ACN) and methanol (MeOH) were purchased from BDH Laboratory Supplies (Poole, UK). Blank, drug-free plasma was obtained from the National Blood Service (Liverpool, UK). De-ionised water was used throughout. All further chemicals were obtained from Sigma-Aldrich (Poole, UK).

6.2.2 HPLC and Mass Spectrometry apparatus

The high-performance liquid chromatography (HPLC) system used to analyse rifampicin, pyrazinamide, and isoniazid consisted of a variable wavelength detector (HPLC detector 432), an automatic sample injection device (HPLC autosampler 360), a delivery pump (325 system) and a degasser (DEG-104) purchased from Kontron Instruments Ltd., Hertfordshire, UK. Analytical runs were processed using Chromeleon software (Dionex Ltd; Camberley, UK).

Rifampicin analysis was determined by reverse-phase high-pressure liquid chromatography (HPLC) interfaced with a mass spectrometer. Equipment consisted of a mass spectrometer (Finnigan MAT TSQ 7000 triple quadrupole), an autosampler (SpectraSystem AS3000, Thermo Separation Products, Hemel Hempstead, UK), a pump (SpectraSystem P2000, Thermo Separation Products, Hemel Hempstead, UK), a degasser (TSP), a rotary vacuum pump (2X E2M30, Aztech Trading, Loughborough, Leicestershire, UK), a nitrogen generator and a 2000-40M air compressor (Jun Air). Assays were processed by Xcalibur Software (Thermo Electron Corporation, Hemel Hempstead, UK).

6.2.3 Rifampicin HPLC Method

The HPLC method for the detection of rifampicin is a novel method developed for the detection of plasma rifampicin at concentrations above 0.823 μg/mL.

Column: Separation of rifampicin from the internal standard (IS: p-hydroxybenzoic acid n-butyl ester) and the mobile front was achieved with a Luna C_8 reverse phase column (5 μm, 150 x 4.6 mm), (phenomenex, Macclesfield, UK), protected by a guard column (Si 60, 5μ; Merck, Germany).

Mobile phase: A gradient mobile phase consisting of 50mM ammonium formate (pH 5) and acetonitrile (mobile phase A: 65:35 (v/v), Mobile phase B: 30:70 (v/v)) was used to ensure optimum separation and peak shape for rifampicin and internal standard. For the first 2 min 100 % mobile phase A was kept isocratic at a flow rate of 1 ml/min, followed by a linear gradient to 100 % mobile phase B at 7 min. From 7 min to 12 min the mobile phase was returned to mobile phase A, to allow the column to equilibrate.

Preparation of stock rifampicin and internal standard solutions: Stock solution of rifampicin (1 mM or 0.823 mg/mL) and internal standard (IS: p-hydroxybenzoic acid n-butyl ester, 1mg/ml) was prepared by dissolving the appropriate amount of compound, accurately weighed, in 100% HPLC grade methanol (kept at -20 °C and in the dark to prevent breakdown of the drug). Stock IS solutions were further diluted in 100 % HPLC grade methanol to generate a working IS solution of 1 μg/ml.

Preparation of Quality control samples: Low (LQC: 1.07 μg/mL), medium (MQC: 7.41 μg/mL) and high (HQC 16.46 μg/mL) quality control samples were prepared by respectively adding 26, 180 and 400 μL of stock 0.823 mg/mL rifampicin to a 20 ml volumetric flasks. Following the evaporation of the methanol from the added rifampicin (under gasseus nitrogen), blank drug free plasma (centrifuged at 3200 g, 10 min) was then added to the mark. Following thorough mixing, 1 mL aliquots of each quality control sample were transferred to plasma vials and frozen down at -80 °C. LQC, MQC and HQC samples were defrosted prior to and incorporated into each analytical run.

Preparation of standard curves: On the day of experimental setup, a top rifampicin concentration was generated by adding 30 μL of stock 0.823 mg/mL rifampicin to 1470 μL of blank drug free plasma (centrifuged at 3200 g, 10 min) to give 16.46 μg/mL solutions. A rifampicin standard curve (0.412, 0.823, 1.65, 3.29, 6.58, 9.88, 11.52, 16.46 μg/mL) was constructed by mixing the appropriate amount of the top standard (16.46 μg/mL), with blank plasma in 5 ml glass culture tubes.

Sample treatment: 200 μL (in duplicate) of each of the standard, quality control sample (QC) and test samples were transferred into a clean glass 5 ml culture tube. Proteins were then precipitated by adding 1 mL of 1 μg/ml IS working solution (in HPLC grade methanol). The solutions were vortexed thoroughly and allowed to stand for 1 hr to allow for protein precipitation (1 h, 4 °C, in the dark). Samples were centrifuged (3200 g, 10 min) and supernatant transferred to a clean 5 ml culture tube. The supernatant was then dried down to complete dryness under nitrogen (in the dark). The residue was re-suspended in 200 μL HPLC grade methanol, vortexed and

transferred to an autosample vial (with insert). 20 µL of sample was injected into the HPLC system and analysed at 254 nm.

6.2.4 Pyrazinamide HPLC Method

The detection and quantification of plasma pyrazinamide concentrations is based on a method described by (Conte *et al.*, 2000) with minor modifications.

Column: Separation of pyrazinamide and the internal standard from each other and the solvent front was achieved using a HyPURITY C_{18} column (5µ, 250 x 4.6 mm) (Thermo Electron Corporation, Runcorn, Cheshire, UK) protected by a guard column (Si 60, 5µ; Merck, Germany).

Mobile phase: Separation was achieved with an isocratic mobile phase consisting of 20 mM KH_2PO_4 (pH 2.6 with phosphoric acid) and acetonitrile (98:2, v/v), at a flow rate of 1.2 ml/min, and a runtime of 45 min.

Preparation of stock pyrazinamide and internal standard solutions: Stock solution of pyrazinamide (10 mg/ml) and internal standard (IS: acetazolamide: 5 mg/ml) was prepared by dissolving the appropriate amount of compound, accurately weighed, in 50% HPLC grade methanol (kept at –20 °C and in the dark). On each experimental day the working IS stock solution was diluted in acetonitrile to 5 µg/ml.

Preparation of Quality Control Samples: Low (LQC: 3µg/ml), medium (MQC: 15 µg/ml) and high (HQC: 75 µg/ml) quality control samples were prepared by respectively adding 15, 75 and 375 µL of 10 mg/ml pyrazinamide in methanol to 50 ml volumetric flasks. Following the evaporation of the methanol from the added

pyrazinamide (under gaseous nitrogen), blank drug free plasma (centrifuged at 3200 g, 10 min) was then added to the mark and mixed thoroughly. 1 ml aliquots of each quality control sample were transferred to plasma vials and frozen down at –80 °C. LQC, MQC and HQC samples were defrosted prior to and incorporated into each analytical run.

Preparation of standards curves: On the day of experimental setup, a top pyrazinamide concentration was generated by adding 80 µL of stock 1 mg/ml pyrazinamide to 920 µL of blank drug free plasma (centrifuged at 3200 g, 10 min) to give 80 µg/ml solutions. A pyrazinamide standard curve (1.25, 2.5, 5.0, 10.0, 20.0, 40.0, 80.0 µg/ml) was constructed by performing serial 1 in 2 dilutions of the top standard (80 µg/ml), with blank plasma in 5 ml glass culture tubes.

Sample treatment: 200 µL (all in duplicate) of each of the standards, quality control sample (QC) and test samples were transferred into a clean 1.5 ml microfuge tube. 400 µL of IS working solution (5 µg/ml in ACN) was added and mixed thoroughly to allow for sample protein precipitation. Following centrigugation (10 min, 10000 x g), the top organic layer was transferred to a glass 5 ml tube and dried down to complete dryness under nitrogen. The residue was then reconstituted in 200 µl of mobile phase, vortexed and transferred to an autosample vial (with insert). 20 µL of sample was injected into the HPLC system and analysed at 268 nm.

6.2.5 Isoniazid and acetylisoniazid HPLC Method

The detection of isoniazid and acetylisoniazid by HPLC was originally described by (Hutchings *et al.*, 1983) (as well as further modifications by Hutchings A, University of Cardiff by personal communication), briefly:

Column: Separation of isoniazid, acetylisoniazid and the internal standard (iproniazid) from each other and the mobile front was achieved using a Spherisorb nitrile column (5μ, 250 x 4.5 mm) (Waters, Hertsfordshire, UK). Because of the vigorous extraction procedure, a guard column was deemed unnecessary.

Mobile phase: Separation was achieved with an isocratic mobile phase consisted of 8 mM citric acid and acetonitrile (80:20, v:v), at a flow rate of 2 ml/min, and a runtime of 10 min.

Preparation of acetylisoniazid: The preparation of acetylisoniazid was as described by (Fox, 1953) and modified by (Lauterberg BH, 1981). Briefly, 10 ml of tetrahydrofuran was added to a clean conical flask containing 1.37 g of isoniazid. The solution was mixed until the isoniazid was dissolved and in drop wise fashion 1.9 ml of acetic anhydride was carefully added (in fume hood). Following the completion of the reaction the samples was cooled (4 °C, 24 hr) to aid the spontaneous precipitation of acetylisoniazid. The acetylisoniazid was then separated from the solution by filtration and allowed to dry. The purity of the acetylisoniazid was then confirmed using chromatography and NMR.

Preparation of stock isoniazid, acetylisoniazid and internal standard solutions: Stock solution of isoniazid (1 mg/ml), acetylisoniazid (1 mg/ml), and internal standard (iproniazid: 1 mg/ml) was prepared by dissolving the appropriate amount of compound, accurately weighed, in 50% HPLC grade methanol and (kept at –80 °C and in the dark). Working solutions of IS (100 μg/ml) was prepared in water.

Preparation of Quality Control Samples: Low (LQC: 0.3 μg/ml), medium (MQC: 1.5 μg/ml) and high (HQC: 10 μg/ml) quality control samples were prepared by respectively adding 30, 150 and 1000 μL of stock isoniazid and acetylisoniazid solutions (1 mg/ml) to 100 ml volumetric flasks. Following the evaporation of the methanol from the added isoniazid and acetylisoniazid (under gaseous nitrogen), blank drug free plasma (centrifuged at 3200 g, 10 min) was then added to the mark and mixed thoroughly. 3300 μl aliquots of each quality control sample were transferred to 10 ml glass tube and frozen down at –80 °C. LQC, MQC and HQC samples were defrosted prior to and incorporated into each analytical run.

Preparation of standard curve: On the day of experimental setup a top isoniazid/ acetylisoniazid solution was prepared by mixing 30.72 μL of isoniazid (1 mg/ml) and 30.72 μL of acetylisoniazid (1 mg/ml) with 2340 μL of blank, drug free plasma (centrifuged at 3200 g, 10 min) to give a final concentration of 12.8 μg/ml for each drug. A isoniazid/ acetylisoniazid standard curve (0.2, 0.4, 0.8, 1.6, 3.2, 6.4 and 12.8 μg/ml) was constructed by performing serial 1 in 2 dilutions of the top standard (12.8 μg/ml), with blank plasma in 5 ml glass culture tubes.

Sample Treatment: 1000 μL of each standard, quality control sample (QC) and test samples were transferred into a clean 5 ml glass tube and 100 μL of IS working solution (iproniazid 100μg/ml) was added. 500 μL of 30 % (w/v) perchloric acid was then added (to precipitate all the proteins and to break down isoniazid hydrazones to isoniazid) and vortexed thoroughly and left for 10 min. The samples were then centrifuged (10 min, 3000 g) and supernatant transferred to a clean 5 ml glass tube.

To neutralise the acid, 1500 µL of di-potassium hydrogen phosphate buffer (3M) was added and the sample was vortexed and centrifuged (10 min, 3000 g). The supernatant was transferred into 3 ml ISOLUTE extraction column (Kinesis Ltd, Beds, UK) and left to distribute evenly for 30 min. 3 volumes of 4 ml chloroform: butanol (70:30) were then used to extract the isoniazid and acetylisoniazid from the column and the elutent collected in a clean 10 ml glass tube. 500 µL of phosphoric acid (0.05 M) was added to the elutent (to back extract the isoniazid and acetylisoniazid) and tubes were tumbled for 30 min. The tubes were then centrifuged (10 min, 3200 g) and the inorganic layer transferred to an autosample vial (with insert). 20 µL of sample was injected into the HPLC system and analysed at 266 nm.

6.2.6 Rifampicin HPLC-MS Method

The HPLC-MS method for the detection of rifampicin is a novel method developed for the detection of both plasma and cell associated rifampicin concentrations.

Column: Ideal chromatography was achieved using a Betasil Phenyl-Hexyl column (5 µm, 50 x 2.1 mm) (Thermo Electron Corporation, Runcorn, Cheshire, UK), protected with a betasil hexyl pre-column (5µ).

Mobile phase: To ensure separation of rifampicin and the internal standard from the solvent front, but retaining a short runtime, an isocratic mobile phase of 10 mM ammonium acetate (pH 4.0) and acetonitrile (60:40 v:v), at a flow rate of 0.4 ml/min was used.

Preparation of stock rifampicin and internal standard solutions: Stock solution of rifampicin (1 mg/ml) and internal standard (IS: rifamycin SV, 1 mg/ml) was

prepared by dissolving the appropriate amount of compound, accurately weighed, in 100% HPLC grade methanol (kept at –80 °C and in the dark). On each experimental day the working IS stock solution was diluted in acetonitrile to 1 μg/ml.

Preparation of Quality Control Samples: Low (LQC: 150 ng/ml), medium (MQC: 1200 ng/ml) and high (HQC: 10000 ng/ml) quality control samples were prepared by adding 37.5 μL (of 100 μg/ml rifampicin), 30 μl and 250 μL (of 1000 μg/ml rifampicin) respectively to a 25 ml volumetric flasks. Following the evaporation of the methanol from the added rifampicin (under gaseous nitrogen), blank drug free plasma (centrifuged at 3200 g, 10 min) was then added to the mark and mixed thoroughly. 1 ml aliquots of each quality control sample were transferred to plasma vials and frozen down at –80 °C.

Preparation of rifampicin standard curve: On the day of experimental setup a top rifampicin solution was prepared by mixing 12.8 μL of stock rifampicin (1 mg/ml) with 987.2 μL of blank drug free plasma (centrifuged at 3200 g, 10 min) to give a final rifampicin concentration of 12.8 μg/ml. A rifampicin standard curve (0.1, 0.2, 0.4, 0.8, 1.6, 3.2, 6.4, 12.8 μg/ml) was constructed by performing 1 in 2 dilutions of the top standard, with blank plasma in 1.5 ml microfuge tube.

Sample treatment: 50 μL (all in duplicate) of each of the standards, quality control sample (QC) and test samples were transferred into a clean 1.5 ml microfuge tube. 150 μL of internal standard (rifamycin SV, 1 μg/ml in ACN) was added to allow for protein precipitation. Following vigorous vortexing, the samples were centrifuged (10 min, 12000 x g). 100 μL of supernatant was transferred to an autosample vial

(with insert) and mixed with 150 µL of HPLC grade water. 10µL of sample was injected into the HPLC/MS machine.

HPLC-MS conditions: Mass spectral analyses for rifampicin and the IS were carried out using electrospray ionisation (ESI) in the positive ion mode, an ESI voltage of 4.5 kV and a heated capillary temperature of 250 °C. For single ion monitoring (SIM) analysis, the first quadripole was set to scan for the scan ranges indicated in Table 6.1. The sum of three m/z products (m/z: 791.9, 824.0 and 846.0) was used for the quantification of rifampicin. The different m/z for rifampicin represent MH+ (m/z = 824.00), MNa+ (m/z = 846.00) and a truncated rifampicin (without a methoxy: m/z = 791.9; also shown by (Korfmacher *et al.*, 1993)). The single m/z product of rifamycin SV (m/z: 720.6) was used to analyse the IS area.

Table 6.1: The single ion monitoring (SIM) settings and conditions for the detection of rifampicin and rifamycin SV by HPLC-MS.

Drug	Centre Mass (m/z)	Width (m/z)	Scan time (sec)
Rifamycin SV	720.60	0.60	0.20
Rifampicin	791.90	0.60	0.20
Rifampicin	824.00	0.60	0.20
Rifampicin	846.00	0.60	0.20

6.3 Results

6.3.1 Detection and chromatography:

Rifampicin and the IS (p-hydroxybenzoic acid n-butyl ester) were detected by UV-HPLC detection at 254 nm over a total run time of 12 min. Rifampicin and IS peaks were detected at retention times of 5.3 and 9.0 min respectively and blank plasma did not interfere with either of the peaks (Fig. 6.1). Pyrazinamide was detected by UV-HPLC at 268 nm, over a total run time of 20 min. Pyrazinamide and the IS were detected at a retention time of 4.7 and 14.0 min respectively (Fig. 6.2). Isoniazid and acetylisoniazid was detected by UV-HPLC detection at 266 nm over a total run time of 8 min. Isoniazid, acetylisoniazid and IS had a retention time of 4.1, 2.2, and 6.5 min respectively (Fig. 6.3).

Rifampicin was detected by HPLC-MS single ion monitoring over a total run time of 6 min. Rifampicin detection was optimised by measuring 3 rifampicin ions, all of which producing a single peak of equal retention time (Fig. 6.4 and 6.5). Rifampicin and IS peaks eluted at a retention time of 1.1 and 1.7 min respectively and blank plasma did not interfere with either of the peaks (Fig. 6.6).

6.3.2 Validation of all assays quality control samples

A minimum of 6 standard curves (in duplicate) and QC samples (LQC, MQC and HQC) were analysed for each of the anti-tuberculosis drug assays. All standard curves for all the assays were adequately described by a 1/concentration^2 linear weighted. All points of the standard curve were within 15 % of the target

concentration (Table 6.3) and the correlation co-efficient (r^2) for all standard curves were above 0.995.

Upper and lower limits of quantification (ULQ, LLQ) were arbitrarily set as the top and bottom concentrations of the standard curve, respectively. The limit of detection (LOD) was set at the concentration where the accuracy exceeds 20%. The ULQ, LLQ and the LOD for each of the assays is summarised in Table 6.2.

Accuracy was evaluated by calculating the percentage bias of the QC samples (% bias: difference in the measured and target concentration as a percentage of the target concentration). Precision was evaluated by measuring the co-efficient of variation of the QC samples (% CV: standard deviation / mean x 100). Intra-assay variability was calculated from a minimum 8 replicates of each of the QC samples assayed within one run, while the inter-assay variability was determined from the mean QC samples concentration (each in quadruplicate) from a minimum of 6 independent assays. For all the described analytical assays the inter- and intra-assay precision (% CV) of the QC concentrations was below 15 % (Table 6.4 and 6.5). The inter- and intra-assay accuracy (% bias) for all the QC concentrations was within 15 % bias (Table 6.4 and 6.5).

6.3.3 Rifampicin stability

Rifampicin stability of the HQC, MQC and LQC was determined by UV-HPLC following 3 days storage at -20°C, 4°C, following 3 freeze-thaw cycles and following heat treatment compared to the control -80°C storage (Table 6.6). Only the rifampicin concentration of the LQC was found to be significantly decreased following heat treatment (11 % decrease, $P<0.05$).

6.3.4 Results Tables

Table 6.2: Summary of lower and upper limits of quantification (LLQ, ULQ) and limits of detection (LOD).

Drug (method)	LLQ (ng/ml)	ULQ (ng/ml)	LOD (ng/ml)
Rifampicin (HPLC)	823	16460	412
Pyrazinamide (HPLC)	2500	80000	1000
Isoniazid (HPLC)	200	12800	200
Acetylisoniazid (HPLC)	200	12800	100
Rifampicin (HPLC-MS)	100	12800	< 100

Table 6.3: Inter-assay precision (% CV) and accuracy (% bias) of each point on the standard curves for RIF, PYR, INH and AcINH as measured by the various analytical methods (n=6).

Drug Assay	Theoretical Conc. (ng/ml)	Measured Conc. (ng/ml) Mean (± s.d.)	Precision CV (%)	Accuracy Mean % bias (± s.d.)
RIF HPLC	823	889 (± 33)	3.5	8.1 (± 3.6)
	1646	1662 (± 58)	3.5	2.8 (± 1.7)
	3292	3292 (± 66)	2.1	1.5 (± 0.9)
	6584	6518 (± 173)	2.6	1.6 (± 1.8)
	9876	9727 (± 206)	2.1	1.1 (± 0.8)
	13168	13093 (± 173)	1.3	1.1 (± 0.6)
	16460	16649 (± 247)	1.5	1.2 (± 0.7)
PYR HPLC	1250	1180 (± 119)	10.1	8.1 (± 4.7)
	2500	2500 (± 76)	3.0	0.8 (± 0.4)
	5000	5149 (± 191)	3.7	2.6 (± 1.4)
	10000	10241 (± 576)	4.6	4.0 (± 1.6)
	20000	20553 (± 576)	2.8	1.8 (± 1.0)
	40000	39793 (± 1116)	2.8	1.0 (± 0.7)
	80000	79029 (± 1652)	2.1	1.3 (± 0.7)
INH HPLC	200	217 (± 22)	10.2	8.7 (± 3.9)
	400	407 (± 20)	5.0	3.6 (± 3.1)
	800	804 (± 64)	8.0	6.6 (± 3.6)
	1600	1533 (± 121)	7.9	6.2 (± 4.2)
	3200	2990 (± 196)	6.6	5.6 (± 2.6)
	6400	6167 (± 348)	5.7	3.5 (± 4.3)
	12800	13312 (± 317)	2.4	1.8 (± 1.3)
AcINH HPLC	200	205 (± 24)	11.8	9.4 (± 6.0)
	400	402 (± 21)	5.2	4.1 (± 2.8)
	800	821 (± 45)	5.5	4.4 (± 2.9)
	1600	1543 (± 79)	5.1	3.9 (± 2.9)
	3200	3177 (± 84)	2.7	2.1 (± 1.3)
	6400	6190 (± 216)	3.5	2.4 (± 2.3)
	12800	13074 (± 291)	2.2	1.8 (± 1.1)
RIF HPLC-MS	100	102 (± 11)	11.9	7.2 (± 7.1)
	200	195 (± 29)	15.0	8.2 (± 4.0)
	400	395 (± 54)	13.7	7.4 (± 4.3)
	800	825 (± 43)	5.2	4.1 (± 3.5)
	1600	1620 (± 98)	6.0	4.3 (± 2.0)
	3200	3304 (± 217)	6.6	4.8 (± 3.9)
	6400	6238 (± 354)	5.7	4.7 (± 1.4)
	12800	13054 (± 977)	7.5	3.5 (± 4.8)

Table 6.4: Intra-assay precision and accuracy of the low (LQC), medium (MQC) and high (HQC) QC samples for RIF, PYR, INH and AcINH as measured by the various analytical methods. The target concentration was defined as the mean QC concentration over all assays (n=6). The actual measured concentrations (mean ± s.d.), coefficient of variation (CV %) and accuracy (% bias) were measure relative to the target values (n=8).

Drug Assay	QC Level	Target Conc. (ng/ml)	Measured Conc. (ng/ml) Mean (± s.d.)	Precision CV (%)	Accuracy Mean % bias (± s.d.)
RIF HPLC	LQC	1097	1043 (± 50)	4.7	6.1 (± 2.1)
	MQC	7337	7188 (± 140)	2.0	2.0 (± 1.9)
	HQC	16476	16649 (± 354)	2.1	2.1 (± 1.1)
PYR HPLC	LQC	2852	2734 (± 120)	4.3	4.3 (± 3.9)
	MQC	15187	14109 (± 560)	4.0	7.1 (± 3.7)
	HQC	78156	73468 (± 1490)	2.0	6.0 (± 1.9)
INH HPLC	LQC	283	281 (± 34)	11.9	9.4 (± 4.1)
	MQC	1377	1390 (± 115)	8.3	5.1 (± 3.9)
	HQC	9967	9706 (± 174)	1.8	3.9 (± 3.1)
AcINH HPLC	LQC	247	254 (± 27)	10.6	6.4 (± 5.5)
	MQC	1092	1157 (± 27)	2.4	5.1 (± 3.3)
	HQC	7050	7362 (± 337)	4.6	5.4 (± 3.5)
RIF HPLC-MS	LQC	118	118 (± 5)	4.0	3.1 (± 2.3)
	MQC	1209	1212 (± 26)	2.1	1.7 (± 1.1)
	HQC	10189	10120 (± 474)	4.7	3.5 (± 2.8)

% bias = [(measured concentration - target concentration)/measured concentration] x 100

Table 6.5: Inter-assay precision and accuracy of the low (LQC), medium (MQC) and high (HQC) QC samples for RIF, PYR, INH and AcINH as measured by the various analytical methods (n=6).

Drug Assay	QC Level	Drug Conc. (ng/ml) Mean (± s.d.)	Precision CV (%)	Accuracy Mean % bias (± s.d.)
RIF HPLC	LQC	1097 (± 82)	7.6	6.6 (± 2.5)
	MQC	7337 (± 189)	2.6	2.1 (± 1.2)
	HQC	16476 (± 346)	2.1	1.6 (± 1.2)
PYR HPLC	LQC	2852 (± 360)	12.5	10.2 (± 5.6)
	MQC	15187 (± 1020)	6.7	5.4 (± 3.1)
	HQC	78156 (± 4390)	5.6	4.7 (± 2.3)
INH HPLC	LQC	283 (± 36)	12.8	10.1 (± 6.6)
	MQC	1377 (± 108)	7.9	5.4 (± 5.3)
	HQC	9967 (± 516)	5.2	3.3 (± 3.6)
AcINH HPLC	LQC	247 (± 30)	12.0	9.1 (± 6.9)
	MQC	1092 (±85)	7.8	6.1 (± 4.1)
	HQC	7050 (± 482)	6.8	5.1 (± 4.0)
RIF HPLC-MS	LQC	119 (± 6)	4.9	4.0 (± 2.3)
	MQC	1210 (± 37)	3.0	2.1 (± 1.9)
	HQC	10190 (± 469)	4.6	3.3 (± 2.9)

% bias = [(measured concentration - target concentration)/measured concentration] x 100

Table 6.6: The amount of rifampicin detected in QC samples that have gone through 4 different conditions. (* = $P < 0.05$)

Condition	Level	Mean Concentration (± SD) (µg/ml)	Difference to Control (%)
Control	LQC	1.27 (± 0.07)	N/A
	MQC	7.56 (± 0.12)	N/A
	HQC	16.89 (± 0.16)	N/A
- 20 °C	LQC	1.32 (± 0.02)	3.48
	MQC	7.46 (± 0.05)	-1.34
	HQC	16.56 (± 0.21)	-1.96
4 °C	LQC	1.28 (± 0.02)	-0.35
	MQC	7.42 (± 0.06)	-1.96
	HQC	16.66 (± 0.14)	-1.36
3 freeze-thaw cycles	LQC	1.30 (± 0.03)	2.52
	MQC	7.31 (± 0.10)	-3.32
	HQC	16.16 (± 0.14)	-4.34
Heat treatment	LQC	1.14* (± 0.04)	-11.00
	MQC	7.00 (± 0.22)	-7.53
	HQC	16.00 (± 0.06)	-5.30

6.3.5 Results Figures

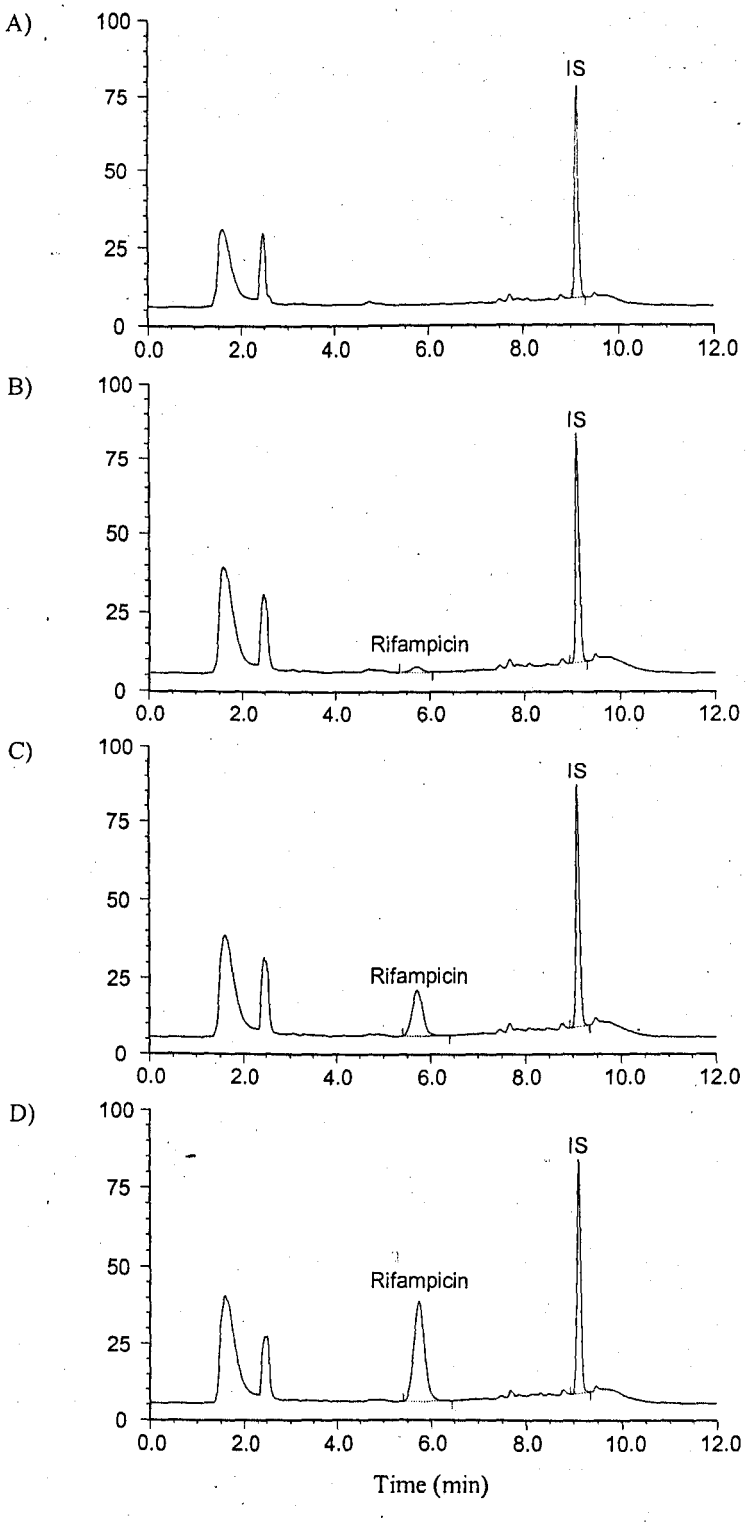

Figure 6.1: Representative chromatographic traces of rifampicin as measured by HPLC using drug free plasma (A), LQC (B), MQC (C) and HQC (D) with internal standard (IS).

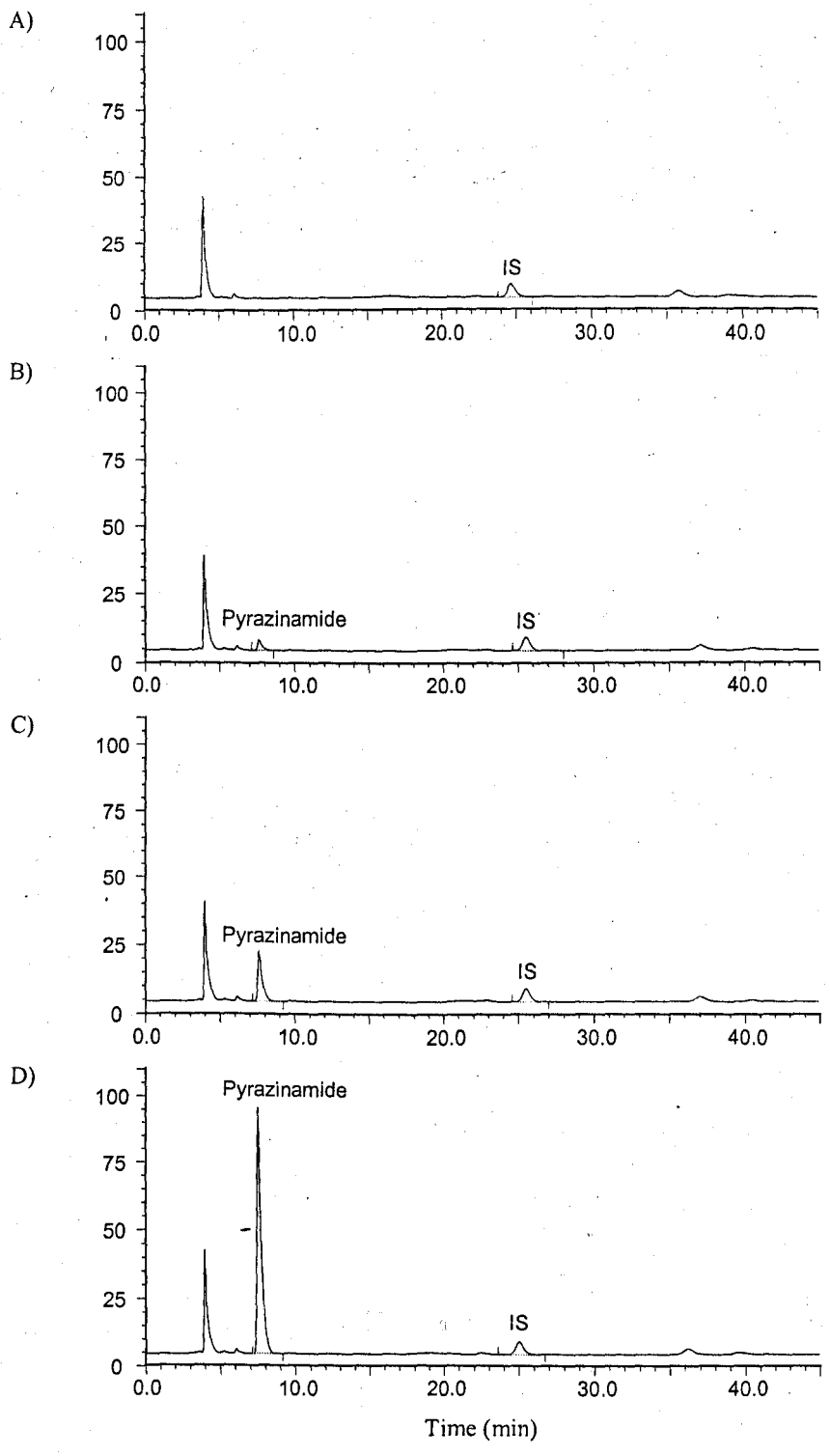

Figure 6.2: Representative chromatographic traces of pyrazinamide as measured by HPLC using drug free plasma (A), LQC (B), MQC (C) and HQC (D) with internal standard (IS).

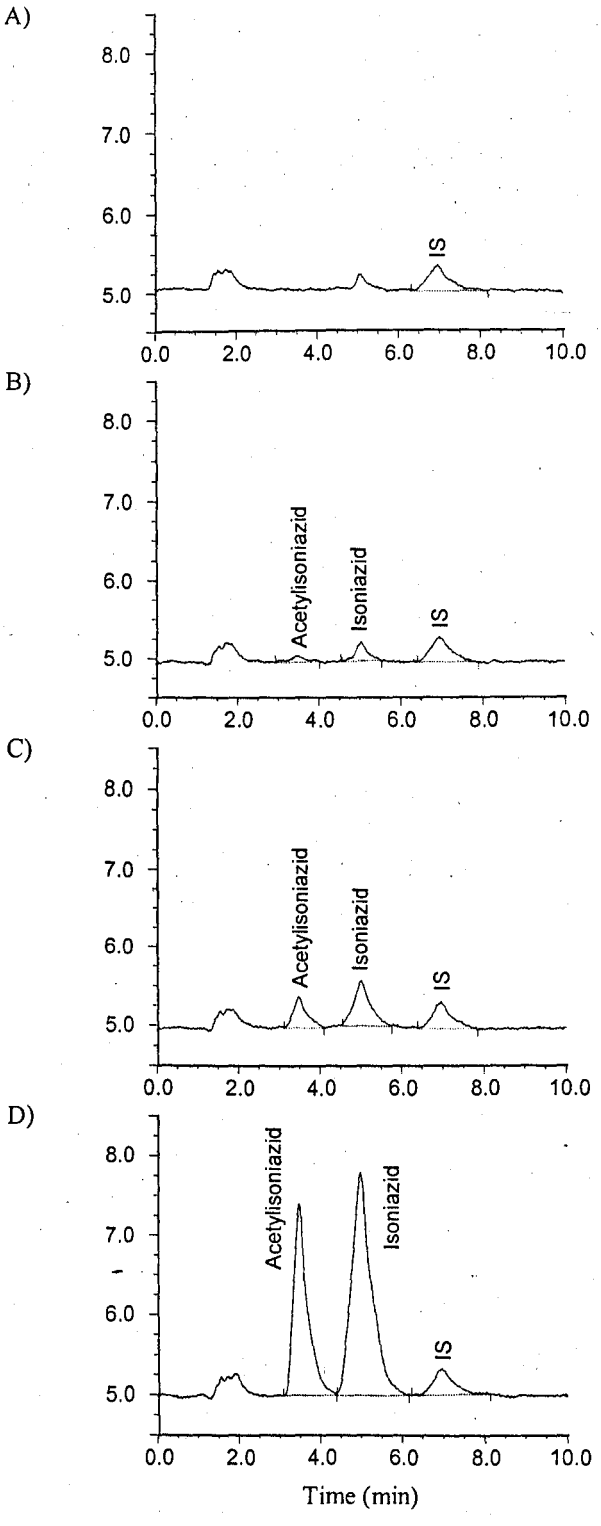

Figure 6.3: Representative chromatographic traces of isoniazid and Acetylisoniazid as measured by HPLC using drug free plasma (A), LQC (B), MQC (C) and HQC (D) with internal standard (IS).

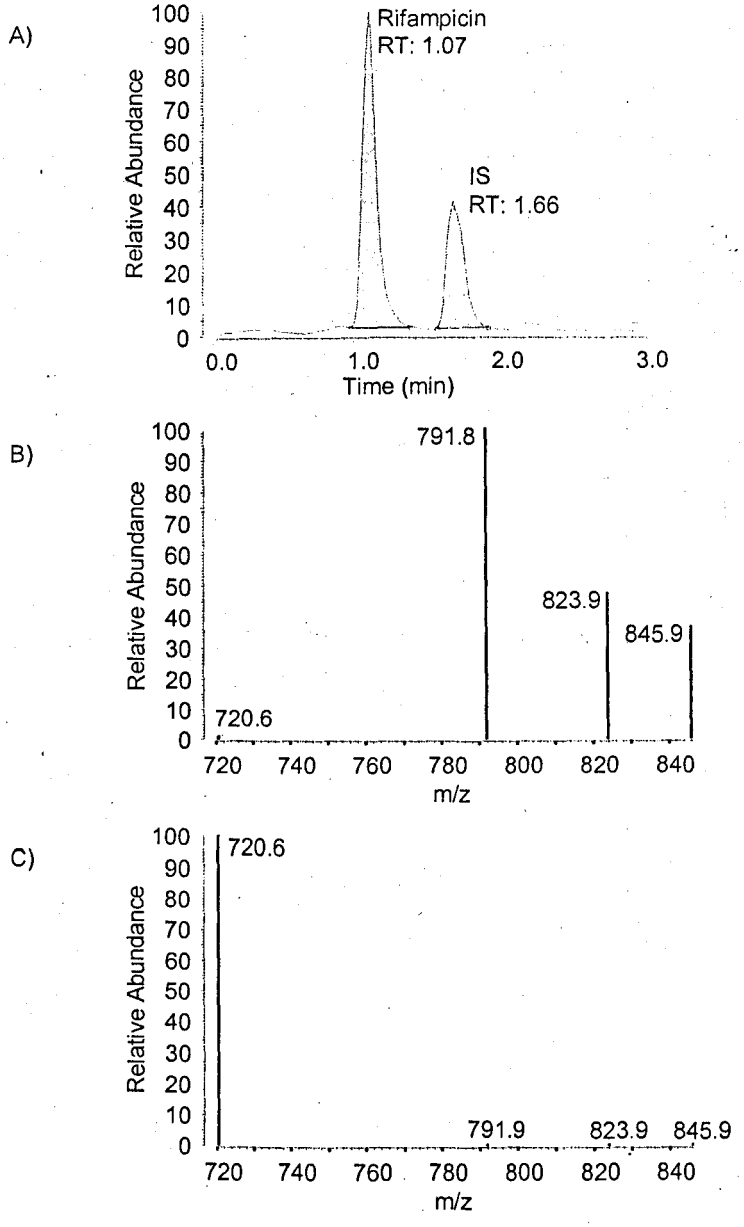

Figure 6.4: Representative total ion current (TIC) trace of rifampicin and internal standard (IS) as measured by HPLC-MS (A). The relative abundance of the 4 measured ions at the rifampicin peak (retention time 1.07 min) is depicted in (B) and that of the internal standard (retention time 1.66 min) is depicted in (C).

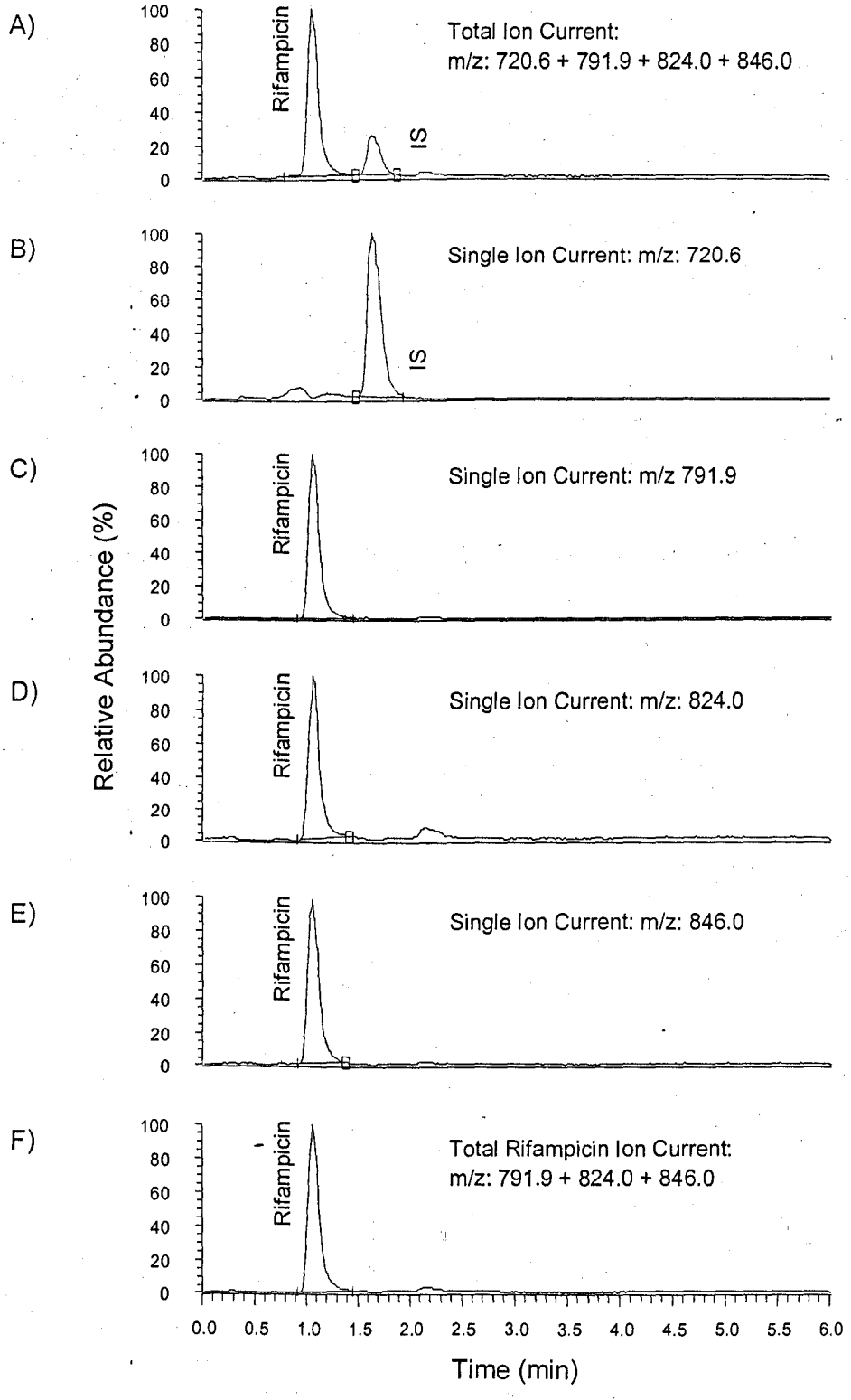

Figure 6.5: Representative chromatographic traces of rifampicin (HQC) as measured by HPLC-MS. A total ion current trace is depicted in (A).Single ion monitoring (SIM) allows for more accurate peak integration and traces of the internal standard ion (B) and of the 3 rifampicin ions (C, D, E), as well as the combination of the 3 rifampicin ions (F) are shown. SIM traces (B) and (F) are used for th quantification of the internal standard and rifampicin respectively.

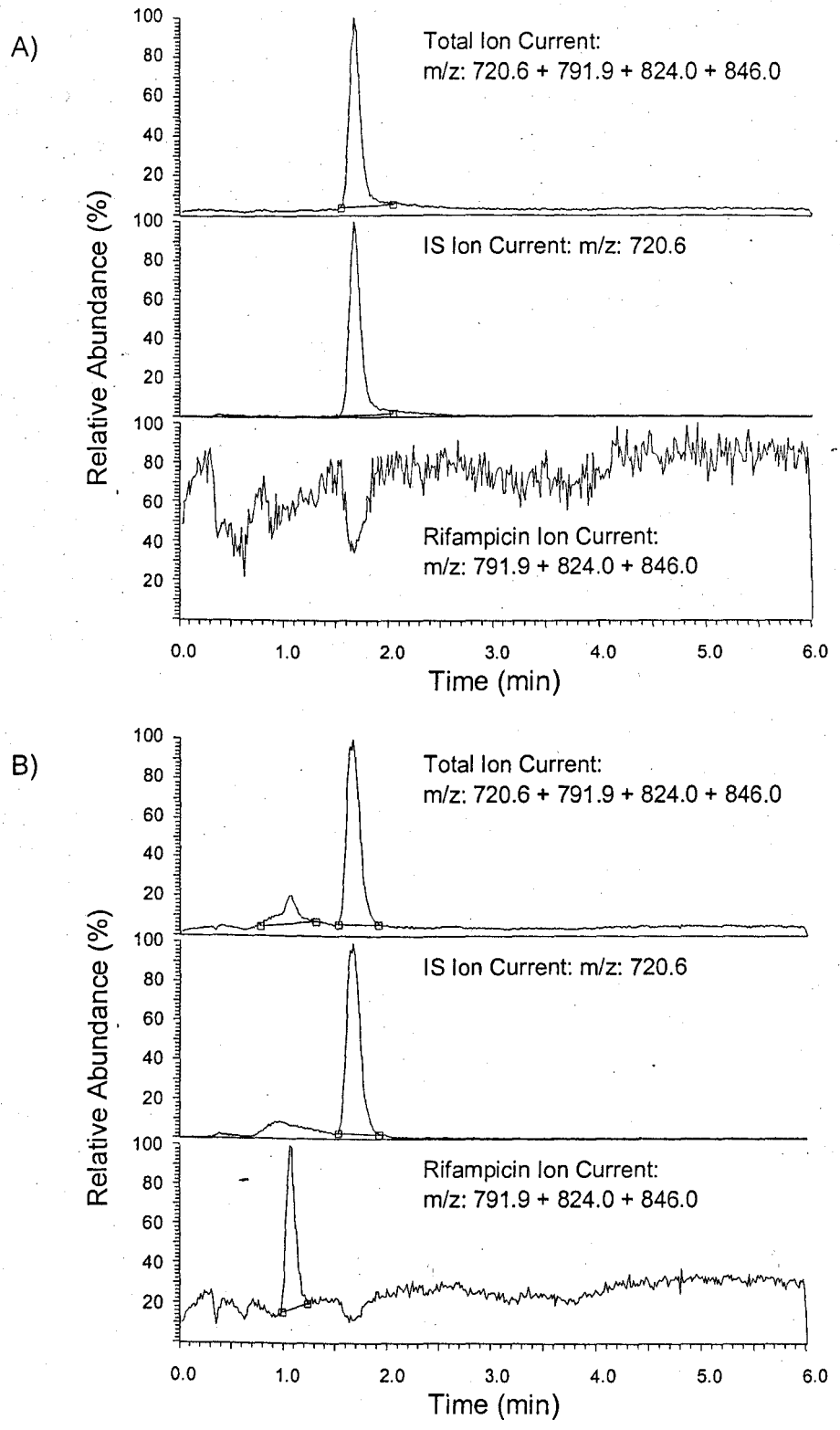

Figure 6.6: Representative chromatographic traces of rifampicin as measured by HPLC-MS using drug free plasma (A) and LQC (B) samples with internal standard (IS). Top panels show the total ion current (TIC) chromatograms, middle panels the SIM for the internal standard (IS) and the bottom panels combined SIM for the 3 rifampicin ions.

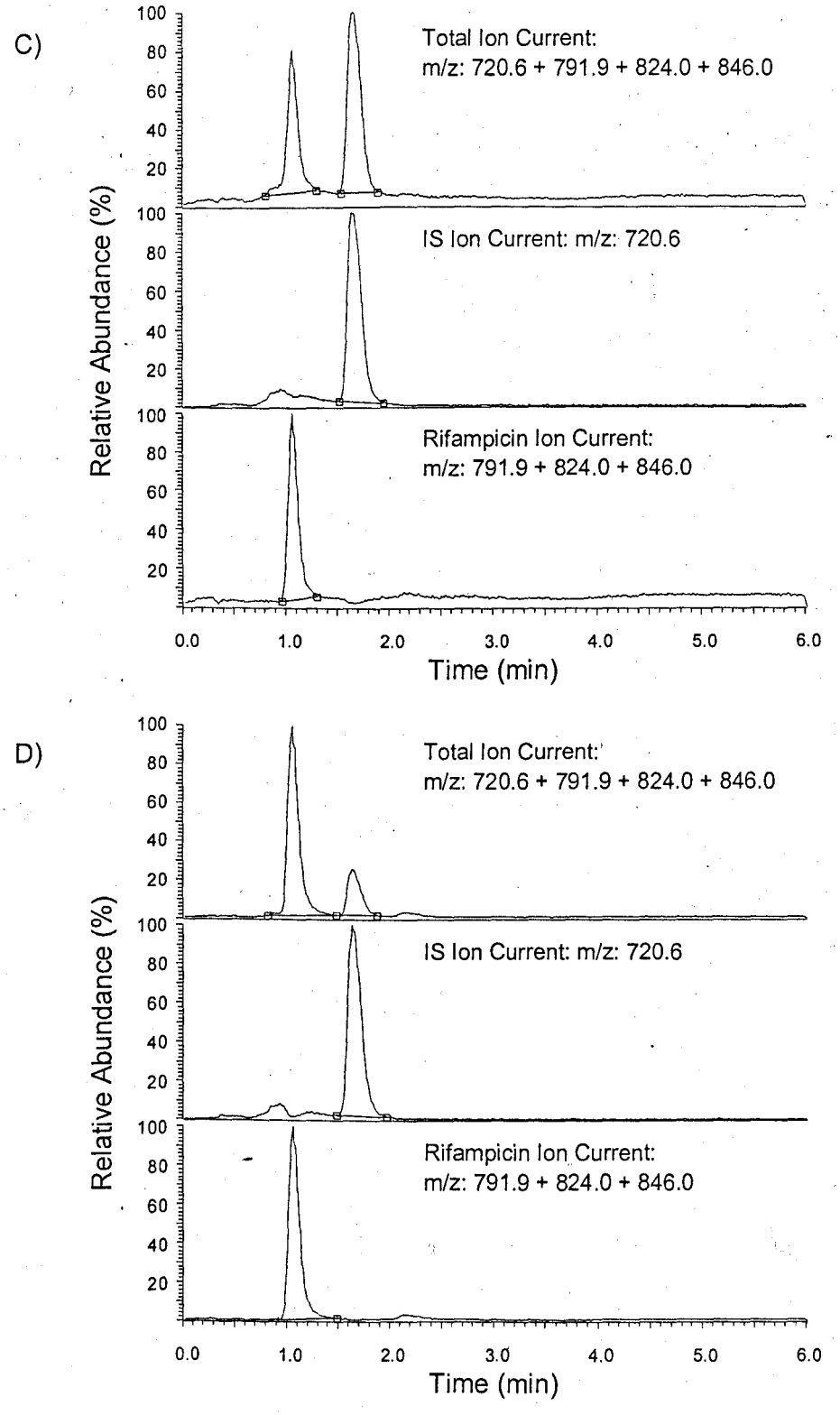

Figure 6.6: Cont. Representative chromatographic traces of rifampicin as measured by HPLC-MS using MQC (C) and HQC (D) samples with internal standard (IS). Top panels show the total ion current (TIC) chromatograms; middle panels the SIM for the internal standard (IS) and the bottom panels combined SIM for the 3 rifampicin ions.

6.4 Discussion

Drug pharmacokinetic studies require an accurate and precise way to measure drug concentrations at a range of time points that will accurately determine the pharmacokinetic parameters involved. Mean rifampicin, pyrazinamide and isoniazid pharmacokinetic profiles and estimates of the individual pharmacokinetic parameters have previously been published by (Peloquin, 2002) (Table 6.7, Fig. 6.7). The drug assays developed here have been designed primarily to accurately determine pharmacokinetic profiles over 12 hr for each of the drugs.

An ideal drug assay would by highly sensitive, selective, accurate and precise whilst simultaneously determining all anti-tuberculosis drug concentrations. However, there are large differences in the chemical properties (lipophilicity, pKa) between rifampicin (lipophilic), pyrazinamide and isoniazid (both lipophobic). This has a dramatic influence on both the retention of the drug and the extraction efficiency. Further, the optimum UV absorbance for the drugs are also slightly different (rifampicin: 254 nm, pyrazinamide: 268 and isoniazid: 266). Assays have been described that analyse all 3 anti-TB drugs at once (Table 6.8), however, many of them compromise the sensitivity and often the chromatography of the assay to achieve this. Many of the previously published analytical drug assays also lack an internal standard, which is essential to correct for changes in the extraction efficiency, injection volume and the evaporation of sample.

There are numerous HPLC assays for the detection of rifampicin, however many lack sensitivity or an internal standard. Because of this, a new HPLC method was developed here that was accurate, precise and sensitive enough to be able to measure

down to 0.823 μg/mL (sensitive enough for a normal 12 hr pharmacokinetic plasma profiles - Fig. 6.7).

The HPLC-MS method developed here however has a 10 fold greater sensitivity to that of the UV detection. This sensitivity was found to be optimum when measuring the main parent (MH+, m/z = 824) as well as a truncated rifampicin adducts (m/z = 792 loss of a methoxy) and a sodium adduct (MNa+, m/z = 846), both of which were previously identified by (Korfmacher *et al.*, 1993). The increased sensitivity in the HPLC-MS assay is important when measuring low drug concentration in sanctuary site (cerebral spinal fluid and cell associated rifampicin) and for studies involving children where only very small sample volumes (50 μL) can be obtained. A further advantage of this assay is that a very simple extraction procedure is used which is both cheap and time saving.

Rifampicin was found to be stable when store at -80°C, as well as during short term storage at -20°C, 4°C and at room temperature. Freeze-thaw cycles and heat inactivation of samples didn't have an influence on rifampicin stability either other than for low level rifampicin (LQC) where significant breakdown was measured following heat inactivation.

Pyrazinamide plasma concentrations are normally high (Fig. 6.7), and therefore assay sensitivity is not problematic. The method established here was developed from a published method by (Conte *et al.*, 2000). This method was chosen because its sensitivity was sufficient to determine plasma pharmacokinetic profiles and the sample preparation procedure by precipitation was rapid. However, because of the

hydrophilic nature of pyrazinamide, and the simple extraction procedure, water-soluble plasma components are retained on the column and can elute late on in the run. This leads to a long run time that can only be shortened with a more elaborate extraction procedure or a different column. However, the pyrazinamide assay is accurate, precise and sensitive enough for the effective determination of plasma pharmacokinetic profiles.

The HPLC method for the detection of isoniazid and acetylisoniazid was developed from a published method (Hutchings *et al.*, 1983) as well as from personal communications with A. Hutchings. This method was considered superior to previously published methods (Table 6.8) despite its long extraction procedure. The reason for this is that the assay contains an internal standard, the extraction efficiency is good (around 80%- (Hutchings *et al.*, 1983)) and the assay is sufficiently sensitive for the determination of plasma pharmacokinetic parameters. This assay also utilises a nitrile separation column which gives superior chromatography and separation of isoniazid from the mobile front compared to the standard C_8 or C_{18} columns. Further the assay has the added advantage of having a short run time and being able to detect the primary isoniazid metabolite; acetylisoniazid. This allows simultaneous determination of acetylator phenotype (fast or slow acetylator).

The main drawback with most HPLC assays compared to HPLC-MS methods is the potential lack of specificity due to the co-elution of other drugs or plasma components and the decreased sensitivity. Attempts were made at quantifying pyrazinamide and isoniazid by HPLC-MS and HPLC-MS/MS. Both drugs produced a good m/z signals and chromatography when pure standards were injected.

However, following extraction of isoniazid and pyrazinamide spiked plasma samples by precipitation or liquid-liquid extraction (hexane, ethyl acetate mixtures) the chromatography and sensitivity became very poor. The main reason for this is thought to be due to the lack of separation between the drug peaks and the mobile front. Their co-elution may suppress the ionisation of the drugs and therefore detection (especially with isoniazid).

The HPLC and HPLC-MS analytical methods described here are precise, accurate, sensitive and fully validated for the detection of rifampicin, pyrazinamide, isoniazid and acetylisoniazid in plasma. These assays can be used in pharmacokinetic studies, whilst the increased sensitivity of the rifampicin HPLC-MS method also potentially allows for the measurement of cerebral spinal fluid and cell associated rifampicin

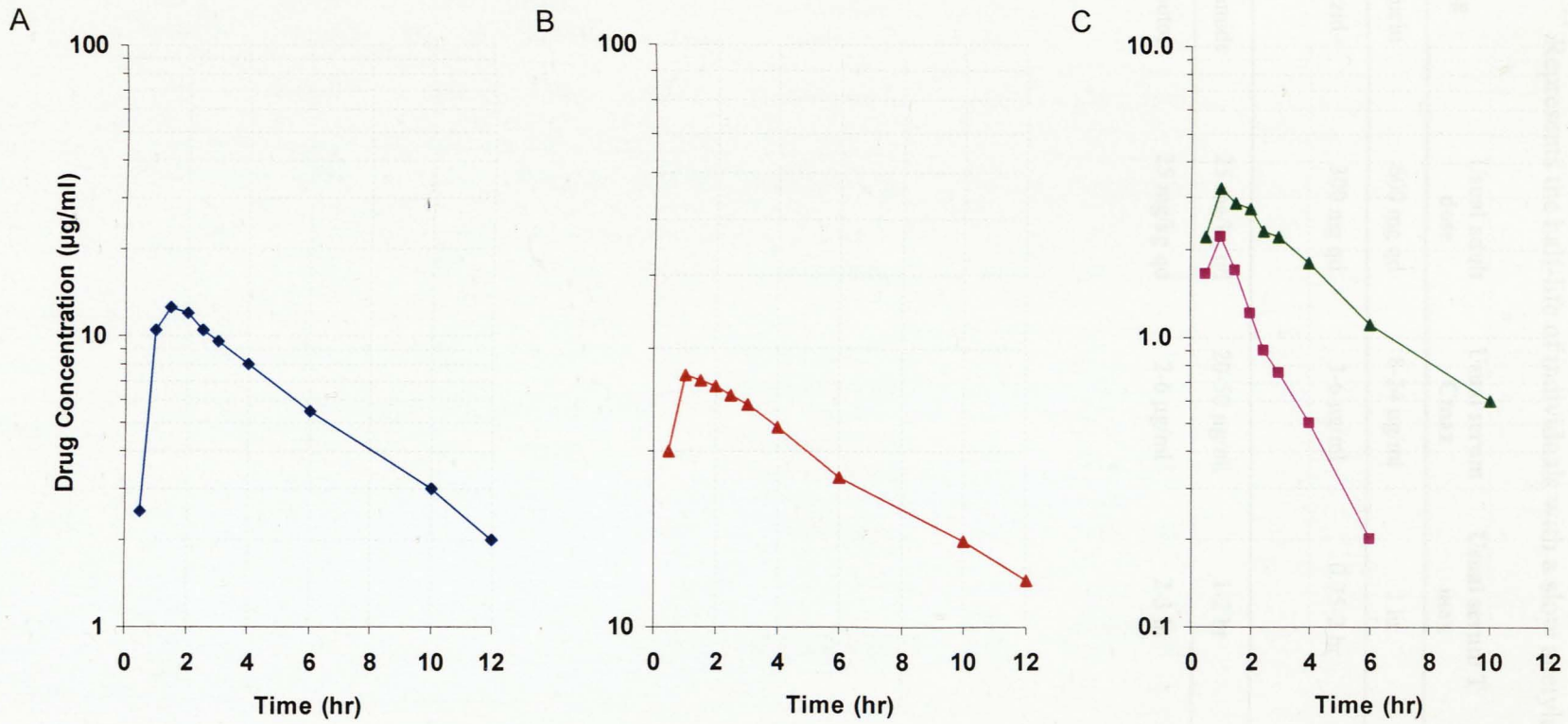

Figure 6.7: Simulation of the (A) rifampicin, (B) pyrazinamide and (C) isoniazid (slow acetylator: —▲— and fast acetylator: —■—) pharmacokinetic curves as observed by (Peloquin, 2002)

Table 6.7: Pharmacokinetic parameters of four anti-tuberculosis drugs as published by (Peloquin, 2002). $^{+}$ Represents the half-life of individuals with a fast acetylator phenotype. $^{++}$ Represents the half-life of individuals with a slow acetylator phenotype

Drug	Usual adult dose	Usual serum Cmax	Usual serum T max	Normal serum T1/2
Rifampicin	600 mg qd	8-24 µg/ml	2 hr	3 hr
Isoniazid	300 mg qd	3-6 µg/ml	0.75-2 hr	1.5hr (fast^{+}) 4 hr (slow^{++})
Pyrazinamide	25 mg/kg qd	20-50 µg/ml	1-2 hr	9 hr
Ethambutol	25 mg/kg qd	2-6 µg/ml	2-3 hr	2-4 hr

Table 6.8: Summary of the drug quantification variables by HPLC and HPLC-MS as described here and from previous publications.

Paper	Drug analysed	Internal Standard	LOD (ng/ml)	Standards (µg/mL)	Plasma Volume	Extraction method	Run time (min)	Detection method	Column type	Comment
	RIF	HBABE	500	1-20	0.2 mL	Precipitation	12	HPLC (254 nm)	C_8 (5 µm, 150x4.6 mm)	
	RIF	RFM	<100	0.1-12.8	0.05 mL	Precipitation	6	HPLC-MS	Phe-H (5 µm, 50x2.1 mm)	
	PZA	AZA	1000	2.5-80	0.2 mL	Precipitation	45	HPLC (268 nm)	C_{18} (5 µm, 250x4.6 mm)	
	INH	IPR	200	0.2-12.8	1 mL	Precipitation + liquid extraction	10	HPLC (266 nm)	CN (5 µm, 250x4.6 mm)	
(Hutchings *et al.*, 1983)	INH	IPR	200	0.1-15	1 mL	Precipitation and liquid extraction	8	HPLC (266 nm)	CN (5 µm, 250x4.6 mm)	
(Conte *et al.*, 2000)	PZA	AZA	1000	0.5-80	200	Precipitation	22	HPLC (268 nm)	C_{18} (5 µm, 250x4.6 mm)	
(Seifart *et al.*, 1993)	INH PZA RIF				0.2 mL 0.2 mL 0.2 mL	Liquid extraction	20 20 20	HPLC (280 nm) HPLC (280 nm) HPLC (254 nm)	C_8 (10 µm, 250x4.6 mm)	Not good separation No Internal Standard No LLQ
(Khuhawar and Rind, 2002)	INH PZA RIF		22 40 2600	0-34.25 0-61.56 0-658.3	1 mL 1 mL 1 mL	Derivatization + precipitation	4 8 8	HPLC (337 nm)	C_{18} (5 µm, 150x4.6 mm)	No Internal Standard No LLQ

Rifampicin (RIF), Isoniazid (INH), Pyrazinamide (PZA), p-hydrogenbenzoic acid n-butyl ester (HBABE), Rifammycin SV (RFM), Acetazolamide (AZA), Iproniazid (IPR) and Ion Interaction Reagent (IIR), Phenyl-Hexyl (Phe-H)

Table 6.8: Continued.

Paper	Drug analysed	Internal Standard	LOD (ng/ml)	Standards (µg/mL)	Plasma Volume	Extraction method	Run time (min)	Detection method	Column type	Comment
(Calleri *et al.*, 2002)	INH PZA RIF	External					40	HPLC (261 nm) HPLC (265 nm) HPLC (254 nm)	C_{18} (5 µm, 250x4.6 mm)	Not in Plasma
(Mohan *et al.*, 2003)	INH PZA RIF	RQ					25	HPLC (238 nm)	C_{18} (5 µm, 250x4.6 mm)	Not in Plasma
(Walubo *et al.*, 1994)	PZA RIF	NBAP NBAP	500 200	0.5-8 0.5-8	2 mL 2 mL	Liquid extraction Liquid extraction	15 15	HPLC (248 nm) HPLC (248 nm)	C_8 (5 µm, 250x4.6 mm)	
(Gennaro *et al.*, 2001)	INH, PZA		91 63			Dilution	30 45	(IIR) HPLC (264 nm)	C_{18} (5 µm, 250x4.6 mm)	No Internal Standard No LLQ
(Walubo *et al.*, 1994)	INH,	PHEN	250	0.5-8	2 mL	Liquid extraction + Derivatization	17	HPLC (280 nm)	C_8 (5 µm, 250x4.6 mm)	
(Smith *et al.*, 1999)	INH PZA		50 50	0.1-20 0.1-60	0.5 mL 0.5 mL	Solid phase extraction	± 8	HPLC (254 nm) HPLC (254 nm)	C_8 (5 µm, 150x4.6 mm)	No Internal Standard
(Gaitonde and Pathak, 1990)	INH PZA	RIF	200 200	0.2-0.8 0.2-0.8	2 mL	Solid phase extraction	5	HPLC (265 nm)	CN (5 µm, 250x4.6 mm)	
(Delahunty *et al.*, 1998)	INH	External	500	0.5-3	1 mL	Precipitation and liquid extraction	± 12	HPLC (266 nm)	CN (5 µm, 250x4.6 mm)	

Rifampicin (RIF), Isoniazid (INH), Pyrazinamide (PZA), N-butarylaminophenol (NBAP), Rifampicin (RIF), Rifampicin quinone (RQ), Phenelzine (PHEN) and Iproniazid (IPR)

Table 6.8: Continued.

Paper	Drug analysed	Internal Standard	LOD (ng/ml)	Standards (µg/mL)	Plasma Volume	Extraction method	Run time (min)	Detection method	Column type	Comment
(Moussa *et al.*, 2002)	INH	NIC	500	0.5-8	0.5 mL	Precipitation	15	HPLC (275 nm)	C_{18} (300x3.9 mm)	
(Seifart *et al.*, 1995)	INH		1000	1-25	0.2 mL	Derivatization	15	HPLC (340 nm)	C_8 (5 µm, 250x4.6 mm)	No Internal Standard
(Kraemer *et al.*, 1998)	PZA	M-PZA	1000	1-80	0.5 mL	Solid phase extraction	16	HPLC (268 nm)	C_{18} (3 µm, 150x4.6 mm)	
(Revankar *et al.*, 1994)	PZA	NIC		1-25	0.05 mL	Precipitation	± 8	HPLC (268 nm)	C_{18} (5 µm, 150x4.6 mm)	
(Mehmedagic *et al.*, 1997)	PZA			0.375-7.5	0.02 mL	Dilution	35	HPLC (254 nm) GC-MS	C_{18} (5 µm, 250x4 mm)	No Internal Standard Only in Urine
(Korfmacher *et al.*, 1993)	RIF						17	HPLC-MS	C_{18} (5 µm, 150x4.6 mm)	Not in Plasma No Internal Standard
(Calleja *et al.*, 2004)	RIF		50	0.1-50	0.1 mL	Liquid Extraction	± 6	HPLC (333 nm)	C_{18} (5 µm, 250x4.6 mm)	No Internal Standard
{Smith, 1999 #119	RIF		50	0.1-20	0.5 mL	Solid phase extraction	± 5	HPLC (270 nm)	C_8 (5 µm, 250x4.6 mm)	No Internal Standard
(Panchagnula *et al.*, 1999)	RIF	RPT	2000	2-20	0.1 mL	Precipitation	17	HPLC (254 nm)	C_{18} (4 µm, 250x4 mm)	

Rifampicin (RIF), Isoniazid (INH), Pyrazinamide (PZA), Nicotinamide (NIC), N-Methylol-pyrazinamide (M-PZA) and Rifapentine (RPT)

CHAPTER 7

The impact of drug transporters on rifampicin cellular accumulation *in vivo*

7.1 Introduction 224

7.2 Methods 225

7.2.1 Materials 225

7.2.2 Subjects 225

7.2.3 Blood sampling 225

7.2.4 Isolation and storage of plasma 226

7.2.5 Isolation and storage of PBMCs for cellular rifampicin concentration 226

7.2.6 Isolation and storage of PBMCs for transporter expression 226

7.2.7 Drug concentration quantification 226

7.2.8 Determination of transporter expression 226

7.2.9 Data analysis 227

7.3 Results 229

7.3.1 Results Tables 231

7.3.2 Results Figures 234

7.4 Discussion 245

7.1 Introduction

Rifampicin penetration into cells is of great importance in the eradication of intracellular bacteria. The presence of active drug efflux pumps may however be able to limit rifampicin accumulation. Rifampicin has been shown to be a substrate for P-gp in T-lymphoblastoid and MDCKII cell lines (chapter 2). However, rifampicin is also able to induce P-gp on cells (Geick *et al.*, 2001; Kauffmann *et al.*, 2002) and thereby potentially affect its own accumulation.

Pharmacokinetics of tuberculosis drugs in healthy volunteers has been well characterised by (Peloquin *et al.*, 1997). Induction of drug transporters and drug metabolising enzymes by rifampicin as well as the influence of disease state will however impact on the pharmacokinetics of rifampicin and other co-administered drugs.

Rifampicin is routinely administered to patients with tuberculosis and staphylococcal infections. The aim of this study is to characterise rifampicin pharmacokinetics both in plasma and in PBMCs in these patients, and to determine if there is any correlation with the expression of P-gp, MRP1 and BCRP. This study also investigates the inductive effect of rifampicin on P-gp, MRP1 and BCRP on PBMCs. Further, the pharmacokinetics of pyrazinamide and isoniazid were also determined in patients with tuberculosis in order to evaluate the utility of the analytical methods developed in Chapter 6 for determining the *in vivo* pharmacokinetics.

7.2 Methods

7.2.1 Materials

The primary antibody: BXP-21 was purchased from AbCam (Cambridge, UK) and the secondary rPE-conjugated anti IgG2a was purchased from Serotec (oxford, UK). All other materials were purchased from Sigma-Aldrich (Poole, UK).

7.2.2 Subjects

18 subjects (9 male, 9 female) were enrolled into this study. Each subject provided written informed consent, which was approved by the local ethics committee. All subjects were over the age of 18 years, were able to give informed consent and received routine rifampicin containing therapy for the treatment of tuberculosis (13 patients) or staphylococcal infection (5 patients). None of the subjects suffered from hepatic impairment (as graded by elevated ALT) or anaemia (as graded haemoglobin). 12 healthy volunteers (6 male, 6 female) were also recruited to act as a control group for basal drug transporter expression.

7.2.3 Blood sampling

On the day of the study, patients received observed medication on an empty stomach. In order to determine plasma rifampicin, isoniazid, pyrazinamide and cellular rifampicin pharmacokinetics as well as PBMC transporter expression, 6 heparinised blood samples (collected using 5 mL monovette collection tubes,) were provided by each of the participants over 8 hr. The first blood sample (25 mL) was taken 30 min post dose, followed by 19 mL blood samples at 1, 2, 4, 6 and 8 hr post dose. The total blood volume donated equated to no more than 120 mL.

7.2.4 Isolation and storage of plasma

From each sampling time-point, 4 mL of heparinised blood was centrifuged (10 min, 2700 x g) to separate the plasma from the cells. Plasma (approx. 2 mL) was then transferred to 2 labelled 1.5 mL plasma tubes and stored at -80°C (in the dark).

7.2.5 Isolation and storage of PBMCs for cellular rifampicin concentration

From each sampling time-point, PBMCs were isolated from 14 mL of heparinised blood as described in section 2.2.3. Isolated PBMCs were then washed 3 times in PBS (20 mL, 4°C, 4 min, 800 x g), counted by NucleoCounter and pelleted (4°C, 4 min, 800 x g). Cell pellets were then frozen (-80°C) prior to rifampicin quantification.

7.2.6 Isolation and storage of PBMCs for transporter expression

Following the first sampling time-point, PBMCs were also isolated from 5 mL of heparinised blood as described in section 2.2.3. Isolated PBMCs were then washed 3 times in PBS (20 mL, 4°C, 4 min, 800 x g) and cryo-preserved (2 mL of FCS 10 % DMSO, -80°C) prior to drug transporter quantification.

7.2.7 Drug concentration quantification

Plasma and cellular rifampicin concentrations were determined by HPLC-MS as described in section 6.2.6. Plasma pyrazinamide, isoniazid and acetylisoniazid concentrations were measured as described in section 6.2.4 and 6.2.5.

7.2.8 Determination of transporter expression

P-gp and MRP1 expression was determined by flow cytometry as described in section 2.2.11. Flow cytometry was also used for the determination of BCRP

expression by a method similar to that described by (Minderman *et al.*, 2002). Briefly, an appropriate number of cells were pelleted (800 x g, 6 min) and fixed (1 x 10^6 cells/mL in 1:10 CellFIX, 25min). 100 µL aliquots (2 x 10^5 cells) were then transferred to a 96 well plate (U bottom) and pelleted (800 x g, 10 min). Cells were then fixed in 90% methanol (4°C, 10 min), washed in PBS (containing 2% BSA and 0.01% Tween 20; 800 x g, 6 min) and blocked with pooled human serum (50 µL, 30 min). Following a further wash, cells were stained for BCRP using primary mouse-anti-human BCRP antibody (BXP-21: 50µL, 2.5 µg/mL, 1 hr). Non-specific antibody binding was determined by staining cells with primary mouse-anti-human IgG_{2A} isotype control (IgG_{2A}: 50 µL, 2.5 µg/mL, 1 hr). Following 3 washes (200 µL PBS containing 2% BSA and 0.01% Tween 20; 800 x g, 6 min) cell pellets (both specific and isotype control stained cells) were stained with secondary goat-anti-mouse IgG_{2A} conjugated to r-phycoerythrin (50 µL, 5 µg/ml, 1 hr). Following 3 washes (200 µL, 0.1 $mg.ml^{-1}$ saponin in PBS, 800 x g, 10 min) cell pellets were resuspended (300 µL of 1:10 CellFix) and transferred into 5 ml FACS tubes. BCRP expression was then measured by flow cytometry with r-phycoerythrin fluorescence being detected in FL2.

7.2.9 Data analysis

P-gp, MRP1 and BCRP transporter expression was quantified using relative fluorescence units (RFU) as described in section 2.2.11. Cellular rifampicin concentrations were calculated based on cell density and a cell volume of 0.4 pL as determined by (Gao *et al.*, 1993).

Pharmacokinetic parameters (AUC, $t_{1/2}$, CL, C_{max} and T_{max}) were calculated from the measured cellular and plasma drug concentration profiles for each individual patient

by first-order, compartmental (with lag) analysis using WinNonLin 5.1. (Pharsight Co. Mountainview, CA, USA).

Data were tested for normality using a Shapiro-Wilk test, which showed evidence of non-normality. Statistical analysis of simple linear regression was performed by Spearman's Rank Correlation Coefficient analysis, and between sample groups by Mann Whitney U-test.

7.3 Results

Demographics for the 18 subjects enrolled into the study are summarised in Table 7.1. Further, the number of patients receiving doses of rifampicin, pyrazinamide and isoniazid is given in Table 7.2.

A blood sampling strategy was designed around predicted plasma rifampicin pharmacokinetic parameters as published by (Peloquin, 2002). The variance inflation factors of different sampling schemes were compared to minimise the standard error of parameter estimates (AUC and $t_{1/2}$). The most effective sampling strategy was found to be 0.5, 1, 2, 4, 6 and 8 hr post dose (because of the lag in drug absorption and drug trough levels below assay quantification limits, a blood sample at time 0 was not deemed necessary).

Individual and mean plasma and cellular rifampicin pharmacokinetic profiles are illustrated in Fig. 7.1 and 7.2. A significant positive linear correlation (Rho = 0.79, $P < 0.001$) was observed between cellular and plasma rifampicin AUC (Fig. 7.3). Individual and mean pyrazinamide, isoniazid and acetyl-isoniazid pharmacokinetic profiles are illustrated in Fig. 7.4, 7.5 and 7.6. AUC, $t_{1/2}$, V_d, clearance, C_{max} and t_{max} (median and range) of the drugs as measured by first order, compartmental analysis (with a lag time) are summarised in Table 7.3. A frequency histogram illustrates the wide range in isoniazid $t_{1/2}$ (Fig. 7.7).

When correlating drug AUC against patient body mass index (BMI), a significant negative correlation was observed with rifampicin plasma AUC (Rho = -0.66, $P < 0.01$), but not with pyrazinamide and isoniazid plasma AUC (Fig. 7.8).

Patients receiving rifampicin were found to have 4.3 fold greater P-gp expression compared to healthy volunteer controls (3.50 ± 1.24 vs 0.81 ± 0.17 RFU, $P < 0.0001$) (Fig 7.9). BCRP expression was also significantly greater in patients receiving rifampicin by 2 fold compared to healthy controls (0.85 ± 0.46 vs 0.41 ± 0.17 RFU, $P < 0.001$) (Fig 7.9). No significant difference was seen in PBMC MRP1 expression (Fig 7.9). The effect of the duration of drug exposure on PBMC transporter expression is shown in Fig. 7.10. When looking at the correlation between rifampicin CAR and PBMC transporter expression (Fig. 7.11), it was found that there was a significant positive correlation with Pgp expression (Rho = 0.70, $P < 0.01$), but not with MRP1 or BCRP expression.

7.3.1 Results Tables

Table 7.1: Demographic characteristics of the 18 patients recruited

	Number (%) of patients
Diagnosis	
Tuberculosis	13 (72%)
Staphylococcal infection	5 (28%)
Gender	
Male	9 (50%)
With TB	7 (78%)
With Staphylococcal infection	2 (22%)
Female	9 (50%)
With TB	6 (67%)
With Staphylococcal infection	3 (33%)
Ethnicity	
Caucasian	12 (67%)
African	3 (17%)
Indian	2 (11%)
Mixed Ethnicity	1 (6%)
HIV status	
Positive	3 (17%)
Negative	6 (33%)
Untested	9 (50%)

Table 7.2: Range of anti-TB drug doses given to the 18 patients

	Dose (mg)	Number (%) of patient
Rifampicin		
	300	4 (22%)
	450	3 (17%)
	600	10 (56%)
	900	1 (6%)
Pyrazinamide		
	1500	2 (17%)
	2000	9 (75%)
	2500	1 (8%)
Isoniazid		
	225	2 (15%)
	300	10 (77%)
	450	1 (8%)

Table 7.3: Summary of the parameters measured

	n	Mean ± SD	Median	Range
Patient details				
BMI	18	20.6 ± 4.9	20.8	13.0 – 32.1
Rifampicin Exposure (days)	18	11.8 ± 14.4	6	1 – 65
Serum albumin (g/L)	18	33.0 ± 4.6	33	25 – 41
Rifampicin				
Plasma AUC_{0-24} (ng.hr/mL)	18	33958 ± 26010	24876	8462 – 105724
Plasma $T_{1/2}$ (hr)	18	2.18 ± 0.78	2.00	1.21 – 4.28
Plasma Vd (mL)	18	66812 ± 39063	64577	12110 – 156261
Plasma Vd (mL/kg)	18	1099 ± 517	1028	378 – 2112
Plasma Cl (mL/hr)	18	21750 ± 11463	21605	4256 – 47595
Plasma Cmax (ng/mL)	18	7326 ± 4856	6576	1787 – 21468
Plasma Tmax (hr)	18	1.71 ± 0.78	1.54	0.71 – 3.29
Cellular AUC_{0-24} (ng.hr/mL)	16	61899 ± 52962	47283	8430 – 201003
Cellular $T_{1/2}$ (hr)	16	2.37 ± 0.83	2.09	1.38 – 3.95
Cellular Cmax (ng/mL)	16	13432 ± 12222	11218	1413 – 50066
Cellular Tmax (hr)	16	1.83 ± 0.85	1.64	0.71 – 4.11
CAR	16	1.82 ± 0.88	1.61	0.65 – 3.73
Pyrazinamide				
Plasma AUC_{0-24} (ng.hr/mL)	12	699772 ± 450299	603585	263892 – 1997106
Plasma $T_{1/2}$ (hr)	12	8.12 ± 3.61	8.39	4.16 – 17.28
Plasma Vd (mL)	12	35542 ± 9183	36552	22174 – 47789
Plasma Vd (mL/kg)	12	606 ± 152	597	364 – 937
Plasma Cl (mL/hr)	12	3572 ± 1698	3350	1001 – 7112
Plasma Cmax (ng/mL)	12	51517 ± 11526	49629	36520 – 77459
Plasma Tmax (hr)	12	1.32 ± 0.98	1.02	0.47 – 3.95
Isoniazid				
Plasma AUC_{0-24} (ng.hr/mL)	13	27036 ± 12024	26841	10637 – 50348
Plasma $T_{1/2}$ (hr)	13	2.59 ± 1.77	1.99	0.18 – 3.69
Plasma Vd (mL)	13	54330 ± 39360	43138	15896 – 170086
Plasma Vd (mL/kg)	13	898 ± 436	662	485 – 1790
Plasma Cl (mL/hr)	13	13641 ± 7249	10813	5959 – 28205
Plasma Cmax (ng/mL)	13	6716 ± 2726	6652	1685 – 12037
Plasma Tmax (hr)	13	0.73 ± 0.38	0.74	0.17 – 1.47
Acetylisoniazid				
Plasma AUC_{0-24} (ng.hr/mL)	9	27940 ± 17975	21152	9641 – 65436
Plasma $T_{1/2}$ (hr)	9	7.65 ± 5.47	6.32	1.52 – 18.05
Plasma Cmax (ng/mL)	9	2193 ± 1549	1634	850 – 5530
Plasma Tmax (hr)	9	2.74 ± 1.00	2.72	1.39 – 4.35
Transporter expression				
P-gp (RFU)	18	3.50 ± 1.24	3.27	1.61 – 6.31
MRP1 (RFU)	18	4.15 ± 0.92	4.39	2.31 – 5.60
BCRP (RFU)	18	0.85 ± 0.46	0.69	0.32 – 1.66

7.3.2 Results Figures

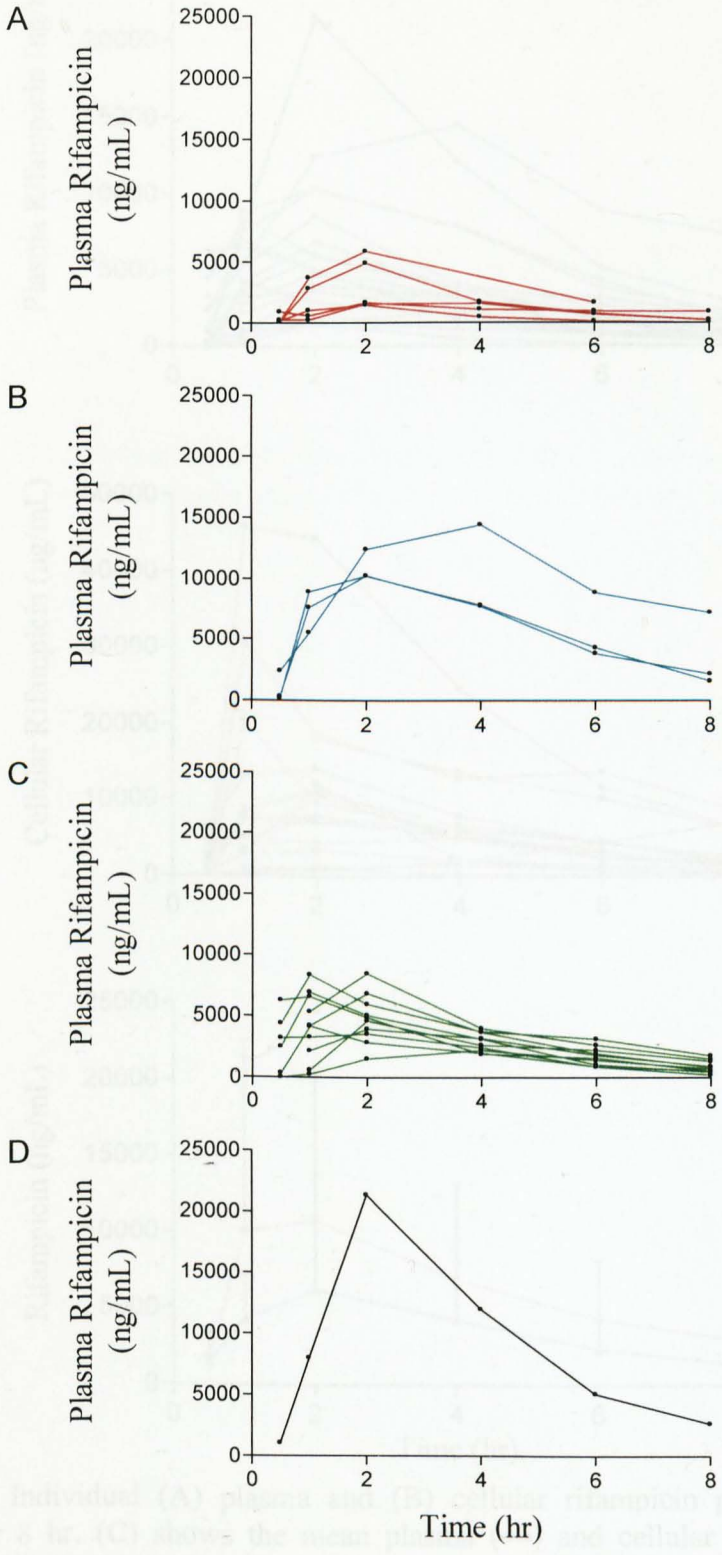

Figure 7.1: Individual rifampicin plasma pharmacokinetic profiles over 8 hr following a rifampicin dose of (A) 300 mg, (B) 450 mg, (C) 600 mg and (D) 900 mg.

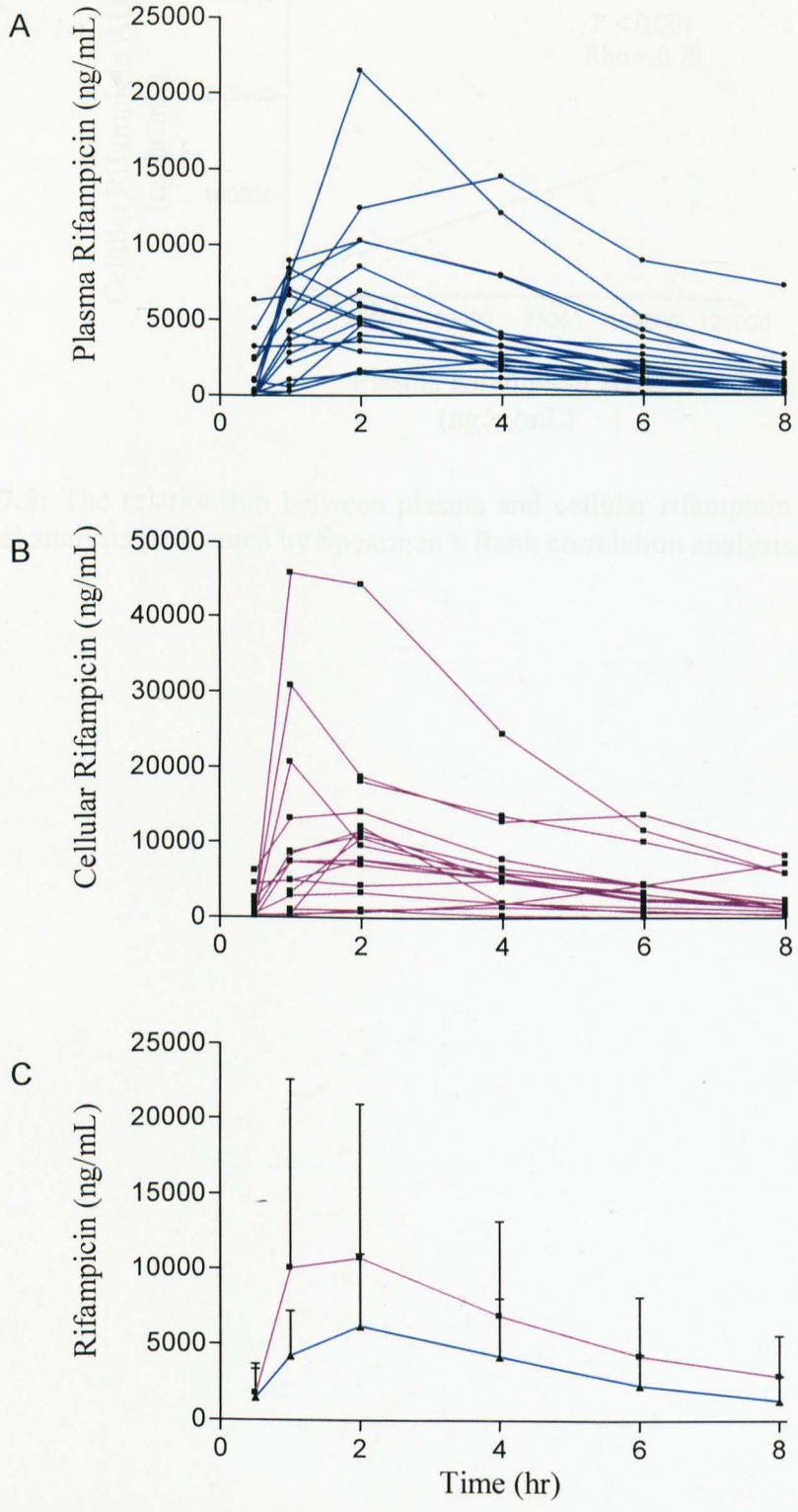

Figure 7.2: Individual (A) plasma and (B) cellular rifampicin pharmacokinetic profiles over 8 hr. (C) shows the mean plasma (—) and cellular (—) rifampicin pharmacokinetic (±SD) of the patients.

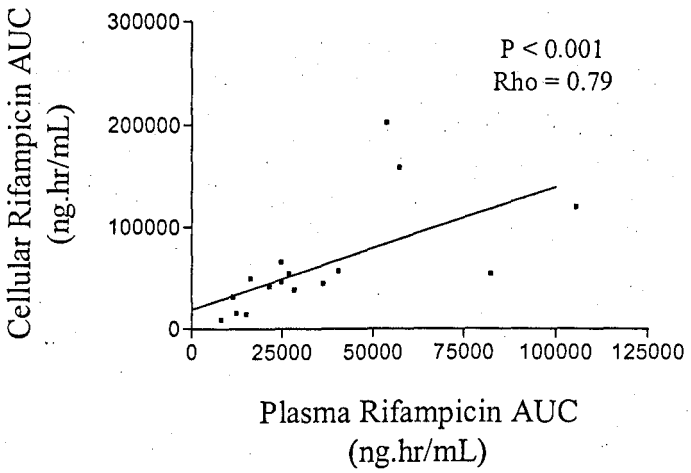

Figure 7.3: The relationship between plasma and cellular rifampicin AUC (n=16). Statistical analysis performed by Spearman's Rank correlation analysis.

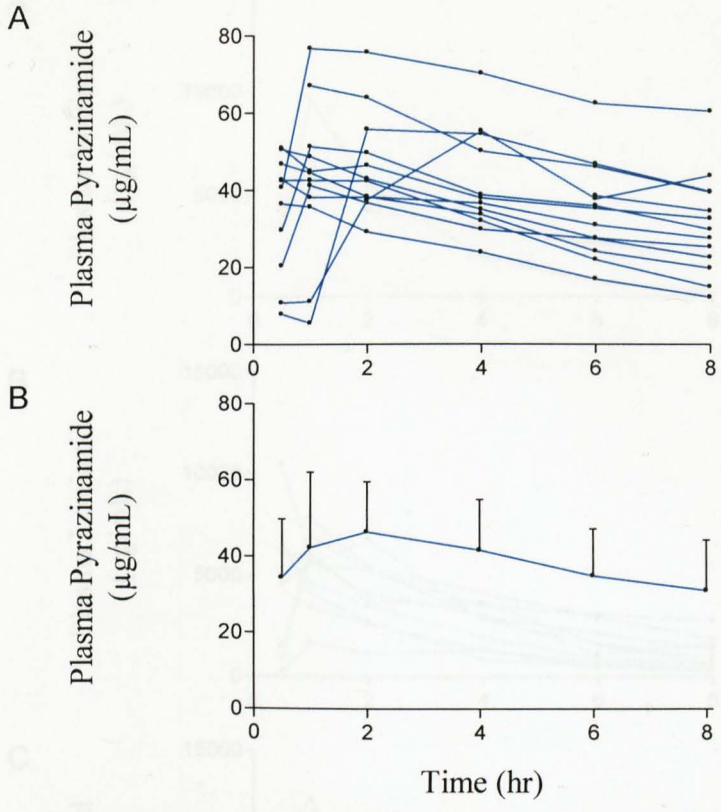

Figure 7.4: Individual (A) pyrazinamide pharmacokinetic profiles over 8 hr following a pyrazinamide dose and the mean (B) plasma pyrazinamide pharmacokinetic (±SD) of the patients.

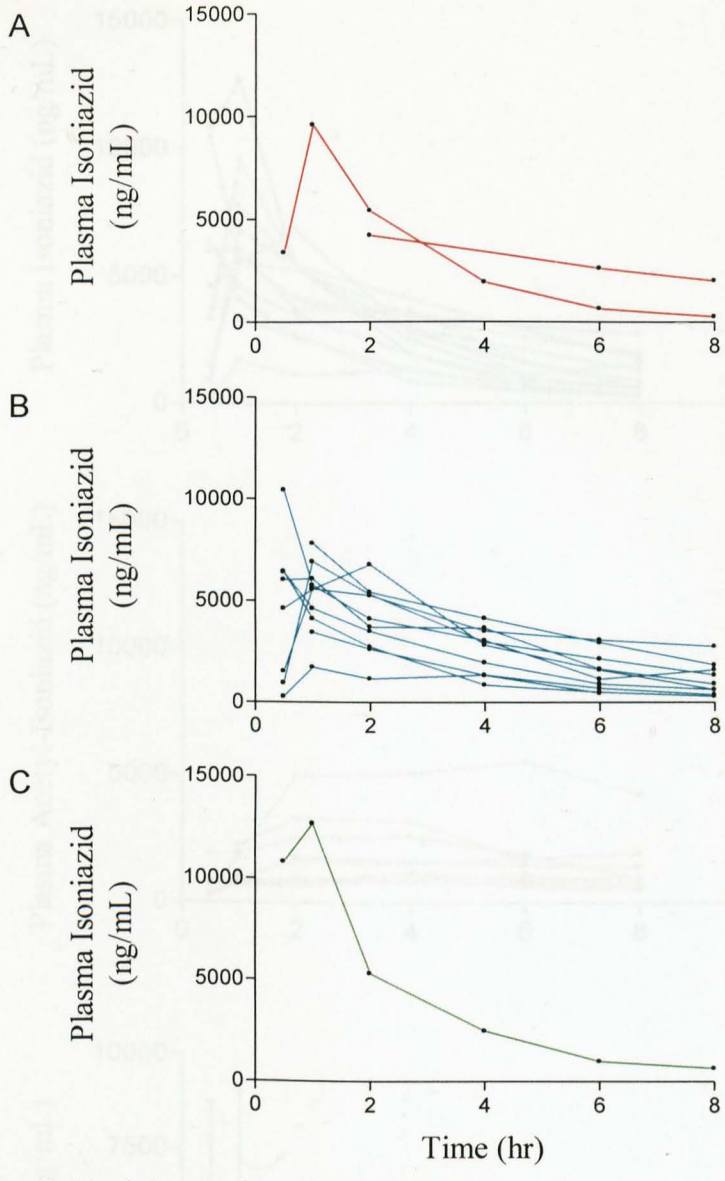

Figure 7.5: Individual isoniazid pharmacokinetic profiles over 8 hr following an isoniazid dose of (A) 225 mg, (B) 300 mg and (C) 450 mg.

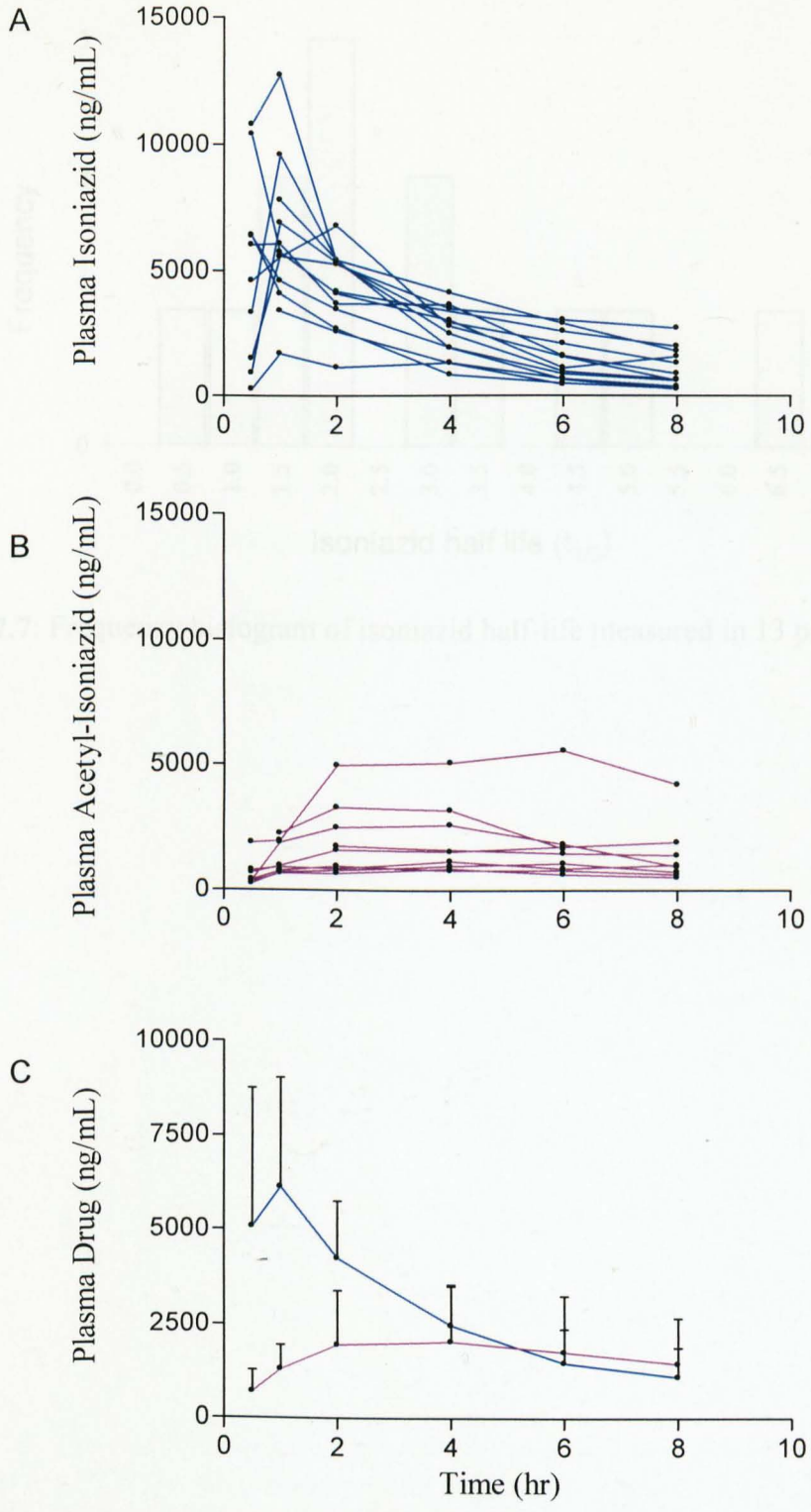

Figure 7.6: Individual (A) isoniazid and (B) acetyl-isoniazid pharmacokinetic profiles over 8 hr. (C) shows the mean patients plasma isoniazid (—) and acetyl-isoniazid (—) pharmacokinetics (+SD).

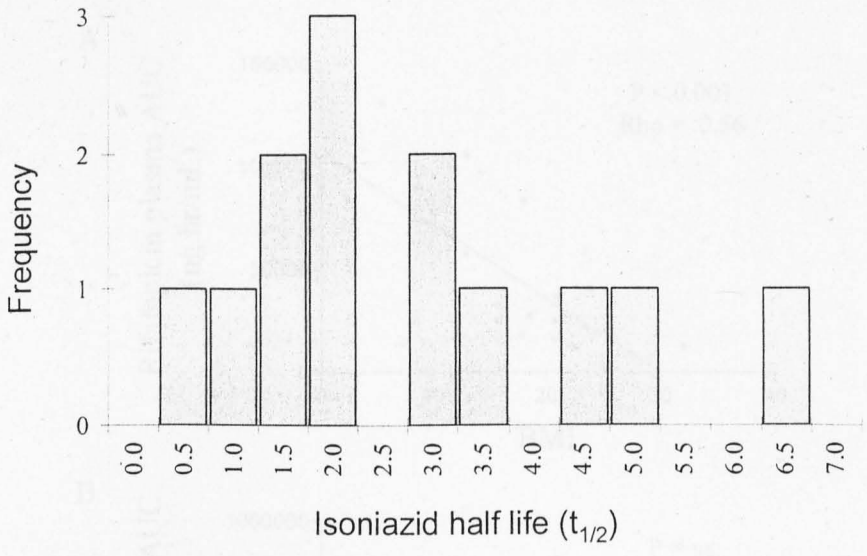

Figure 7.7: Frequency histogram of isoniazid half-life measured in 13 patients.

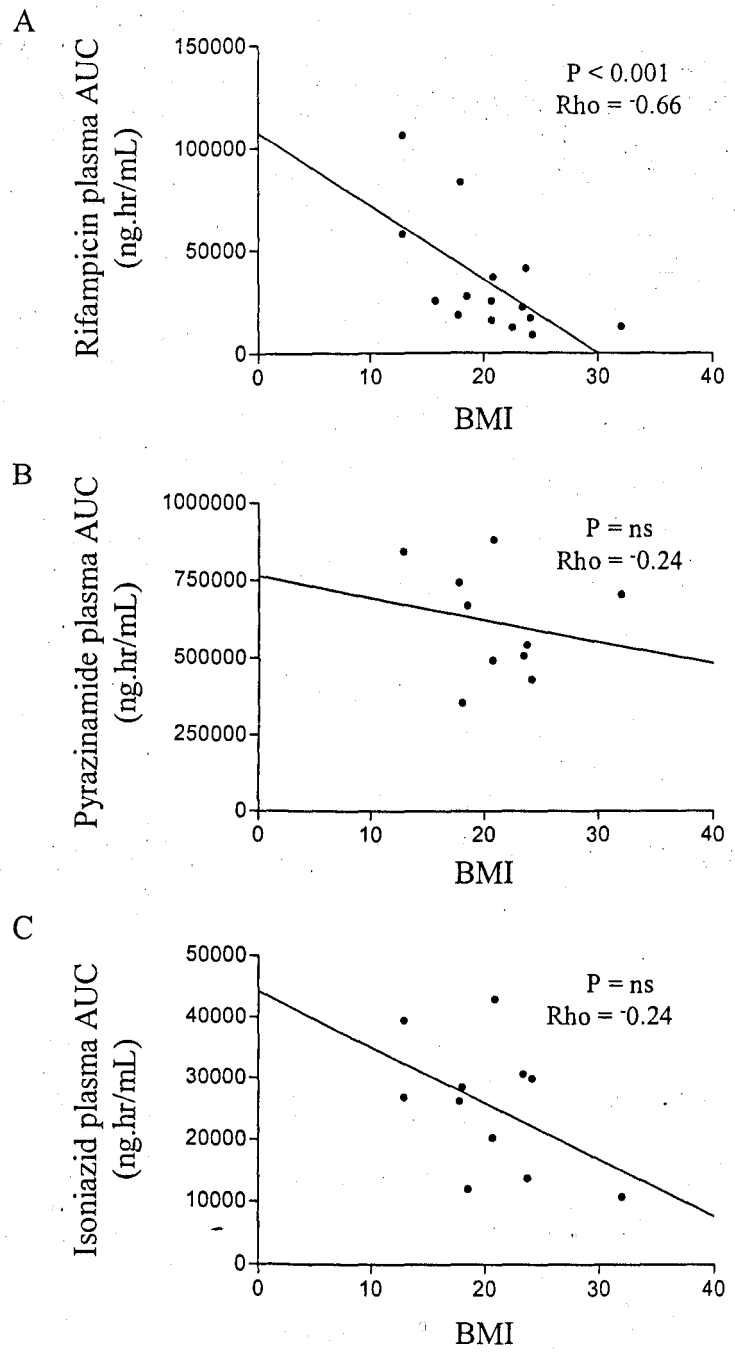

Figure 7.8: The relationship between (A) rifampicin (●300 mg, ●450 mg, ●600 mg and ●900 mg), (B) pyrazinamide (●1500 mg, ●2000 mg and ●2500 mg) and (C) isoniazid (●225 mg, ●300 mg and ●750 mg) AUC and the body mass index (BMI) of the patients. Statistical analysis performed by Spearman's Rank correlation analysis.

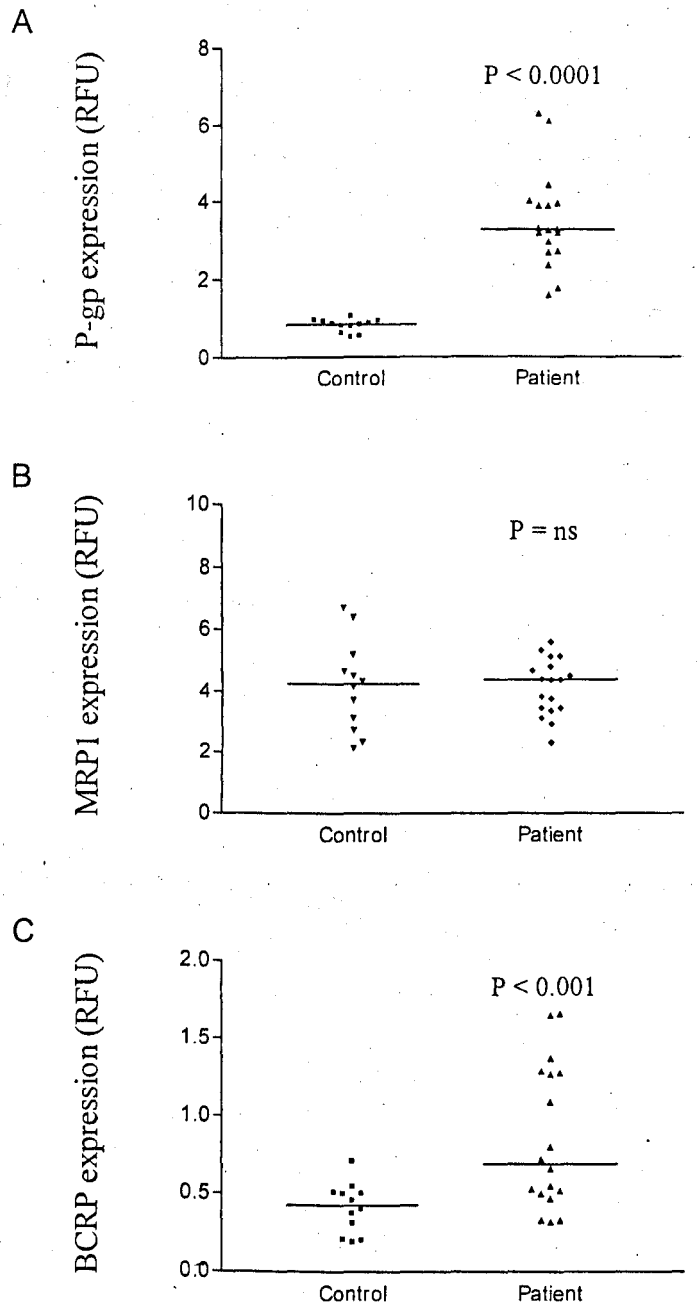

Figure 7.9: (A) Pgp, (B) MRP1 and (C) BCRP transporter expression as determined on healthy volunteer PBMCs (n=12) and on PBMCs of patients receiving rifampicin containing medication (n=18). Statistical analysis performed by Mann Whitney U-test analysis.

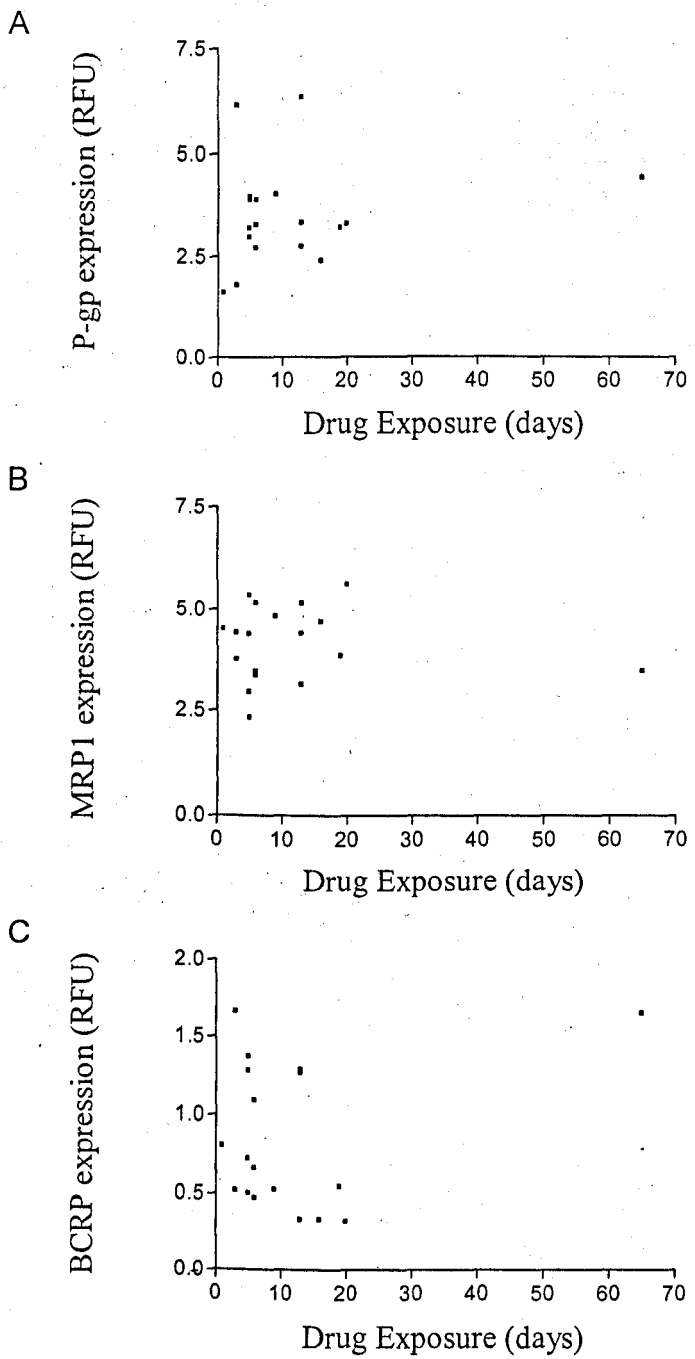

Figure 7.10: The relationship between (A) Pgp, (B) MRP1 and (C) BCRP transporter expression on PBMCs and the length of time the individual patients have been receiving rifampicin containing medication.

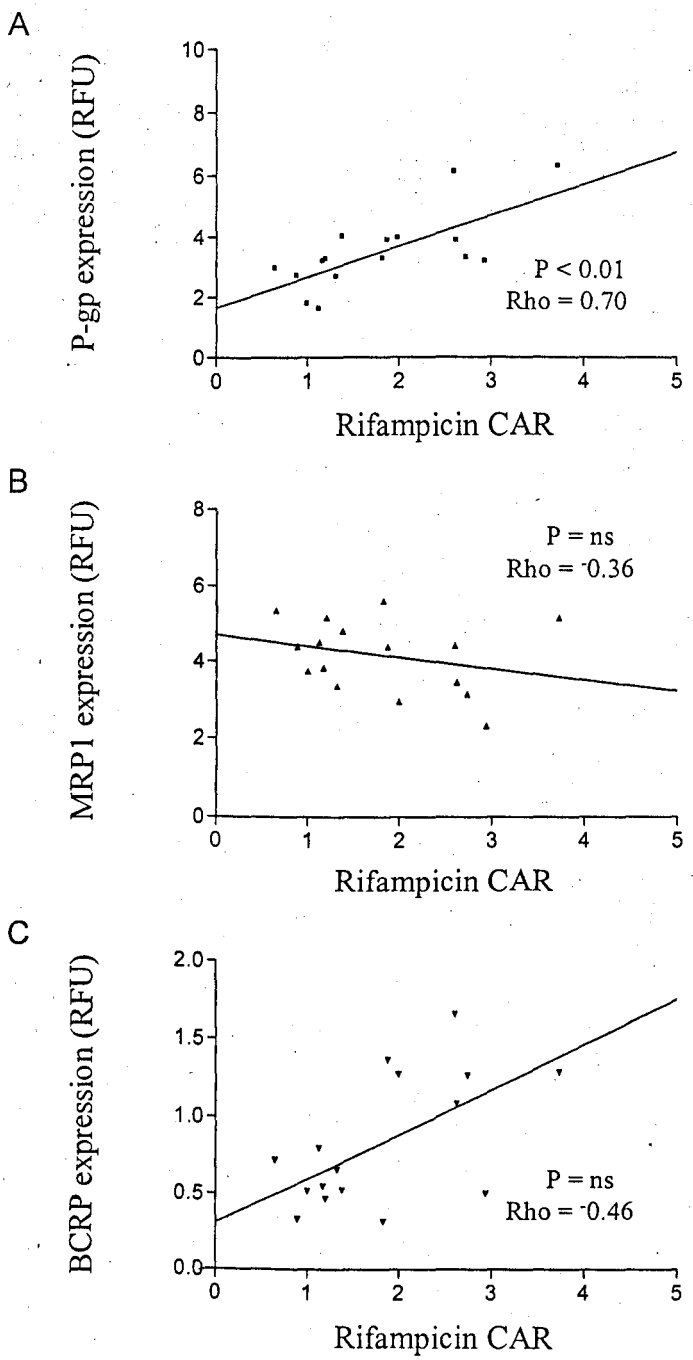

Figure 7.11: The relationship between (A) Pgp, (B) MRP1 and (C) BCRP transporter expression on PBMCs and the cellular accumulation of rifampicin (CAR) within those PBMCs (n=16). Statistical analysis performed by Spearman's Rank correlation.

7.4 Discussion

This study was designed to ascertain the cellular and plasma pharmacokinetics of anti-tuberculosis drugs and to determine the impact of drug transporters. Rifampicin is a known inducer of P-gp (Greiner *et al.*, 1999; Asghar *et al.*, 2002) and in chapter 2 it was demonstrated also to be a substrate for Pgp. The initial aim of the study was to compare cellular rifampicin pharmacokinetic accumulation before (day 0) and following full rifampicin mediated P-gp induction (day 14). However, due to the extent of the illness in both the tuberculosis and staphylococcal patients, it did not prove possible to sample large volumes of blood on day 0. This study could therefore only be performed on patients that had already commenced rifampicin therapy.

The rifampicin pharmacokinetic profiles and parameters obtained here are in the same range as those observed by (Peloquin *et al.*, 1997). However, unlike (Peloquin *et al.*, 1997) where rifampicin pharmacokinetics were determined on healthy volunteers receiving their first rifampicin dose, data obtained here are from patients suffering from different diseases, receiving different doses of rifampicin (depending on body weight and disease type) for different periods of time. These differences all contribute to the increased variation in the rifampicin pharmacokinetic profiles.

Rifampicin is routinely given to patients with tuberculosis and staphylococcal infections at 600 and 300 mg respectively. In the case of tuberculosis meningitis, dosage is increased to 900 mg of rifampicin. Rifampicin dosage for the treatment of tuberculosis is only corrected for body mass (to 450 mg) if the patients weigh less than 60 kg (to 450 mg). It is therefore not surprising that plasma rifampicin AUC is significantly correlated to BMI.

Although rifampicin accumulates in PBMCs, the number of cells that can be obtained from blood samples obtained from patients is limited and a sensitive assay is therefore needed for its detection. The HPLC-MS method described in Chapter 6, with a limit of detection of 100 ng/mL was found to be sensitive enough to measure cell associated rifampicin over the sampling time-points.

Rifampicin accumulation ratios were measured using the ratio of the cell associated vs plasma AUC, rather than at a particular sampling time point in order to decrease the potential error. The CARs of rifampicin in PBMCs measured here are however lower than those seen in the *in vitro* cell lines and *in vitro* PBMC studies (chapter 2). This phenomenon has also been seen with saquinavir which has a published *in vivo* CAR of 3.31 (range, 1.49 to 6.69) (Ford *et al.*, 2004), while *in vitro* it appears greater at 25.3 (range, 6.4 to 50.7) (Janneh *et al.*, 2005). The difference betweeen *in vivo* and *in vitro* rifampicin CAR may be due to physiological conditions such as the increase of drug transporter expression on PBMCs by rifampicin mediated induction of P-gp (Fig. 7.9) or differences in protein binding. However, as rifampicin is lipophilic, it is likely that a loss of cell associated rifampicin occurs during the separation of PBMCs from blood on Ficoll-Paque.

Rifampicin is known to be a dose and time dependent inducer of MDR1 through the activation of the nuclear hormone receptor pregnane X receptor (PXR) (Geick *et al.*, 2001; Kauffmann *et al.*, 2002). When comparing P-gp expression of rifampicin receiving patients to that of healthy volunteers it can be seen that there is a large increase in P-gp expression on PBMCs. The P-gp induction is seen in both

tuberculosis and staphylococcal patients which makes it unlikely that either the disease or other co-administered medication is responsible for the observed induction. Nonetheless, the control group would ideally comprise non rifampicin receiving patients. Further, because of the lack of data on P-gp expression between day 0 and day 3 following the start of rifampicin medication, the time during which induction is expected to be most evident, a good fit cannot be placed on the rate of induction (Fig 7.10).

Data also indicate that the patients receiving rifampicin have an increased expression of BCRP. Previous studies have shown that PXR plays a role in the regulation of BCRP in mice (Anapolsky *et al.*, 2006) and that there is a correlation between PXR and BCRP mRNA expression in human PBMCs (Albermann *et al.*, 2005). Our data agree with these findings and show for the first time that rifampicin has an impact on BCRP expression *in vivo* at a protein level.

The induction of MRP1 is not well understood and is thought to depend on glutathione (GSH) concentrations (Muller *et al.*, 1994; Zaman *et al.*, 1994; O'Brien *et al.*, 1999; Akan *et al.*, 2004). Conflicting data have been presented on the involvement of PXR and/or rifampicin in the induction of MRP1. Data shown here demonstrate no induction of MRP1 expression on PBMCs in rifampicin receiving patients (Fig. 7.9). The lack of MRP1 induction is in agreement with previous reports showing a lack of induction by RT-PCR (Schrenk *et al.*, 2001; Kauffmann *et al.*, 2002). Other work found that rifampicin was able to induce MRP1 mRNA but not protein expression in LLC-PK1 cell lines (Magnarin *et al.*, 2004).

In chapter 2, rifampicin was shown to be a substrate for P-gp in cell lines. Further it was shown that basal P-gp levels in PBMC had no effect on rifampicin accumulation. When commencing the study described in the present chapter we hypothesised that an increase in P-gp expression due to rifampicin induction would have a greater impact on rifampicin accumulation and therefore negatively correlate with rifampicin CAR. However the data show a significant positive correlation between rifampicin CAR and P-gp expression and demonstrate that despite rifampicin being a substrate for P-gp, the impact of P-gp on the accumulation of rifampicin in PBMCs *in vivo* is limited. Moreover, it seems that increased P-gp expression actually leads to increased rifampicin accumulation within cells. The likely reason for this is that increased intracellular accumulation of rifampicin will mediate a greater inducing effect on P-gp expression.

Previous work has indicated a significant correlation between P-gp and saquinavir CAR (Ford *et al.*, 2004), despite saquinavir being a well known P-gp substrate that can be modulated by inhibition of P-gp (Janneh *et al.*, 2005). This demonstrates that correlating transporter expression to drug CAR may not necessarily be a good way of determining if a drug is a substrate. However, our data demonstrate that P-gp is not the main determinant of rifampicin accumulation in PBMCs; and that transport is mediated through other influx and efflux transporters or through diffusion.

Ideally, the concentration of rifampicin would have been measured in alveolar macrophages, as they are the main site of intra-cellular bacilli. However, due to the difficulty in obtaining alveolar macrophages from tuberculosis patients and the limited sensitivity of our assays, this was unachievable. Being able to determine

intracellular accumulation of isoniazid and pyrazinamide *in vivo* would also give us a feel for the concentrations of drug acting on intracellular bacilli. However due to the hydrophilicity of these drugs, accumulation would be limited and therefore more sensitive analytical assays are needed.

Pharmacokinetic plasma drug profiles for isoniazid and pyrazinamide were performed to demonstrate the functionality of the HPLC assays described in chapter 6 and to determine the inter-individual variability. Both of these drugs were only given to the tuberculosis patients, which is why fewer patients were studied compared to rifampicin. As with rifampicin, the pharmacokinetic parameters determined for pyrazinamide, isoniazid and acetyl-isoniazid were similar to those observed by (Peloquin *et al.*, 1997). With both drugs a trend was seen towards BMI dependent AUC. Further, the presence of both fast and slow acetylators were likely to have been present in our patient population as indicated by the range of isoniazid half-lives (similar to that seen by (Peloquin *et al.*, 1997)).

Data obtained here show that we are able to accurately determine the pharmacokinetic profiles of plasma rifampicin, pyrazinamide and isoniazid *in vivo*. Further, we have provided the first indication of the extent of rifampicin accumulation in PBMCs *in vivo*. Rifampicin accumulation does not seem to be primarily governed by the expression of surface P-gp, MRP1 or BCRP, however rifampicin was an inducer of both P-gp and BCRP.

CHAPTER 8

General discussion

Despite the availability of numerous anti-tuberculosis drugs, the duration of tuberculosis therapy is still at least 6 months. Partially, the reason for this is that tuberculosis infection consists of a 'mixed population' containing bacilli in different metabolic states as well as within or outside alveolar macrophages and granuloma. Current drugs are highly effective at killing actively growing bacilli in the extracellular space (i.e. they have good EBA), however they are less effective at killing semi-dormant and intracellular bacilli (persisting bacilli) (Mitchison, 2000).

Previously published data show that active drug efflux transporters are associated with decreased activity of anti-cancer drugs (Juliano and Ling, 1976), anti-microbials (Van Bambeke *et al.*, 2000; Seral *et al.*, 2003a; Seral *et al.*, 2003b; Seral *et al.*, 2003c; Seral *et al.*, 2005) and anti-retrovirals (Jones *et al.*, 2001a; Jones *et al.*, 2001b; Owen *et al.*, 2005). The involvement of active drug transporters in the chemotherapy of tuberculosis has as yet not been determined. It is hypothesised here that active efflux transporters may contribute to the decreased efficiency with which current anti-tuberculosis drugs kill intracellular bacteria by limiting their intracellular accumulation.

The focus of this PhD has been to establish the expression of both P-gp and MRP1 on alveolar macrophages and to determine their impact on the accumulation of first line anti-tuberculosis drugs. Also, the extent to which OATP influx transporters have an influence on drug uptake in alveolar macrophages is evaluated. Further aims were to develop novel assays for the determination of EBA and sterilising activity of drugs. These assays are utilised to provide a unique insight into the time and concentration dependent bactericidal activity of current first line drugs, and allow us

to evaluate differential efficacy of drugs in macrophages compared to extracellular bacilli. In addition, novel and pre-existing analytical methods are introduced and validated for the measurement of plasma rifampicin, isoniazid and ethambutol concentrations.

Initial studies detailed in chapter 2 show for the first time that alveolar macrophages and monocyte derived macrophages express both P-gp and MRP1. This is an important finding because it means that both transporters may be able to impact on the cellular accumulation of the anti-tuberculosis drugs.

Here it has been demonstrated, using established *in vitro* cell line models (T-lymphoblastoid and MDCKII) in combination with the potent P-gp inhibitor tariquidar, that rifampicin is a substrate for P-gp. However, contrasting data is observed in PBMCs derived from healthy volunteers (*ex vivo*) and patients (*in vivo*) where rifampicin cellular accumulation does not correlate with P-gp expression. In addition, inhibition of P-gp on PBMCs (*ex vivo*) does not significantly alter rifampicin accumulation. However, interestingly, and probably most importantly, *in vitro* inhibition of P-gp on activated macrophages (activated THP1 cells) leads to a significant increase in rifampicin bactericidal activity on intracellular H37Rv and this increase in rifampicin activity is related to its increase in accumulation.

The inconsistency in the extent to which P-gp is able to modulate rifampicin accumulation may to be best explained by the differences in P-gp expression between the cell lines, PBMC and activated THP1 cells. The cell line models utilise cells that are drug selected or transfected to express P-gp (CEM_{VBL100} and

$MDCKII_{MDR1}$ respectively). The P-gp expression levels in these cells is therefore high, accounting for the marked observed modulation of rifampicin accumulation. Activation of THP1 cells into macrophage like cells causes a marked induction of P-gp, resulting in expression levels greater than basal expression, but below that of the T-lymphoblastoid and MDCKII cell lines. This clear induction of P-gp allows for modulation of rifampicin in the activated THP1 cells but not the parental THP1 cells. Basal P-gp expression on PBMC is the lowest compared to that of other models, and data suggest that it is too low to result in significant modulation of rifampicin accumulation by its inhibition. Rifampicin is therefore a substrate for P-gp, although relatively high P-gp expression is required to be able to significantly modulate rifampicin accumulation. The extent to which P-gp expression on alveolar macrophages modulates rifampicin accumulation is not yet known and further studies are needed to determine this. Data suggest that *in vivo* the impact on rifampicin accumulation, and therefore its intracellular activity, will be limited in cells expressing basal amounts of P-gp (i.e. PBMCs). However it may be of importance in cells that express higher levels, such as intestinal, liver cell and possibly activated alveolar macrophages.

The clinical studies also show the induction of both P-gp and BCRP on PBMC from patients receiving rifampicin. Even though this induction has not been shown to be of particular importance in rifampicin transport, P-gp induction by rifampicin may alter the accumulation of other co-administered drugs that are substrates for P-gp.

Like rifampicin, ethambutol shows differential toxicity in T-lymphoblastoid cells and its intracellular activity against H37Rv in activated THP1 cells is enhanced by

inhibition of P-gp. However, a lack of commercially available radioactive ethambutol precludes determination of the impact of basal P-gp expression on its accumulation. Nonetheless, data suggest that P-gp expression alters ethambutol accumulation and that this can affect its antimicrobial activity against intracellular MTB. Again, further studies are needed to determine the degree to which alveolar macrophage P-gp expression modulates ethambutol accumulation.

Isoniazid and pyrazinamide proved not to be differentially toxic in the T-lymphoblastoid cell lines. Further, isoniazid accumulation was not altered in T-lymphoblastoid cell lines and inhibition of P-gp did not improve its intracellular anti-tuberculosis activity. These data suggest that neither of the two drugs are substrates for P-gp and that P-gp activity will not alter their intracellular activity.

With regards to MRP1, experiments in cell lines and in ex-vivo PBMCs provide no conclusive evidence that MRP1 modulates the efflux of any of the first line anti-tuberculosis drugs.

As well as P-gp and MRP1, it is demonstrated here that alveolar macrophages express active influx transporters in the form of SLCO3A1 and SLCO1B3. Interestingly rifampicin has previously been found to be a substrate for OATP1B3 (encoded by SLCO1B3) (Vavricka *et al.*, 2002). OATP1B3 may therefore be an important determinant for the amount of rifampicin accumulation in alveolar macrophages, and may therefore have a pivotal role in the degree of intracellular anti-tuberculosis activity by rifampicin. The study of OATP influx transporters is a relatively new field, and therefore commercially available specific antibodies and

inhibitors have as yet not been developed. Both antibodies and inhibitors will be vital tools needed to determine the extent to which OATPs play a role in tuberculosis therapy.

A further aim of the thesis was to investigate time and concentration dependent killing of extracellular bacilli by first line anti-tuberculosis drugs. Numerous methods have been developed for the analysis of anti-tuberculosis activity including the traditional proportion method, MABA (Collins and Franzblau, 1997; Abate *et al.*, 1998; Franzblau *et al.*, 1998; Mshana *et al.*, 1998; De Logu *et al.*, 2001; Caviedes *et al.*, 2002; Foongladda *et al.*, 2002; Luna-Herrera *et al.*, 2003; Abate *et al.*, 2004; Reis *et al.*, 2004)and BACTEC (Collins and Franzblau, 1997; Jayaram *et al.*, 2003; Jayaram *et al.*, 2004). Here it has been established that MABA is a flexible assay that can be effectively modified to determine the influence of time and concentration on EBA. Results indicate that rifampicin, isoniazid and ethambutol show concentration dependent killing of MTB. Pyrazinamide shows no activity against extracellular H37Rv, a phenomenon explained by previous work suggesting that an acidified environment is needed for pyrazinamide to be bactericidal (Heifets *et al.*, 2000; Zhang and Mitchison, 2003).

Interestingly, it is shown here that H37Rv develops a time dependent tolerance to both rifampicin and isoniazid (not ethambutol) over 3 weeks of culture in the presence of the drug. Tolerance developed against isoniazid is not reversed in the absence of drug pressure, suggesting the selection or generation of genotypically resistant MTB. Further, ethionamide susceptibility of the isoniazid resistant MTB strain is similar to that of wild-type H37Rv. As isoniazid and ethionamide share the

same target proteins (DeBarber *et al.*, 2000; Lee *et al.*, 2000; Morlock *et al.*, 2003), this suggests that the genetic mutation occurs in the gene responsible for isoniazid bioactivation (KatG). Also, the rate of emergence of isoniazid resistance shown here is greater than previously predicted by (David, 1970). This result emphasises the need for combination therapy in the treatment of tuberculosis, and may provide a further explanation for the decrease in bacterial killing following EBA.

Contrary to isoniazid, time dependent development of rifampicin tolerant MTB was reversed in the absence of drug pressure. These data suggest a novel mechanism by which MTB is able to alter its susceptibility to rifampicin (phenotypic switch) without having to undergo a mutation. MTB is known to alter its transcriptome during phagocytosis in order to compensate for attack by the host immune system (Schnappinger *et al.*, 2003) which may also occur following drug mediated pressure. MTB tolerance to rifampicin may partially provide an explanation for the long period needed for tuberculosis therapy.

MTB is known for its ability to manipulate the human immune system and utilise the macrophage as a sanctuary site. Drug mediated killing of intracellular MTB is thought to be a constituent of the sterilising phase (Jindani *et al.*, 1980; Jindani *et al.*, 2003). To shorten tuberculosis therapy, drugs that improve MTB kill during the sterilising phase are essential. A novel high throughput assay for the analysis of intracellular bactericidal/static activity of drugs against MTB is described here. By using macrophage viability as a marker of MTB viability, this assay provides a new approach to analysis of anti-tuberculosis activity, and may prove to be a useful model in developing new anti-tuberculosis drugs against persisting bacilli. A drawback with

the intracellular assay is that it is difficult to differentiate between bactericidal and bacteriostatic activity of drugs. The intracellular assay may also be used to look at the importance of host proteins, by transfecting the genes of interest into THP1 cells prior to activation and infection.

With regard to the intracellular activity of rifampicin, isoniazid and ethambutol all three drugs showed concentration dependent activity. For both isoniazid and ethambutol, intracellular activity was at a similar concentration to that needed to control extracellular bacteria. Rifampicin intracellular kill was however less efficient, than with extracellular bacilli. This difference may be at least partially a consequence of protein binding and drug accumulation. Further, it must be noted that trough rifampicin concentrations achieved *in vivo* are below those needed to kill intracellular bacteria *in vitro*, and may be another reason for the long period needed to sterilise MTB.

In chapter 6 the successful development and validation of novel and pre-existing analytical assays for measuring plasma rifampicin, pyrazinamide and isoniazid from plasma is described. These assays are utilised to measure plasma drug concentration in rifampicin receiving patients, giving pharmacokinetic parameters similar to those previously published (Peloquin *et al.*, 1997). Further, rifampicin HPLC-MS proved sensitive enough to measure cellular rifampicin pharmacokinetics in PBMCs, which allowed the determination of *in vivo* rifampicin accumulation. The analytical methods developed can provide a useful tool in measuring plasma drug concentration for further clinical studies.

Work presented here provides evidence that P-gp (not MRP1) and OATPs may have a role in the bactericidal activity of rifampicin and ethambutol within macrophages. It must be remembered however, that drug accumulation is often a complex interplay between active efflux and influx transporters, and that other untested transporters may also play a role in governing the accumulation of anti-tuberculosis drugs. Further, this thesis describes novel assays that underpin the future determination of extracellular and intracellular activity of novel anti-tuberculosis drugs.

REFERENCES

Abate G, Aseffa A, Selassie A, Goshu S, Fekade B, WoldeMeskal D and Miorner H (2004) Direct colorimetric assay for rapid detection of rifampin-resistant Mycobacterium tuberculosis. *J Clin Microbiol* **42**:871-873.

Abate G, Mshana RN and Miorner H (1998) Evaluation of a colorimetric assay based on 3-(4,5-dimethylthiazol-2-yl)-2,5-diphenyl tetrazolium bromide (MTT) for rapid detection of rifampicin resistance in Mycobacterium tuberculosis. *Int J Tuberc Lung Dis* **2**:1011-1016.

Abe T, Kakyo M, Tokui T, Nakagomi R, Nishio T, Nakai D, Nomura H, Unno M, Suzuki M, Naitoh T, Matsuno S and Yawo H (1999) Identification of a novel gene family encoding human liver-specific organic anion transporter LST-1. *J Biol Chem* **274**:17159-17163.

Acocella G, Nicolis FB and Tenconi LT (1965) The effect of an intravenous infusion of rifamycin SV on the excretion of bilirubin, bromsulphalein, and indocyanine green in man. *Gastroenterology* **49**:521-525.

Acocella G, Pagani V, Marchetti M, Baroni GC and Nicolis FB (1971) Kinetic studies on rifampicin. I. Serum concentration analysis in subjects treated with different oral doses over a period of two weeks. *Chemotherapy* **16**:356-370.

Adachi H, Suzuki T, Abe M, Asano N, Mizutamari H, Tanemoto M, Nishio T, Onogawa T, Toyohara T, Kasai S, Satoh F, Suzuki M, Tokui T, Unno M, Shimosegawa T, Matsuno S, Ito S and Abe T (2003) Molecular characterization of human and rat organic anion transporter OATP-D. *Am J Physiol Renal Physiol* **285**:F1188-1197.

Ahn CH, Kong JY, Choi WC and Hwang MS (1996) Selective inhibition of the effects of phorbol ester on doxorubicin resistance and P-glycoprotein by the protein kinase C inhibitor 1-(5-isoquinolinesulfonyl)-2-methylpiperazine (H7) in multidrug-resistant MCF-7/Dox human breast carcinoma cells. *Biochem Pharmacol* **52**:393-399.

Akan I, Akan S, Akca H, Savas B and Ozben T (2004) N-acetylcysteine enhances multidrug resistance-associated protein 1 mediated doxorubicin resistance. *Eur J Clin Invest* **34**:683-689.

Albermann N, Schmitz-Winnenthal FH, Z'Graggen K, Volk C, Hoffmann MM, Haefeli WE and Weiss J (2005) Expression of the drug transporters MDR1/ABCB1, MRP1/ABCC1, MRP2/ABCC2, BCRP/ABCG2, and PXR in peripheral blood mononuclear cells and their relationship with the expression in intestine and liver. *Biochem Pharmacol* **70**:949-958.

Alsaadi AI and Smith DW (1973) The fate of virulent and attenuated Mycobacteria in guinea pigs infected by the respiratory route. *Am Rev Respir Dis* **107**:1041-1046.

Ameyaw MM, Regateiro F, Li T, Liu X, Tariq M, Mobarek A, Thornton N, Folayan GO, Githang'a J, Indalo A, Ofori-Adjei D, Price-Evans DA and McLeod HL (2001) MDR1 pharmacogenetics: frequency of the C3435T mutation in exon 26 is significantly influenced by ethnicity. *Pharmacogenetics* **11**:217-221.

Anapolsky A, Teng S, Dixit S and Piquette-Miller M (2006) The role of pregnane x receptor in 2-acetylaminofluorene-mediated induction of drug transport and -metabolizing enzymes in mice. *Drug Metab Dispos* **34**:405-409.

Armstrong JA and Hart PD (1971) Response of cultured macrophages to Mycobacterium tuberculosis, with observations on fusion of lysosomes with phagosomes. *J Exp Med* **134**:713-740.

Armstrong JA and Hart PD (1975) Phagosome-lysosome interactions in cultured macrophages infected with virulent tubercle bacilli. Reversal of the usual nonfusion pattern and observations on bacterial survival. *J Exp Med* **142**:1-16.

Asghar A, Gorski JC, Haehner-Daniels B and Hall SD (2002) Induction of multidrug resistance-1 and cytochrome P450 mRNAs in human mononuclear cells by rifampin. *Drug Metab Dispos* **30**:20-26.

Barnes PF, Lu S, Abrams JS, Wang E, Yamamura M and Modlin RL (1993) Cytokine production at the site of disease in human tuberculosis. *Infect Immun* **61**:3482-3489.

Bean AG, Roach DR, Briscoe H, France MP, Korner H, Sedgwick JD and Britton WJ (1999) Structural deficiencies in granuloma formation in TNF gene-targeted mice underlie the heightened susceptibility to aerosol Mycobacterium tuberculosis infection, which is not compensated for by lymphotoxin. *J Immunol* **162**:3504-3511.

Beck WT, Mueller TJ and Tanzer LR (1979) Altered surface membrane glycoproteins in Vinca alkaloid-resistant human leukemic lymphoblasts. *Cancer Res* **39**:2070-2076.

Benet LZ, Izumi T, Zhang Y, Silverman JA and Wacher VJ (1999) Intestinal MDR transport proteins and P-450 enzymes as barriers to oral drug delivery. *J Control Release* **62**:25-31.

Berg JD, Pandov HI and Sammons HG (1984) Serum total bile acid levels in patients receiving rifampicin and isoniazid. *Ann Clin Biochem* **21 (Pt 3)**:218-222.

Bermudez LE and Goodman J (1996) Mycobacterium tuberculosis invades and replicates within type II alveolar cells. *Infect Immun* **64**:1400-1406.

Bernstein J, Lott WA, Steinberg BA and Yale HL (1952) Chemotherapy of experimental tuberculosis. V. Isonicotinic acid hydrazide (nydrazid) and related compounds. *Am Rev Tuberc* **65**:357-364.

Blackwood KS, Burdz TV, Turenne CY, Sharma MK, Kabani AM and Wolfe JN (2005) Viability testing of material derived from Mycobacterium tuberculosis prior to removal from a containment level-III laboratory as part of a Laboratory Risk Assessment Program. *BMC Infect Dis* **5**:4.

Borst P, Evers R, Kool M and Wijnholds J (2000) A family of drug transporters: the multidrug resistance-associated proteins. *J Natl Cancer Inst* **92**:1295-1302.

Borst P, Schinkel AH, Smit JJ, Wagenaar E, Van Deemter L, Smith AJ, Eijdems EW, Baas F and Zaman GJ (1993) Classical and novel forms of multidrug resistance and the physiological functions of P-glycoproteins in mammals. *Pharmacol Ther* **60**:289-299.

Brightbill HD, Libraty DH, Krutzik SR, Yang RB, Belisle JT, Bleharski JR, Maitland M, Norgard MV, Plevy SE, Smale ST, Brennan PJ, Bloom BR, Godowski PJ and Modlin RL (1999) Host defense mechanisms triggered by microbial lipoproteins through toll-like receptors. *Science* **285**:732-736.

Calleja I, Blanco-Prieto MJ, Ruz N, Renedo MJ and Dios-Vieitez MC (2004) High-performance liquid-chromatographic determination of rifampicin in plasma and tissues. *J Chromatogr A* **1031**:289-294.

Calleri E, De Lorenzi E, Furlanetto S, Massolini G and Caccialanza G (2002) Validation of a RP-LC method for the simultaneous determination of isoniazid,

pyrazinamide and rifampicin in a pharmaceutical formulation. *J Pharm Biomed Anal* **29**:1089-1096.

Campbell IA and Elmes PC (1975) Letter: Ethambutol and the eye; zinc and copper. *Lancet* **2**:711.

Carlone NA, Acocella G, Cuffini AM and Forno-Pizzoglio M (1985) Killing of macrophage-ingested mycobacteria by rifampicin, pyrazinamide, and pyrazinoic acid alone and in combination. *Am Rev Respir Dis* **132**:1274-1277.

Carryn S, Van Bambeke F, Mingeot-Leclercq MP and Tulkens PM (2002) Comparative intracellular (THP-1 macrophage) and extracellular activities of beta-lactams, azithromycin, gentamicin, and fluoroquinolones against Listeria monocytogenes at clinically relevant concentrations. *Antimicrob Agents Chemother* **46**:2095-2103.

Caruso AM, Serbina N, Klein E, Triebold K, Bloom BR and Flynn JL (1999) Mice deficient in CD4 T cells have only transiently diminished levels of IFN-gamma, yet succumb to tuberculosis. *J Immunol* **162**:5407-5416.

Cavalli V, Vilbois F, Corti M, Marcote MJ, Tamura K, Karin M, Arkinstall S and Gruenberg J (2001) The stress-induced MAP kinase p38 regulates endocytic trafficking via the GDI:Rab5 complex. *Mol Cell* **7**:421-432.

Caviedes L, Delgado J and Gilman RH (2002) Tetrazolium microplate assay as a rapid and inexpensive colorimetric method for determination of antibiotic susceptibility of Mycobacterium tuberculosis. *J Clin Microbiol* **40**:1873-1874.

Chan J, Tanaka K, Carroll D, Flynn J and Bloom BR (1995) Effects of nitric oxide synthase inhibitors on murine infection with Mycobacterium tuberculosis. *Infect Immun* **63**:736-740.

Chan J, Xing Y, Magliozzo RS and Bloom BR (1992) Killing of virulent Mycobacterium tuberculosis by reactive nitrogen intermediates produced by activated murine macrophages. *J Exp Med* **175**:1111-1122.

Chandra P and Brouwer KL (2004) The complexities of hepatic drug transport: current knowledge and emerging concepts. *Pharm Res* **21**:719-735.

Changsen C, Franzblau SG and Palittapongarnpim P (2003) Improved green fluorescent protein reporter gene-based microplate screening for antituberculosis compounds by utilizing an acetamidase promoter. *Antimicrob Agents Chemother* **47**:3682-3687.

Chatterjee D and Khoo KH (1998) Mycobacterial lipoarabinomannan: an extraordinary lipoheteroglycan with profound physiological effects. *Glycobiology* **8**:113-120.

Chen CJ, Chin JE, Ueda K, Clark DP, Pastan I, Gottesman MM and Roninson IB (1986) Internal duplication and homology with bacterial transport proteins in the mdr1 (P-glycoprotein) gene from multidrug-resistant human cells. *Cell* **47**:381-389.

Cheng AF, Li MS, Chan CY, Chan CH, Lyon D, Wise R and Lee JC (1994) Evaluation of three culture media and their combinations for the isolation of Mycobacterium tuberculosis from pleural aspirates of patients with tuberculous pleurisy. *J Trop Med Hyg* **97**:249-253.

Choudhuri BS, Sen S and Chakrabarti P (1999) Isoniazid accumulation in Mycobacterium smegmatis is modulated by proton motive force-driven and ATP-dependent extrusion systems. *Biochem Biophys Res Commun* **256**:682-684.

Christoforidis S, McBride HM, Burgoyne RD and Zerial M (1999) The Rab5 effector EEA1 is a core component of endosome docking. *Nature* **397**:621-625.

Chua J and Deretic V (2004) Mycobacterium tuberculosis reprograms waves of phosphatidylinositol 3-phosphate on phagosomal organelles. *J Biol Chem* **279**:36982-36992.

Chua J, Vergne I, Master S and Deretic V (2004) A tale of two lipids: Mycobacterium tuberculosis phagosome maturation arrest. *Curr Opin Microbiol* **7**:71-77.

Clark J and Wallace A (1967) The susceptibility of mycobacteria to rifamide and rifampicin. *Tubercle* **48**:144-148.

Clemens DL and Horwitz MA (1996) The Mycobacterium tuberculosis phagosome interacts with early endosomes and is accessible to exogenously administered transferrin. *J Exp Med* **184**:1349-1355.

Co DO, Hogan LH, Kim SI and Sandor M (2004) Mycobacterial granulomas: keys to a long-lasting host-pathogen relationship. *Clin Immunol* **113**:130-136.

Cole SP, Bhardwaj G, Gerlach JH, Mackie JE, Grant CE, Almquist KC, Stewart AJ, Kurz EU, Duncan AM and Deeley RG (1992) Overexpression of a transporter gene in a multidrug-resistant human lung cancer cell line. *Science* **258**:1650-1654.

Cole ST, Brosch R, Parkhill J, Garnier T, Churcher C, Harris D, Gordon SV, Eiglmeier K, Gas S, Barry CE, 3rd, Tekaia F, Badcock K, Basham D, Brown D, Chillingworth T, Connor R, Davies R, Devlin K, Feltwell T, Gentles S, Hamlin N, Holroyd S, Hornsby T, Jagels K, Krogh A, McLean J, Moule S, Murphy L, Oliver K, Osborne J, Quail MA, Rajandream MA, Rogers J, Rutter S, Seeger K, Skelton J, Squares R, Squares S, Sulston JE, Taylor K, Whitehead S and Barrell BG (1998) Deciphering the biology of Mycobacterium tuberculosis from the complete genome sequence. *Nature* **393**:537-544.

Collins L and Franzblau SG (1997) Microplate alamar blue assay versus BACTEC 460 system for high-throughput screening of compounds against Mycobacterium tuberculosis and Mycobacterium avium. *Antimicrob Agents Chemother* **41**:1004-1009.

Conte JE, Jr., Golden JA, Kipps J, Lin ET and Zurlinden E (2001) Effects of AIDS and gender on steady-state plasma and intrapulmonary ethambutol concentrations. *Antimicrob Agents Chemother* **45**:2891-2896.

Conte JE, Jr., Lin E and Zurlinden E (2000) High-performance liquid chromatographic determination of pyrazinamide in human plasma, bronchoalveolar lavage fluid, and alveolar cells. *J Chromatogr Sci* **38**:33-37.

Cooper AM, Magram J, Ferrante J and Orme IM (1997) Interleukin 12 (IL-12) is crucial to the development of protective immunity in mice intravenously infected with mycobacterium tuberculosis. *J Exp Med* **186**:39-45.

Courtois A, Payen L, Vernhet L, de Vries EG, Guillouzo A and Fardel O (1999) Inhibition of multidrug resistance-associated protein (MRP) activity by rifampicin in human multidrug-resistant lung tumor cells. *Cancer Lett* **139**:97-104.

Cui Y, Konig J, Leier I, Buchholz U and Keppler D (2001) Hepatic uptake of bilirubin and its conjugates by the human organic anion transporter SLC21A6. *J Biol Chem* **276**:9626-9630.

Cui Y, Konig J, Nies AT, Pfannschmidt M, Hergt M, Franke WW, Alt W, Moll R and Keppler D (2003) Detection of the human organic anion transporters SLC21A6 (OATP2) and SLC21A8 (OATP8) in liver and hepatocellular carcinoma. *Lab Invest* **83**:527-538.

Dallas S, Ronaldson PT, Bendayan M and Bendayan R (2004) Multidrug resistance protein 1-mediated transport of saquinavir by microglia. *Neuroreport* **15**:1183-1186.

Danelishvili L, McGarvey J, Li YJ and Bermudez LE (2003) Mycobacterium tuberculosis infection causes different levels of apoptosis and necrosis in human macrophages and alveolar epithelial cells. *Cell Microbiol* **5**:649-660.

David HL (1970) Probability distribution of drug-resistant mutants in unselected populations of Mycobacterium tuberculosis. *Appl Microbiol* **20**:810-814.

De Logu A, Uda P, Pellerano ML, Pusceddu MC, Saddi B and Schivo ML (2001) Comparison of two rapid colorimetric methods for determining resistance of mycobacterium tuberculosis to rifampin, isoniazid, and streptomycin in liquid medium. *Eur J Clin Microbiol Infect Dis* **20**:33-39.

De Rossi E, Ainsa JA and Riccardi G (2006) Role of mycobacterial efflux transporters in drug resistance: an unresolved question. *FEMS Microbiol Rev* **30**:36-52.

DeBarber AE, Mdluli K, Bosman M, Bekker LG and Barry CE, 3rd (2000) Ethionamide activation and sensitivity in multidrug-resistant Mycobacterium tuberculosis. *Proc Natl Acad Sci U S A* **97**:9677-9682.

Delahunty T, Lee B and Conte JE (1998) Sensitive liquid chromatographic technique to measure isoniazid in alveolar cells, bronchoalveolar lavage and plasma in HIV-infected patients. *J Chromatogr B Biomed Sci Appl* **705**:323-329.

Deng L, Mikusova K, Robuck KG, Scherman M, Brennan PJ and McNeil MR (1995) Recognition of multiple effects of ethambutol on metabolism of mycobacterial cell envelope. *Antimicrob Agents Chemother* **39**:694-701.

Denis M (1991) Interferon-gamma-treated murine macrophages inhibit growth of tubercle bacilli via the generation of reactive nitrogen intermediates. *Cell Immunol* **132**:150-157.

Dollery C ed (1998) *Therapeutic Drugs*. Churchill Livingstone, Edinburgh.

Dollery CT (1999) Drug discovery and development in the molecular era. *Br J Clin Pharmacol* **47**:5-6.

Drennan MB, Nicolle D, Quesniaux VJ, Jacobs M, Allie N, Mpagi J, Fremond C, Wagner H, Kirschning C and Ryffel B (2004) Toll-like receptor 2-deficient mice succumb to Mycobacterium tuberculosis infection. *Am J Pathol* **164**:49-57.

Duman N, Cevikbas A and Johansson C (2004) The effects of rifampicin and fluoroquinolones on tubercle bacilli within human macrophages. *Int J Antimicrob Agents* **23**:84-87.

Ehrt S, Shiloh MU, Ruan J, Choi M, Gunzburg S, Nathan C, Xie Q and Riley LW (1997) A novel antioxidant gene from Mycobacterium tuberculosis. *J Exp Med* **186**:1885-1896.

Endicott JA and Ling V (1989) The biochemistry of P-glycoprotein-mediated multidrug resistance. *Annu Rev Biochem* **58**:137-171.

Faber KN, Muller M and Jansen PL (2003) Drug transport proteins in the liver. *Adv Drug Deliv Rev* **55**:107-124.

Fardel O, Loyer P, Lecureur V, Glaise D and Guillouzo A (1994) Constitutive expression of functional P-glycoprotein in rat hepatoma cells. *Eur J Biochem* **219**:521-528.

Fattinger K, Cattori V, Hagenbuch B, Meier PJ and Stieger B (2000) Rifamycin SV and rifampicin exhibit differential inhibition of the hepatic rat organic anion transporting polypeptides, Oatp1 and Oatp2. *Hepatology* **32**:82-86.

Feng CG, Bean AG, Hooi H, Briscoe H and Britton WJ (1999) Increase in gamma interferon-secreting CD8(+), as well as CD4(+), T cells in lungs following aerosol infection with Mycobacterium tuberculosis. *Infect Immun* **67**:3242-3247.

Fenhalls G, Stevens-Muller L, Warren R, Carroll N, Bezuidenhout J, Van Helden P and Bardin P (2002) Localisation of mycobacterial DNA and mRNA in human tuberculous granulomas. *J Microbiol Methods* **51**:197-208.

Foongladda S, Roengsanthia D, Arjrattanakool W, Chuchottaworn C, Chaiprasert A and Franzblau SG (2002) Rapid and simple MTT method for rifampicin and isoniazid susceptibility testing of Mycobacterium tuberculosis. *Int J Tuberc Lung Dis* **6**:1118-1122.

Ford J, Boffito M, Wildfire A, Hill A, Back D, Khoo S, Nelson M, Moyle G, Gazzard B and Pozniak A (2004) Intracellular and plasma pharmacokinetics of saquinavir-ritonavir, administered at 1,600/100 milligrams once daily in human immunodeficiency virus-infected patients. *Antimicrob Agents Chemother* **48**:2388-2393.

Fox HH (1952) The chemical approach to the control of tuberculosis. *Science* **115**:129-134.

Fox HH, Gibas, J.T. (1953) Synthetic tuberculostats. VIII. acyl derivatives of isonicotinyl hydrazine. *J Org Chem* **18**:1375-1379.

Franzblau SG, Witzig RS, McLaughlin JC, Torres P, Madico G, Hernandez A, Degnan MT, Cook MB, Quenzer VK, Ferguson RM and Gilman RH (1998) Rapid, low-technology MIC determination with clinical Mycobacterium tuberculosis isolates by using the microplate Alamar Blue assay. *J Clin Microbiol* **36**:362-366.

Fratti RA, Backer JM, Gruenberg J, Corvera S and Deretic V (2001) Role of phosphatidylinositol 3-kinase and Rab5 effectors in phagosomal biogenesis and mycobacterial phagosome maturation arrest. *J Cell Biol* **154**:631-644.

Fratti RA, Chua J and Deretic V (2003a) Induction of p38 mitogen-activated protein kinase reduces early endosome autoantigen 1 (EEA1) recruitment to phagosomal membranes. *J Biol Chem* **278**:46961-46967.

Fratti RA, Chua J, Vergne I and Deretic V (2003b) Mycobacterium tuberculosis glycosylated phosphatidylinositol causes phagosome maturation arrest. *Proc Natl Acad Sci U S A* **100**:5437-5442.

Fremond CM, Nicolle DM, Torres DS and Quesniaux VF (2003) Control of Mycobacterium bovis BCG infection with increased inflammation in TLR4-deficient mice. *Microbes Infect* **5**:1070-1081.

Fremond CM, Yeremeev V, Nicolle DM, Jacobs M, Quesniaux VF and Ryffel B (2004) Fatal Mycobacterium tuberculosis infection despite adaptive immune response in the absence of MyD88. *J Clin Invest* **114**:1790-1799.

Fromm MF, Kauffmann HM, Fritz P, Burk O, Kroemer HK, Warzok RW, Eichelbaum M, Siegmund W and Schrenk D (2000) The effect of rifampin treatment on intestinal expression of human MRP transporters. *Am J Pathol* **157**:1575-1580.

Fulton SA, Cross JV, Toossi ZT and Boom WH (1998) Regulation of interleukin-12 by interleukin-10, transforming growth factor-beta, tumor necrosis factor-alpha, and interferon-gamma in human monocytes infected with Mycobacterium tuberculosis H37Ra. *J Infect Dis* **178**:1105-1114.

Gaitonde CD and Pathak PV (1990) Rapid liquid chromatographic method for the estimation of isoniazid and pyrazinamide in plasma and urine. *J Chromatogr* **532**:418-423.

Galeazzi R, Lorenzini I and Orlandi F (1980) Rifampicin-induced elevation of serum bile acids in man. *Dig Dis Sci* **25**:108-112.

Gao WY, Cara A, Gallo RC and Lori F (1993) Low levels of deoxynucleotides in peripheral blood lymphocytes: a strategy to inhibit human immunodeficiency virus type 1 replication. *Proc Natl Acad Sci U S A* **90**:8925-8928.

Gehring AJ, Rojas RE, Canaday DH, Lakey DL, Harding CV and Boom WH (2003) The Mycobacterium tuberculosis 19-kilodalton lipoprotein inhibits gamma interferon-regulated HLA-DR and Fc gamma R1 on human macrophages through Toll-like receptor 2. *Infect Immun* **71**:4487-4497.

Geick A, Eichelbaum M and Burk O (2001) Nuclear receptor response elements mediate induction of intestinal MDR1 by rifampin. *J Biol Chem* **276**:14581-14587.

Gennaro MC, Calvino R and Abrigo C (2001) Ion interaction reagent reversed-phase high-performance liquid chromatography determination of anti-tuberculosis drugs and metabolites in biological fluids. *J Chromatogr B Biomed Sci Appl* **754**:477-486.

Gerosa F, Nisii C, Righetti S, Micciolo R, Marchesini M, Cazzadori A and Trinchieri G (1999) CD4(+) T cell clones producing both interferon-gamma and interleukin-10 predominate in bronchoalveolar lavages of active pulmonary tuberculosis patients. *Clin Immunol* **92**:224-234.

Girling DJ (1977) Adverse reactions to rifampicin in antituberculosis regimens. *J Antimicrob Chemother* **3**:115-132.

Gomes MS, Florido M, Pais TF and Appelberg R (1999) Improved clearance of Mycobacterium avium upon disruption of the inducible nitric oxide synthase gene. *J Immunol* **162**:6734-6739.

Gong JH, Zhang M, Modlin RL, Linsley PS, Iyer D, Lin Y and Barnes PF (1996) Interleukin-10 downregulates Mycobacterium tuberculosis-induced Th1 responses and CTLA-4 expression. *Infect Immun* **64**:913-918.

Gottesman MM and Ambudkar SV (2001) Overview: ABC transporters and human disease. *J Bioenerg Biomembr* **33**:453-458.

Gottesman MM and Pastan I (1993) Biochemistry of multidrug resistance mediated by the multidrug transporter. *Annu Rev Biochem* **62**:385-427.

Greiner B, Eichelbaum M, Fritz P, Kreichgauer HP, von Richter O, Zundler J and Kroemer HK (1999) The role of intestinal P-glycoprotein in the interaction of digoxin and rifampin. *J Clin Invest* **104**:147-153.

Grumbach F and Rist N (1967) [Experimental antitubercular activity of rifampicin, a derivative of rifamycin SV]. *Rev Tuberc Pneumol (Paris)* **31**:749-762.

Guerin I and de Chastellier C (2000) Disruption of the actin filament network affects delivery of endocytic contents marker to phagosomes with early endosome characteristics: the case of phagosomes with pathogenic mycobacteria. *Eur J Cell Biol* **79**:735-749.

Hadjikoutis S, Morgan JE, Wild JM and Smith PE (2005) Ocular complications of neurological therapy. *Eur J Neurol* **12**:499-507.

Hediger MA, Romero MF, Peng JB, Rolfs A, Takanaga H and Bruford EA (2004) The ABCs of solute carriers: physiological, pathological and therapeutic implications of human membrane transport proteinsIntroduction. *Pflugers Arch* **447**:465-468.

Heifets L, Higgins M and Simon B (2000) Pyrazinamide is not active against Mycobacterium tuberculosis residing in cultured human monocyte-derived macrophages. *Int J Tuberc Lung Dis* **4**:491-495.

Heldwein KA and Fenton MJ (2002) The role of Toll-like receptors in immunity against mycobacterial infection. *Microbes Infect* **4**:937-944.

Hellberg C, Molony L, Zheng L and Andersson T (1996) Ca2+ signalling mechanisms of the beta 2 integrin on neutrophils: involvement of phospholipase C gamma 2 and Ins(1,4,5)P3. *Biochem J* **317 (Pt 2)**:403-409.

Henderson HJ, Dannenberg AM, Jr. and Lurie MB (1963) Phagocytosis of Tubercle Bacilli by Rabbit Pulmonary Alveolar Macrophages and Its Relation to Native Resistance to Tuberculosis. *J Immunol* **91**:553-556.

Herbert D, Paramasivan CN, Venkatesan P, Kubendiran G, Prabhakar R and Mitchison DA (1996) Bactericidal action of ofloxacin, sulbactam-ampicillin, rifampin, and isoniazid on logarithmic- and stationary-phase cultures of Mycobacterium tuberculosis. *Antimicrob Agents Chemother* **40**:2296-2299.

Hickman SP, Chan J and Salgame P (2002) Mycobacterium tuberculosis induces differential cytokine production from dendritic cells and macrophages with divergent effects on naive T cell polarization. *J Immunol* **168**:4636-4642.

Hirsch CS, Toossi Z, Othieno C, Johnson JL, Schwander SK, Robertson S, Wallis RS, Edmonds K, Okwera A, Mugerwa R, Peters P and Ellner JJ (1999) Depressed T-cell interferon-gamma responses in pulmonary tuberculosis: analysis of underlying mechanisms and modulation with therapy. *J Infect Dis* **180**:2069-2073.

Hoffmeyer S, Burk O, von Richter O, Arnold HP, Brockmoller J, Johne A, Cascorbi I, Gerloff T, Roots I, Eichelbaum M and Brinkmann U (2000) Functional polymorphisms of the human multidrug-resistance gene: multiple sequence variations and correlation of one allele with P-glycoprotein expression and activity in vivo. *Proc Natl Acad Sci U S A* **97**:3473-3478.

Honer Zu Bentrup K, Miczak A, Swenson DL and Russell DG (1999) Characterization of activity and expression of isocitrate lyase in Mycobacterium avium and Mycobacterium tuberculosis. *J Bacteriol* **181**:7161-7167.

Hooijberg JH, Broxterman HJ, Kool M, Assaraf YG, Peters GJ, Noordhuis P, Scheper RJ, Borst P, Pinedo HM and Jansen G (1999) Antifolate resistance mediated by the multidrug resistance proteins MRP1 and MRP2. *Cancer Res* **59**:2532-2535.

Hsiang B, Zhu Y, Wang Z, Wu Y, Sasseville V, Yang WP and Kirchgessner TG (1999) A novel human hepatic organic anion transporting polypeptide (OATP2). Identification of a liver-specific human organic anion transporting polypeptide and identification of rat and human hydroxymethylglutaryl-CoA reductase inhibitor transporters. *J Biol Chem* **274**:37161-37168.

Huang S, Hendriks W, Althage A, Hemmi S, Bluethmann H, Kamijo R, Vilcek J, Zinkernagel RM and Aguet M (1993) Immune response in mice that lack the interferon-gamma receptor. *Science* **259**:1742-1745.

Huisman MT, Smit JW, Crommentuyn KM, Zelcer N, Wiltshire HR, Beijnen JH and Schinkel AH (2002) Multidrug resistance protein 2 (MRP2) transports HIV protease inhibitors, and transport can be enhanced by other drugs. *Aids* **16**:2295-2301.

Huisman MT, Smit JW, Wiltshire HR, Hoetelmans RM, Beijnen JH and Schinkel AH (2001) P-glycoprotein limits oral availability, brain, and fetal penetration of saquinavir even with high doses of ritonavir. *Mol Pharmacol* **59**:806-813.

Hutchings A, Monie RD, Spragg B and Routledge PA (1983) High-performance liquid chromatographic analysis of isoniazid and acetylisoniazid in biological fluids. *J Chromatogr* **277**:385-390.

Itoh T and Takenawa T (2002) Phosphoinositide-binding domains: Functional units for temporal and spatial regulation of intracellular signalling. *Cell Signal* **14**:733-743.

Jacquemin E, Hagenbuch B, Stieger B, Wolkoff AW and Meier PJ (1994) Expression cloning of a rat liver Na(+)-independent organic anion transporter. *Proc Natl Acad Sci U S A* **91**:133-137.

Jang S, Uematsu S, Akira S and Salgame P (2004) IL-6 and IL-10 induction from dendritic cells in response to Mycobacterium tuberculosis is predominantly dependent on TLR2-mediated recognition. *J Immunol* **173**:3392-3397.

Janneh O, Owen A, Chandler B, Hartkoorn RC, Hart CA, Bray PG, Ward SA, Back DJ and Khoo SH (2005) Modulation of the intracellular accumulation of saquinavir in peripheral blood mononuclear cells by inhibitors of MRP1, MRP2, P-gp and BCRP. *Aids* **19**:2097-2102.

Jayaram R, Gaonkar S, Kaur P, Suresh BL, Mahesh BN, Jayashree R, Nandi V, Bharat S, Shandil RK, Kantharaj E and Balasubramanian V (2003) Pharmacokinetics-pharmacodynamics of rifampin in an aerosol infection model of tuberculosis. *Antimicrob Agents Chemother* **47**:2118-2124.

Jayaram R, Shandil RK, Gaonkar S, Kaur P, Suresh BL, Mahesh BN, Jayashree R, Nandi V, Bharath S, Kantharaj E and Balasubramanian V (2004) Isoniazid pharmacokinetics-pharmacodynamics in an aerosol infection model of tuberculosis. *Antimicrob Agents Chemother* **48**:2951-2957.

Jindani A, Aber VR, Edwards EA and Mitchison DA (1980) The early bactericidal activity of drugs in patients with pulmonary tuberculosis. *Am Rev Respir Dis* **121**:939-949.

Jindani A, Dore CJ and Mitchison DA (2003) Bactericidal and sterilizing activities of antituberculosis drugs during the first 14 days. *Am J Respir Crit Care Med* **167**:1348-1354.

Johnsson K and Schultz PG (1994) Mechanistic studies of the oxidation of isoniazid by catalase peroxidase from Mycobacterium tuberculosis. *J. Am. Chem. Soc.* **116**:7425-7426.

Johnstone RW, Ruefli AA and Smyth MJ (2000) Multiple physiological functions for multidrug transporter P-glycoprotein? *Trends Biochem Sci* **25**:1-6.

Jones BW, Means TK, Heldwein KA, Keen MA, Hill PJ, Belisle JT and Fenton MJ (2001a) Different Toll-like receptor agonists induce distinct macrophage responses. *J Leukoc Biol* **69**:1036-1044.

Jones K, Bray PG, Khoo SH, Davey RA, Meaden ER, Ward SA and Back DJ (2001b) P-Glycoprotein and transporter MRP1 reduce HIV protease inhibitor uptake in CD4 cells: potential for accelerated viral drug resistance? *Aids* **15**:1353-1358.

Jones K, Hoggard PG, Sales SD, Khoo S, Davey R and Back DJ (2001c) Differences in the intracellular accumulation of HIV protease inhibitors in vitro and the effect of active transport. *Aids* **15**:675-681.

Jouanguy E, Lamhamedi-Cherradi S, Altare F, Fondaneche MC, Tuerlinckx D, Blanche S, Emile JF, Gaillard JL, Schreiber R, Levin M, Fischer A, Hivroz C and Casanova JL (1997) Partial interferon-gamma receptor 1 deficiency in a child with tuberculoid bacillus Calmette-Guerin infection and a sibling with clinical tuberculosis. *J Clin Invest* **100**:2658-2664.

Juliano RL and Ling V (1976) A surface glycoprotein modulating drug permeability in Chinese hamster ovary cell mutants. *Biochim Biophys Acta* **455**:152-162.

Kauffmann HM, Pfannschmidt S, Zoller H, Benz A, Vorderstemann B, Webster JI and Schrenk D (2002) Influence of redox-active compounds and PXR-activators on human MRP1 and MRP2 gene expression. *Toxicology* **171**:137-146.

Kelley VA and Schorey JS (2003) Mycobacterium's arrest of phagosome maturation in macrophages requires Rab5 activity and accessibility to iron. *Mol Biol Cell* **14**:3366-3377.

Kelley VA and Schorey JS (2004) Modulation of cellular phosphatidylinositol 3-phosphate levels in primary macrophages affects heat-killed but not viable Mycobacterium avium's transport through the phagosome maturation process. *Cell Microbiol* **6**:973-985.

Kerb R, Hoffmeyer S and Brinkmann U (2001) ABC drug transporters: hereditary polymorphisms and pharmacological impact in MDR1, MRP1 and MRP2. *Pharmacogenomics* **2**:51-64.

Khuhawar MY and Rind FM (2002) Liquid chromatographic determination of isoniazid, pyrazinamide and rifampicin from pharmaceutical preparations and blood. *J Chromatogr B Analyt Technol Biomed Life Sci* **766**:357-363.

Kim RB (2003) Organic anion-transporting polypeptide (OATP) transporter family and drug disposition. *Eur J Clin Invest* **33 Suppl 2**:1-5.

Kim RB, Fromm MF, Wandel C, Leake B, Wood AJ, Roden DM and Wilkinson GR (1998) The drug transporter P-glycoprotein limits oral absorption and brain entry of HIV-1 protease inhibitors. *J Clin Invest* **101**:289-294.

Knutson KL, Hmama Z, Herrera-Velit P, Rochford R and Reiner NE (1998) Lipoarabinomannan of Mycobacterium tuberculosis promotes protein tyrosine dephosphorylation and inhibition of mitogen-activated protein kinase in human mononuclear phagocytes. Role of the Src homology 2 containing tyrosine phosphatase 1. *J Biol Chem* **273**:645-652.

Konig J, Cui Y, Nies AT and Keppler D (2000) A novel human organic anion transporting polypeptide localized to the basolateral hepatocyte membrane. *Am J Physiol Gastrointest Liver Physiol* **278**:G156-164.

Korfmacher WA, Bloom J, Churchwell MI, Getek TA, Hansen EB, Jr., Holder CL and McManus KT (1993) Characterization of three rifamycins via electrospray mass spectrometry and HPLC-thermospray mass spectrometry. *J Chromatogr Sci* **31**:498-501.

Kraemer HJ, Feltkamp U and Breithaupt H (1998) Quantification of pyrazinamide and its metabolites in plasma by ionic-pair high-performance liquid chromatography. Implications for the separation mechanism. *J Chromatogr B Biomed Sci Appl* **706**:319-328.

Krutzik SR and Modlin RL (2004) The role of Toll-like receptors in combating mycobacteria. *Semin Immunol* **16**:35-41.

Kullak-Ublick GA, Hagenbuch B, Stieger B, Schteingart CD, Hofmann AF, Wolkoff AW and Meier PJ (1995) Molecular and functional characterization of an organic anion transporting polypeptide cloned from human liver. *Gastroenterology* **109**:1274-1282.

Kullak-Ublick GA, Ismair MG, Stieger B, Landmann L, Huber R, Pizzagalli F, Fattinger K, Meier PJ and Hagenbuch B (2001) Organic anion-transporting polypeptide B (OATP-B) and its functional comparison with three other OATPs of human liver. *Gastroenterology* **120**:525-533.

Kusner DJ (2005) Mechanisms of mycobacterial persistence in tuberculosis. *Clin Immunol* **114**:239-247.

Lambert PA (2002) Cellular impermeability and uptake of biocides and antibiotics in Gram-positive bacteria and mycobacteria. *J Appl Microbiol* **92 Suppl**:46S-54S.

Laudano OM (1972) [Effects of rifampicin on the blood clearance and biliary excretion of sulfobromophthalein in man]. *Farmaco [Prat]* **27**:622-627.

Lauterberg BH SC, Mitchell JR (1981) Determination of isoniazid and its hydrazine metabolites, acetylisoniazid, acetylhydrazine, and diacetylhydrazine in human plasma by gas chromatography-mass spectrometry. *J Chromatogr* **224**:431-438.

Lee CG, Gottesman MM, Cardarelli CO, Ramachandra M, Jeang KT, Ambudkar SV, Pastan I and Dey S (1998) HIV-1 protease inhibitors are substrates for the MDR1 multidrug transporter. *Biochemistry* **37**:3594-3601.

Lee CS, Gambertoglio JG, Brater DC and Benet LZ (1977) Kinetics of oral ethambutol in the normal subject. *Clin Pharmacol Ther* **22**:615-621.

Lee H, Cho SN, Bang HE, Lee JH, Bai GH, Kim SJ and Kim JD (2000) Exclusive mutations related to isoniazid and ethionamide resistance among Mycobacterium tuberculosis isolates from Korea. *Int J Tuberc Lung Dis* **4**:441-447.

Leibold JE (1966) The ocular toxicity of ethambutol and its relation to dose. *Ann N Y Acad Sci* **135**:904-909.

Levin ME and Hatfull GF (1993) Mycobacterium smegmatis RNA polymerase: DNA supercoiling, action of rifampicin and mechanism of rifampicin resistance. *Mol Microbiol* **8**:277-285.

Lopez M, Sly LM, Luu Y, Young D, Cooper H and Reiner NE (2003) The 19-kDa Mycobacterium tuberculosis protein induces macrophage apoptosis through Toll-like receptor-2. *J Immunol* **170**:2409-2416.

Lu B, Rutledge BJ, Gu L, Fiorillo J, Lukacs NW, Kunkel SL, North R, Gerard C and Rollins BJ (1998) Abnormalities in monocyte recruitment and cytokine expression in monocyte chemoattractant protein 1-deficient mice. *J Exp Med* **187**:601-608.

Lucia MB, Rutella S, Rumi C, Ventura G, Caldarola G and Cauda R (1997) Detection of P-glycoprotein efflux activity on peripheral blood lymphocyte subsets from HIV+ patients. *Eur J Histochem* **41 Suppl 2**:195-196.

Luna-Herrera J, Martinez-Cabrera G, Parra-Maldonado R, Enciso-Moreno JA, Torres-Lopez J, Quesada-Pascual F, Delgadillo-Polanco R and Franzblau SG (2003) Use of receiver operating characteristic curves to assess the performance of a microdilution assay for determination of drug susceptibility of clinical isolates of Mycobacterium tuberculosis. *Eur J Clin Microbiol Infect Dis* **22**:21-27.

Lurie MB, Zappasodi P and Tickner C (1955) On the nature of genetic resistance to tuberculosis in the light of the host-parasite relationships in natively resistant and susceptible rabbits. *Am Rev Tuberc* **72**:297-329.

MacMicking JD, North RJ, LaCourse R, Mudgett JS, Shah SK and Nathan CF (1997) Identification of nitric oxide synthase as a protective locus against tuberculosis. *Proc Natl Acad Sci U S A* **94**:5243-5248.

Magnarin M, Morelli M, Rosati A, Bartoli F, Candussio L, Giraldi T and Decorti G (2004) Induction of proteins involved in multidrug resistance (P-glycoprotein, MRP1, MRP2, LRP) and of CYP 3A4 by rifampicin in LLC-PK1 cells. *Eur J Pharmacol* **483**:19-28.

Malik ZA, Denning GM and Kusner DJ (2000) Inhibition of Ca(2+) signaling by Mycobacterium tuberculosis is associated with reduced phagosome-lysosome fusion and increased survival within human macrophages. *J Exp Med* **191**:287-302.

Malik ZA, Iyer SS and Kusner DJ (2001) Mycobacterium tuberculosis phagosomes exhibit altered calmodulin-dependent signal transduction: contribution to inhibition of phagosome-lysosome fusion and intracellular survival in human macrophages. *J Immunol* **166**:3392-3401.

Malik ZA, Thompson CR, Hashimi S, Porter B, Iyer SS and Kusner DJ (2003) Cutting edge: Mycobacterium tuberculosis blocks Ca2+ signaling and phagosome maturation in human macrophages via specific inhibition of sphingosine kinase. *J Immunol* **170**:2811-2815.

Markowitz N, Hansen NI, Hopewell PC, Glassroth J, Kvale PA, Mangura BT, Wilcosky TC, Wallace JM, Rosen MJ and Reichman LB (1997) Incidence of tuberculosis in the United States among HIV-infected persons. The Pulmonary Complications of HIV Infection Study Group. *Ann Intern Med* **126**:123-132.

Martinez E, Collazos J and Mayo J (1999) Hypersensitivity reactions to rifampin. Pathogenetic mechanisms, clinical manifestations, management strategies, and review of the anaphylactic-like reactions. *Medicine (Baltimore)* **78**:361-369.

McDermott W and Tompsett R (1954) Activation of pyrazinamide and nicotinamide in acidic environments in vitro. *Am Rev Tuberc* **70**:748-754.

McFarland J (1907) An instrument for estimating the number of bacteria in suspentsions used for calculating the opsonic index and for vaccines. *Jama* **49**:1176-1178.

McKinney JD and Gomez JE (2003) Life on the inside for Mycobacterium tuberculosis. *Nat Med* **9**:1356-1357.

McKinney JD, Honer zu Bentrup K, Munoz-Elias EJ, Miczak A, Chen B, Chan WT, Swenson D, Sacchettini JC, Jacobs WR, Jr. and Russell DG (2000) Persistence of Mycobacterium tuberculosis in macrophages and mice requires the glyoxylate shunt enzyme isocitrate lyase. *Nature* **406**:735-738.

Means TK, Wang S, Lien E, Yoshimura A, Golenbock DT and Fenton MJ (1999) Human toll-like receptors mediate cellular activation by Mycobacterium tuberculosis. *J Immunol* **163**:3920-3927.

Mehmedagic A, Verite P, Menager S, Tharasse C, Chabenat C, Andre D and Lafont O (1997) Determination of pyrazinamide and its main metabolites in rat urine by high-performance liquid chromatography. *J Chromatogr B Biomed Sci Appl* **695**:365-372.

Mehta PK, King CH, White EH, Murtagh JJ, Jr. and Quinn FD (1996) Comparison of in vitro models for the study of Mycobacterium tuberculosis invasion and intracellular replication. *Infect Immun* **64**:2673-2679.

Michot JM, Seral C, Van Bambeke F, Mingeot-Leclercq MP and Tulkens PM (2005) Influence of efflux transporters on the accumulation and efflux of four quinolones (ciprofloxacin, levofloxacin, garenoxacin, and moxifloxacin) in J774 macrophages. *Antimicrob Agents Chemother* **49**:2429-2437.

Michot JM, Van Bambeke F, Mingeot-Leclercq MP and Tulkens PM (2004) Active efflux of ciprofloxacin from J774 macrophages through an MRP-like transporter. *Antimicrob Agents Chemother* **48**:2673-2682.

Mikusova K, Slayden RA, Besra GS and Brennan PJ (1995) Biogenesis of the mycobacterial cell wall and the site of action of ethambutol. *Antimicrob Agents Chemother* **39**:2484-2489.

Miller BH, Fratti RA, Poschet JF, Timmins GS, Master SS, Burgos M, Marletta MA and Deretic V (2004) Mycobacteria inhibit nitric oxide synthase recruitment to phagosomes during macrophage infection. *Infect Immun* **72**:2872-2878.

Minderman H, Suvannasankha A, O'Loughlin KL, Scheffer GL, Scheper RJ, Robey RW and Baer MR (2002) Flow cytometric analysis of breast cancer resistance protein expression and function. *Cytometry* **48**:59-65.

Mistry P, Stewart AJ, Dangerfield W, Okiji S, Liddle C, Bootle D, Plumb JA, Templeton D and Charlton P (2001) In vitro and in vivo reversal of P-

glycoprotein-mediated multidrug resistance by a novel potent modulator, XR9576. *Cancer Res* **61**:749-758.

Mitchell JR, Long MW, Thorgeirsson UP and Jollow DJ (1975) Acetylation rates and monthly liver function tests during one year of isoniazid preventive therapy. *Chest* **68**:181-190.

Mitchell JR, Zimmerman HJ, Ishak KG, Thorgeirsson UP, Timbrell JA, Snodgrass WR and Nelson SD (1976) Isoniazid liver injury: clinical spectrum, pathology, and probable pathogenesis. *Ann Intern Med* **84**:181-192.

Mitchison DA (2000) Role of individual drugs in the chemotherapy of tuberculosis. *Int J Tuberc Lung Dis* **4**:796-806.

Mitchison DA and Nunn AJ (1986) Influence of initial drug resistance on the response to short-course chemotherapy of pulmonary tuberculosis. *Am Rev Respir Dis* **133**:423-430.

Mohan B, Sharda N and Singh S (2003) Evaluation of the recently reported USP gradient HPLC method for analysis of anti-tuberculosis drugs for its ability to resolve degradation products of rifampicin. *J Pharm Biomed Anal* **31**:607-612.

Moore AV, Kirk SM, Callister SM, Mazurek GH and Schell RF (1999) Safe determination of susceptibility of Mycobacterium tuberculosis to antimycobacterial agents by flow cytometry. *J Clin Microbiol* **37**:479-483.

Mor N, Simon B, Mezo N and Heifets L (1995) Comparison of activities of rifapentine and rifampin against Mycobacterium tuberculosis residing in human macrophages. *Antimicrob Agents Chemother* **39**:2073-2077.

Mor N, Vanderkolk J and Heifets L (1994) Inhibitory and bactericidal activities of levofloxacin against Mycobacterium tuberculosis in vitro and in human macrophages. *Antimicrob Agents Chemother* **38**:1161-1164.

Morlock GP, Metchock B, Sikes D, Crawford JT and Cooksey RC (2003) ethA, inhA, and katG loci of ethionamide-resistant clinical Mycobacterium tuberculosis isolates. *Antimicrob Agents Chemother* **47**:3799-3805.

Mosmann T (1983) Rapid colorimetric assay for cellular growth and survival: application to proliferation and cytotoxicity assays. *J Immunol Methods* **65**:55-63.

Moussa LA, Khassouani CE, Soulaymani R, Jana M, Cassanas G, Alric R and Hue B (2002) Therapeutic isoniazid monitoring using a simple high-performance liquid chromatographic method with ultraviolet detection. *J Chromatogr B Analyt Technol Biomed Life Sci* **766**:181-187.

Mshana RN, Tadesse G, Abate G and Miorner H (1998) Use of 3-(4,5-dimethylthiazol-2-yl)-2,5-diphenyl tetrazolium bromide for rapid detection of rifampin-resistant Mycobacterium tuberculosis. *J Clin Microbiol* **36**:1214-1219.

Muller I, Cobbold SP, Waldmann H and Kaufmann SH (1987) Impaired resistance to Mycobacterium tuberculosis infection after selective in vivo depletion of L3T4+ and Lyt-2+ T cells. *Infect Immun* **55**:2037-2041.

Muller M, Meijer C, Zaman GJ, Borst P, Scheper RJ, Mulder NH, de Vries EG and Jansen PL (1994) Overexpression of the gene encoding the multidrug resistance-associated protein results in increased ATP-dependent glutathione S-conjugate transport. *Proc Natl Acad Sci U S A* **91**:13033-13037.

Mwandumba HC, Russell DG, Nyirenda MH, Anderson J, White SA, Molyneux ME and Squire SB (2004) Mycobacterium tuberculosis resides in nonacidified vacuoles in endocytically competent alveolar macrophages from patients with tuberculosis and HIV infection. *J Immunol* **172**:4592-4598.

Nguyen M, Claparols C, Bernadou J and Meunier B (2001) A fast and efficient metal-mediated oxidation of isoniazid and identification of isoniazid-NAD(H) adducts. *Chembiochem* **2**:877-883.

Nitti V, Catena E, Bariffi F and Delli Veneri F (1967) [Therapeutic activity of the Rifampicin in pulmonary tuberculosis]. *Arch Tisiol Mal Appar Respir* **22**:417-462.

North RJ and Jung YJ (2004) Immunity to tuberculosis. *Annu Rev Immunol* **22**:599-623.

Noss EH, Harding CV and Boom WH (2000) Mycobacterium tuberculosis inhibits MHC class II antigen processing in murine bone marrow macrophages. *Cell Immunol* **201**:63-74.

Noss EH, Pai RK, Sellati TJ, Radolf JD, Belisle J, Golenbock DT, Boom WH and Harding CV (2001) Toll-like receptor 2-dependent inhibition of macrophage class II MHC expression and antigen processing by 19-kDa lipoprotein of Mycobacterium tuberculosis. *J Immunol* **167**:910-918.

O'Brien ML, Vulevic B, Freer S, Boyd J, Shen H and Tew KD (1999) Glutathione peptidomimetic drug modulator of multidrug resistance-associated protein. *J Pharmacol Exp Ther* **291**:1348-1355.

Oddo M, Renno T, Attinger A, Bakker T, MacDonald HR and Meylan PR (1998) Fas ligand-induced apoptosis of infected human macrophages reduces the viability of intracellular Mycobacterium tuberculosis. *J Immunol* **160**:5448-5454.

Owen A, Chandler B and Back DJ (2005a) The implications of P-glycoprotein in HIV: friend or foe? *Fundam Clin Pharmacol* **19**:283-296.

Owen A, Chandler B, Bray PG, Ward SA, Hart CA, Back DJ and Khoo SH (2004) Functional correlation of P-glycoprotein expression and genotype with expression of the human immunodeficiency virus type 1 coreceptor CXCR4. *J Virol* **78**:12022-12029.

Owen A, Hartkoorn RC, Khoo S and Back D (2003) Expression of P-glycoprotein, multidrug-resistance proteins 1 and 2 in CEM, CEM(VBL), CEM(E1000), MDCKII(MRP1) and MDCKII(MRP2) cell lines. *Aids* **17**:2276-2278.

Owen A, Janneh O, Hartkoorn RC, Chandler B, Bray PG, Martin P, Ward SA, Hart CA, Khoo SH and Back DJ (2005b) In vitro synergy and enhanced murine brain penetration of saquinavir coadministered with mefloquine. *J Pharmacol Exp Ther* **314**:1202-1209.

Pallanza R, Arioli V, Furesz S and Bolzoni G (1967) Rifampicin: a new rifamycin. II. Laboratory studies on the antituberculous activity and preliminary clinical observations. *Arzneimittelforschung* **17**:529-534.

Panchagnula R, Sood A, Sharda N, Kaur K and Kaul CL (1999) Determination of rifampicin and its main metabolite in plasma and urine in presence of pyrazinamide and isoniazid by HPLC method. *J Pharm Biomed Anal* **18**:1013-1020.

Pauwels R, De Clercq E, Desmyter J, Balzarini J, Goubau P, Herdewijn P, Vanderhaeghe H and Vandeputte M (1987) Sensitive and rapid assay on MT-4 cells for detection of antiviral compounds against the AIDS virus. *J Virol Methods* **16**:171-185.

Peloquin CA (2002) Therapeutic drug monitoring in the treatment of tuberculosis. *Drugs* **62**:2169-2183.

Peloquin CA, Jaresko GS, Yong CL, Keung AC, Bulpitt AE and Jelliffe RW (1997) Population pharmacokinetic modeling of isoniazid, rifampin, and pyrazinamide. *Antimicrob Agents Chemother* **41**:2670-2679.

Pettit EJ and Hallett MB (1996) Localised and global cytosolic Ca2+ changes in neutrophils during engagement of Cd11b/CD18 integrin visualised using confocal laser scanning reconstruction. *J Cell Sci* **109 (Pt 7)**:1689-1694.

Piddock LJ, Williams KJ and Ricci V (2000) Accumulation of rifampicin by Mycobacterium aurum, Mycobacterium smegmatis and Mycobacterium tuberculosis. *J Antimicrob Chemother* **45**:159-165.

Quesniaux V, Fremond C, Jacobs M, Parida S, Nicolle D, Yeremeev V, Bihl F, Erard F, Botha T, Drennan M, Soler MN, Le Bert M, Schnyder B and Ryffel B (2004a) Toll-like receptor pathways in the immune responses to mycobacteria. *Microbes Infect* **6**:946-959.

Quesniaux VJ, Nicolle DM, Torres D, Kremer L, Guerardel Y, Nigou J, Puzo G, Erard F and Ryffel B (2004b) Toll-like receptor 2 (TLR2)-dependent-positive and TLR2-independent-negative regulation of proinflammatory cytokines by mycobacterial lipomannans. *J Immunol* **172**:4425-4434.

Raja A (2004) Immunology of tuberculosis. *Indian J Med Res* **120**:213-232.

Ramaswamy S and Musser JM (1998) Molecular genetic basis of antimicrobial agent resistance in Mycobacterium tuberculosis: 1998 update. *Tuber Lung Dis* **79**:3-29.

Raviglione MC (2003) The TB epidemic from 1992 to 2002. *Tuberculosis (Edinb)* **83**:4-14.

Raynaud C, Laneelle MA, Senaratne RH, Draper P, Laneelle G and Daffe M (1999) Mechanisms of pyrazinamide resistance in mycobacteria: importance of lack of uptake in addition to lack of pyrazinamidase activity. *Microbiology* **145 (Pt 6)**:1359-1367.

Reed MB, Domenech P, Manca C, Su H, Barczak AK, Kreiswirth BN, Kaplan G and Barry CE, 3rd (2004) A glycolipid of hypervirulent tuberculosis strains that inhibits the innate immune response. *Nature* **431**:84-87.

Reis RS, Neves I, Jr., Lourenco SL, Fonseca LS and Lourenco MC (2004) Comparison of flow cytometric and Alamar Blue tests with the proportional method for testing susceptibility of Mycobacterium tuberculosis to rifampin and isoniazid. *J Clin Microbiol* **42**:2247-2248.

Revankar SN, Desai ND, Vaidya AB, Bhatt AD and Anjaneyulu B (1994) Determination of pyrazinamide in human by high performance liquid chromatography. *J Postgrad Med* **40**:7-9.

Roach TI, Barton CH, Chatterjee D and Blackwell JM (1993) Macrophage activation: lipoarabinomannan from avirulent and virulent strains of Mycobacterium tuberculosis differentially induces the early genes c-fos, KC, JE, and tumor necrosis factor-alpha. *J Immunol* **150**:1886-1896.

Rojas M, Garcia LF, Nigou J, Puzo G and Olivier M (2000) Mannosylated lipoarabinomannan antagonizes Mycobacterium tuberculosis-induced macrophage apoptosis by altering Ca+2-dependent cell signaling. *J Infect Dis* **182**:240-251.

Rozwarski DA, Grant GA, Barton DH, Jacobs WR, Jr. and Sacchettini JC (1998) Modification of the NADH of the isoniazid target (InhA) from Mycobacterium tuberculosis. *Science* **279**:98-102.

Russell DG (2001) Mycobacterium tuberculosis: here today, and here tomorrow. *Nat Rev Mol Cell Biol* **2**:569-577.

Russell DG, Dant J and Sturgill-Koszycki S (1996) Mycobacterium avium- and Mycobacterium tuberculosis-containing vacuoles are dynamic, fusion-competent vesicles that are accessible to glycosphingolipids from the host cell plasmalemma. *J Immunol* **156**:4764-4773.

Salgame P (2005) Host innate and Th1 responses and the bacterial factors that control Mycobacterium tuberculosis infection. *Curr Opin Immunol* **17**:374-380.

Sarich TC, Adams SP, Petricca G and Wright JM (1999) Inhibition of isoniazid-induced hepatotoxicity in rabbits by pretreatment with an amidase inhibitor. *J Pharmacol Exp Ther* **289**:695-702.

Sarich TC, Youssefi M, Zhou T, Adams SP, Wall RA and Wright JM (1996) Role of hydrazine in the mechanism of isoniazid hepatotoxicity in rabbits. *Arch Toxicol* **70**:835-840.

Sato K, Tomioka H, Sano C, Shimizu T, Sano K, Ogasawara K, Cai S and Kamei T (2003) Comparative antimicrobial activities of gatifloxacin, sitafloxacin and levofloxacin against Mycobacterium tuberculosis replicating within Mono Mac 6 human macrophage and A-549 type II alveolar cell lines. *J Antimicrob Chemother* **52**:199-203.

Schaeffeler E, Eichelbaum M, Brinkmann U, Penger A, Asante-Poku S, Zanger UM and Schwab M (2001) Frequency of C3435T polymorphism of MDR1 gene in African people. *Lancet* **358**:383-384.

Schaible UE, Collins HL, Priem F and Kaufmann SH (2002) Correction of the iron overload defect in beta-2-microglobulin knockout mice by lactoferrin abolishes their increased susceptibility to tuberculosis. *J Exp Med* **196**:1507-1513.

Schell RF, Ealey WF, Harding GE and Smith DW (1974) The influence of vaccination on the course of experimental airborne tuberculosis in mice. *J Reticuloendothel Soc* **16**:131-138.

Schiffer R, Neis M, Holler D, Rodriguez F, Geier A, Gartung C, Lammert F, Dreuw A, Zwadlo-Klarwasser G, Merk H, Jugert F and Baron JM (2003) Active influx transport is mediated by members of the organic anion transporting polypeptide family in human epidermal keratinocytes. *J Invest Dermatol* **120**:285-291.

Schlesinger LS, Bellinger-Kawahara CG, Payne NR and Horwitz MA (1990) Phagocytosis of Mycobacterium tuberculosis is mediated by human monocyte complement receptors and complement component C3. *J Immunol* **144**:2771-2780.

Schnappinger D, Ehrt S, Voskuil MI, Liu Y, Mangan JA, Monahan IM, Dolganov G, Efron B, Butcher PD, Nathan C and Schoolnik GK (2003) Transcriptional Adaptation of Mycobacterium tuberculosis within Macrophages: Insights into the Phagosomal Environment. *J Exp Med* **198**:693-704.

Schnare M, Barton GM, Holt AC, Takeda K, Akira S and Medzhitov R (2001) Toll-like receptors control activation of adaptive immune responses. *Nat Immunol* **2**:947-950.

Schrenk D, Baus PR, Ermel N, Klein C, Vorderstemann B and Kauffmann HM (2001) Up-regulation of transporters of the MRP family by drugs and toxins. *Toxicol Lett* **120**:51-57.

Schuetz EG, Schinkel AH, Relling MV and Schuetz JD (1996) P-glycoprotein: a major determinant of rifampicin-inducible expression of cytochrome P4503A in mice and humans. *Proc Natl Acad Sci U S A* **93**:4001-4005.

Schuetz EG, Umbenhauer DR, Yasuda K, Brimer C, Nguyen L, Relling MV, Schuetz JD and Schinkel AH (2000) Altered expression of hepatic cytochromes P-450 in mice deficient in one or more mdr1 genes. *Mol Pharmacol* **57**:188-197.

Schwebach JR, Jacobs WR, Jr. and Casadevall A (2001) Sterilization of Mycobacterium tuberculosis Erdman samples by antimicrobial fixation in a biosafety level 3 laboratory. *J Clin Microbiol* **39**:769-771.

Scior T, Meneses Morales I, Garces Eisele SJ, Domeyer D and Laufer S (2002) Antitubercular isoniazid and drug resistance of Mycobacterium tuberculosis--a review. *Arch Pharm (Weinheim)* **335**:511-525.

Seifart HI, Gent WL, Parkin DP, van Jaarsveld PP and Donald PR (1995) High-performance liquid chromatographic determination of isoniazid, acetylisoniazid and hydrazine in biological fluids. *J Chromatogr B Biomed Appl* **674**:269-275.

Seifart HI, Kruger PB, Parkin DP, van Jaarsveld PP and Donald PR (1993) Therapeutic monitoring of antituberculosis drugs by direct in-line extraction on a high-performance liquid chromatography system. *J Chromatogr* **619**:285-290.

Selwyn PA, Hartel D, Lewis VA, Schoenbaum EE, Vermund SH, Klein RS, Walker AT and Friedland GH (1989) A prospective study of the risk of tuberculosis among intravenous drug users with human immunodeficiency virus infection. *N Engl J Med* **320**:545-550.

Seral C, Barcia-Macay M, Mingeot-Leclercq MP, Tulkens PM and Van Bambeke F (2005) Comparative activity of quinolones (ciprofloxacin, levofloxacin, moxifloxacin and garenoxacin) against extracellular and intracellular infection by Listeria monocytogenes and Staphylococcus aureus in J774 macrophages. *J Antimicrob Chemother* **55**:511-517.

Seral C, Carryn S, Tulkens PM and Van Bambeke F (2003a) Influence of P-glycoprotein and MRP efflux pump inhibitors on the intracellular activity of azithromycin and ciprofloxacin in macrophages infected by Listeria monocytogenes or Staphylococcus aureus. *J Antimicrob Chemother* **51**:1167-1173.

Seral C, Michot JM, Chanteux H, Mingeot-Leclercq MP, Tulkens PM and Van Bambeke F (2003b) Influence of P-glycoprotein inhibitors on accumulation of macrolides in J774 murine macrophages. *Antimicrob Agents Chemother* **47**:1047-1051.

Seral C, Van Bambeke F and Tulkens PM (2003c) Quantitative analysis of gentamicin, azithromycin, telithromycin, ciprofloxacin, moxifloxacin, and oritavancin (LY333328) activities against intracellular Staphylococcus aureus in mouse J774 macrophages. *Antimicrob Agents Chemother* **47**:2283-2292.

Shoeb HA, Bowman BU, Jr., Ottolenghi AC and Merola AJ (1985) Peroxidase-mediated oxidation of isoniazid. *Antimicrob Agents Chemother* **27**:399-403.

Siddiqi N, Das R, Pathak N, Banerjee S, Ahmed N, Katoch VM and Hasnain SE (2004) Mycobacterium tuberculosis isolate with a distinct genomic identity overexpresses a tap-like efflux pump. *Infection* **32**:109-111.

Simonsen A, Gaullier JM, D'Arrigo A and Stenmark H (1999) The Rab5 effector EEA1 interacts directly with syntaxin-6. *J Biol Chem* **274**:28857-28860.

Simonsen A, Lippe R, Christoforidis S, Gaullier JM, Brech A, Callaghan J, Toh BH, Murphy C, Zerial M and Stenmark H (1998) EEA1 links PI(3)K function to Rab5 regulation of endosome fusion. *Nature* **394**:494-498.

Slayden RA and Barry CE, 3rd (2000) The genetics and biochemistry of isoniazid resistance in mycobacterium tuberculosis. *Microbes Infect* **2**:659-669.

Slayden RA, Lee RE and Barry CE, 3rd (2000) Isoniazid affects multiple components of the type II fatty acid synthase system of Mycobacterium tuberculosis. *Mol Microbiol* **38**:514-525.

Smith PJ, van Dyk J and Fredericks A (1999) Determination of rifampicin, isoniazid and pyrazinamide by high performance liquid chromatography after their simultaneous extraction from plasma. *Int J Tuberc Lung Dis* **3**:S325-328; discussion S351-322.

Smith PK, Krohn RI, Hermanson GT, Mallia AK, Gartner FH, Provenzano MD, Fujimoto EK, Goeke NM, Olson BJ and Klenk DC (1985) Measurement of protein using bicinchoninic acid. *Anal Biochem* **150**:76-85.

Solotorovsky M, Gregory FJ, Ironson EJ, Bugie EJ, O'Neill RC and Pfister R, 3rd (1952) Pyrazinoic acid amide; an agent active against experimental murine tuberculosis. *Proc Soc Exp Biol Med* **79**:563-565.

Somoskövi A, Parsons LM and Salfinger M (2001) The molecular basis of resistance to isoniazid, rifampin, and pyrazinamide in Mycobacterium tuberculosis. *Respir Res* **2**:164-168.

Spears KJ, Ross J, Stenhouse A, Ward CJ, Goh LB, Wolf CR, Morgan P, Ayrton A and Friedberg TH (2005) Directional trans-epithelial transport of organic anions in porcine LLC-PK1 cells that co-express human OATP1B1 (OATP-C) and MRP2. *Biochem Pharmacol* **69**:415-423.

Spiegel S and Milstien S (2002) Sphingosine 1-phosphate, a key cell signaling molecule. *J Biol Chem* **277**:25851-25854.

Sreevatsan S, Stockbauer KE, Pan X, Kreiswirth BN, Moghazeh SL, Jacobs WR, Jr., Telenti A and Musser JM (1997) Ethambutol resistance in Mycobacterium tuberculosis: critical role of embB mutations. *Antimicrob Agents Chemother* **41**:1677-1681.

Srinivas RV, Middlemas D, Flynn P and Fridland A (1998) Human immunodeficiency virus protease inhibitors serve as substrates for multidrug transporter proteins MDR1 and MRP1 but retain antiviral efficacy in cell lines expressing these transporters. *Antimicrob Agents Chemother* **42**:3157-3162.

Stokes RW and Doxsee D (1999) The receptor-mediated uptake, survival, replication, and drug sensitivity of Mycobacterium tuberculosis within the macrophage-like cell line THP-1: a comparison with human monocyte-derived macrophages. *Cell Immunol* **197**:1-9.

Su Y, Zhang X and Sinko PJ (2004) Human organic anion-transporting polypeptide OATP-A (SLC21A3) acts in concert with P-glycoprotein and multidrug resistance protein 2 in the vectorial transport of Saquinavir in Hep G2 cells. *Mol Pharm* **1**:49-56.

Takayama K and Kilburn JO (1989) Inhibition of synthesis of arabinogalactan by ethambutol in Mycobacterium smegmatis. *Antimicrob Agents Chemother* **33**:1493-1499.

Takayama K, Wang L and David HL (1972) Effect of isoniazid on the in vivo mycolic acid synthesis, cell growth, and viability of Mycobacterium tuberculosis. *Antimicrob Agents Chemother* **2**:29-35.

Tamai I, Nezu J, Uchino H, Sai Y, Oku A, Shimane M and Tsuji A (2000) Molecular identification and characterization of novel members of the human organic anion transporter (OATP) family. *Biochem Biophys Res Commun* **273**:251-260.

Tan B, Piwnica-Worms D and Ratner L (2000) Multidrug resistance transporters and modulation. *Curr Opin Oncol* **12**:450-458.

Tarshis MS and Weed WA, Jr. (1953) Lack of significant in vitro sensitivity of Mycobacterium tuberculosis to pyrazinamide on three different solid media. *Am Rev Tuberc* **67**:391-395.

Telenti A, Imboden P, Marchesi F, Lowrie D, Cole S, Colston MJ, Matter L, Schopfer K and Bodmer T (1993) Detection of rifampicin-resistance mutations in Mycobacterium tuberculosis. *Lancet* **341**:647-650.

Telenti A, Philipp WJ, Sreevatsan S, Bernasconi C, Stockbauer KE, Wieles B, Musser JM and Jacobs WR, Jr. (1997) The emb operon, a gene cluster of

Mycobacterium tuberculosis involved in resistance to ethambutol. *Nat Med* **3**:567-570.

Theus SA, Cave MD and Eisenach KD (2004) Activated THP-1 cells: an attractive model for the assessment of intracellular growth rates of Mycobacterium tuberculosis isolates. *Infect Immun* **72**:1169-1173.

Thiemer-Kruger E (1958) Isonicotinic acid hypothesis of the antituberculous action of isoniazid. *Am Rev Tuberc* **77**:364-367.

Thomas JP, Baughn CO, Wilkinson RG and Shepherd RG (1961) A new synthetic compound with antituberculous activity in mice: ethambutol (dextro-2,2'-(ethylenediimino)-di-l-butanol). *Am Rev Respir Dis* **83**:891-893.

Tirona RG and Kim RB (2002) Pharmacogenomics of organic anion-transporting polypeptides (OATP). *Adv Drug Deliv Rev* **54**:1343-1352.

Tirona RG, Leake BF, Wolkoff AW and Kim RB (2003) Human organic anion transporting polypeptide-C (SLC21A6) is a major determinant of rifampin-mediated pregnane X receptor activation. *J Pharmacol Exp Ther* **304**:223-228.

Ullrich HJ, Beatty WL and Russell DG (1999) Direct delivery of procathepsin D to phagosomes: implications for phagosome biogenesis and parasitism by Mycobacterium. *Eur J Cell Biol* **78**:739-748.

Ulrichs T, Kosmiadi GA, Jorg S, Pradl L, Titukhina M, Mishenko V, Gushina N and Kaufmann SH (2005) Differential organization of the local immune response in patients with active cavitary tuberculosis or with nonprogressive tuberculoma. *J Infect Dis* **192**:89-97.

Van Bambeke F, Balzi E and Tulkens PM (2000) Antibiotic efflux pumps. *Biochem Pharmacol* **60**:457-470.

van Crevel R, Ottenhoff TH and van der Meer JW (2002) Innate immunity to Mycobacterium tuberculosis. *Clin Microbiol Rev* **15**:294-309.

Vavricka SR, Van Montfoort J, Ha HR, Meier PJ and Fattinger K (2002) Interactions of rifamycin SV and rifampicin with organic anion uptake systems of human liver. *Hepatology* **36**:164-172.

Velasco-Velazquez MA, Barrera D, Gonzalez-Arenas A, Rosales C and Agramonte-Hevia J (2003) Macrophage--Mycobacterium tuberculosis interactions: role of complement receptor 3. *Microb Pathog* **35**:125-131.

Vergne I, Chua J and Deretic V (2003) Tuberculosis toxin blocking phagosome maturation inhibits a novel Ca2+/calmodulin-PI3K hVPS34 cascade. *J Exp Med* **198**:653-659.

Vergne I, Fratti RA, Hill PJ, Chua J, Belisle J and Deretic V (2004) Mycobacterium tuberculosis phagosome maturation arrest: mycobacterial phosphatidylinositol analog phosphatidylinositol mannoside stimulates early endosomal fusion. *Mol Biol Cell* **15**:751-760.

Vieira OV, Botelho RJ and Grinstein S (2002) Phagosome maturation: aging gracefully. *Biochem J* **366**:689-704.

Vieira OV, Botelho RJ, Rameh L, Brachmann SM, Matsuo T, Davidson HW, Schreiber A, Backer JM, Cantley LC and Grinstein S (2001) Distinct roles of class I and class III phosphatidylinositol 3-kinases in phagosome formation and maturation. *J Cell Biol* **155**:19-25.

Vieira OV, Bucci C, Harrison RE, Trimble WS, Lanzetti L, Gruenberg J, Schreiber AD, Stahl PD and Grinstein S (2003) Modulation of Rab5 and Rab7 recruitment to phagosomes by phosphatidylinositol 3-kinase. *Mol Cell Biol* **23**:2501-2514.

Visintin A, Mazzoni A, Spitzer JH, Wyllie DH, Dower SK and Segal DM (2001) Regulation of Toll-like receptors in human monocytes and dendritic cells. *J Immunol* **166**:249-255.

Viveiros M, Portugal I, Bettencourt R, Victor TC, Jordaan AM, Leandro C, Ordway D and Amaral L (2002) Isoniazid-induced transient high-level resistance in Mycobacterium tuberculosis. *Antimicrob Agents Chemother* **46**:2804-2810.

Walburger A, Koul A, Ferrari G, Nguyen L, Prescianotto-Baschong C, Huygen K, Klebl B, Thompson C, Bacher G and Pieters J (2004) Protein kinase G from pathogenic mycobacteria promotes survival within macrophages. *Science* **304**:1800-1804.

Wallis RS, Patil S, Cheon SH, Edmonds K, Phillips M, Perkins MD, Joloba M, Namale A, Johnson JL, Teixeira L, Dietze R, Siddiqi S, Mugerwa RD, Eisenach K and Ellner JJ (1999) Drug tolerance in Mycobacterium tuberculosis. *Antimicrob Agents Chemother* **43**:2600-2606.

Walubo A, Smith P and Folb PI (1994) Comprehensive assay for pyrazinamide, rifampicin and isoniazid with its hydrazine metabolites in human plasma by column liquid chromatography. *J Chromatogr B Biomed Appl* **658**:391-396.

Wengenack NL, Lopes H, Kennedy MJ, Tavares P, Pereira AS, Moura I, Moura JJ and Rusnak F (2000) Redox potential measurements of the Mycobacterium tuberculosis heme protein KatG and the isoniazid-resistant enzyme KatG(S315T): insights into isoniazid activation. *Biochemistry* **39**:11508-11513.

Wilson M, DeRisi J, Kristensen HH, Imboden P, Rane S, Brown PO and Schoolnik GK (1999) Exploring drug-induced alterations in gene expression in Mycobacterium tuberculosis by microarray hybridization. *Proc Natl Acad Sci U S A* **96**:12833-12838.

Wolucka BA, McNeil MR, de Hoffmann E, Chojnacki T and Brennan PJ (1994) Recognition of the lipid intermediate for arabinogalactan/arabinomannan biosynthesis and its relation to the mode of action of ethambutol on mycobacteria. *J Biol Chem* **269**:23328-23335.

Yamamoto T, Moriwaki Y, Takahashi S, Hada T and Higashino K (1987a) In vitro conversion of pyrazinamide into 5-hydroxypyrazinamide and that of pyrazinoic acid into 5-hydroxypyrazinoic acid by xanthine oxidase from human liver. *Biochem Pharmacol* **36**:3317-3318.

Yamamoto T, Moriwaki Y, Takahashi S, Hada T and Higashino K (1987b) Rapid and simultaneous determination of pyrazinamide and its major metabolites in human plasma by high-performance liquid chromatography. *J Chromatogr* **413**:342-346.

Yeager RL, Munroe WG and Dessau FI (1952) Pyrazinamide (aldinamide) in the treatment of pulmonary tuberculosis. *Am Rev Tuberc* **65**:523-546.

Zaman GJ, Flens MJ, van Leusden MR, de Haas M, Mulder HS, Lankelma J, Pinedo HM, Scheper RJ, Baas F, Broxterman HJ and et al. (1994) The human multidrug resistance-associated protein MRP is a plasma membrane drug-efflux pump. *Proc Natl Acad Sci U S A* **91**:8822-8826.

Zeng H, Chen ZS, Belinsky MG, Rea PA and Kruh GD (2001) Transport of methotrexate (MTX) and folates by multidrug resistance protein (MRP) 3 and MRP1: effect of polyglutamylation on MTX transport. *Cancer Res* **61**:7225-7232.

Zhang Y and Amzel LM (2002) Tuberculosis drug targets. *Curr Drug Targets* **3**:131-154.

Zhang Y, Heym B, Allen B, Young D and Cole S (1992) The catalase-peroxidase gene and isoniazid resistance of Mycobacterium tuberculosis. *Nature* **358**:591-593.

Zhang Y and Mitchison D (2003) The curious characteristics of pyrazinamide: a review. *Int J Tuberc Lung Dis* **7**:6-21.

Zhang Y, Scorpio A, Nikaido H and Sun Z (1999) Role of acid pH and deficient efflux of pyrazinoic acid in unique susceptibility of Mycobacterium tuberculosis to pyrazinamide. *J Bacteriol* **181**:2044-2049.

Zhang Y, Wade MM, Scorpio A, Zhang H and Sun Z (2003) Mode of action of pyrazinamide: disruption of Mycobacterium tuberculosis membrane transport and energetics by pyrazinoic acid. *J Antimicrob Chemother* **52**:790-795.

Ziglam HM, Baldwin DR, Daniels I, Andrew JM and Finch RG (2002) Rifampicin concentrations in bronchial mucosa, epithelial lining fluid, alveolar macrophages and serum following a single 600 mg oral dose in patients undergoing fibre-optic bronchoscopy. *J Antimicrob Chemother* **50**:1011-1015.

Zimhony O, Cox JS, Welch JT, Vilcheze C and Jacobs WR, Jr. (2000) Pyrazinamide inhibits the eukaryotic-like fatty acid synthetase I (FASI) of Mycobacterium tuberculosis. *Nat Med* **6**:1043-1047.